Isolation and Characterization of Antiplasmodial Metabolites from South African Marine Algae

A Thesis Submitted in Fulfillment of the Requirements
for the degree of

Master of Science (Pharmacy)
of Rhodes University

By

Anthonia Folake Afolayan

January 2008

Acknowledgements

Firstly, I would like to say a big thank you to my supervisor, Dr. Denzil Beukes for his patience, guidance and advice throughout my project. Thanks boss for not giving up on me.

A special thank you to Dr. Linda Stephens for her supervision and contributions towards the over-production of *E. coli* DXR

Many people have been contributed to the successful completion of this research and I would like to express my sincere gratitude

- Jessica Goble for her kind donation of over-produced *Plasmodium falciparum* DXR
- Professor Philip Proteau from Oregon State University for donating DOXP
- Mr Andy Soper for his technical assistance with NMR and Mr Aubrey Soneman for his assistance with low resolution mass spectroscopy.
- Dr Edith Antunes for her help especially with NMR
- From the University of Cape Town, Professor John Bolton for the identification of algae, Professor Peter Smith for his help with antiplasmodial assays and Catherine Whibley for her help with anti-oesophageal assays.
- Dr. Louis Fourie and professor Johan Jordaan from the University of the North West for obtaining HRFABMS
- Dr Marietjie Stander from Stellenbosch University for her help with APCI-MS.
- My mentor and tutor, Ms Carmen Oltmann
- Mr David Morley for his technical assistance through the years
- My labmates, Yolisa and Maryssa. Yols thank you for your encouragement and for always answering my many questions. Maryssa thank you for your support and contribution towards the algae extraction
- Pharmacy Faculty staff and Post-graduate students for their support
- My two friends, Vongani and Dubekile, making up the "three musketeers". Thank you for your constant support and encouragement, proof reading and being there for me when times were tough. Dubs thank for hosting me while I was writing up.

- The Nigerian community at Rhodes University, thank you for always looking out for me
- Segun and David, thank you believing in me, for your moral support and always listening to my complaints. Georgina, I could not have asked for a better flatmate, thank you for the nights you stayed up to make sure I worked. Nana, thanks for your support.
- A big thank you to the Mellon Foundation Scholarship and the National Research Foundation for funding my research

Finally, my family who has been a pillar of strength to me. To my parents, Professor Anthony and Mrs Theresa Afolayan, for your unfailing support. Dad, thank you for your guidance and advice. Mum thank you for your prayers and words of encouragement all the way. My brother Sola and my sister Lola, thank you for believing in me and supporting my dreams. I could not have done it without you all.

Table of contents

List of Figures

List of Schemes

List of Tables

List of Abbreviations

°C	Degrees Celsius
bp	Basepair
BSA	Bovine serum albumin
$CdCl_3$	Deuterated chloroform
CH_2Cl_2	Dichloromethane
COSY	^1H-^1H Homonuclear Correlation Spectroscopy
d	Doublet
dd	Doublet doublet
DEPT	Distortionless Enhancement of Polarisation Transfer
DOXP	1-deoxy-$_D$-xylulose-5-phosphate
DXR	DOXP reductoisomerase
E. coli	*Escherichia coli*
*Ec*DXR	*E. coli* DOXP reductoisomerase
EIMS	Electron Impact Mass Spectrometry
EtOAc	Ethyl Acetate
eV	electron Volt
Fr	Fraction
HMBC	Heteronuclear Multiple Bond Correlation
HPLC	High Performance Liquid Chromatography
HREIMS	High Resolution Electron Impact Mass Spectrometry
HRFABMS	High resolution fast atom bombardment
HSQC	Heteronuclear Single Bond Correlation
Hz	Hertz
IC_{50}	Inhibitory Concentration 50 %
IPTG	Isopropyl-β-D-galactopyranoside
IR	Infrared
J	Spin-Spin coupling constant (Hz)
m	Multiplet
m/*z*	Mass to charge ratio
m/z	Mass to charge ratio
MeOH	Methanol

MEP	2-C-methyl-$_D$-erythritol 4-phosphate
MHz	Megahertz
multi	Multiplicity
multi	Multiplicity
MW	Molecular weight
NADPH	Nicotinamide adenine dinucleotide
NMR	Nuclear magnetic resonance
NMR	Nuclear Magnetic Resonance Specroscopy
NOESY	Nuclear Overhauser enhancement spectroscopy
OD	Optical density
P. falciparum	*Plasmodium falciparum*
PAGE	Polyacrylamide gel electrophoresis
*Pf*DXR	*P. falciparum* DOXP reductoisomerase
PMSF	Phenylmethylsulfonylfluoride
ppm	Parts per million
q	Quartet
s	Singlet
SDS-PAGE	Sodium dodecyl sulphate polyacrylamide gel electrophoresis
t	Triplet
THF	Tetrahydrofuran
TLC	Thin Layer Chromatography
UV	Ultra Violet
δ	Chemical shift (ppm)

Abstract

Malaria is one of the three most deadly diseases in Africa. Although there are available treatments, their efficacy has been greatly reduced over the past two decades due to the development of resistance to currently available drugs. This has necessitated the search for new and effective antimalarial agents.

This project approached the search for new antimalarial compounds in two ways: (i) by screening natural products isolated from marine algae against the *Plasmodium* parasite and (ii) by modification of selected isolated active compounds to target 1-deoxy-$_D$-xylulose 5-phosphate reductoisomerase (DXR), an enzyme found in the non-mevalonate isoprenoid biosynthetic pathway of *Plasmodium falciparum*. It was envisaged that such a compound would exhibit dual action on the *Plasmodium* parasite.

Extracts obtained from 22 marine algae were prefractionated by solvent partitioning and were screened for antiplasmodial activity against the chloroquine sensitive (CQS) *P. falciparum* D10 strain. Overall, 50% of the algae screened produced at least one crude fraction with activity against *P. falciparum*. Extracts of the algae *Sargassum heterophyllum*, *Plocamium cornutum*, *Amphiroa ephedrea* and *Pterosiphonia cloiophylla* gave the most promising results. Fractionation of *S. heterophyllum* afforded three tetraprenyltoluquinols (**3.1**, **3.2** and **3.5**) and an *all-trans*-fucoxanthin (**3.6**).Three new compounds (**4.5**, **4.6** and **4.7**) and two known halogenated monoterpenes (4.1 and 4.4) were isolated from *P. cornutum*. Each of the isolated compounds from both *S. heterophyllum* and *P. cornutum* showed antiplasmodial activity with IC_{50} values ranging from 2.0 – 15.3 μM for *S. heterophyllum* and 13 – 230 μM for *P. cornutum*.

Attempts to synthetically modify halogenated monoterpene **4.4** by dihydroxylation and phosphorylation in order to inhibit the DXR enzyme was unsuccessful. However, the hemiterpene analogue (**5.42**) of the halogenated monoterpenes was successfully phosphorylated and dihydroxylated to give compound **5.45** which showed promising activity against DXR. The result obtained indicated that the proposed phosphorylation

and dihydroxylation of the halogenated monoterpene **4.4** would result in the synthesis of a potent DXR inhibitor and therefore a potential antimalarial agent with dual mode of action on the *Plasmodium* parasite.

Chapter 1

Literature review

1.1 General Introduction to Malaria

Malaria is one of the leading infectious diseases in the world. It is reported to cause morbidity in 300 – 500 million people and fatality in 1.5 – 3 million people annually (Fidock *et al.*, 2004). Most of these cases (over 90%) occur amongst children and pregnant women in the sub-Saharan Africa (Watkins and Meshnick, 2000). Over 40% of the world's population is estimated to be exposed to the disease (O'Neill *et al.*, 1998). The major problem at present is the development of resistance by these strains of *Plasmodium* to the traditional antimalarial agents such as the quinoline derivatives and the antifolates. As a result of the decreased efficacy due to the resistance, the cost and severity of the disease have increased significantly; thus, there is an urgent need for the development of affordable and effective antimalarial agents.

1.1.1 History of Malaria

Malaria has been around since the existence of mankind on earth (about 4000 years ago). Its symptoms were noted as far back as 2700 BC. In 1889, Alphonse Laveran discovered the protozoal cause of malaria and by 1898, Ronald Ross discovered that the vector involved in the transmission of the parasite is the female *Anopheles* mosquito (Guillemin, 2001). Malaria was responsible for the decline of many city-state populations in the fourth century and still continues to kill millions of people annually even in this twenty-first century (Haemers *et al.*, 2006).

1.1.2 Distribution of malaria

Malaria is thought to have started in Africa and spread to other parts of the world due to human population growth, the emergence of agriculture societies and the mosquito vector speciation (Joy *et al.*, 2003). Areas such as North America and Europe have

succeeded in eradicating the disease through the eradication of the vector mosquitoes (Gomes, 1993, Hey *et al.*, 2004) but the middle-belt which includes central and South America, most parts of Africa and South-East Asia still suffer from the disease (Figure 1). The countries most affected by the disease are the underdeveloped and developing countries where affordability of treatment for malaria is difficult for an average patient.

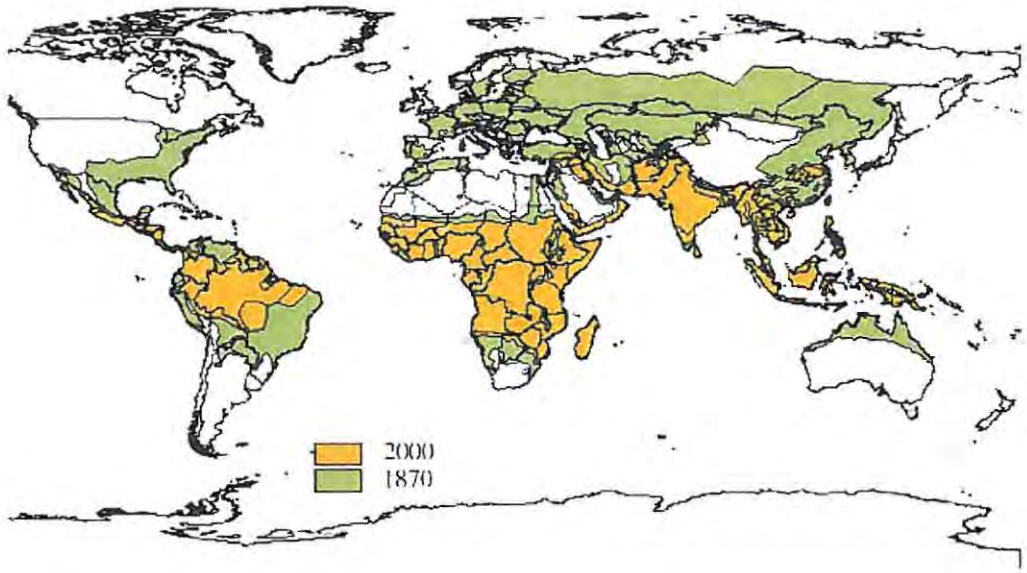

Figure 1.1 Malaria endemic areas: Past and present distribution (van Lieshout *et al.*, 2004)

1.1.3 Causative agents and vector of malaria.

The parasites that cause malaria are of the *Plasmodium* genus. These are apicomplexans or the so-called one-celled organisms. They have a self-replicating organelle known as an apicoplast which is thought to be from algal origin (Ridley, 1999). The *Plasmodium* species considered to be of most importance to human beings include *P. falciparum* (the most dangerous), *P. vivax, P. ovale* and *P. malariae*. The parasites are transferred by the female *Anopheles* mosquitoes (Lemke, 2002).

1.1.4 The life cycle of *Plasmodium* parasites

The transmission of protozoa occurs when female *Anopheles* mosquitoes bite an infected person and ingest the blood containing the *Plasmodium* gametocytes. The gametocytes then reproduce sexually in the mosquito gut over a period of 1 – 2 weeks. The produced infective sporozoites are inoculated into another person when an infected mosquito bites and subsequently infect the hepatocytes where they multiply asexually (Beers and Berkow, 1999). Sporozoites enter the blood stream as merozoites and invade red blood cells where they continue to multiply for 1 – 3 days. The infected red blood cells rupture and release merozoites at about 48 hour intervals giving rise to malaria symptoms (Lemke, 2002). Simultaneously, formation of gametocytes occurs in red blood cells and although they are not clinically important, the gametocytes are the particles that infect mosquitoes (Beers and Berkow, 1999) and are therefore responsible for transmission (Figure 1.2).

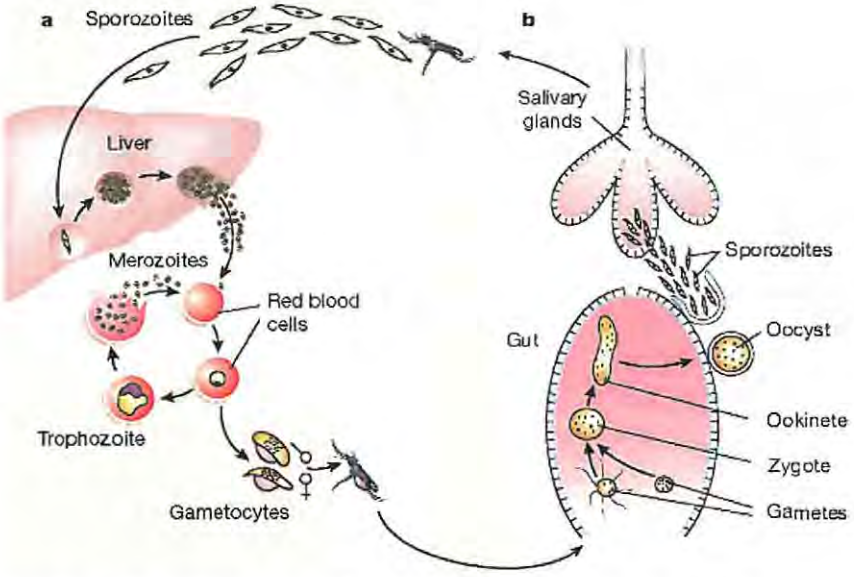

Figure 1.2 The life cycle of a *Plasmodium* parasite in the mosquito and human (Wirth, 2002)

1.1.5 The signs and symptoms of malaria

Each of the different species of *Plasmodium* shows different severity of the disease with *P. falciparum* being the most dangerous. However there are common manifestations of all four species. These include anaemia, jaundice, hepatomegally,

splenomegally and malaria paroxysm. The paroxysm initially involves malaise, chills, rapid pulse, headache and nausea which is then followed by fever, and profuse sweating. The paroxysm occurs at an interval of 48 hours in *P. falciparum* and *P. vivax,* while in *P. ovale* and *P. malariae* it has an interval of 72 hours, which corresponds with the rupture of the red blood cells (Beers and Berkow, 1999).

1.2 Malaria as a major problem in the developing countries

The World Health Organization (WHO) recognizes malaria as one of the major problems facing the developing countries. It is perceived to be the disease of the poor and a cause of poverty. Countries where malaria is endemic have slower growth than those without the disease and the gap in prosperity between countries with malaria and those without malaria increases every year.

The World Bank has estimated that the cost of malaria in Africa as a result of lost productivity is $12 billion a year. In the long run, the cost of preventing the disease is less than the cost required for the treatment of the disease.

Another problem facing developing countries is resistance to the available antimalarial drugs. The development of resistance to the drugs necessitates the discovery and development of new drugs. Unfortunately however, these new drugs are proving to be more expensive than the old drugs and are thus not affordable for the average patient in a developing country.

1.3 Prevention and Treatment of malaria

Malaria can be prevented by drug and non-drug measures (Gibbon *et al.*, 2003).

1.3.1 Non-drug measures for preventing malaria

The saying "prevention is better than cure" is very much applicable to malaria. After contracting the disease, the cost of treatment, the loss of days at work, the potential deformity or death seems a high price to pay for a disease that can be prevented by

simple measure that does not involve medication. These non-drug preventative measures include; avoiding endemic areas during wet season (for people living in areas that are malaria free), applying insect repellants to clothing and exposed skin and wearing light-coloured clothes, long sleeves and long trousers between dark and dawn. Others include using mosquito nets, coils and screens and spraying the house with pyrethroid insecticide.

1.3.2 Drug measures (Chemotherapeutic prevention and treatment of malaria)

This involves the use of chemical compounds to either prevent or treat the disease. These drugs are classified according to the stage of the life cycle of the *Plasmodium* in the host where they act and according to the chemical structure of the drug.

1.3.2.1 Classification of antimalarial drugs based on the stage of *Plasmodium* life cycle.

According to Lemke (2002), malarial drugs could be classified as follows:

1. Tissue shizontizides: These drugs destroy the exoerythrocytic liver-tissue stage of the parasite and thus prevent the parasites from entering the blood. This type of drugs is used as prophylaxis.
2. Blood shizonticides: These are the drugs that eradicate the parasite from the blood stream i.e. they destroy the erythrocytic stage and are therefore able to cure malaria caused by *P. falciparum* and prevent relapses. These drugs are delivered into the blood stream rapidly and thus make this phase of infection the easiest to treat.
3. Gametocides: This drug type wipes out the sexual form of the parasite and as a result prevents the transmission of the disease by preventing the transmission of the parasite to the *Anopheles* mosquitoes.
4. Sporozooiticides: This group of drugs kills the organism (sporozoites) as soon as it enters the blood stream after a mosquito bite and thereby prevents the parasite from infecting the hepatocytes.

None of the available drugs is able to eliminate both the hepatic and the erythrocytic stage (Katzung, 2004), and although they may be effective against more than one species of *Plasmodium*, they may be ineffective against other forms.

1.3.2.2 Structural classification of antimalarial drugs

Quinine (**1.1**) was the first drug used in the treatment of malaria dating back to the 1600s (Figure 1.3). It is a natural product obtained from the bark of the *Cinchona* tree. The bark also contained quinidine (**1.2**) (a diastereomer to quinine) the desmethoxy cinchonine and its diastereomer cinchonidine. The structure of quinine presented evidence that the quinoline nucleus could be a valuable contributor to the antimalarial activity (O'Neill, *et al.*, 1998).

Another class of compounds which exhibited antiplasmodial activity was 9-aminoacridines. A derivative of this class, quinacrine (**1.3**), was synthesized in 1934 and was found to possess weak antimalarial properties. In the effort to produce more effective compounds than quinacrine (**1.3**) and synthetic alternatives to quinine, the structure-activity-relationship (SAR) and chemical similarities between these two classes of compounds were studied. Modifications to the quinoline nucleus and side chains gave rise to compounds that are classified by their chemical structures. These include the 4-aminoquinolines such as choroquine (**1.4**) and the 8-aminoquinolines which includes primaquine (**1.5**). The quinoline-4-methanols, mefloquine (**1.6**) and halofantrine (**1.7**) were also synthetically produced all of which bear similarities to the quinine and quinacrine chemical structure (Lemke, 2002).

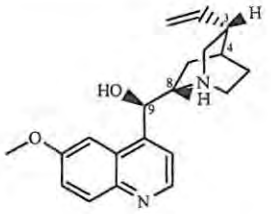

Quinine (**1.1**)

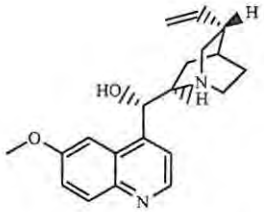

Quinidine (**1.2**)

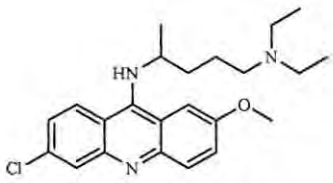

Quinacrine (**1.3**)

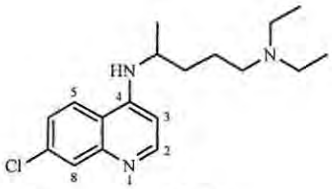

Chloroquine (**1.4**)

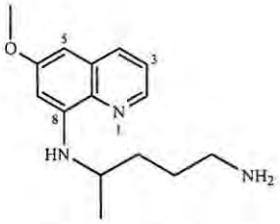

Primaquine (**1.5**)

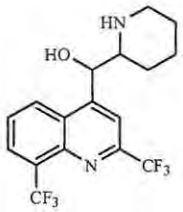

Mefloquine (**1.6**)

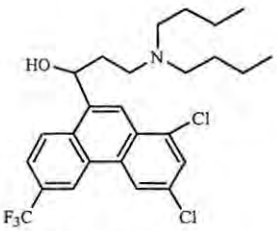

Halofantrine (**1.7**)

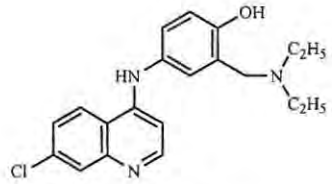

Amodiaquine (**1.8**)

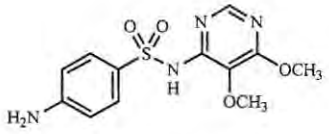

Sulfadoxine (**1.9**)

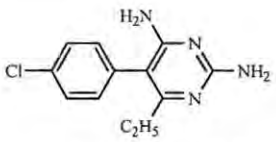

Pyrimethamine (**1.10**)

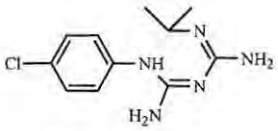

Proguanil (**1.11**)

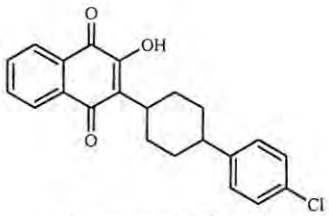

Atovaquone (**1.12**)

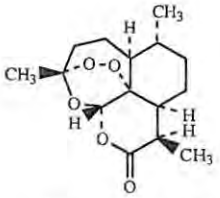

Artemisinin (**1.13**)

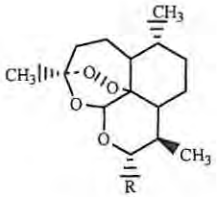

Dihydroartemisinin (**1.14**) R = H
Artesunate (**1.15**) R = $O_2CCH_2CH_2CO_2H$
Ateether (**1.16**) R = OEt
Artemether (**1.17**) R= OMe

Figure 1.3 Structures of some antimalarial compounds

1.3.2.2.1 4-Substituted quinolines

These are a group of antimalarial agents that contain the quinine nucleus and are substituted at C-4 e.g. chloroquine (**1.4**). The five compounds in this group include quinine (**1.1**), chloroquine (**1.4**), mefloquine (**1.6**), hydroxychloroquine and amodiaquine (**1.8**). They have similar modes of action and act on the same stage of the parasite life cycle (O'Neill, *et al.*, 1998 and Lemke, 2002). These compounds act rapidly as blood schizonticides.

These drugs are weak bases, are membrane soluble and are thought to accumulate in the red blood cells where the parasites multiply after leaving the liver. Here the quinolines are able to move into the parasites food vacuole (lysosome) where haemoglobin (Hb) digestion takes place to produce toxic haematin which is then polymerized to detoxify it. The pH in the vacuole is 5.2 while in the red blood cells it is 7.4. At a pH of 7.4 the aminoquinolines are unionized and therefore can cross the membrane. However at pH 5.2 they are diprotonated and cannot move out of the vacuole and as a result accumulate in the vacuole. These drugs then bind to haematin and prevent the formation of non-toxic haemozin or β-haematin. The toxic haematin then leads to parasite death (Warhust, 2003).

Chloroquine as a representative of the 4-substituted aminoquinolines

Chloroquine (**1.4**) has been the drug of choice for prophylaxis and treatment of malaria since the 1940s. However, attempts to eradicate malaria in the 1960s resulted in the overuse of the drug which led to the development of resistance by the parasite. Although chloroquine has been declared ineffective in many parts of the malaria endemic areas, the drug is still useful in some parts of Central America and the Mediterranean. The major problem with the use of chloroquine is resistance. Resistance to the drug has been correlated to the mutation in one of the intrinsic protein transporter (PfCRT) of the drug into the vacuole (Katzung, 2004). Due to its safety and low cost chloroquine is the drug of choice for non-falciparum and sensitive falciparum malaria.

1.3.2.2.2 8-Aminoquinolines

This group of quinolines is substituted at position 8 unlike the 4-substituted quinolines. They are pamaquine and primaquine (**1.5**). Pamaquine was first introduced for malaria treatment in 1926 as a blood schizonticide but has since been replaced with primaquine due to its well known liver toxicity side effect (Lemke, 2002). Primaquine (**1.5**) is a synthetic 8-aminoquinoline marketed as primaquine phosphate. It has an unknown mechanism of action but it is known to generate reactive oxygen species through autooxidation of the 8-amino group (Lemke, 2002). This leads to the formation of radicals such as peroxide, superoxide and hydroxyl radicals that destroy the parasite cells (though they may be toxic to human as well) (Tonnesen, 1998). Primaquine (**1.5**) is the only tissue schizonticide available for the treatment of dormant liver stage or relapsing vivax and ovale infection (Vennerstrom, 1999). It is also active against the gametocyte i.e. its gametocidal to all four *Plasmodium* species. It has very weak erythrocytic activity and is therefore often combined with chloroquine to treat blood stage infection. Primaquine (**1.5**) is used clinically for radical cure of acute vivax and ovale malaria, terminal prophylaxis of vivax and ovale malaria, chemoprophylaxis of malaria and to render *P. falciparum* gametocyte non-infective (Katzung, 2004). However, due to its potential liver toxicity and sensitization, the drug is often used for short term.

1.3.2.2.3 Folate antagonists

Folate antagonists are often used in combinations to prevent and treat malaria. This group of drugs includes sulphadoxine (**1.9**), pyrimethamine (**1.10**) and proguanil (**1.11**). They act by inhibiting folate synthesis in the plasmodium parasites. Folates are necessary for the biosynthesis of pyrimidines, purines and some amino acids (Watkins and Meshnick, 2000). Therefore inhibition of the folate biosynthetic pathway will lead to death of the parasites as a result of low nucleic acid level and protein necessary for survival. Sulphadoxine (**1.9**) is a sulphur-based compound which acts as a structural inhibitor of an interesting enzyme, dihydropteroate synthase, in the folate biosynthetic pathway. It has been demonstrated to compete with para-aminobenzoic acid, a substrate of the enzyme, for binding (Watkins and Meshnick, 2000). Dihydropteroate synthase is not found in humans (Katzung, 2004),

which makes the inhibition of this enzyme specific to the parasite. Pyrimethamine (**1.10**) is a 2,4-diaminopyrimidine which is a structural inhibitor of the enzyme dihydrofolate reductase , a key enzyme in folate synthesis (Lemke, 2002; Katzung, 2004)). Dihydrofolate reductase catalyzes the NADPH-dependent reduction of dihydrofolate to tetrahydrofolate. Pyrimethamine has more affinity for the *Plasmodium* reductase enzyme than the host cell (Watkins and Meshnick, 2000). Pyrimethamine and sulphadoxine are used in combination as they have synergistic effect. Inhibition of dihydropteroate synthase activity leads to reduced production of dihydropteroate which in turn leads to reduced synthesis of dihydrofolate. As a result the activity of dihydrofolate reductase inhibitor increases thus, in the concomitant blockade of the pathway, the activity of one inhibitor potentiates the activity of the other (Nzila, 2006). Both sulphadoxine (**1.9**) and pyrimethamine (**1.10**) act as blood schizonticides. However wide spread resistance is also a problem associated with these drugs.

1.3.2.2.4 Other available antimalalarial agents

Other available antimalarial agents are halofantrine (**1.7**), atovaquone (**1.12**) and a number of antibiotics. Halofantrine (**1.7**) is a tricyclic compound that was introduced in the 1980s (Watkins and Meshnick, 2000). It is classified as a 9-phenanthrenemethanol. The drug is used as a racemic mixture because it has one chiral centre and the two resulting enantiomers appear to have no significant difference (Williams and Lemke, 2002). It produces an active metabolite which contributes to its potency. The mode of action of halofantrine is unknown, however it has been suggested that it might be involved in the chelation of divalent metal ions by the 1,10-phenanthrolic ring system, a metalloprotease inhibitor (Wijayanti *et al.*, 2006). Clinically, halofantrine is used as a second-line agent which is effective against the erythrocytic stage of all the four malaria species that affects human. It is also used against both chloroquine-sensitive and chloroquine-resistant strains of *P. falciparum* (Katzung, 2004). However it is not very effective against mefloquine-resistant strain as a high degree of *in vitro* cross resistance has been demonstrated between mefloquine and halofantrine. Halofantrine use is limited due to its variable

bioavailability, cardiotoxicity side effect and high cost (Watkins and Meshnick, 2000).

Atovaquone (**1.12**) is an ubiquinone analogue belonging to the class of hydroxynaphthoquinones. It was developed in the 1980s as an effective antimalarial compound (Watkins and Meshnick, 2000). The antimalarial effect of atovaquone (**1.12**) is due to its specific blockade of the pyrimidine biosynthesis via the inhibition of parasite respiratory system by competing with ubiquinone to bind to the ubiquinol-cytochrome *c* reductase region of the *Plasmodium* mitochondrial electron transport chain. Dihydro-orotate dehydrogenase (DHOOD) is an important enzyme in the synthesis of pyrimidine in the *Plasmodium* parasite unlike in mammals. The hydroxynaphtoquinones disrupts the pyrimidine biosynthesis without altering the Adenosine triphospahte (ATP) levels as it would in mammals because *Plasmodium* parasites are homolactate fermentors and thus require minimum ATP formation from ubiquinone (Hudson, 1993). When used as a monotherapy, atovaquone has a high failure rate. It is therefore used in combination with proguanil (**1.11**), tetracycline or doxycyline.

A number of antibiotics are used as prophylaxis in the treatment of malaria. Although their mode of action is unclear, it is possible that they inhibit protein synthesis or other functions in the mitochondrion and or apicoplast of the *Plasmodium* as these organelles have prokaryotic origin (Katzung, 2004). Tetracycline and doxycycline are active against the erythrocytic schizont in the four *Plasmodium* species. Doxycyline is often used with quinine or quinidine to allow for better tolerance of quinine in the treatment of *P. falciparum* malaria. Doxycycline is also used in some areas as chemoprophylactic agent. In pregnant women and children where doxycyline is contraindicated, clindamycin is used as a substitute. Other antibiotics used in malaria treatment include azithromycin and some fluoroquinolones. None of these antibiotics is used alone for malaria treatment because they act slower than the standard antimalarial agent (Katzung, 2004).

1.3.2.2.5 Artemisinin and its derivatives

Artemisinin (**1.13**) and its derivatives are the latest development in the treatment of malaria. The plant *Artemisia annua* has been in use in China for over 2000 years for the treatment of chills and fever. Artemisinin (**1.13**) was first isolated from *Artemisia annua* in 1972 and its structure was elucidated in 1979 (Van Agtmael *et al.*, 1999). Artemisinin (**1.13**) is a sesquiterpene 1,2,4-trioxane lactone, with a peroxide bridge that is necessary for antimalarial activity. Dihydroartemisinin (**1.14**) has been shown to have more *in vitro* antimalarial activity than artemisinin (**1.13**) and it is easily obtained by the reduction of artemisinin lactone with sodium borohydride. Many derivatives such as artesunate (**1.15**), arteether (**1.16**), and artemether (**1.17**) have been synthesized from dihyroartemisinin (**1.14**). The derivatives were synthesized in order to generate compounds with better physico-chemical properties because artemisinin (**1.13**) has poor water and oil solubility and as a result it is only administered orally. Artesunate, the water soluble hemisuccinate of dihydroartemisin and the oil-soluble ether derivative, arteether, have been developed for intravenous and intramuscular administration respectively. They are also available as oral dosage forms and they exhibit their activity through the active metabolite dihydroartemisinin (**1.14**) which is often present in higher concentration than the parent drug.

Artemisinin (**1.13**) is only active on the blood stage parasite and has no effect on the liver stage. It is active on the gametocyte stage (Katzung, 2004) and therefore reduces transmission of the parasite from an infected person to a mosquito.

During the blood stage, haemoglobin is digested and haem, which is toxic to the parasite, is produced. Haem or Fe^{2+} catalyses the opening of the peroxide bridge in the artemisinin derivatives leading to the formation of free radicals. The intermediates formed during the radical reaction alkylate some important proteins in the parasite causing parasite death (Van Agtmael *et al.*, 1999).

Being the only group of drugs whose *in vivo* resistance has not been reported, the WHO has recommended that artemisinin derivatives be used in combination in order to avoid development of resistance. They are often combined with halofantine or quinine for additive effect and with mefloquine for potentiating effect. They are

reserved for situations where problems of resistance or unwanted side effects to other antimalrial drugs exist. Although no incidence of clinical resistance has been demonstrated, *in vitro* resistance has been reported (Van Agtmael *et al.*, 1999) indicating that uncontrolled use of these drugs might soon lead to plasmodial resistance.

1.4. Approaches to developing new antimalarial agents

To rely exclusively on artemisinin derivatives for the treatment of severe or complicated malarial will be akin to waiting for a major disaster to happen especially since it appears that resistance may well develop to this drug group in future. As a result there is a serious need for continuous research and development of new antimalarial agents. Researchers approach this in different ways. These include synthetic chemistry development and natural product screening.

1.4.1 Synthetic chemistry approach – Modifications of known drugs

This approach involves the total synthesis of new compounds or modification of existing or known compounds to bind to a particular target, inhibit a pathway or increase the potency of a parent drug. Many of the known antimalarial compounds were discovered or designed using this approach. Examples of such agents include the derivatives of quinine (**1.1**) such as chloroquine (**1.4**) with better potency and hydroxychloroquine with better toxicity profile. Mefoloquine (**1.6**) was synthesized with the aim of making it more metabolically stable than quinine (**1.1**) (Lemke, 2002). Sulphadoxine (**1.9**) and pyrimethamine (**1.10**) were synthesized in the effort to produce compounds with similar chemical structure to the substrates of the enzymes in the folic acid biosynthetic pathway which is essential to the *Plasmodium* parasite (Katzung, 2004), but with inhibitory properties.

1.4.2 Natural product screening approach – Target and lead identification

Natural product screening involves the extraction and isolation of compounds from natural source or organism and testing these compounds against the *Plasmodium* parasites for antiplasmodial activity. This is further discussed in chapter two.

Compounds with activity can then be modified against a validated target in the parasite. A desired property of this type of drug would be to have a different mode of action from the existing antimalarial agents.

1.4.3 New approaches to Antimalarial drug discovery

Recently, due to the severity of malaria, researchers have become more interested in the disease and more targets are being identified. This has been made possible due to the complete sequencing of the 22.8 megabase genome of *P. falciparum* which consists of 14 chromosomes and encodes about 5300 genes (Gardner *et al.*, 2002). Several other projects involving the discovery of the enzymes of the non-mevalonate pathway, enzymes necessary for haem biosynthesis and apicoplast-specific carboxylase enzymes and subunits of type II fatty acyl synthase complex have evolved from the *P. falciparum* genome project (Roos *et al.*, 2002).

A plastid is a photosynthetic bacterium living inside a eukaryotic cell (Stuart *et al.*, 2001). The apicomplexan plastid known as apicoplast is believed to have arisen from endosymbiosis of a unicellular alga into the host eukaryotic cell e.g. *Plasmodium* parasite. It services the host cell with multiple functions and is thus indispensable to the host. However they do not photosynthesize (Stuart *et al.*, 2001).

Since the apicoplast is an alga living inside the malaria parasite it has its own cellular processes such as DNA replication, transcription, translation, metabolism and post-translational modification which are separate from that of the *Plasmodium* parasite. Each of these processes can therefore serve as a potential target for the development of antimalarial agents (Stuart *et al.*, 2001).

The apicoplast contains unique metabolic pathways such as fatty acid synthesis, isoprenoid and haem synthesis all of which are absent in the human host (Jana and Paliwal, 2007), therefore they make good drug targets.

1.4.3.1 Fatty acid Biosynthesis (FAS)

Fatty acids are essential for cell growth, homeostasis and differentiation. This is the major function of the apicoplast. The malaria parasite make use of type II fatty acid synthases such as β-ketoacyl-ACP synthase (Fab H), β-ketoacyl-ACP reductase (Fab G) and eroyl-ACP reductase (Fab I) in their fatty acid biosynthetic pathway. Humans however, use type I synthases (Jana and Paliwal, 2007). These two pathways are inherently different that inhibiting the type II pathway should prove to be selective for the malaria parasite. Thiolactomycin and triclosan have been shown to inhibit Fab H and Fab I respectively and thus inhibit plasmodium growth (McLeod *et al.*, 2001 and reviewed in Jana and Paliwal, 2007).

1.4.3.2 Aromatic amino acid synthesis

The presence of this pathway in apicomplexan parasite was confirmed by Robert *et al.*, (1998). Aromatic amino acid such as tryptophan, phenylalanine and thyroxin are synthesized via the shikimate pathway which is absent in human therefore making it a promising target for the development of antimalarial compounds. The pathway comprises of seven enzymes which are involved in the sequential conversion of erythrose-4-phosphate and phosphoenolpyruvate to chorisimate which is then used for the amino acid synthesis and other aromatic compound such as para-aminobenzoic acid and vitamin K. Glyphosate is a herbicide that has been shown to inhibit 5-enolpyruvylshikimate-3-phosphate synthase (an enzyme in the shikimate pathway). The coding DNA sequence of chorisimate synthase has been identified to be required for normal growth in *P. falciparum* and is therefore a validated target for antimalarial drug discovery (Jana and Paliwal, 2007).

1.4.3.3 Isoprenoid Biosynthesis

Both fungi and mammals depend on the mevalonate pathway to produce isoprene units, isopentyl pyrophosphate (IPP, **5.9**) and (dimethylallyl pyrophosphate (DMAPP, **5.10**) required for synthesis of other isoprenoid class compounds. Isoprenoids play important roles in different organisms such as photosynthesis, protein synthesis and electron transport (Testa *et al.*, 2006). However, *P. falciparum*, many bacteria and

some higher plants make use of a non-mevalonate pathway which utilizes 1-deoxy-D-xylulose 5-phosphate (DOXP, **5.3**) as a precursor to produce the isoprene units (Jana and Paliwal, 2007). Several enzymes in the non-mevalonate pathway have been characterized and each one is a potential target for the development of antiplasmodial agents.

1.5 Marine habitat as a source of bioactive compounds

Over the last few decades, the marine environment has become an attractive source of biologically active compounds. Chemical compounds with a variety of biological properties have been isolated from this aquatic habit (Figure 1.4). These include; haliclonacyclamine (**1.18**, antibacterial), basilikamides A (**1.19**, antifungal), cyanthiwigin (**1.20,** antituberculosis), clathsterol (**1.21,** antiviral) and aigialomycin D (**1.22**) which is an antimalarial agent (Mayer and Hamann, 2005). These bioactive compounds were isolated from marine organisms such as bacteria, fungi and sponges, however, sponges appear to be the major source of bioactive compounds.

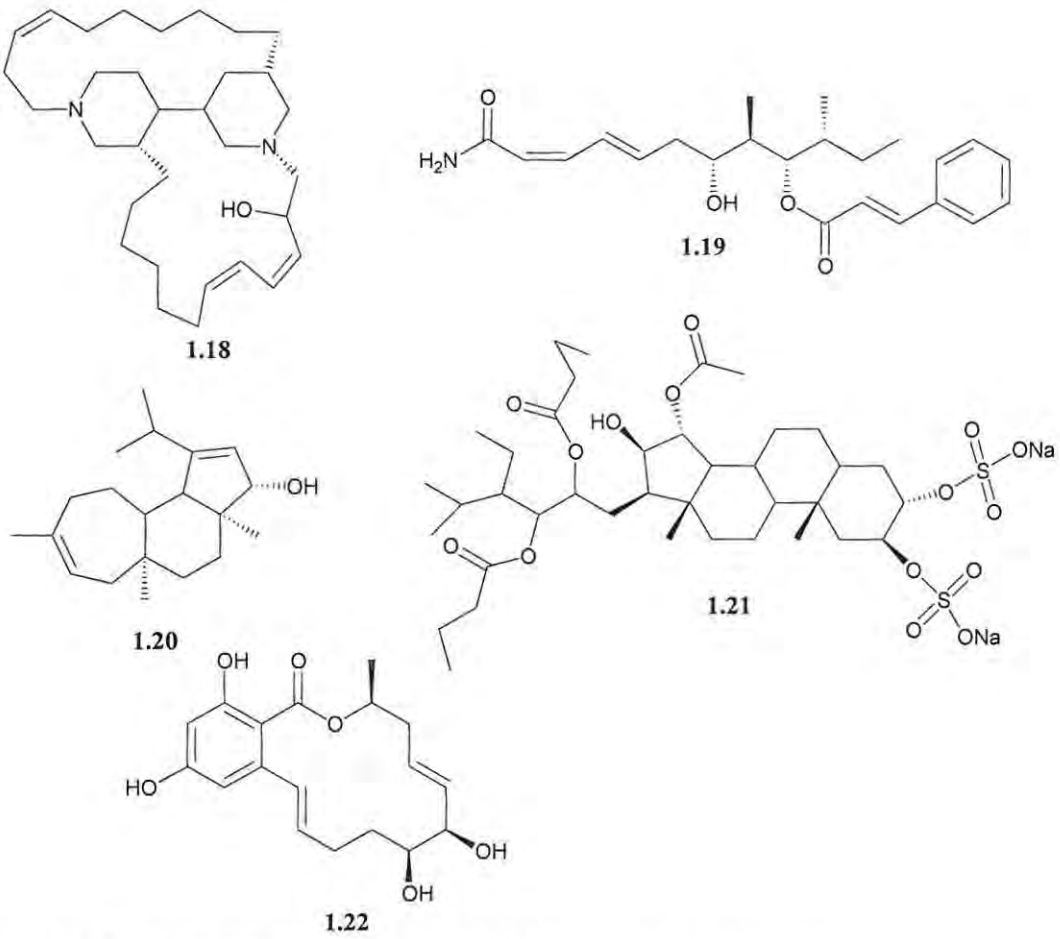

Figure 1.4 Some bioactive compounds from marine organisms

1.5.1 Antimalarial compounds from marine organisms

Many antimalarial and antiplasmodial compounds have been isolated from marine organisms such as fungi, sponges and bacteria but mostly from sponges (Figure 1.5). A highly potent but toxic group of antimalarial agents from sponges is manzamines. Manzamines are complex alkaloids which have been shown to be highly active against rhodent malaria parasite *Plasmodium berghei* (Higa *et al.*, 2001). Manzamine A (**23**), (-)-hydroxymanzamine A (**24**) and manzamine F (**25**) have been tested against *P. berghei* and while manzamine A (**23**) and (-)-hydroxymanzamine A (**24**) showed potent activity, Manzamine F (**25**) did not show any life-prolonging effect on the rhodents used, indicating the importance of the functionality on the 8-memebered ring of the manzamines (Higa *et al.*, 2001) (Figure 1.5).

Several sesquiterpenes and diterpenes with isonitrile (-CN) group have been shown to have antiplasmodial activity. Axisonitrile-3 (**1.26**), a sesquiterpene isolated from the sponge *Acanthella klethra* showed high selectivity for both chloroquine sensitive (D6) and chloroquine resistant (W2) strains of *P. falciparum*. The –CN group appears to be important for antiplasmodial activity as the corresponding analogue of axisonitrile-3, axisothiocynate-3 (**1.27**), with an isocynate group in place of isonitrile exhibited much less activity against the *Plasmodium* parasites (Angerhofer and Pezzuto, 1992).

Polyketide metabolites containing six- or five-membered 1,2-dioxygenated rings have also been isolated from the Plakinidae sponge family. Two six-membered endoperoxide compounds, plakortin (**1.28**) and dihydroplakortin (**1.29**) from *Plakortis simplex* have demonstrated antiplasmodial effect on both chloroquine sensitive and chloroquine resistant *P. falciparum* (Fattorusso *et al.*, 2002). Although the modes of action of these compounds are unknown, it is possible that they share the same mechanism of action with artemisinin derivatives which also contain an endoperoxide moiety in their pharmacophore.

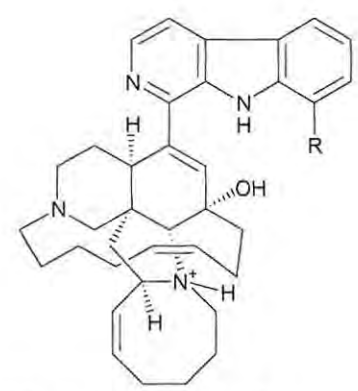

Manzamine A (**23**) R = H
(-)-8-hydroxymanzamine A (**24**) R = OH

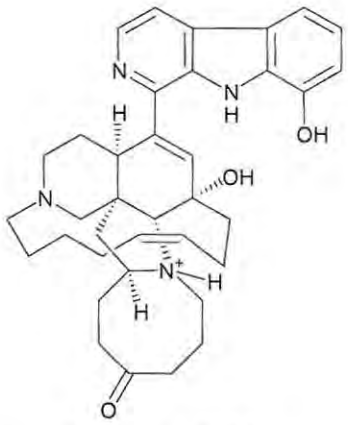

Manzamine F (**25**)

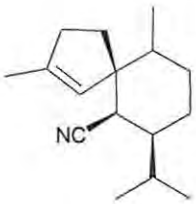

1.26

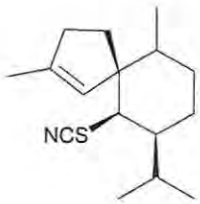

1.27

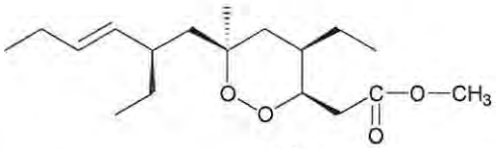

1.28

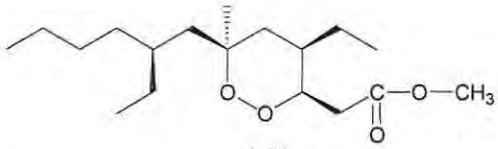

1.29

Figure 1.5 Some antimalarial compounds from marine sponges

1.6 Research objectives

The mortality, morbidy, economic cost and the problems associated with existing antimalarial chemotherapy have prompted this research project. This work aims at searching for antiplasmodial compounds for the production and development of more leads for antimalarial agents. An ideal antimalarial compound is expected to be efficacious, have low toxicity, be active against strains of *Plasmodium* that are resistant to existing chemotherapy, be suitable for use in children and pregnant women and most importantly be affordable. While in many cases all the desired properties might not be possible with one particular compound, a balance can be reached. Taking these into consideration and in order to improve the chances of discovering a suitable compound, this project will approach the development of such a compound by:

i. Screening marine algae extracts for antiplasmodial activity

ii. Isolating and characterizing active natural products

iii. Chemically modifying selected active natural products to improve on their activity.

References

Angerhofer, C. K. and Pezzuto, J. M. Antimalarial Activity of Sesquiterpenes from the Marine Sponge *Acanthella klethra*. *Journal of Natural Products* **1992**, 55 (12), 1787 – 1789.

Beers, M. H. and Berkow, R. (eds). Parasitic infections. *The Merck Manual of Diagnosis and therapy*, 17th edition, Merk Reseach Laboratories, New Jersey, **1999**, pp 1241-1242,

Butcher, G. A. Antimalarial Drugs and the Mosquito Transmission of *Plamodium*. *International Journal of Parasitology* **1997**, 27 (9), 975 – 987.

Fattorusso, E.; Parapini, S.; Campagnuolo, C.; Basilico, N.; Taglialatela-Scafati, O. and Taramelli, D. Activity against *Plasmodium falciparum* of Cycloperoxide Compounds Obtained from the Sponge *Plakortis simplex*. *Journal of Antimicrobial Chemotherapy* **2002**, 50, 883 – 888.

Fidock, D. A.; Rosenthal, P. J.; Croft, S. L.; Brun, R. and Nwaka, S. Antimalarial Drug Discovery: Efficacy Models for Compound Screening. *Nature Reviews Drug Discovery* **2004**, 3, 509 – 520.

Fox, D. T. and Poulter, C. D. Mechanistic Studies with 2-*C*-Methyl-D-Erythritol 4-Phosphate Synthase from *Escherichia coli*. *Biochemistry* **2005**, 44, 8360 – 8368.

Gardner, M. J.; Hall, N.; Fung, E.; White, O.; Berriman, M.; Hyman, R. W.; Carlton, J. M.; Pain, A.; Nelson, K. E.; Bowman, S.; Paulsen, I. T.; James, K.; Eisen, J. A.; Rutherford, K.; Salzberg, S. L.; Craig, A.; Kyes, S.; Chan, M-S.; Nene, V.; Shallom, S. J.; Suh, B.; Peterson, J.; Angiuoli, S.; Pertea, M.; Allen, J.; Selengut, J.; Haft, D.; Mather, M. W.; Vaidya, A. B.; Martin, D. M. A.; Fairlamb, A. H.; Fraunholz, M. J.; Roos, D. S.; Ralph, S. A.; McFadden, G. I.; Cummings, L. M.; Subramanian, G. M.; Mungall, C.; Venter, J. C.; Carucci, D. J.; Hoffman, S. L.; Newbold, C.; Davis, R. W.; Fraser, C. M. and Barrell, B. Genome Sequence of the Human Malaria Parasite *Plasmodium falciparum*. *Nature*, **2002**, 419, 498 – 511.

Gibbon, C. J (eds). Antiparasitic Products. *South Africa Medicines Formulary*, 6th Edition, Health and Medical Publishing group, South Africa, **2003,** pp 454-466,

Gomes, M. Economic and Demographic Research on Malaria: A review of the Evidence. *Society of Science and Medicine* **1993**, 37 (9), 1093 – 1108.

Guillemin, J. Malaria and Method. *Molecular interventions* **2001**, 1, 246 – 249.

Hay, S. I.; Guerra, C. A.; Tatem, A. J.; Noor, A. M. and Snow R. W. The global Distribution and Population at Risk of Malaria: Past, Present and Future. *The Lancet Infectious Disease* **2004**, 4, 327 – 336.

Haynes, R. K. and Krishna S. Artemisinins: Activities and Actions. *Microbes and infection* **2004**, 6, 1339 – 1346.

Higa, T.; Tanaka, J.; Ohtani, I. I.; Musman, M.; Roy, M. C. and Kuroda, I. Bioactive Compounds from Coral Reef Invertebrates. *Pure and Applied Chemistry*, **2001**, 73, 589 – 593.

Hudson, A.T. Atovaquone-A Novel Broad-Spectrum Anti-infective Drug. *Parasitology Today* **1993**, 9 (2), 66 – 68.

Jana, S. and Paliwal, J. Novel Molecular Targets for Antimalarial Chemotherapy. *International Journal of Antimicrobial Agents* **2007**, 30, 4 – 10.

Joy, D. A.; Feng, X.; Mu, J.; Furuya, T.; Chotivanich, K.; Krettli, A. U.; Ho, M.; Wang, A.; White, N. J.; Suh, E.; Beerli, P. and Su, X. Early Origin and Recent Expansion of *Plasmodium falciparum*. *Science* **2003**, 300, 318 – 321.

Katzung, B. G. Basic Principles of Antiparasitic Chemotherapy, *Basic & Clinical Pharmacology* **2004**., Antiprotozoal drugs, nineth edition (Katzung, B. G. ed.), pp 852 – 855, 864 – 875, The MvGraw-Hill Companies, Inc., Singapore.

Koppisch, A. T.; Fox, D. T.; Blagg, B. S. J. and Poulter, C.D. *E. coli* MEP Synthase: Steady-State Kinetic Analysis and Substrate Binding. *Biochemistry* **2002**, 41, 236 – 243.

Lell, B.; Ruangweerayut, R.; Wiesner, J.; Missinou, M.A.; Schindler, A.; Baranek, T.; Hintz, M.; Hutchinson, D.; Jomaa, H. and Kremsner, P. G. Fosmidomycin, a Novel Chemotherapeutic Agent for Malaria. *Antimicrobial Agents and Chemotherapy* **2003**, 47 (2), 735 – 738.

Lemke, T.L. Antiparasitic Agent, In: Williams, D. A.; Lemke, T. L. (eds.), *Foye's Principles of Medicinal Chemistry,* 5th edition, Lippincott Williams and Wilkins, Philadelphia, **2002**, pp 867 – 890.

Llanos-Cuentas, A.; Campos, P.; Clendenes, M.; Canfieled, C. J. and Hutchinson, D. B. A. Atovaquone and Proguanil Hydrochloride Compared with Chloroquine or Pyrimethamine/Sulphadoxine for Treatment of Acute *Plasmodium falciparum* Malaria in Peru. *The Brazilian Journal of Infectious Diseases* **2001**, 5 (2), 67 – 72.

Mayer, A. M. S. and Hamann, M. T. Marine pharmacology in 2001–2002: Marine compounds with anthelmintic, antibacterial, anticoagulant, antidiabetic,

antifungal, anti-inflammatory, antimalarial, antiplatelet, antiprotozoal, antituberculosis, and antiviral activities; affecting the cardiovascular, immune and nervous systems and other miscellaneous mechanisms of action. *Comparative Biochemistry and Physiology, Part C* **2005**, 140, 265 – 286.

McLeod, R.; Muench, S. P.; Rafferty, J. B.; Kyle, D. E.; Mui, E. J.; Kirisits, M. J.; Mack, D. G.; Roberts, C. W.; Samuel, B. U.; Lyons, R. E.; Dorris, M.; Milhous, W. K. and Rice, D. W. Triclosan inhibits the growth of Plasmodium falciparum and Toxoplasma gondii by inhibition of Apicomplexan Fab I. *International Journal of Parasitology* **2002**, 31, 109 – 113.

Meshnick, S. R. Cloroquine as intercalator: A Hypothesis Reviewed. *Parasitology Today* **1990**, 6 (3), 77 – 79.

Nzila, A. Inhibitors of *De Novo* Folate Enzymes in *Plasmodium falciparum*. *Drug Discovery Today* **2006**, 11 (19/20), 939 – 944.

O'Neill P. M.; Bray, P. G.; Hawley, S. R.; Ward, S. A. and Park B. K. 4-Aminoquinolines – Past, Present and Future: A Chemical Perspective. *Pharmacology and Therapeutics* **1998**, 77 (1), 29 – 58.

Ralph, S. A.; D'Ombrian, M. C. and McFadden, G. I. The Apicoplast as an Antimalarial Drug Target. *Drug Resistance Update* **2001**, 4, 145 – 151.

Ridley, R. G. Biomedicine: Enhanced: Planting the Seeds of New Antimalarial Drugs. *Science* **1999**, 285 (5433), 1502 – 1503.

Roberts, F.; Roberts, C. W.; Johnson, J. J.; Kyle, D. E.; Krell, T.; Coggins, J. R.; Coombs, G. H.; Milhous, W. K.; Tzipori, S.; Ferguson, D. J. P.; Chakrabarti, D. and McLeod, R. Evidence for the Shikimate Pathway in Apicomplexan Parasite. *Letters to Nature* **1998**, 393, 801 – 805.

Roos, D. S.; Crawford, M.J.; Donald, R. G. K.; Fraunholz, M.; Harb, O. S.; He, C. Y.; Kissinger, J. C.; Shaw, M. K. and Striepen, B. Mining the Plasmodium Genome Database to Define Organellar Function: What does the Apicoplast Do?. *Philosophical Transactions of the Royal Society B: Biological Sciences*, **2002**, 357 (1417), 35 – 46.

Schmidt, L. H. Relationships Between Chemical Structures of 8-Aminoquinolines and Their Capacity for Radical cure of Infections with *Plasmodium cynomolgi* in Rhesus Monkeys. *Antimicrobial Agent and Chemotherapy* **1983**, 24 (5), 615 – 652.

Sprenger, G. A.; Schörken, U.; Wiegert, T.; Grolle, S.; De Graaf, A. A.; Taylor, S. V.; Begley, T. P.; Bringer-Meyer, S. and Sahm, H. Identification of a Thiamine-dependent Synthase in *Escherichia coli*, Required for the Formation of the 1-Deoxy-D-xylulose -5-Phosphate precursor to Isoprenoids, Thiamin, and Pyridoxol. *Proceedings of National Academy of Sciences* **1997**, 94, 12857 – 12862.

Testa, C. A.; Lherbet, C.; Pojer, F.; Noel, J. P. and Poulter, C. D. Cloning and Expression of *IspDF* from *Mesorhizobium loti*. Characterization of Bifunctional Protein that Catalyzes Non-consecutive Steps in the Methylerythritol Phosphate Pathway. *Biochimica et Biophysica Acta* **2006**, 1764, 85 – 96.

Tonnesen, H.; Kristensen, S. and Nord, K. Photoreactivity of Selected Antimalarial Compounds in Solution and in the Solid State, *Drugs: Photochemistry and Photostability* **1998**. (Albini, A. and Fasani, E. ed.), pp 87 – 99, Royal Society of Chemistry, Great Britain.

Van Agtmael, M. A.; Eggelte, T. A. and Van Boxtel C. J. Artemisinin Drugs in the Treatment of Malaria: From Medicinal Herb to Registered Medication. *Trends in Pharmacological Sciences* **1999**, 20, 199 – 205.

Van Lieshout, M.; Kovats, R. S.; Livermore M. T. J. and Martens, P. Limate Change and Malaria: Analysis of the SRES Climate and Socio-economic Scenarios. *Global Environmental Chang,* **2004**, 14, 87 – 99.

Vennerstrom, J. L.; Nuzum, E. O.; Miller, R. E.; Dorn, A.; Gerena, L.; Dande, P. A.; Ellis, W. Y.; Rideley, R. G. and Milhous, W. K. 8-Aminoquinolines Active against Blood Stage *Plasmodium falciparum* In Vitro Inhibit Hematin Polymerization. *Antimicrobial Agents and Chemotherapy* **1999**, 43 (3), 598 – 602.

Warhust, D. C.; Steele, J. C. P.; Adagu, I. S.; Craig, J. C. and Cullander, C. Hydroxychloroquine is much less active than Chloroquine against Chloroquine-resistant *Plasmodium falciparum*, in agreement with its physicochemical properties. *Journal of Antimicrobial Chemotherapy* **2003**, 52, 188 – 193.

Watkins, E. R. and Meshnicks, S. R. Drugs for Malaria. *Seminars in Paediatric Infectious Diseases* **2000**, 11 (3), 202 – 212.

Wijayanti, M. A.; Sholikhah, E. N.; Tahir, I.; Hadanu, R.; Jumina, Supargiyono and Mustofa. Antiplasmodial Activity and Acute Toxicity of *N*-Alkyl and *N*-benzyl-1,10-Phenanthroline Derivatives in Mouse Malaria Model. *Journal of Health Sciences* **2006**, 52 (6), 794 – 799.

Wirth, D. F. Biological Revelations. *Nature* **2002**, 419, 495 – 496.

Chapter 2

In Vitro Screening of Crude Extracts from South African Marine Algae for Antiplasmodial Activity

2.1 Introduction

Natural product screening has been and still remains a major component of drug discovery. Many drugs are obtained from natural sources, for example quinine and artemisinin which are extracted from the bark of the *Cinchona* tree and *Artemisia annua*, respectively. While terrestrial plants have been extensively studied for their secondary metabolites, marine algae appear to be a relatively untapped potential source for biologically active compounds.

Drug discovery involves the identification of an active compound against a target which could either be an organism such as the *Plasmodium* parasite or specific enzymes and receptors. The identification of the compound is followed by full pharmacological and pharmacokinetics properties analysis after which the compound is then modified chemically to improve on its activity and clinical applications (Kumar and Clark, 2006).

This chapter deals with the *in vitro* screening of extracts from several South African marine algae against the chloroquine sensitive (CQS) D10 strain of *Plasmodium falciparum* in a search to discover antiplasmodial compounds or potential antimalarial lead compounds.

2.1.1 Preparation of natural product extracts for screening

There are different methods by which compounds can be extracted from their natural sources. The most commonly used methods include extraction of fresh (wet) or dried (air dried, oven dried or freeze dried) plant material prior to extraction with different solvents or solvent combinations. The concentration and bioactive nature of the secondary metabolites in the crude extract can be affected by the method of extraction

employed. The yield of the secondary metabolites can be affected by heat, light, drying procedure or the solvent of extraction (Cork and Krockenberger, 1991). It is therefore important to use the method that does not change the structure of the metabolites in the algae.

Various studies have been conducted to investigate and compare methods of extraction of natural products. An example is the investigation of different procedures of extraction of lipophilic extracts from the brown algae *Dictyota ciliolata* and *D. menstrualis* (Cronin *et al.*, 1995). It was shown that while freeze-drying of the marine algae before extraction is thought to avoid the loss and chemical conversion of sensitive compounds, it can lead to a decrease in the yield of unstable and volatile compounds. Extracting wet seaweed has the advantage of keeping the compounds unchanged provided the material had been stored correctly with the best result when the seaweed is extracted soon after collection (Cronin *et al.*, 1995).

The extraction solvent used should depend on the type of compounds to be extracted from the alga. To extract non-polar components for example, a non-polar solvent such as dichloromethane (CH_2Cl_2) would be appropriate and would be expected to yield a good result. It was however demonstrated for *D. ciliolata* and *D. menstrualis* that a 2:1 mixture of CH_2Cl_2-MeOH gave as good a yield or better yields than when extracted with CH_2Cl_2 alone (Cronin *et al.*, 1995). This principle is thought to be applicable to a wide variety of lipophilic compounds. The solvent mixture contains both a low-polarity (CH_2Cl_2) and a high-polarity (MeOH) component that allows it to penetrate cell membranes of the seaweed and extract compounds with different lipophilic properties (Cronin *et al.*, 1995). The extracts can then be screened in an appropriate assay for desired biological properties or they can be fractionated to isolate pure compounds.

2.1.2 Screening of extracts or compounds for antimalarial potential

Compounds are screened to identify potentially useful drugs. Preliminary screening of crude extracts saves time and resources required in modifying and purifying a compound which eventually might not produce the activity required.

Different screens have being used in the past for potential antimalarial determination and many are still been developed. Screening of extracts or compounds for antimalarial potential often involve the use of *Plasmodium* cultures. This is usually carried out on the erythrocytic asexual stage of the *Plasmodium* life cycle in a medium with low oxygen and high carbon dioxide level. The culture (*Plasmodium* in erythrocyte) is maintained in a stationary layer covered by a medium that flows slowly and continuously over the cells (Trager and Jensen, 1976). The medium usually consists of RPMI 1640 (Moore *et al.*, 1967)[1], Hepes (N-(2-hydroxyethyl)-piperazine-N-2-ethanesulphonic acid) buffer, hypoxanthine, $NaHCO_3$, gentamycin and human serum. It has been shown however that the human serum can be replaced with bovine serum supplemented with hypoxanthine, though parasite growth is still superior with the human serum (Divo and Jensen, 1982). The bovine serum has the advantage of been less expensive, easier to obtain and contain less inhibitory antibodies (Jensen *et al.*, 1982). A test compound or extract is introduced into the culture and the growth inhibition of the parasite is observed by any of the different methods discussed later.

Culturing of the parasite offers the potential to discover a variety of antimalarial compounds which toxicity and poor pharmacokinetic properties may prevent from been discovered if tested *in vivo*. Such compounds can be synthetically modified to improve on their antimalarial activity (Geary *et al.*, 1983) and reduce their cytotoxicity. The limitations of culturing include the fact that compounds that are effective in the culture might not be useful clinically due to toxicity. The method is also cumbersome, time consuming and costly and therefore may be unsuitable for large scale screening (Brobey *et al.*, 1996). The selectivity of the compounds is also not revealed in this kind of screening.

Other screening methods of antimalarial drugs usually involve specific targets within the *Plasmodium* parasite. Examples of these include the dihydrofolate reductase (DHFR) based screen which is used to discover antifolate compounds. Here the

[1] RPMI (Roswell Park Memorial Institute) 1640 is a basic cell medium developed by Moore *et al.* (1967) and can be used to culture different types of cell by supplementing it with vitamins, amino acids growth factors or serum.

extracts or compounds are tested on recombinant DHFR enzyme using a known antifolate such as pyrimethamine as the control drug (Brobey *et al.*, 1996).

A high through-put screen involving the inhibition of β-haemozoin has also been reported (Huy *et al.*, 2007) as a screen for antimalarial compounds. The malaria parasite is known to degrade haemoglobin to make use of the amino acids from the catabolic process for proliferation. Haem, toxic to both the host and *Plasmodium* cells, is also produced during this process but the parasite detoxifies it by crystallizing it to β-haemozoin. Inhibition of the formation of β-haemozoin is therefore fatal for the parasite. While a screen for compounds with properties to inhibit β-haemozoin formation is cheap and easy (Huy *et al.*, 2007), only quinoline-type compounds can be used as control. This means that to test on quinoline resistant strains there will be no control drug even though the best compound may or may not be active on the sensitive strain.

2.1.3 Assessment of *P. falciparum* growth in a screening application

The efficacy of compounds or extracts on the growth of *P. falciparum* can be assessed by different methods. This includes the use of hypoxanthine marker where hypoxanthine incorporation into the production of nucleic acids of the parasite is measured (Desjardins *et al.*, 1979). The hypoxanthine assessment method, although has the advantage of overcoming time-consuming and tedious visual counting of parasitaemia, has the limitation of being highly dependent on the stage of *P. falciparum* culture and thus may give inconsistent results (Geary *et al.*, 1983).

Another approach to assessing parasite growth is to determine the level of lactate dehydrogenase produced by the parasite. *Plasmodium* lactate dehydrogenase (pLDH) is essential for the production of energy for use by the parasite (Makler *et al.*, 1993). The enzyme catalyses the dehydrogenation of lactate to pyruvate, using NAD^+ as a cofactor (Xu *et al.*, 2007). Makler *et al.*, (1993) reported this assay to be comparable to measuring hypoxanthine uptake and microscopic Giemsa staining methods. It is a colourimetric assay that measures the enzymatic reduction of NAD^+ to NADH. It has the advantage of been less expensive than ^{3}H-hypoxanthine uptake method and in the absence of a spectrophotometer to follow the reduction by visual assessment. The

activity can also be measured using the colourimetric MTT (3-(4,5-dimethylthiazol-2-yl)-2,5-diphenyl tetrazolium bromide) assay where MTT (pale yellow) is reduced to formazan (dark blue) as is discussed later (Mosmann *et al.*, 1983).

Perhaps the most commonly used and the cheapest assessment method of determining parasite growth is the microscopic detection of the parasite in blood smear by staining the cells with Giemsa stain. This involves visual counting of the cells. It is however time consuming and subject to human error.

For the extraction and screening of the marine algae discussed in this chapter, the best methods with consideration given to the availability of resources were selected. This included wet extraction of the seaweed and screening the extracts against a culture of CQS *P. falciparum* D10 strain according to a modified Trager and Jensen methods (1976). Cytotoxicity assay of the extracts was also conducted to obtain information on the selectivity of the extracts for the *Plasmodium* parasite.

2.1.4 The 3-(4,5-dimethylthiazol-2-yl)-2,5-diphenyl tetrazolium bromide (MTT) assay for cytotoxicity

Various methods can be used in the determination or measurement of surviving or proliferating mammalian cells. Examples of these include counting cells with or without dye or measuring the incorporation of radioactive nucleotide or nucleotide precursors during cell proliferation. MTT is a salt that is used in a colourimetric assay to measure cell survival and activity. The pale yellow salt forms a dark blue Formazan product when incubated with live cells as a result of cleavage of the tetrazolium ring (Figure 2.1). The result can be analysed visually for quantitative analysis or by measuring the absorbance of the product with a suitable spectrophotometer. MTT is only cleared by metabolically active cells and as a result the assay only measures living cells and gives an indication of how active the cells are (Mosmann, 1983). The assay is efficient and can be used to process several extracts during a short period of time. This assay was employed for the cytotoxicity assay conducted on the marine algae extract discussed in this chapter.

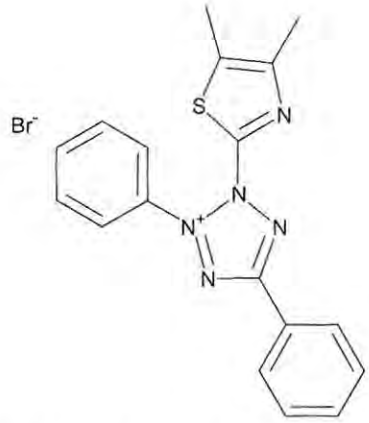

Figure 2.1 The structure of 3-(4,5-dimethylthiazol-2-yl)-2,5-diphenyl tetrazolium bromide (**2.1**)

2.1.5 Cytotoxicity Assay

Many compounds or extracts show biological activity in any given assay due to their general cytotoxicity property. A good antiplasmodial compound with potential antimalarial property would be expected to be selective for the *Plasmodium* parasite with minimum effect on the human cells. In order to make sure of the selectivity, cytotoxicity assays are carried out on potential extracts or compounds. Mammalian cells are used for cytotoxicity assays to be able to determine the toxicity of the extracts to human cells. Several mammalian cell lines are available for this assay. Examples of these include the KB cell lines which is derived from the epidermoid carcinoma of the mouth (DiRienzo *et al.*, 2002), Caco-2 cells, which are human colon carcinoma cell lines (Grasset *et al.*, 1985) and Chinese hamster ovarian (CHO) cell lines. Any extract that is toxic to these cell lines has the potential to exert *in vivo* toxicity in human cells. For the purpose of this study, the available cell line that was used for the cytotoxicity assay was the CHO cell line. The MTT assay (Mosmann, 1983) was used to measure the viability of the cells after incubation with the extracts.

2.1.6 Selectivity index

Antiplasmodial activity and cytotoxic activity of a compound or an extract are independently variable and can be related by the determination of the selectivity index of such a compound or extract. The degree of selectivity is represented as the ratio of

the cytotoxicity (e.g. CHO) IC_{50} value and *P. falciparum* IC_{50} value as shown in the following equation:

$$SI = \frac{\text{CHO } IC_{50} \text{ value}}{P.\ falciparum\ IC_{50} \text{ value}}$$

A SI value greater than 1 represents more selectivity for the parasite relative to the CHO, IC_{50} of 1 represents no selectivity and SI less than 1 means that the extract is more toxic to the mammalian cells than the parasite (Wu *et al.*, 2005). The SI therefore gives an indication of a promising antimalarial extract which may be worth pursuing.

2.1.7 Why marine algae?

Limited information is available in the literature on antiplasmodial and antimalarial compounds from marine algae. This could be due to

i. Lack of interest in the research involving isolation of compounds from marine algae and testing for antiplasmodial activity or that

ii. Marine algae rarely produce compounds with antiplasmodial property.

As a result this group of organisms are yet to be exhausted and promises to be a good source of biologically active compounds which this research project aimed to explore.

2.1.8 The Southern African marine environment

Over 12 000 species of marine plants and animals exist around the southern African coast. These species form almost 6% of the coastal marine species known throughout the world. About 31% of these species are endemic to the southern African region (Branch *et al.*, 2005). The rich and diverse fauna and flora of the southern African marine environment is partly due to the extreme contrast between the water masses on the east and west coasts. One of the most powerful currents in the world, the Agulhas current, sweeps warm water from subtropics down to east coast. Chilled or cold water is found along the west coast as a result of northward drifting cold water. Due to this difference in the waters, diverse organisms are found along the South African coast (Branch *et al.*, 2005).

2.1.9 South African marine algae

The South African coastline consists of diverse types of algae many of which are endemic to this part of the world (e.g. *Plocamium* species). The last decade has seen an increase in the research into the chemistry of the marine algae along South African coastline. Some of these include the isolation of plocoralides or halogenated monoterpenes from endemic *Plocamium corallorhiza* (Knott *et al.*, 2005).

The main objective of the research presented in this chapter was to extract compounds from South African marine algae (while still wet) and test these extracts for antiplasmodial activity against CQS *P. falciparum* using a modified Trager and Jensen (1976) method.

2.2 Results and Discussion

2.2.1 Collection and extraction of South African algae

Twenty-two wet algae (two green, three brown, and seventeen red, Table 2.1) were collected from different locations along South African coast (Kenton on Sea, Noordhoek and Kalk Bay). A standard protocol was employed for the extraction of the algae. This consisted of steeping the algae in MeOH for 1 hour at 4 °C[2] followed by extraction with CH_2Cl_2-MeOH (2:1) at 30 – 40 °C for 30 minutes. Although it was noted that the rate of extraction of compounds from the algae could have been enhanced by mechanically crushing them, it was not carried out on these algae as they were later heated to promote the process. The temperature was kept low to prevent degradation of compounds in the algae or reaction of reactive compounds with MeOH. The solvent combination was expected to allow for the extraction of both polar and non-polar constituents of the algae which might still be present even after the initial extraction with MeOH. Heating the algae with the solvent mixture improves the efficiency of the method in that the compounds are removed at a faster rate and thus the time required to exhaust the algae of their secondary metabolites is reduced. The heating temperature was low enough not to cause a significant degradation of the compounds, however sensitive compounds may be degraded. The pooled CH_2Cl_2-MeOH extracts were separated into organic and aqueous phase by addition of water in a separating funnel. The dried organic extracts were then further fractionated by solvent-solvent partitioning to give hexane (fr A), CH_2Cl_2 (fr B) and EtOAc (fr C) fractions. The aqueous phase of each alga was passed through a column containing HP-20 resin (except for *Plocamium cornutum* (KB06-3)). The HP-20 was sequentially washed with MeOH (fr D) and CH_2Cl_2 (fr E) for the polar components of the algae (Scheme 2.1). HP-20 resin is polyaromatic resin which binds to hydrophobic compounds (Joo *et al.*, 2001). It was used in this extraction in order to remove any polar or slightly polar compounds that might be present in the aqueous phase. The solvent-solvent partitioning of the extracts separate the components of the algae into categories of increasing polarity from non-polar (hexane) to polar (aqueous).

[2] Previous studies have shown that extraction with MeOH at room temperature leads to extensive degradation of certain metabolites (Knott, 2003).

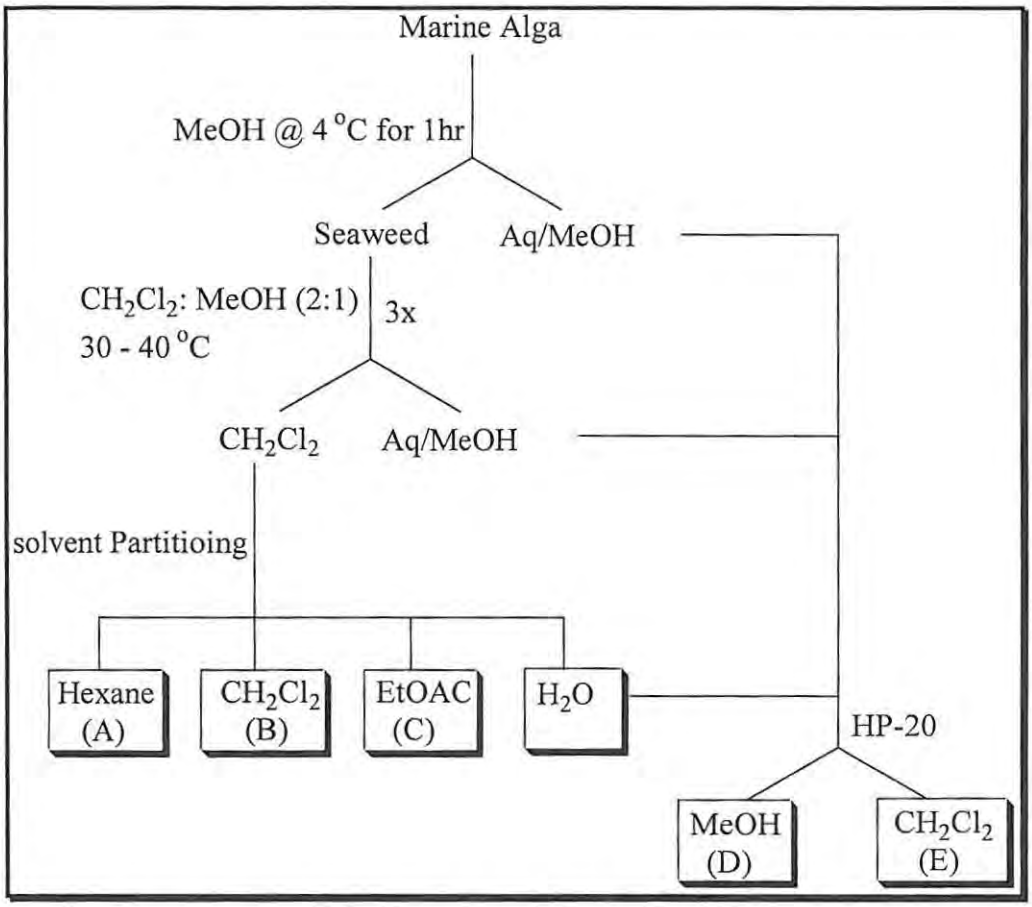

Scheme 2.1 General extraction scheme of the marine algae

Table 2.1 List of algae extracted and masses obtained

Collection code	Alga	Extracted weight (g)	Fr A (mg)	Fr B (mg)	Fr C (mg)	Fr D (mg)	Fr E (mg)
Green algae							
KOS06-13b	*Codium extricatum*	57.1	207.1	270.9	250.9	182.2	nd
KOS06-11	*Cladophora rugulosa*	21.0	197.9	236.6	54.1	76.5	nd
Brown algae							
KB06-5	*Bifurcaria brassicaeformis*	14.3	331.2	654.7	3.4	65.4	8.0
NDK06-5	*Sargassum heterophyllum*	52.6	2012.9	2031.9	108.2	891.5	87.4
KOS06-17	*Sargassum elegans*	15.1	405.4	234.0	717.8	35.9	nd
Red algae							
KB06-8	*Caulacanthus ustulatus*	26.5.	96	190.5	7.3	29.9	10.7
KB06-9	*Pterosiphonia cloiophylla*	8.8	95.4	324	36.4	237.8	33.9
KB06-04	*Grateloupia filicina*	16.9	244.4	169.5	5	312.1	24.7
NDK06-6	*Laurencia flexuosa*	33.3	306.5	554.4	17.7	38.5	18.0
NDK06-9b	*Trematocarpus flabellatus*	73.2	212.4	302.3	8.5	33.9	46.7
NDK06-10	*Gelidium capense*	55.3	320.5	530.0	34.6	110.5	26.0
NDK06-1b	*Plocamium corallorhiza*	33.8	800.4	749.3	39.2	55.7	21.8
NDK06-19	*Polysiphonia incompta*	28.9	128.6	345.1	41.5	371.8	27.5
KB06-3	*Plocamium cornutum*	26.0	784.0	706.0	135.0	nd	nd
KOS06-1	*Gracilaria aculeate*	21.6	356.4	346.8	64.8	1400.0	nd
KOS06-2	*Gelidium abbottiorum*	106.5	1000.0	250.0	50.0	300.0	nd
KOS06-3	*Gelidium pteridifolium*	26.0	394.6	147.6	73.0	385.0	nd
KOS06-23	*Amphiroa ephedraea*	101.3	301.7	223.7	55.4	169.1	nd
KOS06-20	*Spyridia cupressina*	9.0	50.3	28.8	15.5	nd	nd
KOS06-15	*Polysiphonia incompta*	35.1	151.3	407.5	144.9	61.1	nd
KOS06-6	*Laurencia flexuosa*	15.0	241.7	228.8	30.0	123.0	nd
KOS06-14b	*Plocamium corallorhiza*	33.6	1440	378	51	nd	nd

nd = not determined

2.2.2 Antiplasmodial activity of algal extracts

The crude partition extracts (A – E) were screened for antiplasmodial activity against the CQS *P. falciparum* D10 strain at the Division of Pharmacology at University of Cape Town.

A total of 82 extracts, selected on the basis that the mass of the crude extract obtained was mostly more than 30 mg, were tested for antiplasmodial activity against CQS *P. falciparum* D10 strain. The extracts were initially tested at 50, 25 and 12.5 μg/ml concentrations (Appendix 1, Table 2A1)). An extract was considered active if the percentage parasite survival at all three concentrations were less than 35%. This gave 18 active extracts (22%) with 11 different algae (50%) having at least one active extract (Table 2.1). This demonstrates that a large amount of the marine algae in the South African coast could be a potential source of antimalarial compounds or lead compounds. Because of the limited number of brown and green algae extracted it would be premature to speculate on which class of algae produce the most promising antiplasmodial compounds.

All 18 extracts were selected for a full dose response to determine their IC_{50}. The most active extracts were from *Sargassum heterophyllum*. The IC_{50} value of the hexane crude extract, for example, was determined from the plot of the percentage parasite survival against the logarithm of the concentrations of the extracts (Figure 2.2)

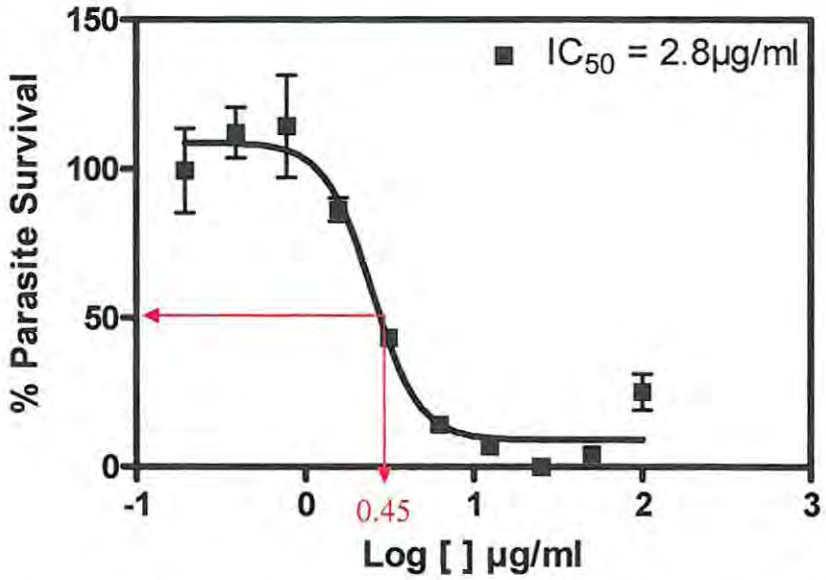

Figure 2.2 Non-linear curve of %parasite survival and log concentration of *S. heterophyllum* hexane extract

An IC_{50} value of 2.8 µg/ml was obtained at 50% parasite survival when *S. heterophyllum* hexane extract was tested.

Extracts with IC_{50} values less than 10 µg/ml were considered more promising than those with IC_{50} value greater than 10 µg/ml. Of the 18 extracts subjected to the full dose response, 15 were promising (Table 2.1). These 15 extracts were from 9 algae of which one is a brown and one is a green alga.

In order to determine whether the extracts contained compounds with selective antiplasmodial activity or whether their antiplasmodial activity was due to general toxicity, a cytotoxicity assay using CHO was conducted on each of the 15 extracts. The IC_{50} of the cytotoxicity assay was determined for all 15 extracts by conducting a full dose response (Table 2.2). The results indicated that four extracts contain compounds with selective antiplasmodial activity.

The selectivity of each of the 15 extracts for the parasite was calculated as a ratio of the CHO IC_{50} and D10 IC_{50}. All the extracts were more selective for the *Plasmodium* parasite than the mammalian cell (SI greater than 1). However, the most promising extracts were selected based on the criterion that the SI be greater than 10. A higher SI target may not be reasonable as the extracts were crude with different types of

compound, some of which may be cytotoxic and some parasite selective. The effect of a highly parasite specific compound may be masked by the presence of even more cytotoxic compound and setting a higher SI target may not allow for the discovery of such a parasite selective compound. A pure compound however would be required to have better selectivity for the parasite e.g. SI of 100 or more to be considered as a potential antimalarial compound. For this reason there were 4 most promising extracts with SI greater than 10 (Table 2.2). It was noted that none of the extracts was as potent as chloroquine on the *Plasmodium* parasite which is understandable as the strain of *Plasmodium* used was chloroquine sensitive. Isolated pure compounds from the active extracts might however be very potent.

Table 2.2 Antiplasmodial and cytotoxicity data of marine algal extracts of the most promising extracts

Algae code	Algae	% Parasite Survival			D10: IC50 (µg/ml)	CHO: IC_{50} (µg/ml)	SI
		50µg/ml	25µg/ml	12.5µg/ml			
KB 06-9-D	*Pterosiphonia cloiophylla*	3.6%	8.8%	19.3%	11.4	nd	nd
KB 06-9-E		4.1%	2.5%	5.7%	4.7	75.0	16
NDK 06-9b-B	*Trematocarpus flabellatus*	4.2%	17.6%	30.0%	7.8	45.9	5.9
NDK 06-5-B	*Sargassum heterophyllum*	3.9%	2.7%	5.6%	2.8	3.7	1.3
NDK 06-5-C		5.2%	8.9%	22.8%	5.9	12.3	2.1
NDK 06-5-E		6.1%	7.3%	10.2%	4.1	9.8	2.4
NDK 06-1b-A	*Plocamium corallorhiza*	2.2%	2.5%	15.2%	3.5	35.1	10
NDK 06-1b-B		8.2%	7.8%	21.0%	6.6	14.0	2.1
NDK 06-19-C	*Polysiphonia incompta*	5.8%	12.7%	8.7%	6.1	19.2	3.1
KB 06-3-A	*Plocamium cornutum*	0.0%	7.3%	12.3%	6.2	7.9	1.3
KB 06-3-B		0.0%	2.0%	18.5%	4.6	57.8	12.6
KOS 06-23-B	*Amphiroa ephedrea*	0.0%	3.7%	23.9%	8.3	>100	>12.1
KOS 06-13B-B	*Codium extricatum*	0.0%	0.0%	0.8%	5.9	32.1	5.4
KOS 06-13B-C		3.5%	7.5%	22.0%	8.2	59.3	7.2
KOS 06-11-A	*Cladophora rugulosa*	0.0%	0.8%	7.0%	11.4	nd	nd
KOS 06-20-C	*Spyridia cupressina*	3.7%	6.2%	16.8%	17.8	nd	nd
KOS 06-14b-A	*Plocamium corallorhiza*	20.4%	24.5%	28.2%	9.6	41.8	4.4
KOS 06-14b-B		11.1%	14.9%	32.8%	7.6	50.7	6.7
		% Parasite Survival for CQ					
		30ng/ml	**15ng/ml**	**7.5ng/ml**			
CQ (n=9)		22.8%	33.3%	61.8%	9.3 ng/ml (n=7)		
Emetine (n=5						0.07	

n = average number of data set, **Bold** = most promising extracts, KB = Kalk Bay, NDK = Noordhoek and KOS = Kenton-on-Sea, nd = not determined. Letters at the end of the algae code represent the fractions with antiplasmodial activity where A = hexane, B = CH_2Cl_2, C = EtOAc, D = MeOH and E = CH_2Cl_2 wash of the HP-20.

Often an organism produces secondary metabolites with different properties to protect itself and compete favourably with other organisms in the environment. A popular example of such metabolites is penicillin G an antibiotic produced by the fungus *Penicillium chrysogenum* (Madigan and Martinko, 2006). The possibility therefore arises that if enough marine algae are screened, possible antimalarial lead compound might be discovered.

In this study, four algae extracts were found to be most promising. The fact that they showed IC_{50} values less than 10 µg/ml was an indication of the possibility that pure compound(s) from each extract could be more potent than the crude. This kind of test could also reveal synergism in a case where more than one compound is isolated from the crude and each one is less potent than the crude extract by showing IC_{50} less than that of the original extract (Innocenti *et al.*, 2007).

The four most promising extracts were extracts from the red algae *P. corallorhiza, Pterosiphonia cloiophylla, Amphiroa ephedrea* and *P. cornutum* (Table 2.2). Due to time constraints, only the *Plocamium* species were further investigated (Chapter 4).With SI greater than 10, the extracts from the four algae were suspected to contain compounds which are selective for the *Plasmodium* parasite and thus present the possibility of discovering new antimalarial lead compounds. The result also shows that while both brown and green algae extracted were initially considered to be active towards the CQS *P. falciparum* D10 strain, the activity was due to the general cytotoxicity of the extract and not a specific activity towards the parasite.

Two *Plocamium* species, *P. cornutum and P. corallorhiza*, had extracts which were amongst the four most promising antiplasmodial extracts. This genus of algae is generally known to be rich in halogenated monoterpenes (Crews and Kho, 1974; Mynderse *et al.*, 1975; Mynderse and Faulkner, 1975). *P. cornutum* chemistry has yet to be studied and the result of this antiplasmodial screening therefore prompted the investigation into the chemical component of this alga that makes it active against this strain of *Plasmodium*. This is discussed in chapter four of this thesis.

P. corallorhiza has been extensively studied and its monterpenes have been shown to be active against oesophageal cancer cell lines (Knott *et al.*, 2005). Two *P. corallorhiza* collections had been made from different locations, Noordhoek and Kenton-on-Sea. While the sample collected from Noordhoek showed selectivity for the *Plasmodium* parasite, the sample from Kenton-on-Sea showed less selectivity (Table 2.2). This result suggested the presence of a compound in the Noordhoek sample that was absent in the sample collected from Kenton-on-sea or may be present at a higher quantity in the sample from Noordhoek. This observation was investigated and discussed in chapter four. This result also indicated that the location and the environment of the organisms play a role in the type and or amount of secondary metabolites produced.

The HP-20 CH_2Cl_2 extract (fr E) of *P. cloiophylla* showed promising antiplasmodial activity. However fractionation of this extract by column chromatography did not yield any compound. Literature search did not reveal any investigation into the chemistry of this alga and further investigation of the organism could be worthwhile.

Although the extracts from *S. heterophyllum* did not show selectivity for the *Plasmodium* parasite, its CH_2Cl_2 extract showed the best antiplasmodial activity of all the extracts tested (Table 2.2). The Sargassaceae family is known to produce plastoquinones and chromenols (Kusumi *et al.*, 1979, Segawa and Shirahama, 1987) to which cytotoxic activity has not been reported. This class of compounds has been investigated for anti-inflammatory and antioxidants properties with positive results (Pérez-Castorena *et al.*, 2002). It became a challenge to investigate the chemical components of this alga and test individual compounds for antiplasmodial activity as it is possible that the cytotoxic activity of the extracts is due to synergy between compounds of the extracts. This is discussed further in chapter three.

Analysis of the antiplasmodial and cytotoxcity screening results from the 18 promising extracts to the 4 most promising extracts showed a greater percentage of the active extracts to be from the non-polar partitions i.e. the hexane (fr A) and CH_2Cl_2 (fr B) extracts. Of the four most promising extracts, three were either from fr A or fr B. This include the CH_2Cl_2 extract of *P. cornutum*, the hexane extract of *P.*

corallorhiza and the CH_2Cl_2 extract of *A. ephedrea*, indicating that the active components of the algae are relatively non-polar.

2.3 Experimental

2.3.1 General experimental

All solvents used for extraction, solvent-solvent partitioning and HP-20 column chromatography were HPLC grade from BDH laboratory supplies. Diaion SUPELCO HP-20 was used for the partitioning of polar extracts from the marine alga.

2.3.2 Collection of marine algae

Marine algae were collected by hand along South African coastline and identified at the Department of Botany at University of Cape Town. They were collected specifically from Kenton-on-Sea, Noordhoek (Eastern Cape) and Kalk Bay (near Cape Town) in January 2006 except for as second *P. cornutum* collection which was collected from Noordhoek in September 2006. After collection the seaweeds were transported in cooler boxes to the laboratory where they were immediately frozen until extraction. The voucher specimens are kept in the freezer at the Division of Pharmaceutical Chemistry at Rhodes University, Grahamstown, South Africa.

2.3.3 Extraction of the Marine Algae

The general extraction of the algae involved submerging the seaweed in methanol (MeOH) at 4 °C for one hour. The MeOH-H_2O solution was decanted and extracted with CH_2Cl_2 to afford the CH_2Cl_2 extract (extract 1) and the aqueous MeOH-water extract (extract 2). The seaweed was re-submerged in a 2:1 solution of CH_2Cl_2-MeOH and heated at 30 – 40 °C for 30 minutes (3 times). The organic phase extract was combined with the CH_2Cl_2 extract from the MeOH-H_2O extraction(extract 1) and concentrated under reduced pressure. MeOH (50 ml) was added to the dried extract and it was extracted with hexane three times (fr A). The resulting aqueous phase was then extracted with CH_2Cl_2 (three times, fr B) with the addition of water to aid separation. MeOH was removed from the aqueous phase under pressure and the

resulting water extract was again extracted three times with EtOAc (fr C). The water phase was then combined with the MeOH-water extract from the cold extraction (fraction 2) and dried under reduced pressure. The resulting water extract was passed through a 50 g HP-20 column. The column was allowed to drain until it was dry and then sequentially washed with MeOH (fr D) and CH_2Cl_2 (fr E).

2.3.4 Sample Preparation for antiplasmodial assay[3]

Stock solutions of the extracts were prepared to 2 mg/ml in 10% methanol or dimethyl sulphoxide (DMSO). Chloroquine, the reference compound for the antiplasmodial activity was prepared to a 2 ng/ml stock solution. The reference compound for the cytotoxicity assay, Emetine, was also prepared to a 2 mg/ml stock solution. All the samples were stored at -20 °C until use at which point they were further diluted to the required concentrations.

2.3.5 Antiplasmodial Assay

Antiplasmodial assay was conducted by Prof. Peter J. Smith at the Division of Pharmacology, University of Cape Town.

All the samples were tested in duplicates against the D10 strain of chloroquine sensitive *P. falciparum*. The continuous *in vitro* culture of the asexual erythrocytic stage used in the experiment was maintained using a modified method of Trager and Jensen (1976). The result was quantitatively assessed to determine the *in vitro* antiplasmodial activity through the lactate dehydrogenase assay according to a modified method of Makler (1993).

The percentage parasite viability of the crude extracts was initially determined at 50, 25 and 12.5 μg/ml. The active extracts, selected on the bases that the percentage parasite viability at the concentrations tested did not exceed 35, were subjected to a full dose response test. Chloroquine used as the reference drug was tested at concentrations of 30, 15 and 7.5 ng/ml. The full dose response experiment of the test

[3] The experimental details were obtained from Professor Peter Smith, Division of Pharmacology, University of Cape Town.

samples was started at a concentration of 100 μg/ml and was serially diluted 2-folds to give 10 concentrations with a minimum of 0.195 μg/ml. Chloroquine was tested at a starting concentration of 100 ng/ml. The highest concentration of solvent used did not have any measurable effect on the parasites.

2.3.6 Cytotoxicity Assay

In this experiment, the samples were tested CHO cell line in triplicate using the 3-(4,5-dimethylthiazol-2-yl)-2,5-diphenyltetrazoliumbromide (MTT) assay. A full dose response was done on the selected extracts starting with a concentration of 100 μg/ml which was diluted serially 10-folds to give five concentrations with minimum of 0.01 μg/ml. Emetine starting concentration was also 100 μg/ml but diluted serially 10-fold to give six concentrations with the lowest being 0.001 μg/ml.

2.3.7 The MTT Assay

The MTT assay was carried out according to the modified method of Mosman (1983) and Rubinstein *et al.*, (1990). Chinese Hamster ovarian cells (1500) were seeded in cell-star 96 well plates and incubated for 24 hours. The extracts were added at varying concentrations described in section 2.3.4 in 0.2% final concentration of DMSO and incubated for 48 hours. MTT solution (10 μL) was then added to each well and incubated for another four hours. Solubilization solution (100 μL) was added to each well for further incubation overnight. The plates were read at 595 nm on an Anthos microplate reader 2001.

2.3.8 Data Analysis

The 50% inhibitory concentration (IC_{50}) values of the reference and test samples were obtained using a non-linear dose response curve fitting analysis by making use of Microsoft Excel GraphPad Prism v.40 software.

Supplementary information: Dose response curve of both the antiplasmodial and cytotoxicity assays are available on CD.

References

Branch, G. M.; Griffiths, C. L.; Branch, M. L. and Beckley, L. E. *Two oceans: A Guide to the Marine Life of Southern Africa* **2005**, Second edition, pp 1 – 2, David Philips Publishers, South Africa.

Brobey, R. K. B.; Sano, G.; Itoh, F.; Aso, K.; Kimura, M.; Mitamura, T. and Horii, T. Recombinant *Plasmodium falciparum* Dihydrofolate Reductase-based *In vitro* Screen for Antifolate Antimalarials. *Molecular and Biochemical Parasitology* **1996**, 81, 225 – 237.

Clarkson, C.; Maharaj, V. J.; Crouch, N. R.; Grace, O. M.; Pillay, P.; Matsabisa M. G.; Bhagwandin, N.; Smith, P. J. and Folb, P. I. *In vitro* Antiplasmodial Activity of Medicinal Plants Native to or Naturalised in South Africa. *Jouranal of Ethnopharmacology* **2004**, 92, 177-191.

Cork, S. J. and Krockenberger, A. K. Methods and Pitfalls of Extracting Condensed Tannis and Other Phenolics from Plant: Insights from Investigations on *Eucalyptus* Leaves. *Journal of Chemical Ecology* **1991**, 17(1), 123 – 134.

Crews, P., and Kho, E. Cartilagineal. An Unusual Monoterpene Aldehyde from Marine Alga. *Journal of Organic Chemistry* **1974**, 39, (22), 3304-3304.

Cronin, G.; Lindquist, N.; Hay, M. E. and Fenical, W. Effects of Storage and Extraction Procedures on Yields of Lipophilic Metabolites from the Brown Seaweeds *Dictyota ciliolata* and *D. menstrualis*. *Marine Ecology Progress Series* **1995**, 119, 265 – 273.

Desjardins, R. E.; Canfield, C. J.; Haynes, J. D. and Chulay, J. D. Quantitative Assessment of Antimalarial Activity *In vitro* by a Semiautomated Microdilution Technique. *Antimicrobial Agents and Chemotherapy* **1979**, 16 (6), 710 – 718.

DiRienzo, J. Kinetics of KB and HEp-2 Cell Responses to an Invasive, Cytolethal Distending Toxin-producing Strain of *Actinobacillus actinomycetemcomitans*, M. *Oral Microbiolgy and immunology* **2002**, 17 (4), 245 – 251.

Divo, A. A. and Jensen, J. B. Studies on Serum Requirements for the Cultivation of *Plasmodium falciparum*. 2. Medium Enrichment. *Bulletin of The World Health Organization* **1982**, 60 (4), 571 – 575.

Geary, T. G.; Divo, A. A. and Jensen, J. B. An *In vitro* Assay System for the Identification of Potential Antimalarial Drugs. *The Journal of Parasitology* **1983**, 69 (3), 577 – 583.

Grasset, E.; Bernaben, J. and Pinto, M. Epithelial properties of human colonic carcinoma cell line Caco-2: effect of secretagogue. *American Journal of Physiology* **1985**, 248, C410 – C418.

Huy, N. T.; Uyen, D. T.; Maeda, A.; Trang, D. T. X.; Oida, T.; Harada, S. and Kamei, K. Simple Colourimetric Inhibition Assay of Haem Crystallization for High-Throughput Screening of Antimalarial Compounds. *Agents and Chemotherapy* **2007**, 51 (1), 350 – 353.

Innocenti, G.; Vegeto, E.; Dall'Acqua, S.; Ciana, P.; Giorgetti, M.; Agradi, E.; sozzi, A.; Fico, G. and Tomè, F. *In vitro* Estrogenic Activity of *Achillea millefolium* L. *Phytomedicine* **2007**, 14, 147 – 152.

Jensen, J. B.; Boland, M. T. and Akood, M. Induction of Crisis Forms in Cultured *Plasmodium falciparum* with Human Immune Serum from Sudan. *Science* **1982**, 216, 1230 – 1233.

Joo, S-H.; Park, G-C.; Kim, K-T.; Paik, S. R.; Chang, C-S. Simple Methods for Alkaline Protease Purification from the Polychaeta, *Periserrula leucophryna*. *Process Biochemistry*, **2001**, 37, 299 – 303.

Knott, M. G. Masters thesis, **2003**, The Natural Product Chemistry of South African *Plocamium* Species.

Knott, M. G.; Mkwananzi, H.; Arendse, C. E.; Hendricks, D. T.; Bolton, J. J. and Beukes, D. R. Plocoralides A-C: Polyhalogenated Monoterpenes from the Marine Alga *Plocamium corallorhiza*. *Phytochemistry* **2005**, 66, 1108-1112.

Kumar, R. A. and Clark, D. S. High-throughput Screening of Biocatalytic Activity: Applications in Drug Discovery. *Current Opinion in Chemical Biology* **2006**, 10, 162 – 168.

Kusumi, T.; Shibata, Y.; Ishitsuka, M. and Kinoshita, T. Structures of New Plastoquinones from the Brown Alga *Sargassum serratifolium*. *Chemistry Letters* **1979**, 277 – 278.

Madigan, M. T. and Martinko, J. M. Microbial Growth Control, *Brock Biology of Microorganisms* **2006.** Eleventh edition, (Carlson, G. eds), pp 686, Pearson Prentice Hall, U.S.A.

Makler, M. T.; Ries, J. M.; Williams, J. A.; Bancroft, J. E.; Piper, R. C., Gibbins, B. L. and Hinrichs, D. J. Parasite lactate dehydrogenase as an assay for *Plasmodium falciparum* drug sensitivity. *The American Society of Tropical Medicine and Hygiene* **1993**, 48, 739 – 741.

Moore, G. E.; Gerner, R. E. and Franklin, H. A. Culture of Normal Human Leukocytes. *Journal of American Medical Association* **1967**, 199, 519 – 524.

Mosmann, T. Rapid colourimetric assay for cellular growth and survival: Application to proliferation and cytotoxicity assays. *Journal of Immunological Methods* **1983**, 65, 55 – 63.

Mynderse, J. S. and Faulkner, D. J. Polyhalogenated Monoterpenes from the Red Alga *Plocamium cartilagineum*. *Tetrahedron* **1975**, 31, 1963 – 1967.

Mynderse, J. S.; Faulkner, D. J.; Finer, J. and Clardy, J. (1R,2S,4S,5R)-1-bromo-trans-2-chlorovinyl-4-5-dichloro-1,5-dimethyl-cyclohexane, a New Monoterpene Skeletal type from the Red Alga, *Plocamium violaceum*. *Tetrahedron Letters* **1975**, 26, 2175 – 2178.

Pérez-Castorena, A. L.; Arciniegas, A.; Apan, M. T.; Villasenor, J. L. and De Vivar, A. R. Evaluation of the Anti-inflammatory and Antioxidant Activities of the Plastoquinone Derivatives Isolated from *Roldana barba-johannis*. *Planta Medica* **2002**, 68, 645 – 647.

Rubinstein, L. V.; Shoemaker, R. H.; Paull, K. D.; Simon, R. M.; Tosini, S.; Skehan, P.; Scudiero, D. A.; Monks, A. and Boyd, M. R. Comparison of *In Vitro* Anticancer-Drug-Screening Data Generated with a Tetrazolium Assay Against a Diverse Panel of Human Tumor Cell Lines. *Journal of the National Cancer Institute* **1990**, 82, 1113 – 8.

Segawa, M. and Shirahama H. New Plastoquinones from the Brown Alga *Sargassum sargamianum* var. *yezoense*. *Chemistry Letters* **1987**, 1365 – 1366.

Trager, W. and Jensen, J. B. Human malaria parasite in continuous culture. *Science* **1976**, 193 (4254), 673 – 675.

Wu, C-P.; van Schalkwyk, D. A.; Taylor, D.; Smith, P. J. and Chibale, K. Reversal of Chloroquine Resistance in *Plasmodium falciparum* by 9*H*-xanthene Derivatives. *International Journal of Antimicrobial Agents* **2005**, 26, 170 – 175.

Xu, X-L.; Yang, R-Y.; Yang, X-Q.; Chen, P-Q. and Zeng, Q-P. A Quantitative Assay of Recombinant Malarial Lactate Dehydrogenase as a Platform for Screening Inhibitors from Crude Herbal Extracts. *Chinese Journal of Biotechnology* **2007**, 23 (4), 593 – 597.

Chapter 3

Tetraprenyltoluquinols and Fucoxanthine from *Sargassum heterophyllum*

3.1 Introduction

Sargassum species belong to the division Phaeophyta (brown algae). The thallus of algae belonging to this division may also be yellow or yellowish green. The Sargassaceae family consists of many species some of which include *Sargassum heterophyllum*, *S. elegans*, and *S. longifolium* (Lubke, 1988). This family of algae is known to produce tetraprenyltoluquinols (e.g. sargaol (**3.1**), Numata *et al.*, 1992), chromenols (e.g. nahocol A (**3.2**), Tsuchiya *et al.*, 1998), polyhydroxyphenyl ethers (e.g. deshydroxytetrafuhalol-C- decaacetate (**3.3**), Glombitza and Keusgen, 1995) and the unusual arsenic containing compounds such as **3.4** (Edmonds, 2000) as secondary metabolites.

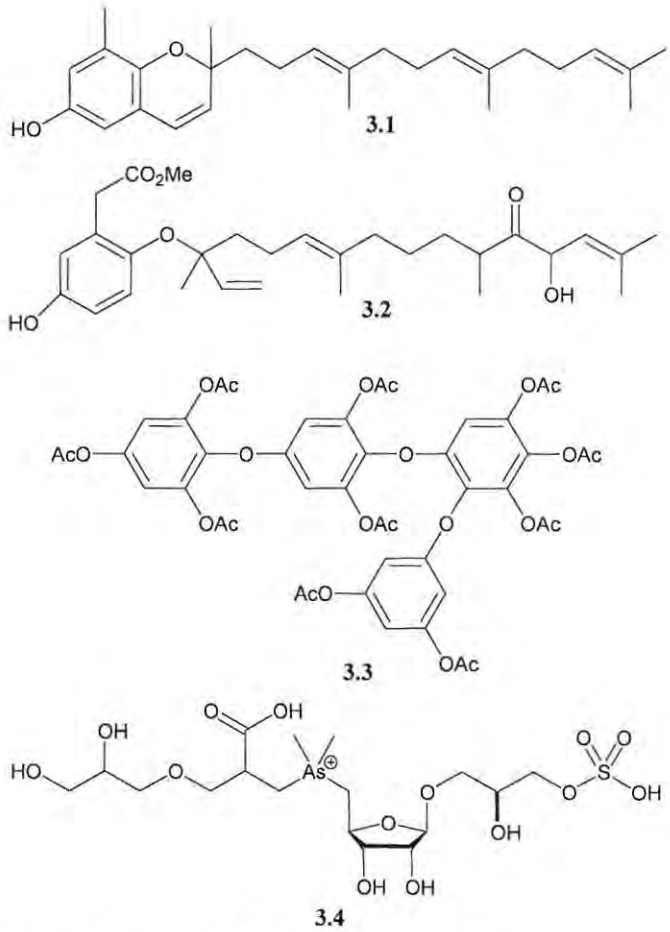

Figure 3.1 Selected compounds from *Sargassum* species

Sargassum heterophyllum is a South African endemic. It has a distinct holdfast with thickened stipe and flattened blades. The stipe of the bushy, yellow-brown thallus is triangular in shape with small air-bladders and two types of blades. The lower 'leaves' are oval with toothed margins while the small spear-shaped upper fronds have smooth margins (Lubke and Seagrief, 1998). *S. heterophyllum* thrives in high tide pools warmed by the sun (Branch *et al.*, 2005).

Figure 3.2 Photograph of *Sargassum heterophyllum*[4]

While the chemistry of several species of *Sargassum* around the world have been investigated very little research has been carried out on the chemical composition of *S. heterophyllum*. However, Mooney and Van Staden (1984a, 1984b, and 1987) have identified endogenous cytokinins and studied the lunar periodicity and the seasonal changes affecting these cytokinins in *S. heterophyllum*.

Organic extracts of *S. heterophyllum* (collection number NDK06-5) showed promising antiplasmodial activity (Chapter 2). The chemical components of these extracts were therefore investigated for potential antiplasmodial and antimalarial lead compounds.

[4] *S. heterophyllum* photograph was obtained form Dr. D. R. Beukes, Division of Pharmaceutical Chemistry, Rhodes University.

3.2 Results and Discussion

3.2.1 Extraction and isolation of metabolites from *S. heterophyllum*

S. heterophyllum (NDK06-5) was collected by hand from Noordhoek in January 2006. The antiplasmodial crude extracts (NDK06-5A – E) were fractionated by silica gel column chromatography using a hexane-EtOAc solvent gradient. This gave rise to fractions (A1-9, B1-9, C1-6, D1-5, E1-6) which were further purified by semi-preparative HPLC (hexane-EtOAc) to afford compounds **3.5** – **3.8** (Scheme 3.1).

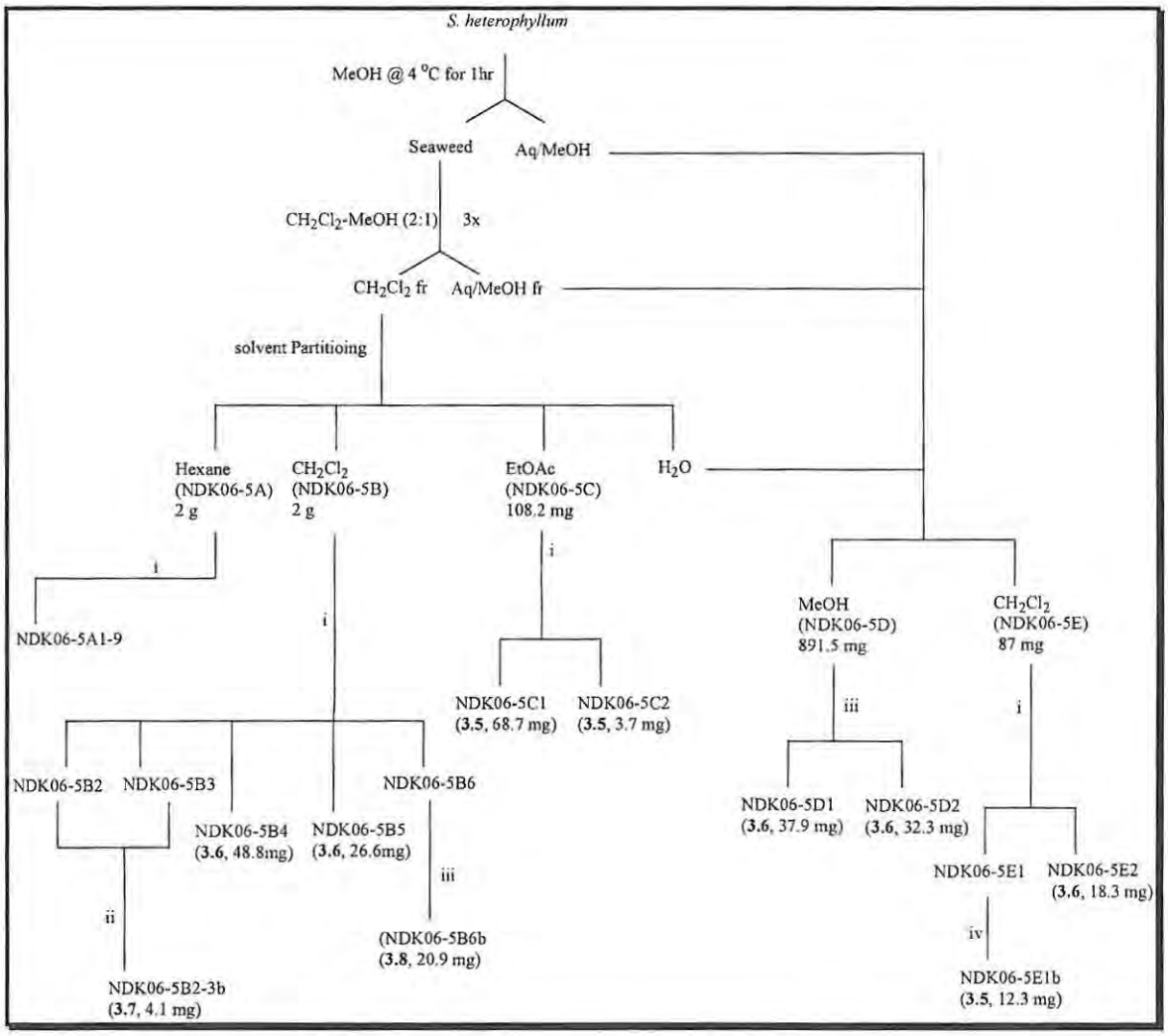

Scheme 3.1 Isolation scheme of *S. heterophyllum* showing only the fractions leading to the isolated compounds i) column chromatography, solvent gradient, Hexane-EtOAC; ii) Normal phase HPLC, hexane-EtOAc (90:10); iii) Normal phase HPLC, hexane-EtOAc (50:50); iv) Reverse phase HPLC, MeOH (100%)

3.2.2 Structure elucidation of NDK06-5C1[5] (3.5)

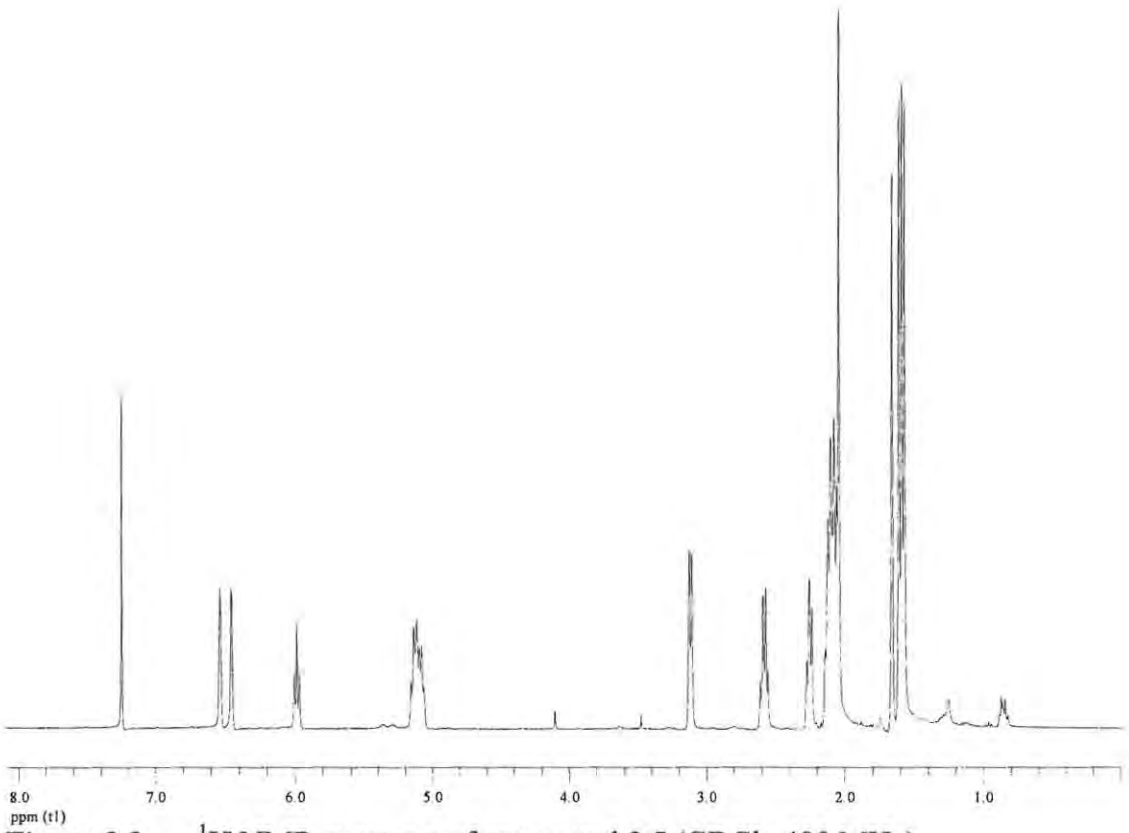

Figure 3.3 ^{1}H NMR spectrum of compound **3.5** ($CDCl_3$, 400 MHz)

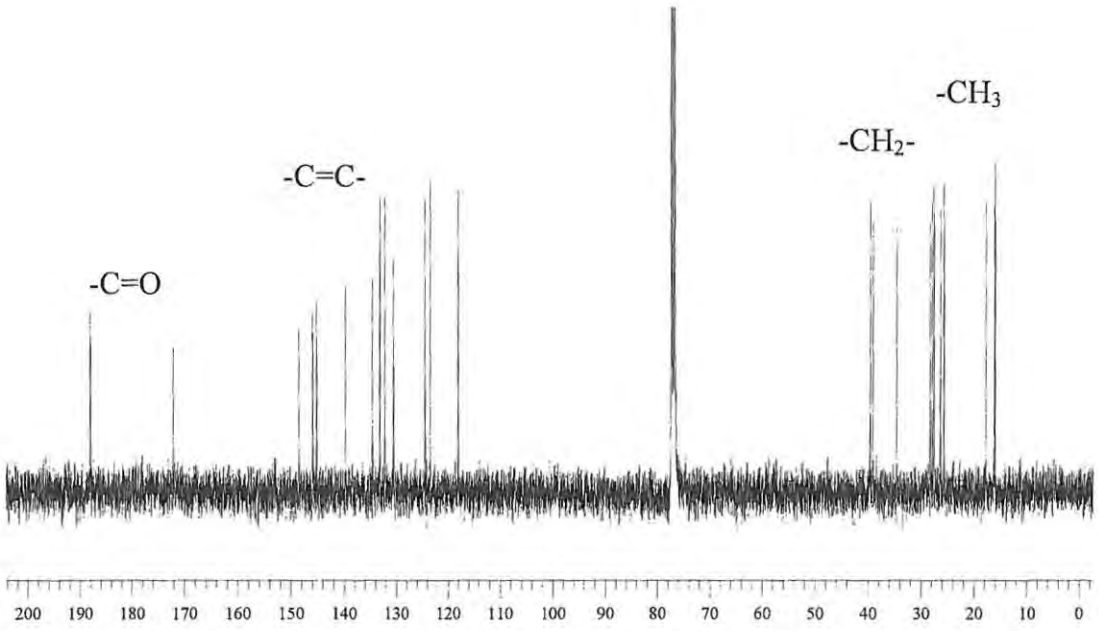

Figure 3.4 ^{13}C NMR spectrum of compound **3.5** ($CDCl_3$, 100 MHz)

[5] NDK06-5C1 = NDK06-5C2 = NDK06-5E1b

The ^{1}H NMR spectrum of compound **3.5** (Figure 3.3) showed signals at δ 5.10, 6.46 and 6.56, indicating the presence of aromatic and or olefinic protons. A total of 27 carbons were observed in the ^{13}C NMR spectrum of compound **3.5**. This, in combination with the DEPT-135 NMR spectrum allowed these to be assigned as five methyl, seven methylene, 12 olefinic and three carbonyl resonances. The two carbon chemical shifts at δ 187.9 and 188.0 indicated the presence of a benzoquinone ring in the structure of the compound while a third carbonyl carbon was observed at δ 172.2 and is indicative of a carboxylic acid group (Figure 3.4, Table 3.1).

The structure and substitution pattern of the substituted benzoquinone ring was deduced by the observation of HMBC correlations between the methyl signal at δ_H 2.05 (H_3-7) to carbons at δ_C 188.0 (C-1), 145.2 (C-2) and 132.2 (C-3) and the methylene at δ_H 3.12 (H-1') to carbons at δ_C 188.0 (C-1), 148.5 (C-6), 132.2 (C-5), 118.0 (C-2'), 139.8 (C-3'). The position of the carboxylic acid group on the diterpene moiety was established from the observation of HMBC correlations between δ_H 1.61 (H_3-20') and δ_C 118.0 (C-2'), 139.8 (C-3') and 39.6 (C-4'), between δ_H 1.59 (H_3-19') and δ 124.5 (C-6'), 134.6 (C-7') and 39.1 (C-8') and between δ5.99 (H-10') and 27.6 (C-9'), 172.2 (C-18') and 34.6 (C-12').

All spectroscopic data for compound **3.5** were in agreement with literature data reported for sargaquinoic acid (Seo *et al.*, 2004). This compound was first isolated from *S. serratifolium* (Kusumi *et al.*, 1979) and subsequently from *S. sagamianum* var *yezoense* (Segawa and Shirahama, 1987). Sargaquinoic acid (**3.5**) has also been isolated from medicinal plants such as *Roldana barba-johannis* (Pérez-Castorena *et al.*, 2002) and the fruits of *Iryanthera juruensis* (Silva *et al.*, 2001).

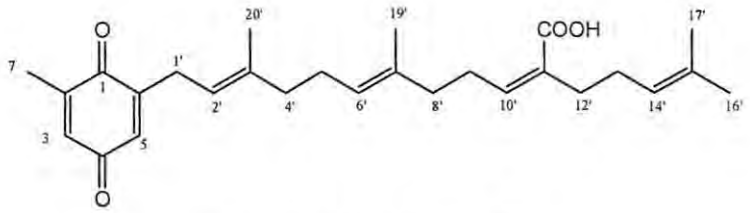

Sargaquinoic acid (**3.5**)

Table 3.1 Comparison of observed and literature ^{1}H (400 MHz) and ^{13}C (100 MHz) NMR and 2D NMR (^{1}H COSY and HMBC) spectroscopic data for compound **3.5**

	Observed			Literature[6]		Observed	
Carbon no.	δ_C	δ_C mult	δ_H, mult, J_{Hz}	δ_C	δ_H, mult, J_{Hz}	COSY	HMBC
1	188.0	C		187.9			
2	145.2	C		145.8			
3	132.2	CH	6.56, quin, 1.5	133.0	6.53, quin, 1.4		C-4
4	187.9	C		187.8			
5	132.2	CH	6.46, m	132.1	6.45, m		C-1
6	148.5	C		148.4			
7	16.0	CH_3	2.05, d, 1.5	16.0	2.05, d, 1.4		
1'	28.2	CH_2	3.12, d, 7.1	27.6	3.12, d, 7.2	H-2'	C-2', C-3', C-6, C-5, C-1
2'	118.0	CH	5.10, m,	117.9	5.13, t, 7.4	H-1'	
3'	139.8	C		139.7			
4'	39.6	CH_2	2.08, m	39.6	2.08, m		C-5', C-20'
5'	26.3	CH_2	2.08, m	26.4	2.09, m	H-6'	
6'	124.5	CH	5.10, m	124.4	5.11, m	H-5'	
7'	134.6	C		134.5			
8'	39.1	CH_2	2.09,m	39.1	2.09, m	H-9'	C-9', C-19'
9'	27.6	CH_2	2.58, q, 7.4	28.3	2.59, q, 7.2	H-8', H-10'	C-7', C-8', C-10', C-11'
10'	145.9	CH	5.99, t, 7.3	145.3	5.99, t, 7.2	H-9'	C-8', C-12', C-18'
11'	130.5	C		130.5			
12'	34.6	CH_2	2.25, t, 7.2	34.6	2.26, t, 7.2	H-13'	C-10', C-11', C-13', C-14', C-18'
13'	27.9	CH_2	2.15, m	27.9	2.12, m	H-12'	C-12'
14'	123.5	CH	5.10, m	123.4	5.07, m		
15'	133.1	C		132.1			
16'	25.7	CH_3	1.66, s	25.7	1.64, s		C-14', C-17'
17'	17.7	CH_3	1.57, s	16.2	1.58, s		C-14'
18'	172.2	C		172.7			
19'	16.0	CH_3	1.59, s	16.1	1.60, s		C-6'
20'	16.1	CH_3	1.61, s	16.2	1.62, s		C-2', C-3'

[6] (Seo *et al.*, 2004)

3.2.3 Structure elucidation of NDK06-5B3[7] (3.6)

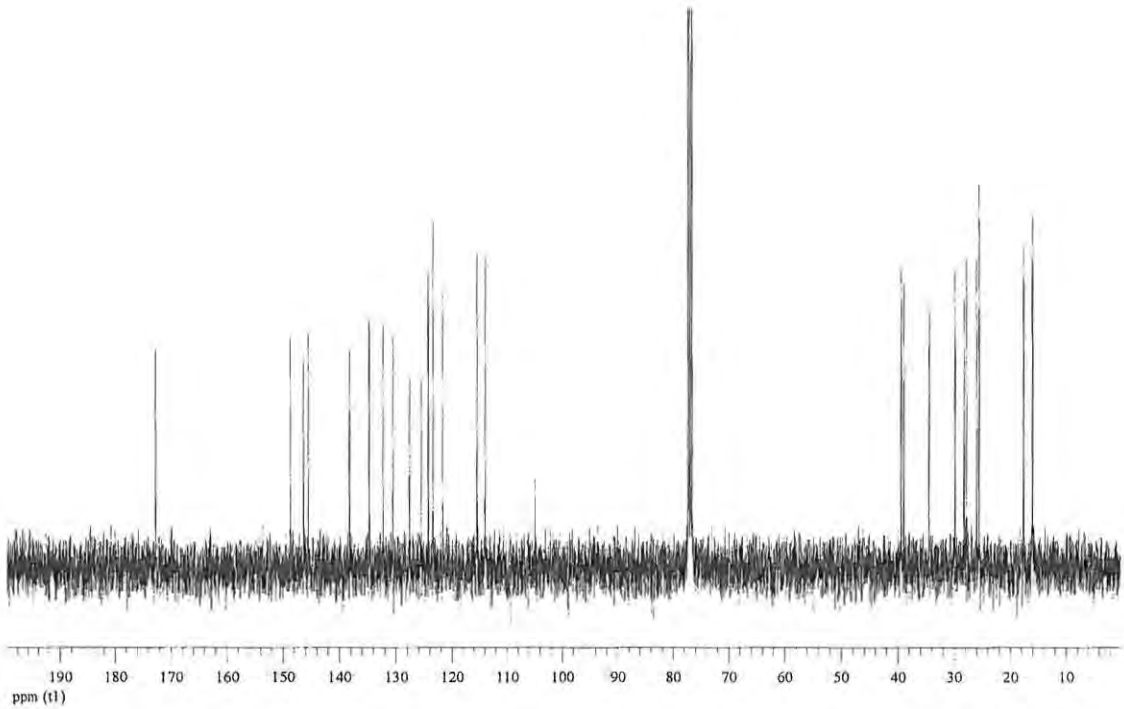

Figure 3.5 ^{13}C NMR spectrum of compound **3.6** ($CDCl_3$, 400 MHz)

The ^{1}H and ^{13}C (Figure 3.5) NMR spectra of compound **3.6** were similar to those of compound **3.5**. The noticeable difference was the absence of the two carbonyl resonances on the benzoquinone ring of sargaquinoic acid (**3.5**) which were replaced with two phenolic carbons (δ 146.4 and 148.7) in compound **3.6**. Thus the compound was considered to be the hydroquinone derivative of compound **3.5**. Analysis of the 1D (^{1}H and ^{13}C) and 2D (HSQC and HMBC) (Table 3.2) NMR data of compound **3.6** and comparison with literature chemical shifts (Seo *et al.*, 2004) suggested the compound to be sargahydroquinoic acid.

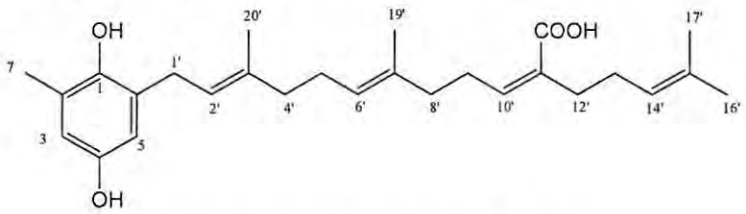

Sargahydroquinoic acid (**3.6**)

[7] NDK06-5B3 = NDK06-5B4 = NDK06-5D1 = NDK06-5E2

Sargahydroquinoic acid (**3.6**) was first isolated from the brown alga *S. sagamianum* var. *yezoense* (Segawa and Shirahama, 1987).

Table 3.2 Comparison of observed and literature ^{1}H (400 MHz) and ^{13}C (100 MHz) NMR and 2D NMR (^{1}H COSY and HMBC) spectroscopic data for compound **3.6**

Observed				Literature[8]		Observed	
Carbon no.	δ_C	δ_C mult	δ_H, mult, J_{Hz}	δ_C	δ_H, mult, J_{Hz}	COSY	HMBC
1	146.4	C		146.2			
2	125.5	C		125.4			
3	115.4	CH	6.49, br s	115.4	6.47, br s		C-4, C-7
4	148.7	C		148.6			
5	114.0	CH	6.47, br s	113.9	6.45, br s		C-6, C-3, C-1
6	127.6	C		127.5			
7	16.0	CH_3	2.17, s	16.2	2.17, s		C-3, C-2, C-1
1'	29.9	CH_2	3.27, d, 7.0	30.0	3.27, d, 7.2	H-2'	C-2', C-3', C-6, C-5, C-1
2'	121.7	CH	5.26, t, 6.9	121.7	5.25, t, 7.2	H-1'	C-1', C-4', C-20
3'	138.2	C		138.0			
4'	39.5	CH_2	2.07, m	39.5	2.08, m	H-5'	C-2', C-3', C-5', C-6', C-20
5'	26.1	CH_2	2.11, m	26.1	2.12, m	H-4', H-6'	C-4', C-6'
6'	124.3	CH	5.09, m	124.2	5.13, t, 6.9	H-5'	C-5', C-8', C-19'
7'	134.7	C		134.6			
8'	39.0	CH_2	2.07, m	39.1	2.08, m	H-9'	C-7', C-9', C-10', C-19'
9'	28.3	CH_2	2.58, q, 7.4	28.4	2.57, dt, 7.0, 7.0	H-8', H-10'	C-7', C-8', C-10', C-11'
10'	145.5	CH	5.99, t, 7.2	145.3	5.97, t, 7.2	H-9'	C-8', C-12', C-18'
11'	130.5	C		130.5			
12'	34.5	CH_2	2.25, t, 7.4	34.6	2.25, t, 7.7	H-13'	C-10', C-11', C-13', C-14', C-18'
13'	27.9	CH_2	2.11, m	27.9	2.12, m	H-12', H-14'	C-12', C-15'
14'	123.4	CH	5.09, m	123.4	5.07, t, 6.9	H-13'	C-13', C-16'
15'	132.3	C		132.1			
16'	25.6	CH_3	1.67, s	25.7	1.67, s		C-14', C-15', C-17
17'	17.7	CH_3	1.58, s	17.8	1.58, s		C-16'
18'	172.7	C		172.5			
19'	16.1	CH_3	1.59, s	16.1	1.59, s		C-6', C-7', C-8'
20'	16.1	CH_3	1.74, s	16.2	1.74, s		C-2', C-3', C-4'

Studies have shown that the exposure of sargahydroquinoic acid (**3.6**) to air could lead to the formation of sargaquinoic acid (**3.5**) due to oxidation (Segawa and Shirahama, 1987). However the studies on this compound were conducted over several months during which the structure of sargahydroquinoic acid (**3.6**) remained intact. This was monitored by repeated ^{1}H NMR experiment over the period. The fact that sargahydroquinoic acid (**3.6**) was not oxidized was presumed to be as a result of its

[8] Seo *et al.*, 2004

storage in hexane at low temperature (less than 4 °C). This was however not investigated further due to time constraint.

3.2.4 Structure elucidation of NDK06-5B2-3b (3.7)

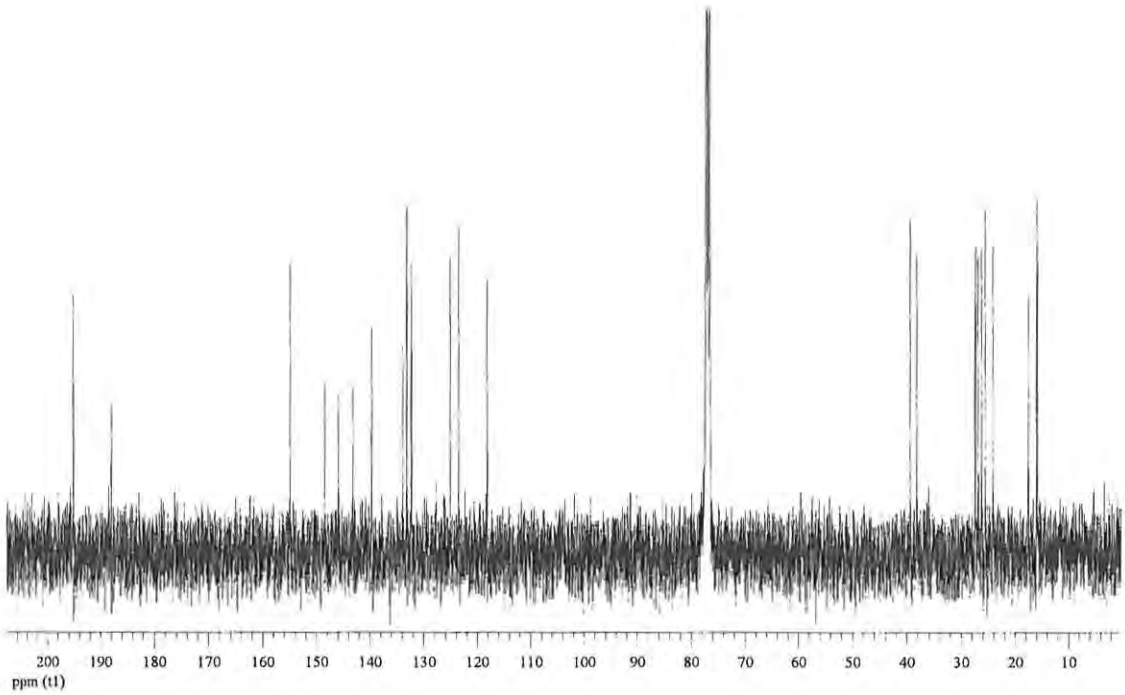

Figure 3.6 ^{13}C NMR spectrum ($CDCl_3$, 400 MHz) of compound **3.7**

The ^{1}H and ^{13}C (Figure 3.6) NMR spectra of compound **3.7** were similar to those of compound **3.5** except for the disappearance of the carbonyl signal at δ 172.2 in the ^{13}C NMR spectrum and the appearance of a new signal at δ 195.1. This, together with a proton signal at δ 9.33, was indicative of an aldehyde functionality in the compound. Although the ^{1}H NMR data for this compound was identical to those reported for sargaquinal (Kusmumi *et al.*, 1979) no additional spectroscopic information was available from the literature. This study therefore presents the first complete NMR data for compound **3.7**.

The 2'*E*,6'*E*-10'*E* geometry of **3.7** is proposed to be the same as that of sargaquinal (**3.7**) from a comparison of ^{1}H NMR data of the two compounds. Kusumi *et al.* (1979) synthesized 2'*E*,6'*E*,'10*Z*- sargaquinal (**3.7**) from sargaquinoic acid (**3.5**) and showed that H-18' (CHO) and H_2-9'resonate at δ 10.06 and 2.65, respectively as opposed to δ9.33 and 2.44 respectively in 2'*E*,6'*E*,10'*E*-sargaquinal (**3.7**).

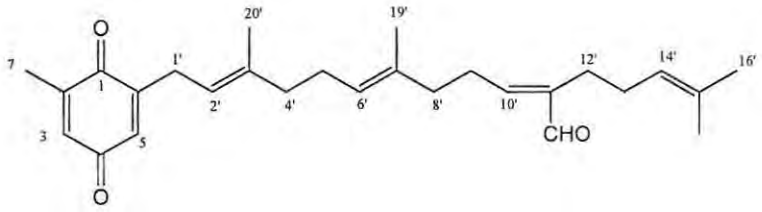

Sargaquinal (**3.7**)

Table 3.3 ^{1}H NMR (400 MHz) and ^{13}C NMR (100 MHz) **3.7** in $CDCl_3$

Carbon no.	δ_C	δ_C mult	δ_H, mult, J_{Hz}	COSY	HMBC
1	188.0	C			
2	146.0	C			
3	132.3	CH	6.54, br s		
4	187.9	C			
5	132.3	CH	6.43, m		
6	148.4	C			
7	16.0	CH_3	2.05, m		C-2, C-1
1'	27.5	CH_2	3.12, d, 7.1	H-2'	C-2', C-3', C-6, C-5, C-1
2'	118.2	CH	5.14, m	H-1'	
3'	139 .7	C			
4'	39.5	CH_2	2.08, m	H-5'	C-3', C-5', C-20'
5'	26.4	CH_2	2.09, m	H-4', H-6'	C-3'
6'	125.1	CH	5.11, m	H-5'	
7'	133.9	C			
8'	38.3	CH_2	2.14, m	H-9'	C-6', C-7'
9'	27.0	CH_2	2.44, q, 7.45	H-8', H-10'	C-8', C-11'
10'	154.9	CH	6.41, m	H-9'	C-12', C-18'
11'	143.2	C			
12'	27.5	CH_2	2.25, t, 7.62	H-13'	C-9', C-11'
13'	25.7	CH_2	2.14, m	H-14'	C-12'
14'	123.6	CH	5.14, m	H-13'	C-12'
15'	133.2	C			
16'	24.3	CH_3	1.66, s		C-14', C-15', C-17'
17'	17.7	CH_3	1.56, br s		C-13, C14, C15
18'	195.1	CH	9.33, s		C-11'
19'	16.0	CH_3	1.63, s		C-6', C-7',
20'	16.1	CH_3	1.62, s		C-2', C-3', C-4'

Compounds **3.5**, **3.6** and **3.7** are thus analogues of each other with compound **3.7** and **3.6** being the aldehyde and the hydroquinone analogues of compound **3.5** respectively (Table 3.4).

Table 3.4 Comparison of ^{1}H and ^{13}C NMR data of compounds **3.1**, **3.2** and **3.5**

	Compound 3.5		**Compound 3.6**		**Compound 3.7**	
Carbon no.	**δ_C**	**δ_H, mult, J_{Hz}**	**δ_C**	**δ_H, mult, J_{Hz}**	**δ_C**	**δ_H, mult, J_{Hz}**
1	28.2	3.12, d, 7.1	29.9	3.27, d, 7.0	27.5	3.12, d, 7.1
2	118.0	5.10, m,	121.7	5.26, t, 6.9	118.2	5.14, m
3	139.8		138.2		139 .7	
4	39.6	2.08, m	39.5	2.07, m	39.5	2.08, m
5	26.3	2.08, m	26.1	2.11, m	26.4	2.09, m
6	124.5	5.10, m	124.3	5.09, m	125.1	5.11, m
7	134.6		134.7		133.9	
8	39.1	2.09,m	39.0	2.07, m	38.3	2.14, m
9	27.6	2.58, q, 7.4	28.3	2.58, q, 7.4	27.0	2.44, q, 7.45
10	145.9	5.99, t, 7.3	145.5	5.99, t, 7.2	154.9	6.41, m
11	130.5		130.5		143.2	
12	34.6	2.25, t, 7.2	34.5	2.25, t, 7.4	27.5	2.25, t, 7.62
13	27.9	2.15, m	27.9	2.11, m	25.7	2.14, m
14	123.5	5.10, m	123.4	5.09, m	123.6	5.14, m
15	133.1		132.3		133.2	
16	25.7	1.66, s	25.6	1.67, s	24.3	1.66, s
17	16.1	1.61, s	16.1	1.74, s	16.1	1.62, s
18	16.0	1.59, s	16.1	1.59, s	16.0	1.63, s
19	172.2		172.7		195.1	9.33, s
20	17.7	1.57, s	17.7	1.58, s	17.7	1.56, br s
21	16.0	2.05, d, 1.5	16.0	2.17, s	16.0	2.05, m
1'	148.5		127.6		148.4	
2'	132.2	6.46, m	114.0	6.47, br s	132.3	6.43, m
3'	187.9		148.7		187.9	
4'	132.2	6.56, quin, 1.5	115.4	6.49, br s	132.3	6.54, br s
5'	145.2		125.5		146.0	
6'	188.0		146.4		188.0	

3.2.5 Structure elucidation of compound NDK06-5B5b (3.8)

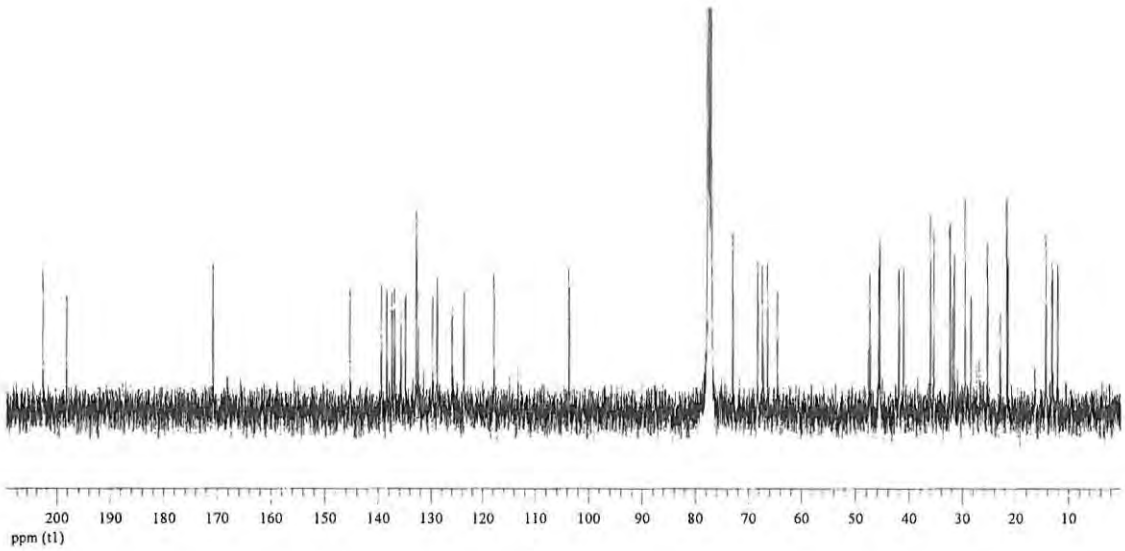

Figure 3.7 ^{13}C NMR spectrum of compound **3.8** ($CDCl_3$, 400 MHz)

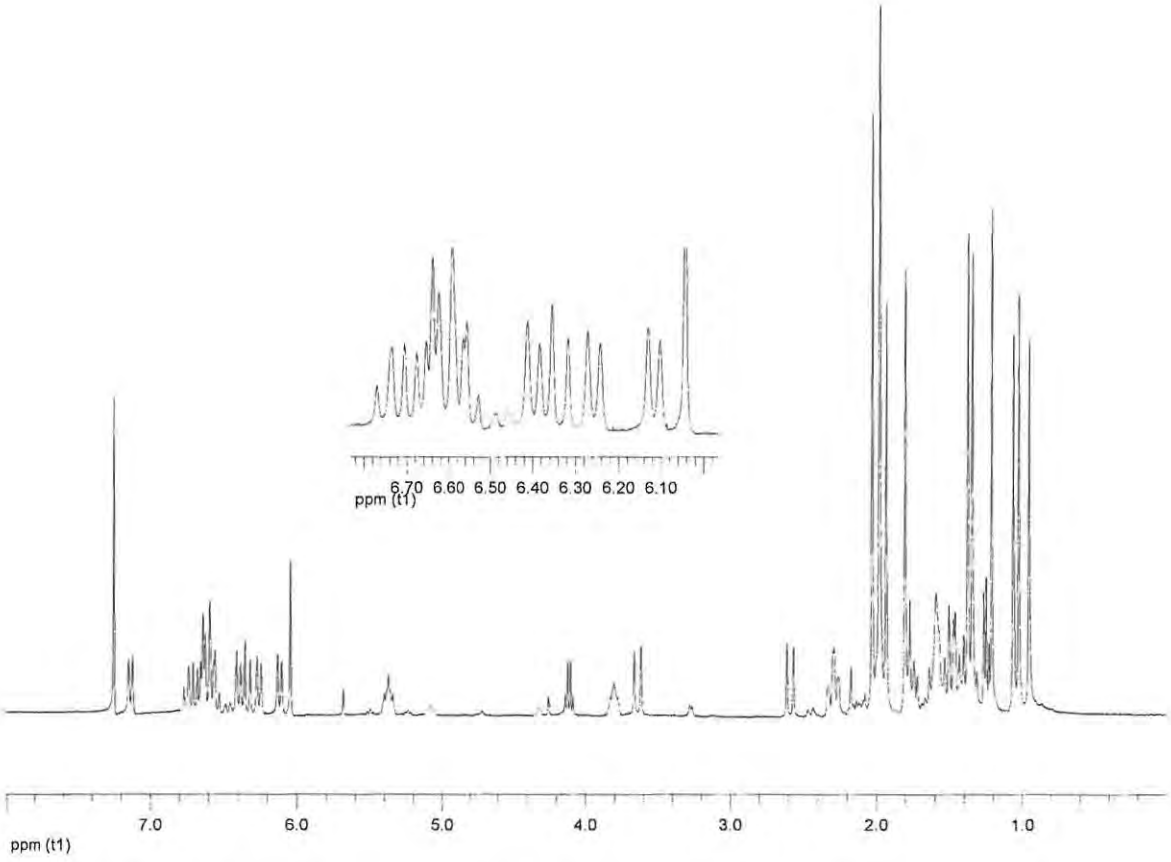

Figure 3.8 ^{1}H NMR spectrum of compound **3.8** ($CDCl_3$, 400 MHz)

The ^{1}H and ^{13}C NMR spectra (Figures 3.7 and 3.8) of compound **3.8** were completely different from those of compounds **3.5 – 3.7**. The ^{13}C NMR spectrum of compound **3.8** was a complicated mesh of resonances, most of which appeared at first glance to be duplicated. A careful analysis of the spectrum revealed 42 resonances. Many of these resonances were found in the olefinic region (δ 100 – 150). Moreover, the pure compound had a strong red-orange colour that suggested the presence of many conjugated double bonds. The ^{1}H NMR spectrum was even more difficult to analyze due to the overlapping of the signals. A comparison of the ^{1}H and ^{13}C NMR data with those of known carotenoids allowed compound **3.8** to be identified as fucoxanthin, a common pigment found in many classes of algae (Englert *et al.*, 1990). Fucoxanthin is one of the most abundant carotenoids in nature and is found especially in brown seaweed and diatoms (Yan *et al.*, 1999).

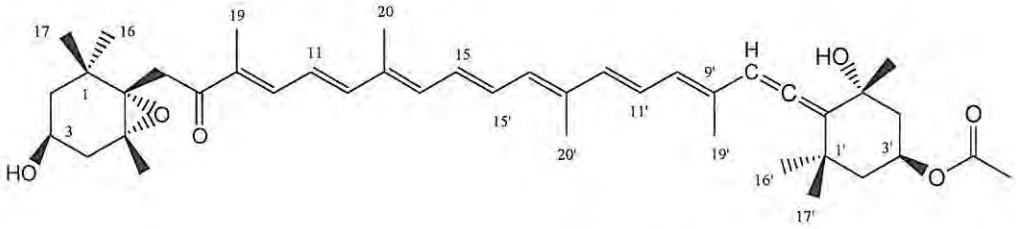

All-*trans*-fucoxanthin (**3.8**)

Table 3.5 A comparison of observed and literature ^{1}H NMR (400 MHz) and ^{13}C NMR (100 MHz) spectroscopic data for compound **3.8**

	Compound 3.8			All-trans-fucoxanthin [9]	
Carbon no.	**δ_C**	**δ_C mult**	**δ_H, mult, J_{Hz}**	**δ_C**	**δ_H, mult, J_{Hz}**
1	35.76	C		35.79	
1'	35.14			35.17	
2	47.07	CH_2		47.11	1.355 ax, 1.498 eq
2'	45.42		1.416	45.45	1.414 ax, 1.998 eq
3	64.30	CH	3.803	64.35	3.818
3'	68.00		5.371	68.01	5.384
4	41.65	CH_2	1.770	41.69	1.788 ax, 2.326 eq
4'	45.23		1.501	45.25	1.516 ax, 2.288 eq
5	66.12	C		66.16	
5'	72.67			72.71	
6	67.08	C		67.09	
6'	117.51			117.53	
7	40.80	CH_2	2.587, 3.641	40.83	2.600, 3.658
7'	202.32			202.37	
8	197.82	C		197.87	
8'	103.36		6.043	103.39	6.056
9	134.51	C		134.55	
9'	132.47			132,51	
10	139.05	CH	7.137	139.11	7.150
10'	128.50		6.117	128.55	6.133
11	123.36	CH	6.549	123.40	6.576
11'	125.65		6.592	125.70	6.605
12	144.98	CH	6.676	145.04	6.673
12'	137.08		6.336	137.16	6.351
13	135.39	C		135.55	
13'	138.04			138.09	
14	136.60	CH	6.398	136.55	6.414
14'	132.13		6.257	132.19	6.270
15	129.39	CH	6.639	129.44	~6.640
15'	132.47		6.742	132.51	6.756
16	25.03	CH_3	1.024	25.06	1.036 ax
16'	21.19		1.803	29.21	1.385 ax
17	28.12	CH_3	0.953	28.15	0.964 eq
17'	32.06		1.061	32.10	1.072 eq
18	21.14	CH_3	1.209	21.18	1.223
18'	31.26		1.342	31.31	1.354
19	11.81	CH_3	1.934	11.84	1.945
19'	13.99		1.803	14.03	1.815
20	12.74	CH_3	1.979	12.78	1.992
20'	12.89		1.979	12.93	1.992
3'-OAc	21.39, 170.39	CH_3 C	2.028		

[9] Englert *et. al.*, 1990

3.2.6 Antiplasmodial and cytotoxic activities of compounds 3.5 – 3.8

The isolated compounds **3.5 – 3.8** are structurally related to vitamin E (**3.9**) and as such have been investigated for antioxidant and anti-inflammatory properties for which vitamin E (**3.9**) is known. Compound **3.6** has been shown to exhibit both antioxidant and the anti-inflammatory properties (Pérez-Castorena *et al.*, 2002). The all-*trans*-fucoxanthin, has been shown to exhibit antioxidant (Yan *et al.*, 1999) and anticarcinogenic (Nishino, 1998) activities and induces cell death in human prostate cancer cells (Kotake-Nara et al., 2005).

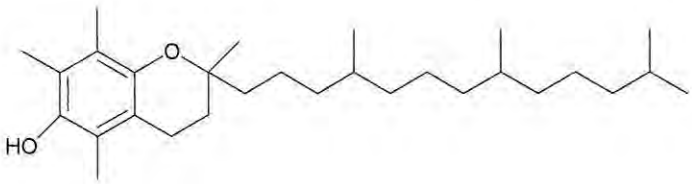

Vitamin E (**3.9**)

The antiplasmodial activity of the crude extracts against CQS *P. falciparum* D10 strain was determined as discussed in chapter 2. The CH_2Cl_2, EtOAc and HP-20 MeOH crude extracts showed good antiplasmodial activity (IC_{50} less than 10 μg/ml). The best activity was observed for the CH_2Cl_2 (NDK06-5B) extract (Table 3.6). The pure compounds were also evaluated for antiplasmodial activity against CQS *P. falciparum*.

Table 3.6 *In vitro* antiplasmodial activity of *S. heterophyllum* crude extracts and pure compounds against *P.falciparum* CQS D10 strain and cytotoxicity against Chinese Hamster Ovarian (CHO) cells.

Extract	D10: IC50(µg/ml)	CHO: IC50(µg/ml)	D10: IC50(µM)	CHO: IC50(µM)	SI (CHO/D10)
NDK06-5A	nd	nd	-	-	nd
NDK06-5B	2.8	3.7	-	-	1.3
NDK06-5C	5.9	12.3	-	-	2.1
NDK06-5D	nd	nd	-	-	nd
NDK06-5E	4.1	9.8	-	-	2.4
3.5	5.1	nd	12.0	nd	nd
3.6	6.5	nd	15.3	nd	nd
3.7	0.8	8.8	2.0	21.6	11
3.8	1.3	70.5	2.0	106.8	54

Selectivity index (SI) = cytotoxicity IC_{50} / antiplasmodial IC_{50}, Nd = not determined

Each compound demonstrated good activity against the parasite when compared to the crude with IC_{50} values less than 10 µg/ml for each one. The two most active compounds were **3.7** and **3.8** with IC_{50} values of 2.0µM respectively (Table 3.6). In order to evaluate the selectivity of these compounds for the *Plasmodium* parasite they were also screened for cytotoxicity against a Chinese Hamster Ovary cell line. Again, compounds **3.7** and **3.8** showed low cytotoxicity against this cell line. The selectivity index (SI) values, obtained for the compounds indicated that they are relatively selective for the *Plasmodium* parasite as compared to the mammalian cell line. However, compound **3.8** was the least toxic to the cell line (SI = 54). As compared to chloroquine however, with an IC_{50} value of 9.3 ng/ml (or 0.029 µM) (Chapter 2), the antiplasmodial activity of the *Sargassum* compounds is low.

At this stage the mode of action of *S. heterophyllum* compounds against *P. falciparum* is unknown. Further investigation of these compounds against chloroquine resistant strains of the parasite might be of value. However, it is interesting to know that the substituent at C-11' of the tetraprenylated toluquinols **3.5 – 3.7** appears to play a role

in the activity of the compounds with the aldehyde (**3.7**) derivative showing better antiplasmodial activity than the carboxylic acid derivatives (**3.5** and **3.6**).

3.3 Experimental

3.3.1 General experimental

HPLC grade solvents (Sigma-Aldrich or BDH) were used in the extraction and purification of the compounds. Purification by column chromatography was carried out using Merck Kieselgel 60 (0.040-0.063). Diaion SUPELCO HP-20 was used for the extraction of polar extracts from the marine alga.

The NMR spectra were recorded on a Bruker Avance 400 NMR spectrometer using standard pulse sequences. Compounds were purified on an HPLC system consisting of a Spectra-Physcis IsoChrom pump; Whatman Partisil 10 semi-preparative column and Spectraseries UV100 detector at a wavelength of 254 nm and a range of 2.0 in AUFs, attached to a Rikadenki chart recorder. Low resolution mass spectroscopy (EIMS) was determined on Finnigan MAT GCQ at 70 eV.

3.3.2 Plant material

S. heterophyllum was collected by hand at low tide from Noordhoek near Port Elizabeth in South Africa in January 2006. The alga was transported to the laboratory and immediately frozen until extracted. A voucher specimen (NDK06-5) is kept at the Division of Pharmaceutical Chemistry, Rhodes University.

3.3.3 Extraction and isolation of metabolites from of *S. heterophyllum*

The frozen alga sample (52.59 g, extracted dry weight) was extracted and prefractionated by solvent-solvent partitioning as described in chapter 2 to give a hexane (fr A, 2.01 g), CH_2Cl_2 (fr B, 2.03 g), EtOAc (fr C, 0.11 g) and H_2O crude fractions. The aqueous extract was passed through an HP-20 column and eluted successively with MeOH (fr D, 0.89 g) and CH_2Cl_2 (fr E, 0.09 g).

Crude extracts A and B were further fractionated by silica gel column chromatography using step-gradient elution (hexane-EtOAc ratio: 10:0, 9:1, 8:2, 7:3, 6:4, 4:6, 2:8, 0:10 and 100% MeOH) to give nine fraction each (A1-9, B1-9); extracts C and E were fractionated also by step-gradient elution (hexane-EtOAc ratio: 10:0, 7:3, 4:6, 2:8, 0:10 and 100% MeOH) to give six fractions each and extract E(hexane-EtOAc ratio: 6:4, 4:6, 2:8, 0:10 and 100% MeOH) gave five fractions after chromatography. Subsequent reverse phase HPLC of fraction 5E1 gave rise to compound **3.5** (0.02% dry wt). Compound **3.6** (5B3, 5B4, 3.7 % dry wt) was obtained from the column chromatography of fraction 5B and 5E (40% hexane-60% EtOAc) and from the HPLC (50% Hexane-50% EtOAc) of 5D. HPLC of 5B2 and 5B3 gave rise to compound **3.7** (0.31 % dry wt), while compound **3.8** (1.6 % dry wt) was obtained from the normal phase HPLC of 5B5 (20% hexane-80% EtOAc).

Sargaquinoic acid (3.5)

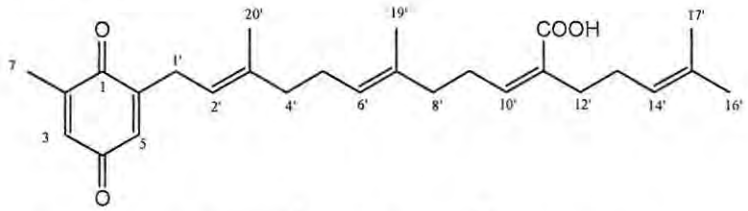

Orange-yellow oil; see Table 3.1 for ^{1}H NMR and ^{13}C NMR data.

Sargahydroquinoic acid (3.6)

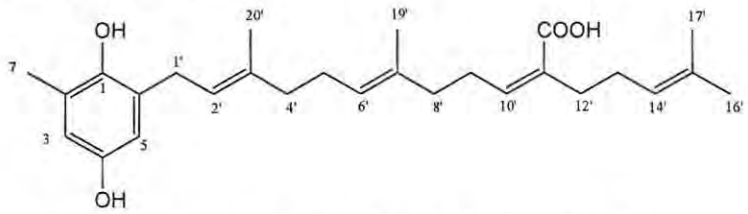

Orange-yellow oil; see Table 3.2 for ^{1}H NMR and ^{13}C NMR data.

Sargaquinal (3.7)

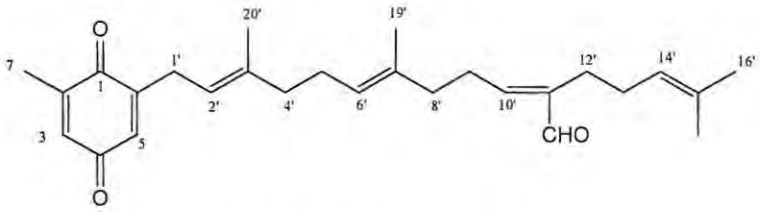

Orange-yellow oil; see Table 3.3 for ^{1}H NMR and ^{13}C NMR data; EIMS (70 eV) *m/z* (int, %) 137 (27), 175 (basepeak), 201 (23), 215 (27), 253 (27), 271 (18), 408 (18).

All-trans-fucoxanthin (3.8)

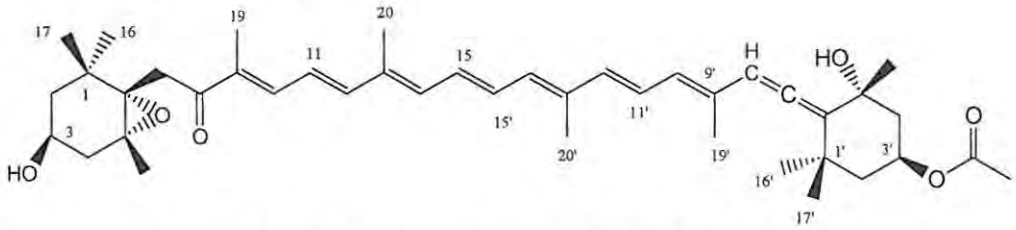

Red-Orange oil; see Table 3.5 for ^{1}H NMR and ^{13}C NMR data.

3.3.4 Antiplasmodial and cytotoxicity assays and data analysis of the crude fractions and pure compounds

The crude extracts and the pure compounds were tested in duplicates against the CQS strain of *P. falciparum* (for the antiplasmodial activity) and in triplicate against the CHO (for the cytotoxicity assay) as described in Section 2.3.4 – 2.3.7. The resulting data was then analysed using the Microsoft Excel GraphPad Prism v.40 software as discussed in section 2.3.8.

Supplementary information: NMR and MS supplementary data are available on CD.

References

Branch, G. M., Griffiths, C. L., Branch, M. L. and Beckley, L. E. *Two oceans: A Guide to the Marine Life of Southern Africa* **2005**. first edition, pp 318, David Philips Publishers, South Africa.

Edmonds, J. S. Diastereoisomers of an 'Arsenomethionine'-Based Structure from *Sargassum lacerifolium*: The formation of the Arsenic-Carbon Bond in Arsenic-Containing Natural Products. *Bioorganic and Medicinal Chemistry Letters* **2000**, 10, 1105 – 1108.

Englert, G.; Bjørnland, T. and Liaanen-Jensen, S. 1D and 2D NMR Study of Some Allenic Carotenoids of the Fucoxanthin Series. *Magnetic Resonance in Chemistry* **1990**, 28, 519 – 528.

Glombitza, K-W. and Keusgen, M. Fuhalols and Deshydroxyfuhalols from the Brown Alga *sargassum Spinuligerum*. *Phytochemistry* **1995**, 38 (4), 987 – 995.

Kotake-Nara, E.; Asai, A.; and Nagao, A. Neoxanthin and fucoxanthin induce apoptosis in PC-3 human prostate cancer cells. *Cancer Letters* **2005**, 220, 75-84.

Kusumi, T.; Shibata, Y.; Ishitsuka, M. and Kinoshita, T. Structures of New Plastoquinones from the Brown Alga *Sargassum serratifolium*. *Chemistry Letters* **1979**, 277 – 278.

Lubke, R. A.; Gess, F. W. and Bruton, M. N., *A Field Guide to the Eastern Cape Coast* **1988**, pp 46, The Grahamstown Centre of the Wildlife Society of South Africa.

Mooney, P. A. and Van Staden, J. Lunar Periodicity of the Levels of Endogenous Cytokinins in *Sargassum heteropyllum* (Phaeophyceae). *Botanica Marina* **1984**a, XXVII, 467 – 472.

Mooney, P. A. and Van Staden, J. Seasonal Changes in the Levels of Endogenous Cytokinins in *Sargassum heterophyllum* (Phaeophyceae). *Botanica Marina* **1984**b, XXVII, 437 – 442.

Mooney, P. A. and Van Staden, J. Tentative identification of Cytokinins in *Sargassum heteropyllum* (Phaeophyceae). *Botanica Marina* **1987**, 30, 323 – 325.

Nishino, H. Cancer Prevention by Carotenoids. *Mutation Research* **1998**, 402, 159 – 163.

Numata, A.; Kanbara, S.; Takahashi, C.; Fujiki, R.; Yoneda, M.; Usami, Y. and Fujita, E. A Cytotoxic Principle of the Brown Alga *Sargassum tortile* and Structures of Chromenes. *Phytochemistry* **1992**, 31 (4), 1209 – 1213.

Pérez-Castorena, A. L.; Arciniegas, A.; Apan, M. T. R.; Villasenor, J. L. and De Vivar, A. R. Evaluation of the Anti-inflammatory and Antioxidant Activities of the Plastoquinone Derivatives Isolated from *Roldana barba-johannis*. *Planta Medica* **2002**, 68, 645 – 647.

Segawa, M. and Shirahama H. New Plastoquinones from the Brown Alga *Sargassum sagamianum* var. *yezoense*. *Chemistry Letters* **1987**, 1365 – 1366.

Seo, Y., Lee; H-J., Park, K. E.; Kim, Y. A.; Ahn, J. W.; Yoo, J. S. and Lee, B.J. Peroxynitrate-scavenging Constituents from the Brown Alga *Sargassum thunbergi*. *Biotechnology and Bioprocess Engineering* **2004**, (9), 212 – 216.

Silva, D. H. S.; Pereira, F. C.; Zanoni, M. V. B and Yoshida, M. Lipophyllic Antioxidants from *Iryanthera juruensis* Fruits. *Phytochemistry* **2001**, 57, 437 – 442.

Tsuchiya, N.; Sato, A.; Haruyama, H.; Watanabe, T. and Iijima, Y. Nahocols and Isonahocols, Endothelin Antagonists from the Brown Alga, *Sargassum autumnale*. *Phytochemistry* **1998**, 48 (6), 1003 – 1011.

Yan, X.; Chuda, Y.; Suzuki, M. and Nagata, T. Fucoxanthin as the Major Antioxidant in *Hijikia fusiformis*, a Common Edible Seaweed. *Bioscience, Biotechnology and Biochemistry* **1999**, 63 (3), 605 – 607.

Chapter 4

Antiplasmodial and cytotoxic polyhalogenated monoterpenes from *Plocamium cornutum* and *Plocamium corallorhiza*

4.1 Introduction

Halogenated monoterpenes are unique secondary metabolites in that they are mainly found in marine algae. They are produced mainly by red algae with a rich source in the Plocamiaceae family of the order Gigartinales (Stierle *et al.*, 1979). Several *Plocamium* species produce arrays of aliphatic (Mynderse and Faulkner, 1975; Crews and Kho, 1974) and alicyclic (Crews and Kho, 1975; Mynderse *et al.*, 1975) polyhalogenated monoterpenes. *Plocamium cartilagineum*, the most studied species to date showed the utmost variety of halogenated monoterpenes. It has been shown to contain several 3,7-dimethyl-1,5,7-octatriene derivatives (Crews and Kho, 1977) such as the acyclic cartilageneal (**4.1**), a polychlorinated monoterpene aldehyde (Crews and Kho, 1974).

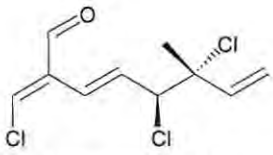

Cartilageneal (**4.1**)

Halogenated monoterpenes were first isolated from the digestive gland of the sea hare *Aplysia californica* (Faulkner and Stallard, 1973) before *P. cartilagineum* (Mynderse and Faulkner, 1974) was identified as the actual source. Halogenated monoterpenes isolated from the digestive glands of *A. limacina* (Imperato *et al.*, 1977), for example, were considered to have been present as a result of the ability of the organism to concentrate compounds from its diet. This organism feeds on marine algae and therefore could have sequestered the halogenated monoterpenes from their algae diet and use these compounds as components of their defensive secretions (De Napoli *et al.*, 1984).

A minimum of six *Plocamium* species are endemic to the Southern African coastline. This includes *P. cornutum*, *P. corallorhiza*, *P. rigidum*, *P. beckeri*, *P. suhrii* and *P.*

glomeratum (Lubke, 1988). Of these the two most common species are *P. cornutum* and *P. corallorhiza.* As discussed in chapter 2, the crude extracts from both *P. cornutum* and *P. corallorhiza* showed good antiplasmodial activity (IC_{50} less than 10 µg/ml) against the chloroquine sensitive (CQS) *P. falciparum* and were therefore, considered for further investigation.

The physical appearance of *P. corallorhiza* (Figure 4.1) is characterized by broad, flattened fronds with claw-like leaflets with serrated margins. The leaflets are arranged in alternating pairs (Figure 4.1). *P. corallorhiza* has been extensively studied and has been found to contain a range of different halogenated monoterpenes, the most intriguing of which contain either a dichloromethyl or aldehyde functionality (Knott *et al.,* 2005 and Mann *et al.,* 2007). *P. corallorhiza* has also shown significant geographical variation in metabolite profile (Davies-Coleman and Beukes, 2004). It thus, came as no surprise when the hexane crude extract of the sample collected from Noordhoek showed good antiplasmodial activity (IC_{50} 3.5 µg/ml) as compared to hexane crude extract from Kenton-on-Sea sample (IC_{50} 9.6 µg/ml). The SI data showed the Noordhoek extract to be more selective for the parasite (SI = 10) than the Kenton-on-Sea extracts (SI = 4.4).

Very little is however known about the chemistry of *P. cornutum* (Figure 4.1). The alga is brownish with a coarse thallus. It is crowed with cylindrical branchlets which are arranged in series of not more than two with claws of about 1 mm wide. Both *P. cornutum* and *P. corallorhiza* grow very well at low sea levels exposed to heavy surf (Branch *et al.*, 2005; Lubke and Seagrief, 1998).

P. cornutum

P. corallorhiza

Figure 4.1 Photographs of *P. cornutum* and *P. corallorhiza* (reproduced with permission)[10]

[10] Permission obtained from Professor Michael Guiry

4.2 Results and Discussion

4.2.1 Isolation of metabolites from *P. corallorhiza* and *P. cornutum*

4.2.1.1 *Plocamium corallorhiza* (NDK06-1b and KOS06-14b)

Previous studies of *P. corallorhiza* from Kenton-On-Sea (Mann *et al.*, 2007) resulted in the isolation of a number of halogenated monoterpenes. In this study we focused our attention on the Noordhoek collection (collection number NDK06-1b) which showed both greater activity against, and selectivity for, CQS *Plasmodium falciparum* (IC_{50} 3.5 μg/ml).

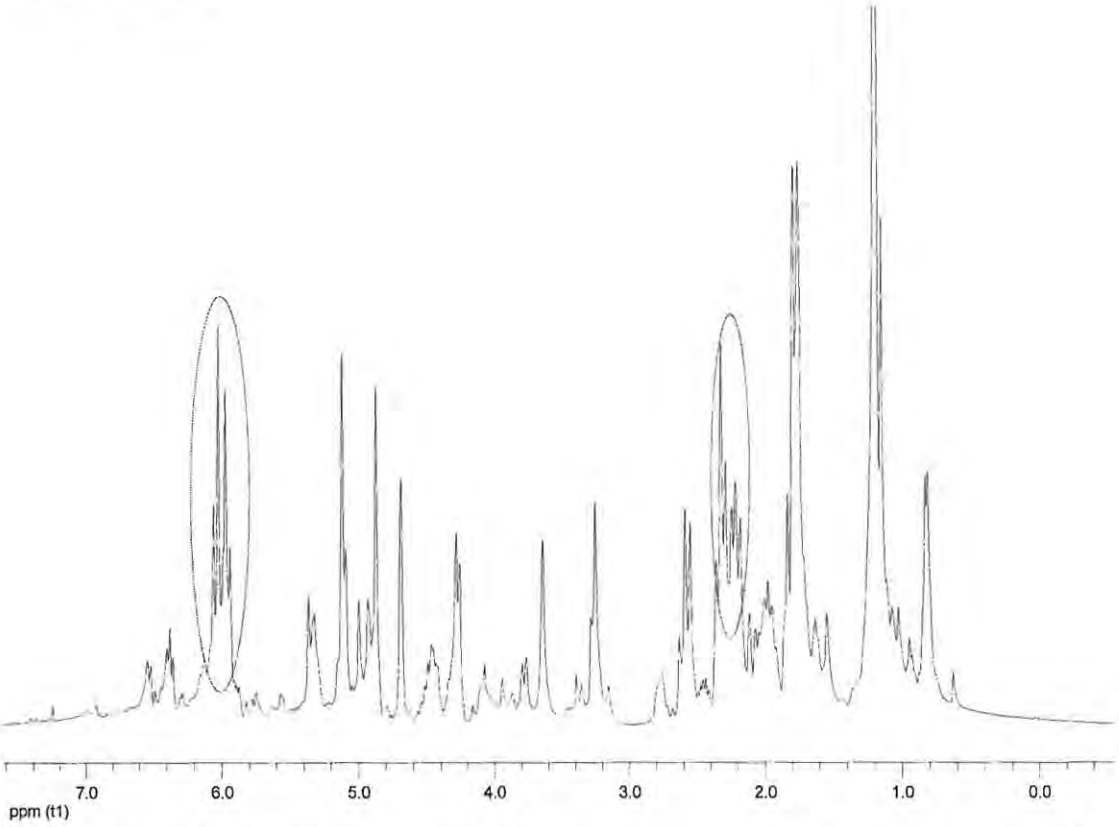

Figure 4.2 ^{1}H NMR spectrum of NDK06-1b-A crude hexane extract ($CDCl_3$, 400MHz)

P. corallorhiza, collected from Noordhoek (NDK06-1b) in the Eastern Cape of South Africa was extracted and pre-fractionated as outlined in section 2.3.3 and shown in in Scheme 4.1. The hexane extract (fr A, Figure 4.2) was firstly fractionated by silica gel column chromatography to afford nine fractions (frs A1-9).

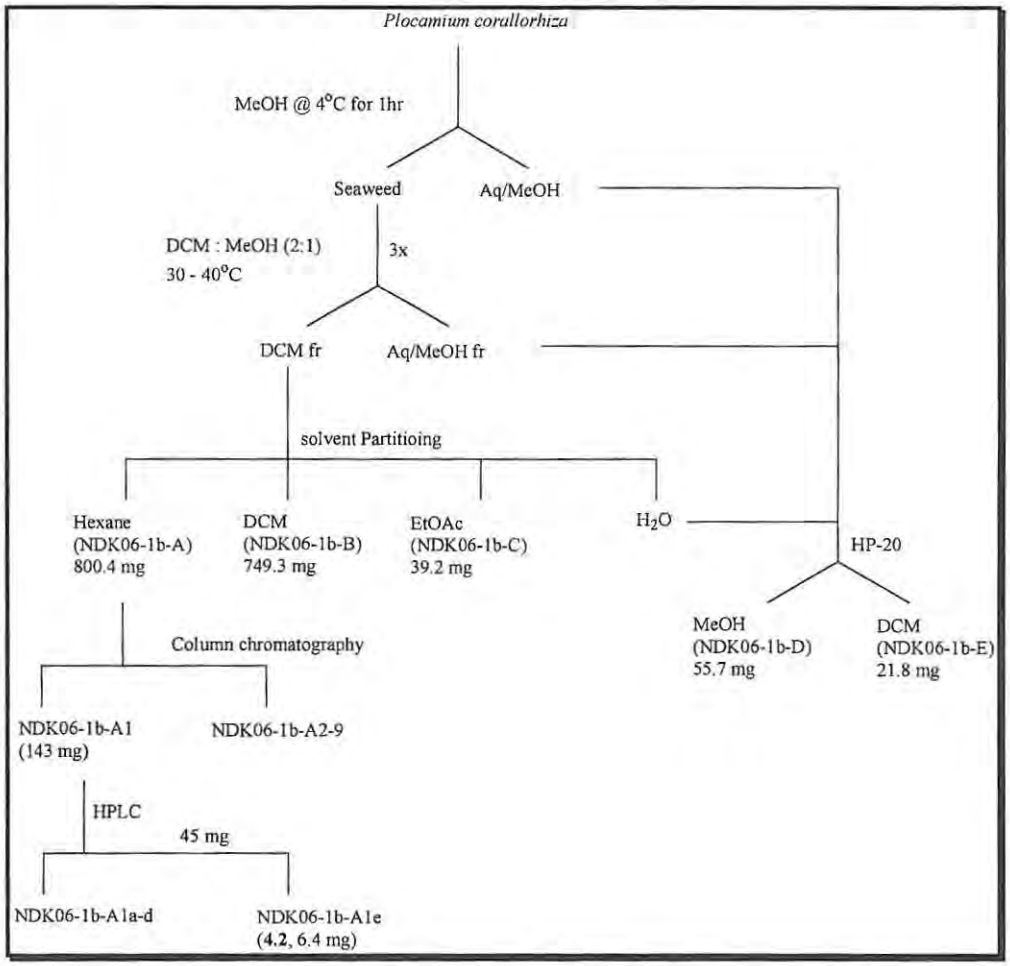

Scheme 4.1 Extraction and isolation scheme of *P. corallorhiza* (NDK06-1b)

Analysis of the ^{1}H NMR spectrum of each of the nine fractions showed fraction A1 (obtained with 100% hexane) to contain the prominent resonances noted (highlighted signals) in the crude hexane fraction (fr A, Figure 4.3) i.e. fraction A (Figure 4.2) was further purified (Scheme 4.1) to obtain fraction A1 (Figure 4.3).

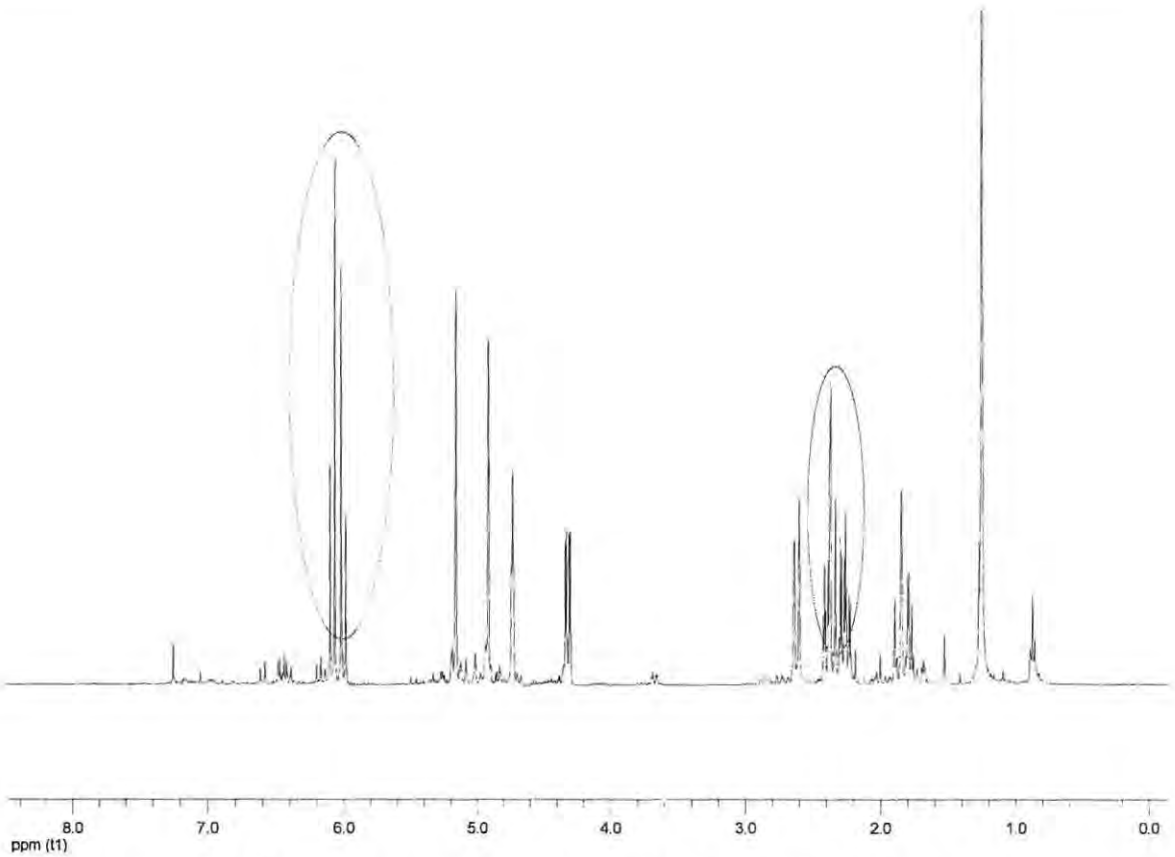

Figure 4.3 ^{1}H NMR spectrum of NDK06-1b-A1 ($CDCl_3$, 400 MHz)

Normal phase semi-preparative HPLC using 100% hexane as mobile phase gave rise to five fractions. However, only fraction A1e showed the presence of a pure compound (Scheme 4.1). Analysis of the ^{1}H and ^{13}C NMR spectra of A1e indicated a monoterpene.

4.2.1.2 *Plocamium cornutum* (KB06-3 and NDK06-36)

KB06-3 was collected from Kalk Bay near Cape Town in South Africa in January 2006. The sample was extracted and prefractionated as previously described for marine algae in section 2.3.3 to give hexane (KB06-3A), CH_2Cl_2 (KB06-3B) and EtOAc (KB06-3C) crude fractions. Fractionation of KB06-3A and KB06-3B using silica gel column chromatography and normal phase semi-preparative HPLC resulted in pure halogenated monoterpenes, compounds **4.1, 4.4 – 4.7** (Scheme 4.2).

Interestingly, a second collection of *P. cornutum* from Noordhoek, near Port Elizabeth gave compound **4.4** as the only identifiable product.

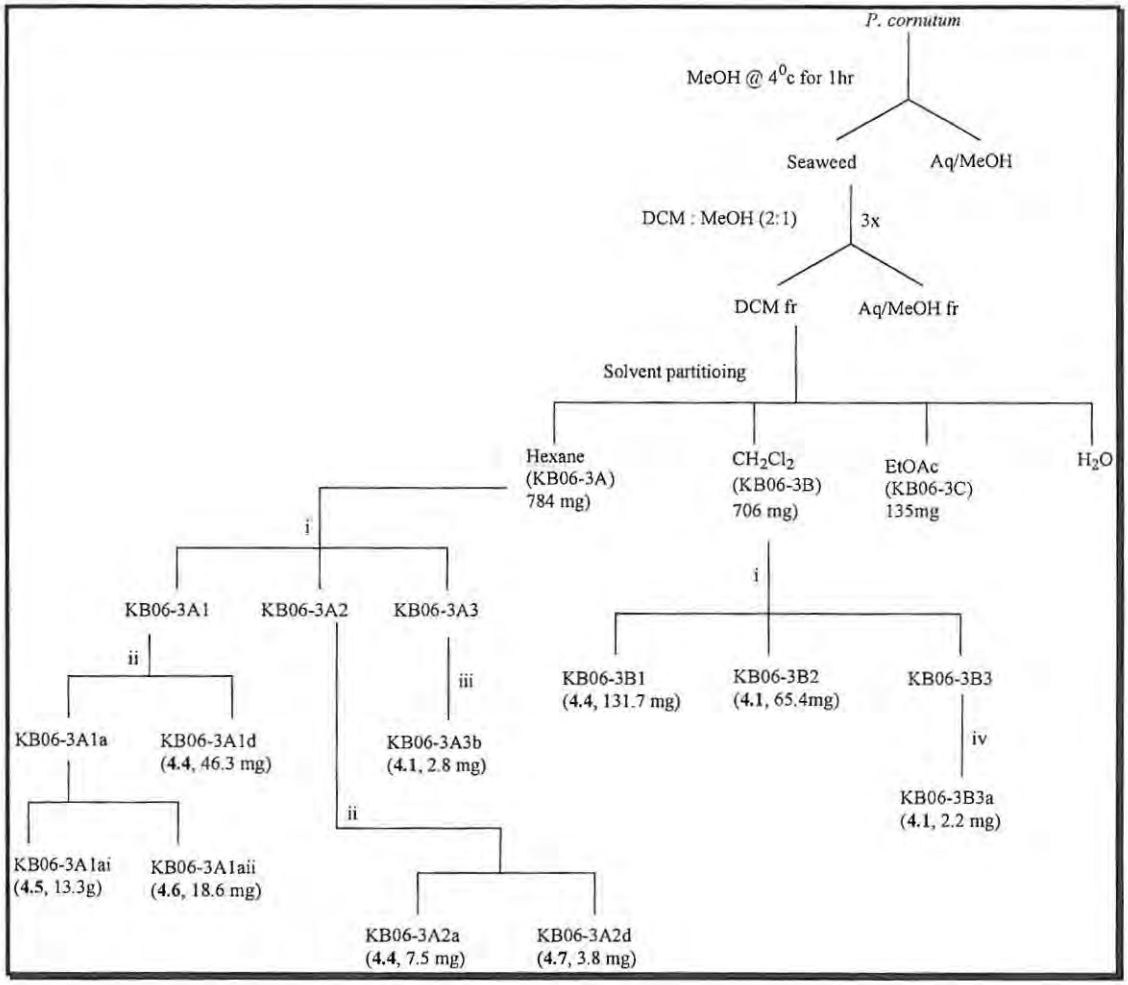

Scheme 4.2 Isolation scheme of *P. cornutum* i) Step-gradient column chromatography; ii) Normal phase HPLC, hexane (100%); iii) Normal phase HPLC, hexane-EtOAc (90:10); iv) Normal phase HPLC, hexane-EtOAc (80:20).

4.2.2 Structure elucidation of halogenated monoterpenes.

4.2.2.1 Compound A1e (4.2)

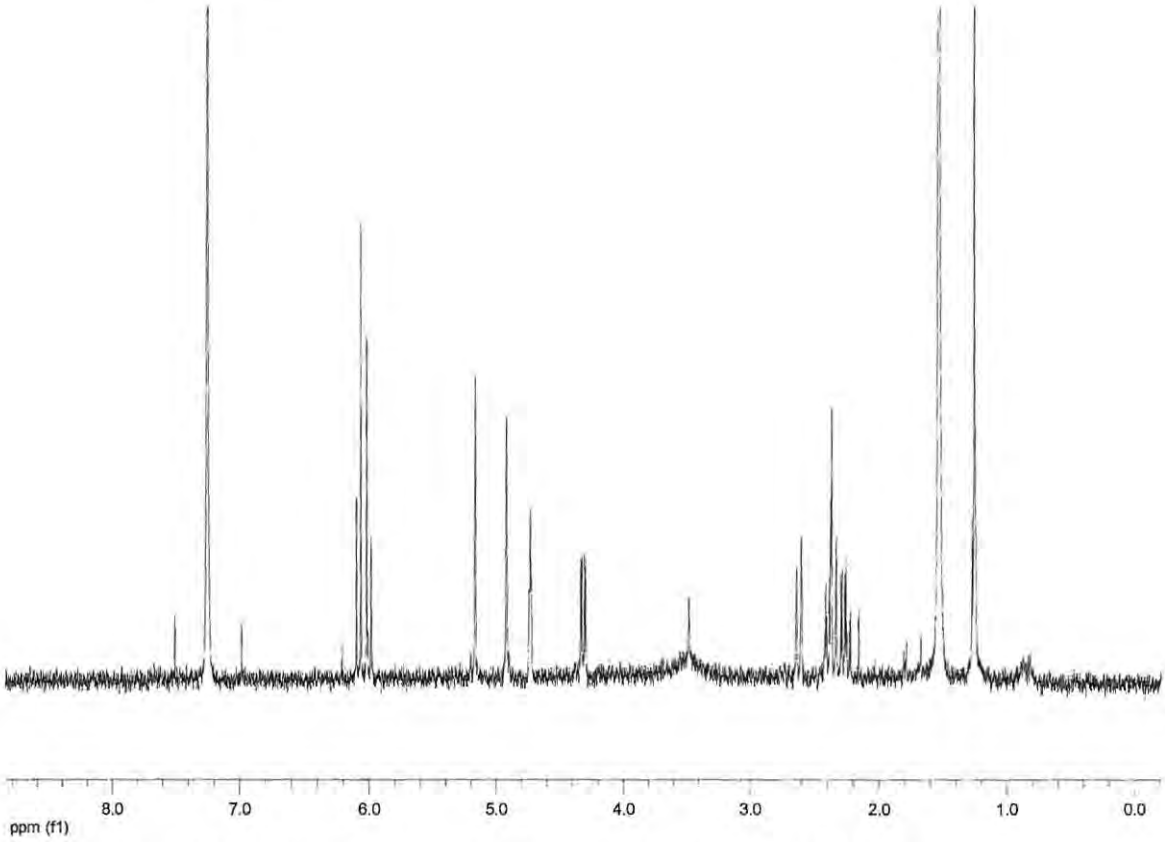

Figure 4.4 ^{1}H NMR spectrum of compound **4.2** ($CDCl_3$, 400MHz)

The ^{1}H NMR spectrum of compound **4.2** (Figure 4.4 and Table 4.1) showed two mutually coupled vinylic methines at δ 6.08 (d, J = 13.6, H-8) and 6.00 (d, J = 13.6 Hz, H-7); two terminal vinylic methylene protons at δ 4.92 (H-10a) and 5.17 (H-10b), and two halomethines at δ 4.32 (dd, J = 11.4, 4 Hz, H-2) and 4.73 (br t, J = 3.3 Hz, H-4).

The ^{13}C and DEPT-135 NMR spectra of compound **4.2** indicated ten carbons of which four were sp^2 hybridized at δ 115.5 (C-10), 120.3 (C-8), 133.9 (C-7) and 142.1 (C-5) and two were halomethines at δ 61.6 (C-4) and 63.1 (C-2). The remaining four resonances constituted a quaternary carbon δ 43.5 (C-1), two methylene carbons at δ 40.9 (C-3) and 41.4 (C-6) and the final shift at δ 26.5 (C-9) indicated a methyl carbon.

Table 4.1 A comparison of observed and literature ^{1}H and ^{13}C NMR spectroscopic data for compound **4.2**

	Observed			**Literature**[11]	
Carbon no.	δ_C	δ_C **mult**	δ_H, **mult,** J_{Hz}	δ_C	δ_H, **mult,** J_{Hz}
1	43.5	C		43.3	
2	63.1	CH	4.32, dd, 11.4, 4	63.0	4.33, dd, 12, 4
3	40.9	CH_2	2.22-2.30, m	40.9	2.2-2.3, m
4	61.6	CH	4.73, t, 3.4	61.2	4.74, br t, 4, 4
5	142.1	C		142.2	
6a	41.4	CH_2	2.35, d, 14.0	41.1	2.35, d, 14.7
6b			2.63, d, 14.4		2.65, d, 14.7
7	133.9	CH	6.00, d, 13.6	134.0	5.92, d, 12
8	120.3	CH	6.08, d, 13.6	120.3	6.08, d, 12
9	26.5	CH_3	1.26, s	26.2	1.26, s
10a	115.5	CH_2	4.92, s	115.2	4.93, br s
10b			5.17, s		5.18, br s

The comparison of the ^{1}H and ^{13}C NMR spectra of **4.2** to known cyclic monoterpenes revealed it to be epi-plocamene D. This had first been isolated from *Plocamium violaceum* (Crews *et al.*, 1984b). It has also been reported as a constituent of *P. cartilagineum* from Antarctica (Stierle and Sims, 1979).

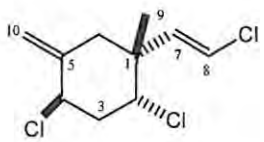

4.2

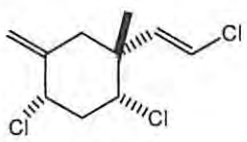

4.3

Compound **4.2** shows NMR spectra data that are identical to plocamene D (**4.3**) except for the broad triplet resonance displayed by **4.2** at δ 4.73 for equatorial H-4 which appears as a broadened double doublets for compound **4.3** at δ 4.26 (Stierle and Sims, 1979).

[11] Abreu and Galindro, 1996

4.2.2.2 Compound 3A3b (4.1)[12]

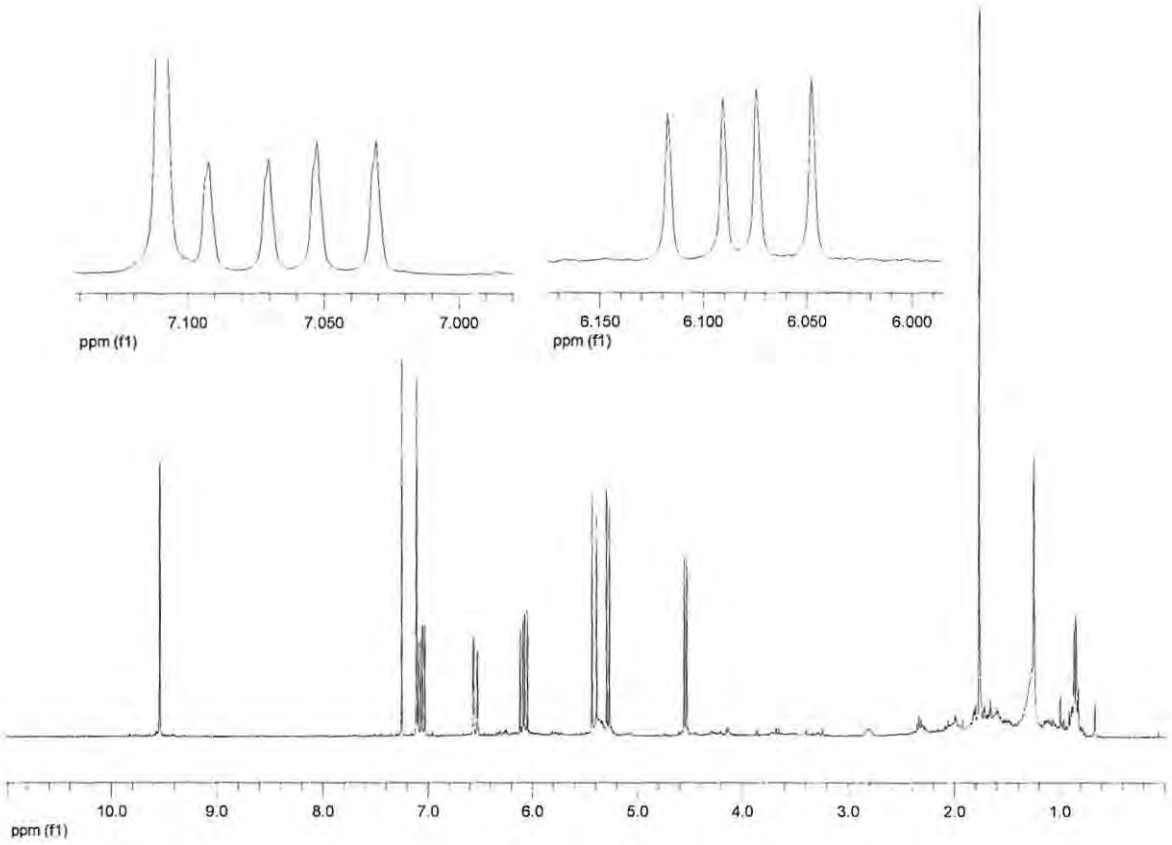

Figure 4.5 ^{1}H NMR spectrum of (**4.1**) ($CDCl_3$, 400 MHz)

The ^{1}H NMR spectrum of compound **4.1** (Figure 4.5) showed a methyl group at δ 1.77 (H_3-10) and a deshielded singlet at δ 7.11 (H-8). Coupled to the deshielded methine at δ 7.06 (dd, J = 8.7, 15.8 Hz, H-5) was a doublet at δ 6.55 (d, J = 15.8 Hz, H-6) and the halomethine proton at δ 4.54 (d, J = 8.7 Hz, H-4). Two terminal alkene protons were indicated by two doublets at δ 5.28 (d, J = 10.6 Hz, H-1a) and 5.41 (d, J = 17.1 Hz, H-1b). These terminal protons were coupled to a methine proton at δ 6.08 (dd, J = 10.7, 17.1 Hz, H-2). The above information suggested –CH=CH-CHX and –CH=CH_2 moieties in compound **4.1**. The ^{13}C NMR spectrum of compound **4.1** showed six sp^2 hybridized carbons (δ 143.9, 139.5, 137.5, 134.1, 122.5, 116.4), one quaternary (δ 71.6) one methine (δ 69.6), one methyl (δ 24.7) and one carbonyl carbon (δ 189.3) indicating an aldehyde monoterpene (Table 4.2). The coupling

[12] The skeleton of the structure were named using the most common numbering system encountered in literature for monoterpene i.e. 3-methyl-1,5,7-octatriene.

constant (J = 15.8 Hz) between H-5 and H-6 indicated an *E* geometry about this double bond (Mynderse and Faulkner, 1975) while the ^{13}C resonance of the methyl group (δ 24.7) indicated a 3,4-*erythro* configuration which is usually associated with this type of compound (Crews *et al.*, 1984b).

All spectroscopic data for compound **4.1** compared favourably with those of cartilagineal, which was originally isolated from *P. cartilagineum* (Crews and Kho, 1974).

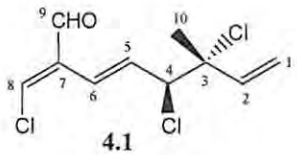

4.1

Table 4.2 A comparison of observed and literature ^{1}H NMR (400 MHz), and ^{13}C NMR (100 MHz) spectroscopic data for compound **4.1**

	Observed			**Literature**[13]	
Carbon no.	δ_C	δ_C **mult**	δ_H, **mult,** J_{Hz}	δ_C	δ_H, **mult,** J_{Hz}
1a	116.4	CH_2	5.28, d, 10.6	116.3	5.26, dd, 10.5, 1.0
1b			5.41, d, 17.1		5.40, dd, 17.0, 1.0
2	139.5	CH	6.08, dd, 10.7, 17.1	139.5/ 134.0	6.06, dd, 10.5, 17.0
3	71.6	C	-	71.5	-
4	69.6	CH	4.54, d, 8.7	69.5	4.47, br d, 8.5
5	134.1	CH	7.06, dd, 8.7, 15.8	134.0/ 139.5	7.05, dd, 8.5, 15.3
6	122.5	CH	6.55, d, 15.8	122.5	6.49, d of dd, 15.3, 2.0, 1.0
7	137.5	C	-	137.3	-
8	143.9	CH	7.11 s	132.3	7.05 s
9	189.3	CH	9.54 br s	189.3	9.04, d, 2.0
10	24.7	CH_3	1.77 s	24.6	1.71 s

[13] Crews and Kho, 1974

4.2.2.3 Compound KB06-3A1d (4.4)

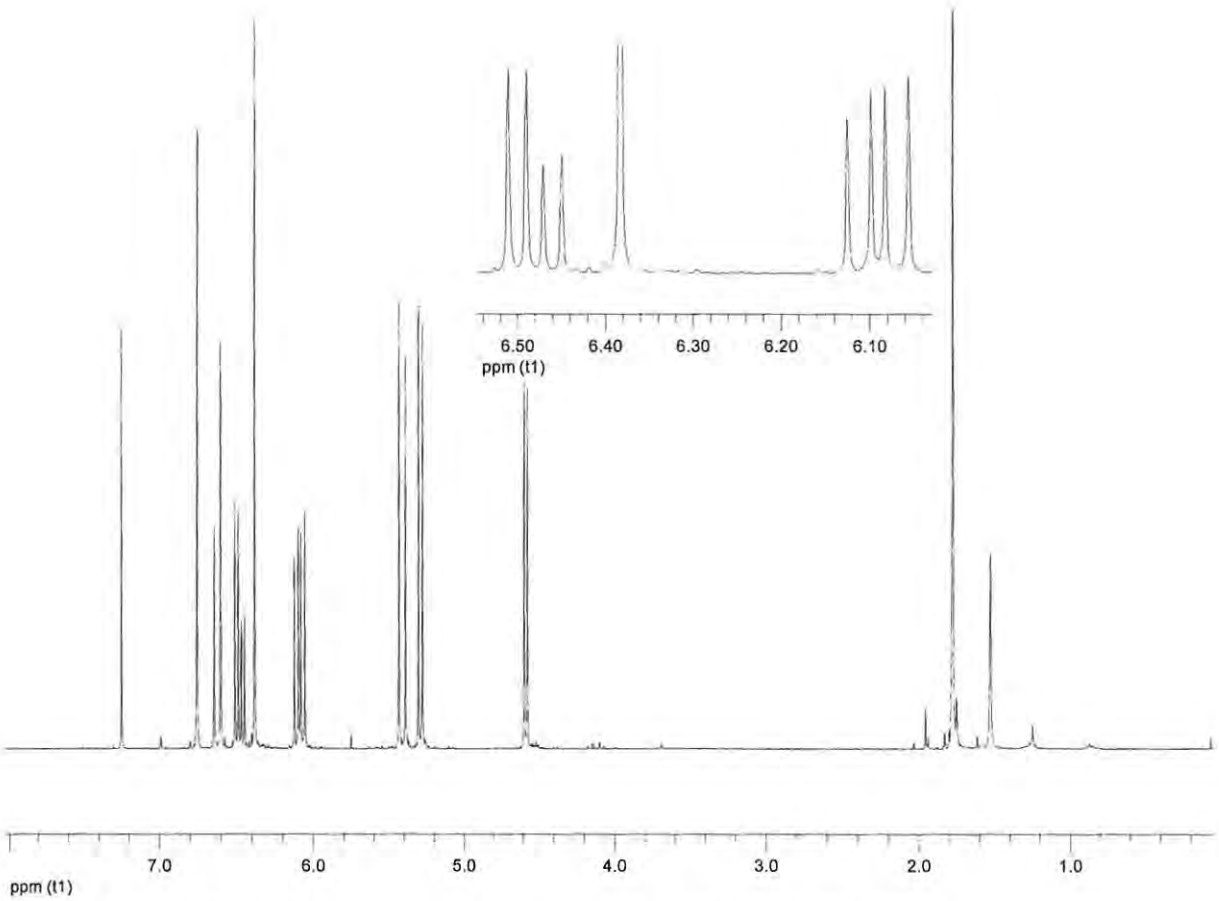

Figure 4.6 ^{1}H NMR spectrum of compound **4.4** ($CDCl_3$, 400 MHz)

A molecular formula of $C_{10}H_{11}Cl_5$ was deduced for compound **4.4** by high resolution fast-atom bombardment mass spectrometry (HRFABMS) which gave a molecular ion at *m/z* 305.9308. The ^{1}H and ^{13}C NMR spectra of compound **4.4** showed similarities to those of compound **4.1**. ^{1}H NMR spectrum of compound **4.4** (Figure 4.6) showed a methyl signal at δ 1.78 (H_3-10) and two deshielded methine protons at δ 6.38 (H-8) and 6.75 (H-9). In addition, it also showed a double doublet at δ 6.48 (dd, J = 8.5, 16.2 Hz, H-5) which was coupled to two deshielded methines at δ 4.58 (d, J = 8.5 Hz, H-4) and 6.62 (d, J = 16.2 Hz, H-6) to give a –CH=CH=CHX-moiety. A second double doublet methine proton at δ 6.09 (dd, J = 10.7, 17.1 Hz, H-2) was coupled to the terminal alkene protons at δ 5.29 (d, J = 10.7 Hz, H-1a) and 5.42 (d, J = 10.7 Hz, H-1b) to give a –CH=CH_2 moiety as was observed for compound **4.1**. The most significant difference between compound **4.4** and **4.1** was the disappearance of the

signal at δ 9.54, observed for the aldehyde functionality in compound **4.1,** and the appearance of a signal at δ 6.75 in the ^{1}H NMR spectrum of compound **4.4**. The ^{13}C NMR data indicated ten carbon resonances (Table 4.3). The spectrum included six resonances indicative of double bonds (δ 116.6, 123.9, 124.2, 131.9, 136.0 and 139.4), two overlapping halomethine carbons (δ 69.4, C-4 and C-9), a quaternary carbon at δ 71.7 (C-3) and a methyl carbon at δ 25.1. The methyl resonance at δ 25.1 is indicative of a 3,4-*erythro* configuration. The comparison of the ^{1}H and ^{13}C NMR data with literature data of known halogenated monoterpenes revealed that compound **4.4** had originally been isolated from *P. cartilagineum* (Mynderse and Faulkner, 1975; Abreu and Galindro, 1996).

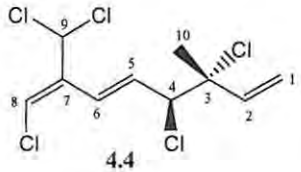

4.4

Table 4.3 A comparison of observed and literature ^{1}H and ^{13}C NMR (100 MHz) spectroscopic data for compound **4.4**

	Observed			**Literature**[14]	
Carbon no.	**δ_C**	**δ_C mult**	**δ_H, mult, J_{Hz}**	**δ_C**	**δ_H, mult, J_{Hz}**
1a	116.6	CH_2	5.29, d, 10.7	116.5	5.29, d, 10.5
1b			5.42, d, 17.1		5.41, d, 17.0
2	139.4	CH	6.09, dd, 10.7, 17.1	139.8	6.09, dd, 10.6, 17.0
3	71.7	C	-	71.8	-
4	69.4	CH	4.58, d, 8.5	69.6	4.58, d, 8.1
5	124.2	CH	6.48, dd, 8.5, 16.2	124.3	6.47, dd, 8.1, 16.3
6	123.9	CH	6.62, d, 16.2	124.2	6.63, d, 16.3
7	136.0	C	-	136.5	-
8	131.9	CH	6.38 s	132.3	6.39 s
9	69.4	CH	6.75 s	69.3	6.76 s
10	25.1	CH_3	1.78 s	25.4	1.78 s

[14] Abreu and Galindro, 1996

4.2.2.4 Compound 3A1a (4.5 and 4.6)

Compounds **4.5** and **4.6** were initially isolated as a mixture (Scheme 4.2). Normal phase TLC with different mobile phase combinations, column chromatography and normal and reversed phase HPLC with different solvents and solvent combinations such as acetonitrile-water (80:20), acetonitrile (100%) and hexane (100%) did not achieve the separation of these compounds. The 1D NMR (^{1}H and ^{13}C) spectra showed signals which appeared duplicated (Figure 4.7a and 4.7b). However, GCMS showed two peaks which were separated by 0.5 minutes. Analysis such as EIMS (Figure 4.8), IR and UV to identify the properties of the components were conducted on the mixture. Fortuitously, in an attempt to isolate additional quantities of material by normal phase HPLC using 100% hexane as mobile phase, resulted in the separation of the two isomers.

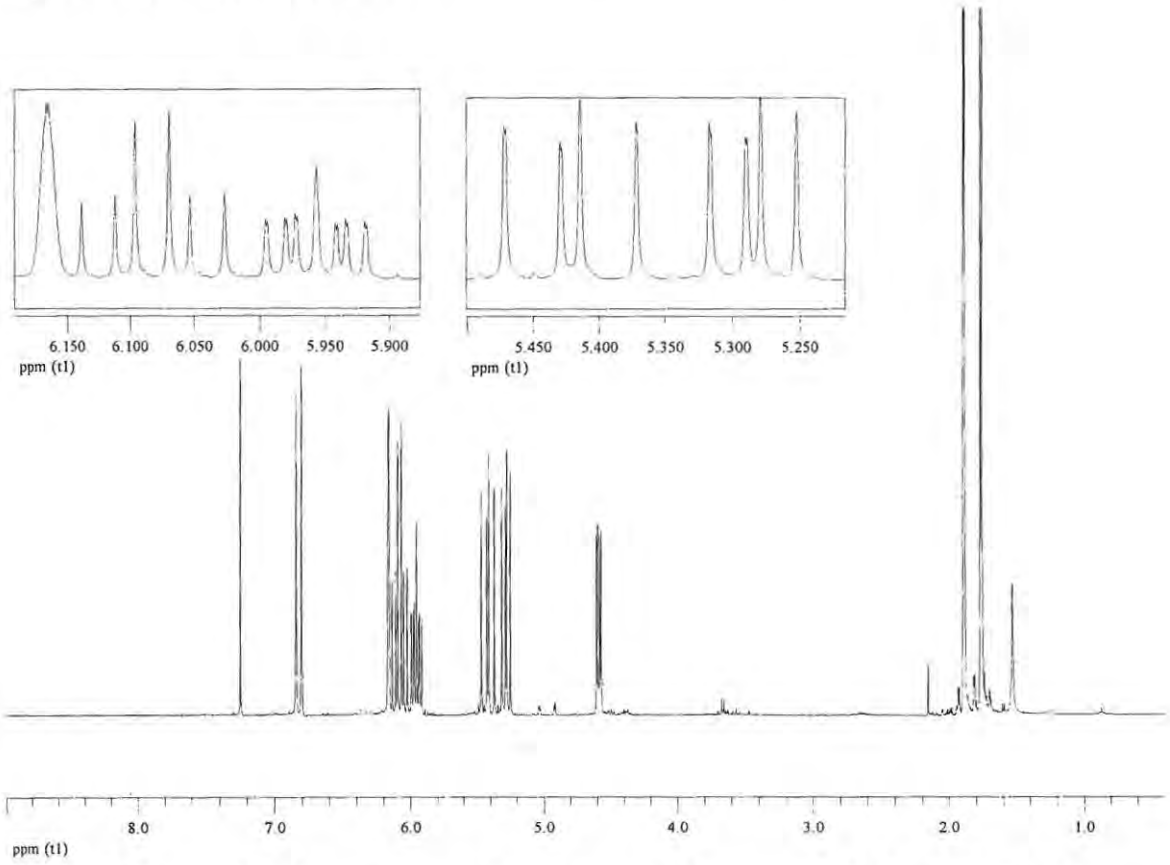

Figure 4.7a ^{1}H NMR spectrum of a mixture of Compounds **4.5** and **4.6** ($CDCl_3$, 400MHz)

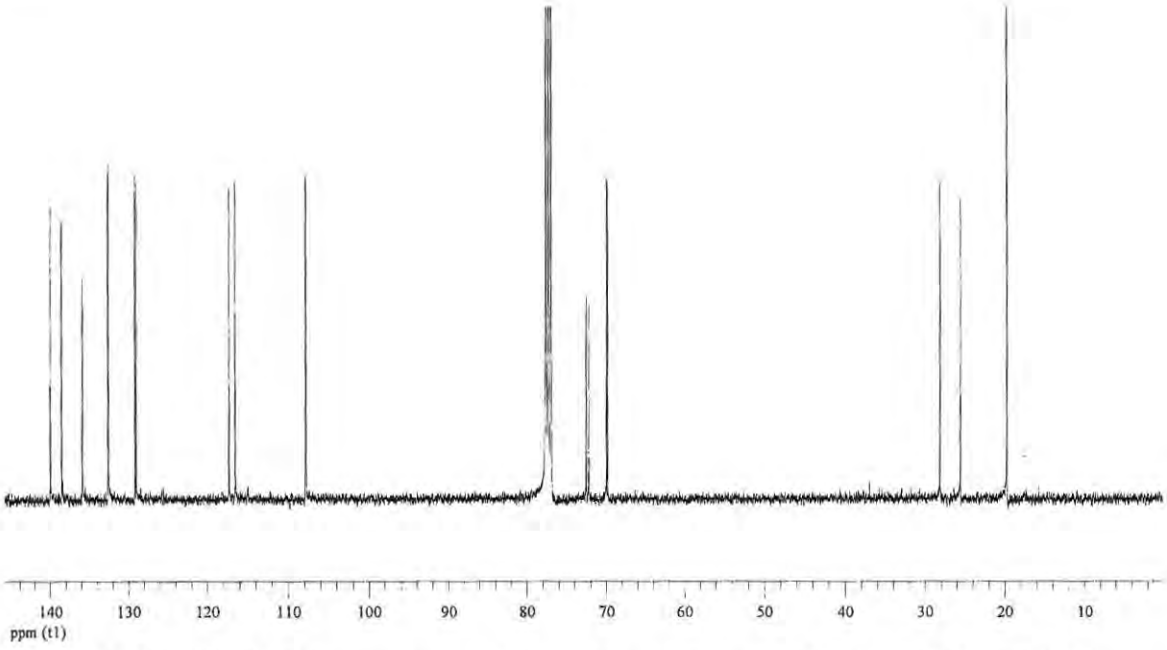

Figure 4.7b ^{13}C NMR spectrum of a mixture of compounds **4.5** and **4.6** ($CDCl_3$, 100MHz)

4.2.2.4.1 Compound 3A1ai (4.5)

A molecular formula of $C_{10}H_{13}BrCl_2$ was deduced from the HRFABMS spectrum which gave a molecular ion at *m/z* 281.9572. The molecular ion of **4.5** could not be obtained on the EIMS. However, ion clusters were observed at *m/z* 167/169 $[M-BrCl]^+$, 193/195 $[C_6H_7BrCl]^+$ and 203/205 $[M-Br]^+$ (Figure 4.8), indicating the halogen content of the compound.

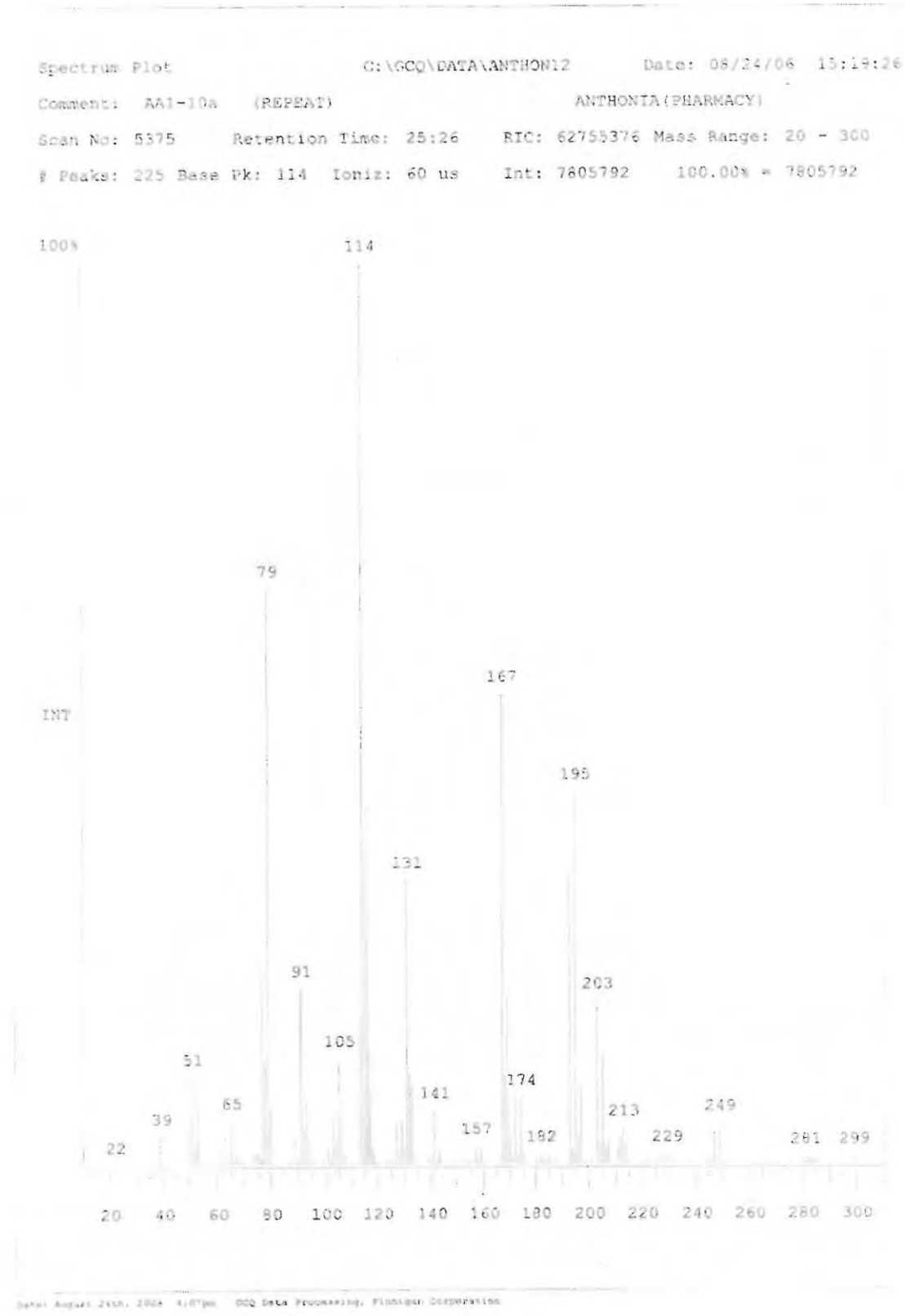

Figure 4.8 EIMS of a mixture of compounds **4.5**

The ^{1}H NMR spectrum (Figure 4.9) of compound **4.5** showed some similarities to those of compounds **4.1** and **4.4**. However, the main difference was the appearance of two methyl signals (δ 1.89, H_3-9 and 1.78, H_3-10) as opposed to one methyl group in compounds **4.1** and **4.4.** As before, the same –CH=CH-CHX- structural motif were apparent from resonances at δ 6.83 (d, J = 15.5 Hz, H-6), 5.95 (dd, J = 15.5, 9.1 Hz, H-5) and δ 4.60 (d, J = 9.1 Hz, H-4); as were the –CH=CH_2 moiety (δ 5.30, d, 10.6 Hz, H-1a; 5.45, d, 16.9 Hz, H-1b; 6.11, dd, 10.7, 16.9 Hz, H-2). The ^{13}C NMR spectrum showed ten carbon resonances (Table 4.4) which included six olefinic carbons (δ 138.3, 135.6, 132.3,128.9,117.0, 107.5), one quaternary carbon (δ 72.2), one methine carbon (δ 69.7) and two methyl carbons at δ 27.9 (C-10) and 19.5 (C-9).

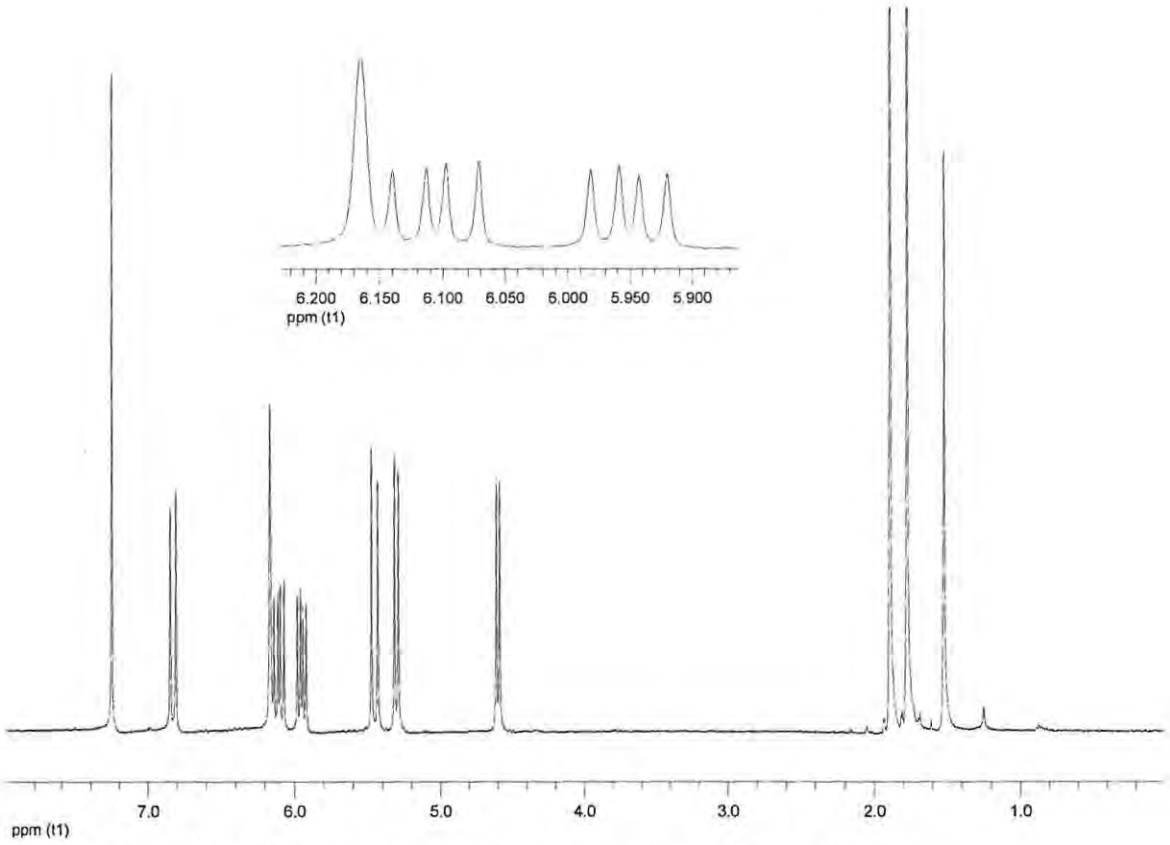

Figure 4.9 ^{1}H NMR spectrum of compounds **4.5** ($CDCl_3$, 400 MHz)

Analysis of the 2D NMR data allowed the assignment of the complete planar structure of compound **4.5** as follows. HMBC correlations were observed from the vinyl methyl protons at δ 1.89 (H_3-9) to carbons resonating at δ 107.5 (C-8), 135.6 (C-7) and 132.3 (C-6) consistent with the substructure CH(X)=C(CH_3)-CH=. A second substructure, =CH-CH(X)-CX(CH_3)-CH=, was deduced from HMBC correlations from the methyl

protons at δ1.78 (H_3-10) to δ 138.3 (C-2), 72.2 (C-3) and 69.7 (C-4) (Table 4.4 and Figure 4.10). The complete structure was consolidated by the observation of direct proton-proton coupling (^{1}H-^{1}H COSY) between δ 4.60 (H-4) and δ 5.95 (H-5) and also between the two doublets at δ 5.30 (H-1a) and 5.45 (H-1b) and the methine proton at δ 6.11 (H-2).

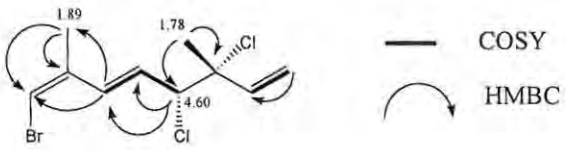

Figure 4.10 Selected HMBC and ^{1}H-^{1}H COSY correlations of compound **4.5**

The presence of a bromine atom at C-8 in compound **4.5** (as opposed to chlorine in compound **4.4**) was indicated by the upfield shift of the carbon resonance from δ 131.9 in compound **4.4** to δ 107.5 in compound **4.5**. The chlorine atoms at C-3 and C-4 were deduced from deshielded resonances at δ 72.2 and 69.7 respectively and also by comparison with those of compounds **4.1** and **4.4**. The geometry of the double bonds was confirmed by a 2D NOESY experiment. NOESY correlations between the protons at δ 6.17 (H-8) and δ 1.89 (H-9) signified a *Z* geometry about the $\Delta^{7,8}$ double bond. The coupling constant (J = 15.5 Hz) observed for the H-5 and H-6 is indicative of an *E* geometry at the $\Delta^{5,6}$ double bond. This was also reinforced by the NOESY correlation of δ 5.95 (H-5) to δ 1.89 (H-9). In contrast to compounds **4.1** and **4.4**, the methyl signal (C-10) for compound **4.5** was slightly downfield at δ 27.9, indicating a 3,4-*threo* configuration.

All spectroscopic data were consistent with the proposed structure 3,4-*threo*-8-bromo-3,4-dichloro-3,7-dimethyl-5*E*,7*Z*-octatriene.

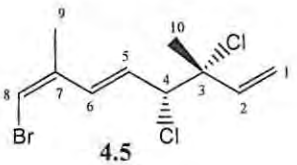

4.5

Table 4.4 ^{1}H (400 MHz, $CDCl_3$), ^{13}C (100 MHz, $CDCl_3$), $^{1}H - {}^{1}H$ COSY and HMBC data for compounds **4.5**

Carbon No.	δ_C	δ_C **mult**	δ_H, **mult,** J_{Hz}	$^{1}H - {}^{1}H$ **COSY**	**HMBC**
1a	117.0	CH_2	5.30, d, 10.6	H-2	C-3
1b			5.45, d, 16.9	H-2	C-3
2	138.3	CH	6.11, dd, 10.7, 16.9	H-1	-
3	72.2	C	-	-	-
4	69.7	CH	4.60, d, 9.1	H-5	C-5, C-6, C-10
5	128.9	CH	5.95, dd, 9.1, 15.5	H-4, H-6	C-3, C-8
6	132.3	CH	6.83, d, 15.5	H-5	C-4, C-8, C-9
7	135.6	C	-	-	-
8	107.5	CH	6.17, s	H-9	-
9	19.5	CH_3	1.89, s	H-8	C-6, C-7, C-8
10	27.9	CH_3	1.78, s	-	C-2, C-3, C-4

4.2.2.4.2 Compound 3A1aii (4.6)

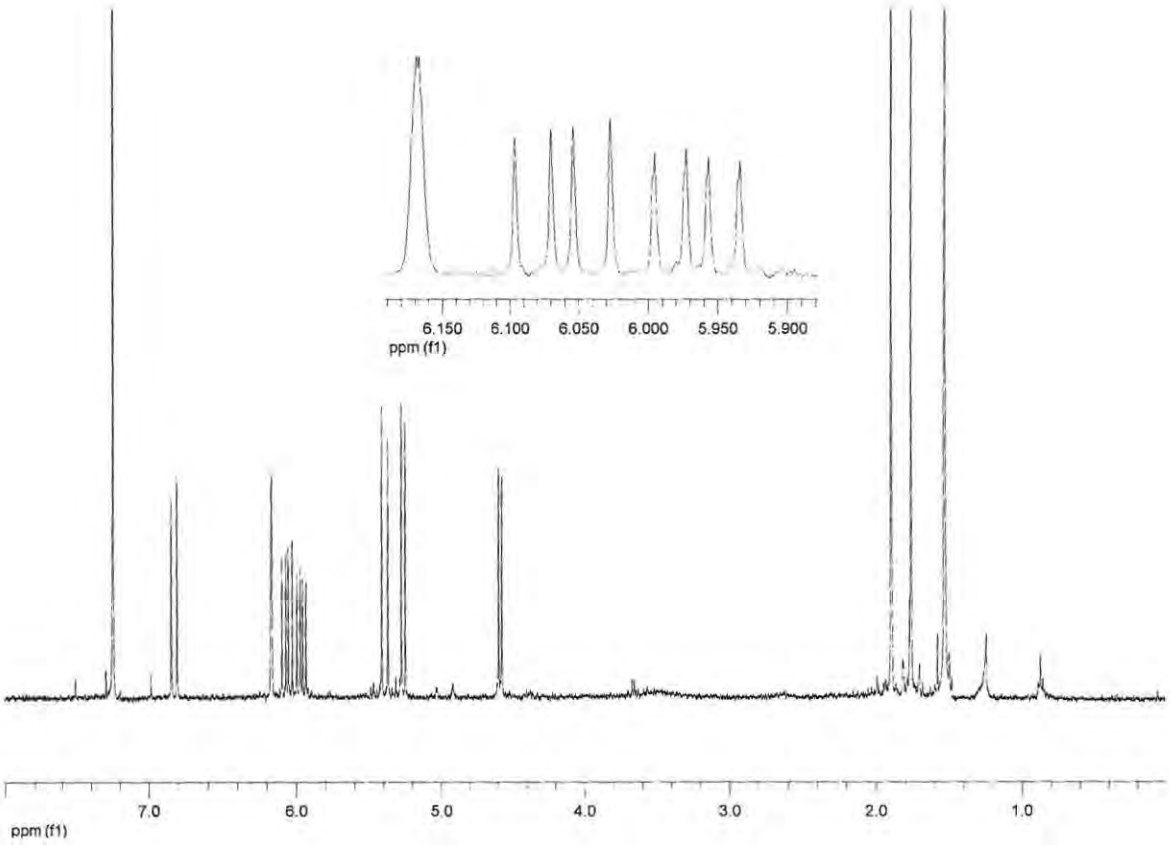

Figure 4.11 ^{1}H NMR spectrum of compound **4.6** ($CDCl_3$, 400 MHz)

As isomers, the spectroscopic data of compounds **4.5** and **4.6** such as IR and MS were expected to be identical and was proven by the identical GCMS obtained for the two compounds. The difference in the isomers was observed in their NMR spectra. The ^{1}H (Figure 4.11) and ^{13}C NMR spectra of compounds **4.5** and **4.6** were very similar with the only difference being the chemical shift of the methyl carbons of the two compounds. While **4.5** showed a methyl carbon resonance at δ 27.9, a resonance at δ 25.3 was observed in the ^{13}C NMR spectrum of compound **4.6**. This indicated that the only difference between the two compounds was the relative configurations at C-3 and C-4. A resonance at δ 25.3 signified a 3,4-*erythro* configuration making compound **4.6** a diastereomer of compound **4.5** (Crews *et al.*, 1984b).

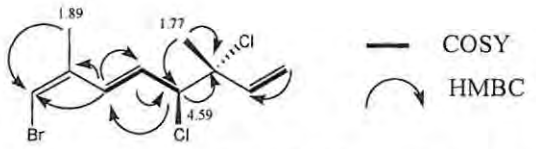

Figure 4.12 Selected HMBC and ^{1}H-^{1}H COSY correlations of compound **4.6**

All spectroscopic data for compound **4.6** were consistent with the proposed structure 3,4-*erythro*-8-bromo-3,4-dichloro-3,7-dimethyl-5*E*,7*Z*-octatriene.

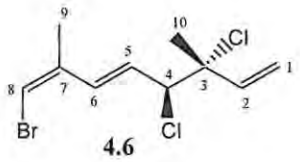

4.6

Table 4.5 ^{1}H (400 MHz, $CDCl_3$), ^{13}C (100 MHz, $CDCl_3$), ^{1}H – ^{1}H COSY and HMBC data for compound **4.6**

Carbon no.	δ_C	**δ_C mult**	**δ_H, mult, J_{Hz}**	**^{1}H – ^{1}H COSY**	**HMBC**
1a	116.2	CH_2	5.27, d, 10.6	H-2	C-3
1b			5.39, d, 17.0	H-2	C-3
2	139.7	CH	6.06, dd, 10.6, 17.0	H-1	-
3	71.9	C	-	-	-
4	69.5	CH	4.59, d, 9.0	H-5	C-2, C-3, C-6,
5	128.7	CH	5.96, dd, 9.1, 15.5	H-4, H-6	C-3, C-4, C-7
6	132.3	CH	6.83, d, 15.5	H-5	C-5, C-7, C-8,
7	135.6	C	-	-	-
8	107.6	CH	6.17, br s	H-9	C7
9	19.5	CH_3	1.89, br s	H-8	C-6, C-7
10	25.3	CH_3	1.77, br s	-	C-2, C-3, C-4

4.2.2.5 Compound 3A2d (4.7)

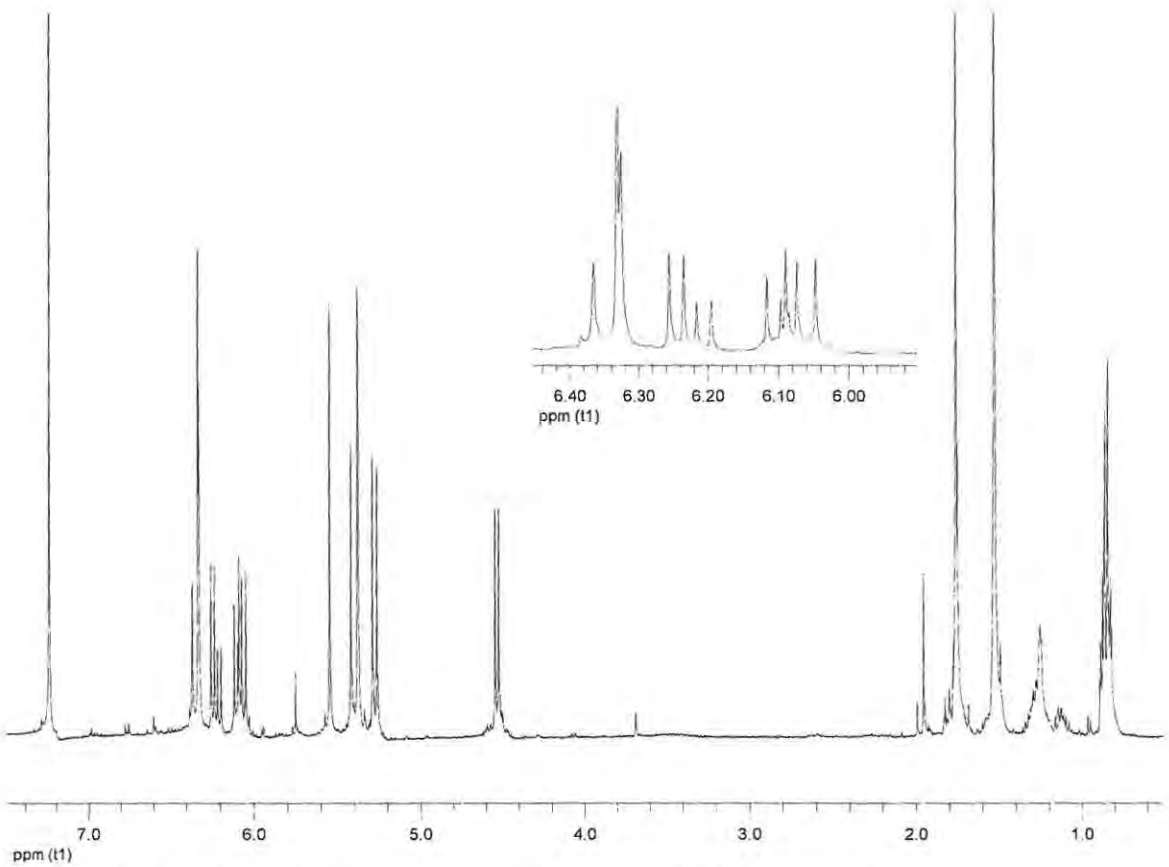

Figure 4.13 ^{1}H NMR spectrum of compound **4.7** ($CDCl_3$, 400 MHz)

HRFABMS showed a molecular ion peak at *m/z* 349.8795 for compound **4.7** suggestive of a molecular formula of $C_{10}H_{11}BrCl_4$. EIMS of compound **4.7** did not give a molecular ion but cluster ions were observed at *m/z* 215/217 $[C_5H_4BrCl_2]^+$ and 165/167 $[C_7H_{10}Cl_2]^+$. The base peak at *m/z* 277 was attributed to the loss of two chlorine atoms $[M^+-Cl_2]$.

NMR spectroscopic data of compound **4.7** showed a number of similarities to those of compound **4.4** including signals corresponding to the –CH=CH-CHX- (δ 6.23, dd, 8.6, 15.9 Hz, H-5; 6.32, d, 15.9 Hz. H-6; 4.54, d, 8.6 Hz, H-4) and $-CH=CH_2$ (δ 5.28, d, 10.6 Hz, H-1a; 5.39, d, 17.0 Hz, H-1b; and 6.09, dd, 10.6, 17.1, H-2) moieties. In addition, the ^{1}H NMR spectrum (Figure 4.13) exhibited a methyl singlet at δ 1.76 and two deshielded singlets at δ 6.37 (H-9) and 5.55 (H-8).

A significant difference between ^{1}H NMR spectrum of compound **4.4** and **4.7** was the presence of the singlet at δ 5.55 as compared to 6.38 for compound **4.4**, suggesting that a different halogen atom, as opposed to a chlorine atom, is attached to C-8. The ^{13}C NMR spectrum showed a methyl carbon at δ 25.1, two methines at δ 70.8 and 69.2, a quaternary carbon at δ 71.9 and six olefinic carbons from δ 143.3 – 116.4 (Table 4.6). A less deshielded carbon was observed at δ 118.4 (C-8) for compound **4.7** in place of 131.9 for compound **4.4**. This contributed to the suspicion that was confirmed by HRFABMS that a bromine and not a chlorine atom is present in the structure of compound **4.7** at position 8.

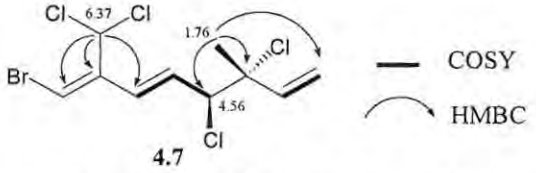

Figure 4.14 Selected HMBC and ^{1}H-^{1}H COSY correlations of compound **4.7**

Analysis of the 2D NMR data (COSY and HMBC) of compound **4.7** confirmed the structural assignment as follows. The vinylic proton at δ 6.37 (H-9) showed HMBC correlations to 129.5 (C-6), 143.3(C-7) and 118.4 (C-8) which was consistent with the substructure CH(X)=C(CHX_2)-CH=. The methyl protons at δ 1.76 (H_3-10) also showed HMBC correlations to δ 139.8 (C-2), 71.9 (C-3) and 69.2 (C-4) and while the proton at δ 4.54 (H-4) correlated to δ 129.0 (C-5) to give a second substructure =CH-CH-CX(CH_3)-CH= (Table 4.6 and Figure 4.14). The two substructures were joined and the structure of compound **4.7** was consolidated by the proton-proton coupling (^{1}H-^{1}H COSY) of 4.54 (H-4) to 6.23 (H-5) and the correlations of the methylene protons at δ 5.28 (H-1a) and 5.39 (H-1b) to 6.09 (H-2).

The geometry of the double bond between C-5 and C-6 was established by the analysis of the NOESY NMR data which correlated δ 4.54 (H-4) to 6.32 (H-6) and on the basis of the coupling constant (J = 15.6 Hz) which is indicative of an *E* geometry (Mynderse and Faulkener, 1975). A careful analysis of the NOESY NMR data also showed the correlation of δ 5.55 (H-8) to 6.32 (H-6) indicating a *Z* geometry of the $\Delta^{7,8}$ double bond.

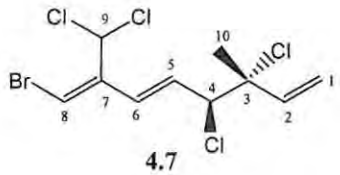

4.7

Table 4.6 ^{1}H -^{1}H (400 MHz, $CDCl_3$), ^{13}C (100 MHz, $CDCl_3$), ^{1}H – ^{1}H COSY and HMBC data for compounds **4.7**

No.	δ_C	δ_C mult	δ_H, mult, J_{Hz}	^{1}H – ^{1}H COSY	HMBC
1a	116.4	CH_2	5.28, d, 10.6	H-2	C-3
1b			5.39, d, 17.0	H-2	C-2, C-3
2	139.8	CH	6.09, dd, 10.6, 17.1	H-1	-
3	71.9	C	-	-	-
4	69.2	CH	4.54, d, 8.6	H-5	C-3, C-6
5	129.0	CH	6.23, dd, 8.6,15.9,	H-4, H-6	C-6
6	129.5	CH	6.32, d, 15.6	H-5	C-4, C-8, C-9
7	143.3	C	-	-	-
8	118.4	CH	5.55, s	-	C-6, C-7, C-9
9	70.8	CH	6.37, s	-	C-6, C-7, C-8
10	25.1	CH_3	1.76, s	-	C-2, C-3, C-4

A significant difference was observed in the number of compounds present in *P. cornutum* obtained from Kalk Bay and Noordhoek. While compounds **4.1** and **4.4** – **4.7** was obtained from KB06-3, only compound **4.4** was present in the algae sample NDK06-36 without further purification of the crude extract. Since the two samples were collected at different times of the year from different locations, it is possible that either the time of collection or the location or both affected the metabolite content of the algae. Collecting and extracting samples from the two locations at the same time of the year or from each location at different times of the year should be able to confirm the effect of seasonal changes on the chemical components of *P. cornutum*.

4.2.3 Biological activities of halogenated monoterpenes

Studies have shown that halogenated monoterpenes have cytotoxic activity towards human tumor cells (Fuller *et al.*, 1994) and halogenated monoterpenes from *P. corallorhiza* have been shown to act against oesophageal cancer cells (Knott *et al.*, 2005). This same group of compounds isolated from *P. cartilagineum* and *P. violaceum* has also been shown to inhibit mosquito larvae emergence (Crews *et al.*, 1984a). This project also investigated the halogenated monoterpenes isolated from *P. cornutum* and *P. corallorhiza* for their antiplasmodial activity and anti-oesophageal property.

4.2.3.1 Antiplasmodial activity of isolated monoterpenes from *P. corallorhiza* and *P. cornutum*

Compounds **4.1** and **4.4** – **4.7** from *P. cornutum* and compound **4.2** from *P. corallorhiza* were tested against the CQS strain of *P. falciparum* D10. The results (Table 4.7), showed compound **4.7** to be the most effective against the parasite with an IC_{50} value of 13 μM followed by compound **4.4** (IC_{50} 16 μM). This insignificant difference (3 μM) in the IC_{50} values between **4.4** and **4.7** indicated that the type of halogen present at position 8 of these compounds did not play a significant role in the antiplasmodial activity of the compounds. The result also revealed that a dichloro moiety at position 9 was preferred for antiplasmodial activity as both compounds **4.4** and **4.7** showed better activity than **4.1** (27 μM) with an aldehyde functionality. However, an electronegative as opposed to a methyl group at position 9 showed a much more potent antiplasmodial activity. This was observed from the IC_{50} values of isomeric compounds **4.5** and **4.6** which were 230 and 210 μM respectively and were far higher than for compound **4.1**, **4.4** and **4.7**. Although compound **4.6** ultimately showed better antiplasmodial activity than **4.5**, it was not significantly different, indicating that the configuration of the atoms at position 4 does not play an important role in the antiplasmodial activity of the compounds.

Compound **4.2** from *P. corallorhiza* showed only moderate antiplasmodial activity (IC_{50} = 79.3 μM). Since the crude hexane extracts is significantly more active than the

pure compounds, it is likely that more active halogenated monoterpenes may have been overlooked in the isolation process.

Table 4.7 *In vitro* antiplasmodial activity and cytotoxicity of compounds **4.1**, **4.2** and **4.4 – 4.7** against CQS D10 strain and CHO respectively

Compound	D10 IC_{50} (μM)	WHCO1 IC_{50} (μM)
4.1	27	47.3
4.2	79.3	nd
4.4	16	17.8
4.5	230	87.6
4.6	210	
4.7	13	40.2

nd = not determined

The oesophageal cancer activity of compounds **4.1** and **4.4 – 4.7** (Table 4.7) showed a similar trend as observed for the antiplasmodial activity, suggesting the dichloromethyl or aldehyde functionality is important for activity.

At the time of testing the compounds, separation of the isomeric compounds **4.5** and **4.6** had not been achieved and thus the anti-oesophageal activity of the isomers was tested as a mixture. The isomers were the least active against the cancer cells with IC_{50} of 87.6 μM.

It can thus be concluded that although the isomers showed the least cytotoxicity and **4.4** showed the most cytotoxic activity, compound **4.7** showed the best antiplasmodial activity relative to cytotoxic activity.

4.3 Experimental

4.3.1 General experimental

All solvents and instruments used were the same as described in section 3.4.1.

UV spectra were obtained using the GBC UV/VIS 916 spectrophotometer. Optical rotations were measured on a Perkin-Elmer 141 polarimeter. The IR spectra were obtained using the Perkin-Elmer Spectrum 2000 FT-IR spectrometer as films on KBr disks. HRFABMS was conducted by Dr Louise Fourie at the University of North West, Potchefstroom on a VG-7070E mass spectrometer.

4.3.2 Plant material (KOS06-14b , KB06-3, NDK06-1b)

P. corallorhiza was collected by hand at Noordhoek in January 2006. *P. cornutum* was collected from Kalk Bay and Noordhoek in January and September 2006 respectively. A voucher specimen of each alga (KOS06-14b, KB06-3 and NDK06-1b) is kept at the Division of Pharmaceutical chemistry, Rhodes University. The algae were identified by Professor John Bolton at the Department of Botany, University of Cape Town.

4.3.3 Extraction and isolation

4.3.3.1 *P. corallorhiza* from Noordhoek (NDK06-1b)

P. corallorhiza was collected from Noordhoek in January 2006. The sample (33.83 g dry weight) was stored frozen until extraction when it was extracted as described in section 2.3.3. The crude fraction was partitioned into hexane (NDK06-1bA, 800.4 mg), CH_2Cl_2 (NDK06-1bB, 734.3 mg), EtOAc (NDK06-1bC, 39.2 mg) and H_2O fractions. The H_2O fraction was passed through an HP-20 column and eluted with MeOH (NDK06-1bD, 55.7 mg) and CH_2Cl_2 (NDK06-1bE, 21.8 mg).

Column chromatography of NDK06-1bA by solvent gradient column chromatography afforded nine fractions (A1-9). Normal phase HPLC of fraction A1 using 100% hexane as the mobile phase afforded compound **4.2** (21.4 mg, 0.06% dry weight).

4.3.3.2 *P. cornutum* from Kalk Bay (KB06-3)

P. cornutum was collected from Kalk Bay near Cape Town in January 2006. The sample (26.02g dry weight) was stored frozen until it was extracted. The frozen sample was extracted as described in section 2.3.3. The crude extract was partitioned into hexane (KB06-3A, 784 mg), CH_2Cl_2 (KB06-3B, 706 mg) and EtOAc (KB06-3C, 135 mg)

Silica gel column chromatography of KB06-3A and KB06-3B using step gradient of *n*-hexane-EtOAc afforded nine fractions each (KB06-3A1 – 9 and KB06-3B1 – 9). Normal phase HPLC (100% hexane) of KB06-3A1 using 100% hexane as mobile phase gave pure **4.4** (491.6 mg, 1.8% dry weight) [15]. Further purification of KB06-3A1a (Scheme 4.2) by normal phase HPLC using 100% hexane gave rise to **4.5** (325.9 mg, 1.2% dry weight) and **4.6** (455.7 mg, 1.7% dry weight). Compound **4.7** (25.5 mg, 0.1% dry weight) and more of compound **4.4** were isolated from normal phase HPLC of KB06-3A2 using100% hexane as mobile phase. Fractionation of the fractions obtained from the silica gel column chromatography of KB06-3B using a solvent gradient method gave compound **4.1** (455.7 mg, 1.7% dry weight). More of **4.1** was also obtained from normal phase HPLC of KB06-3A3 and KB06-3B3 using 90:10 hexane-EtOAc (Scheme 4.2).

4.3.3.3 *P. cornutum* from Noordhoek (NDK06-36)

NDK06-36 (16.93g dry weight) was collected from Noordhoek near Port Elizabeth in September 2006. It was stored frozen and extracted under similar conditions as the sample collected from Kalk Bay. The frozen sample was submerged in methanol and kept in the fridge (4 °C) for one hour. After decanting methanol, the alga sample was

[15] Total mass and % dry weight was calculated based on the amount of each compound expected had the entire extract been purified and not on the actual amount obtained from purifying some of the extracts.

extracted three times with 2:1 CH_2Cl_2-MeOH (500ml) at a temperature of 30 – 40 °C. The combined organic fraction of the crude product after the separation into CH_2Cl_2 gave pure compound **4.4** (1.14 g, 6.7% dry wt) without further purification.

4.3.4 Compounds isolated

Compound 4.1

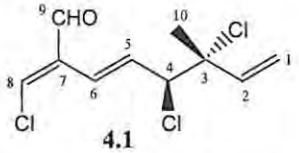

4.1

3,4-*erythro*-3,4,8-trichloro-1,5*E*,7*E*-en-7-al (**4.1**): yellow oil; $[\alpha]_D$ -14.2; ^{1}H NMR and ^{13}C NMR in Table 4.3; EIMS (70 eV) *m/z* (int, %) 115/117 (13/27), 163/165 (15/8), 181 (basepeak); 217/219 (36/20).

Compound 4.2

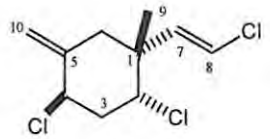

4.2

Epi-ploccamene D (**4.2**): colourless oil; ^{1}H NMR and ^{13}C NMR in Table 4.1.

Compound 4.4

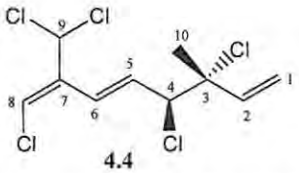

4.4

3,4-*erythro* -7-dichloromethyl-3-methyl-3,4,8-trichloro-1,5*E*,7*E*-octatriene (**4.4**): colourless oil; $[\alpha]_D$ -47.7, lit $[\alpha]_D$ -39.3; ^{1}H NMR and ^{13}C NMR in Table 4.2; EIMS (70 eV) *m/z* (int, %) 54 (80), 128/129 (40/46), 146/147 (34/27); 163/165 (42/36); 181 (basepeak), 183 (88); 199/201 (38/28), 235/237 (17/18);; HRFABMS obsd. *m/z* 305.9308; Calc. *m/z* 281.9303.

Compound 4.5

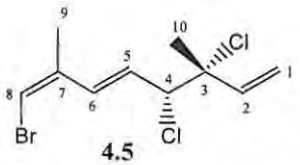

4.5

3,4-threo-8-bromo-3,4-dichloro-3,7-dimethyl-5E,7Z-octatriene ***(4.5)****:* colourless oil; $[\alpha]_D$ +5.0; λ_{max} (hexane) 252nm; IR ν_{max} (KBr): 1460, 2852, 2921 cm^{-1}; ^1H and ^{13}C NMR in Table 4.4; EIMS, *m/z* (int, %) 77/79 (23/65); 91 (19), 114 (base peak), 116 (40), 131 (32), 167/169 (52/19), 193/195 (32/42), 203, 205 (19/12); HRFABMS obsd. *m/z*. 281.9572; Calc. *m/z* 281.9578; COSY, H1-H2, H4-H5, H5-H6

Compound 4.6

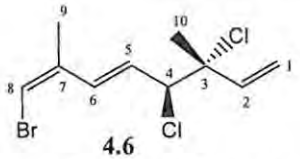

4.6

3,4-erythro-8-bromo-3,4-dichloro-3,7-dimethyl-5E,7Z-octatriene ***(4.6)****:* colourless oil; $[\alpha]_D$ -38.6; λ_{max} (hexane) 252nm; IR ν_{max} (KBr): 1460, 2852, 2921 cm^{-1}; ^1H and ^{13}C NMR in Table 4.5; EIMS, *m/z* (int, %) 77/79 (23/65); 91 (19), 114 (base peak), 116 (40), 131 (32), 167/169 (52/19), 193/195 (32/42), 203, 205 (19/12); HRFABMS obsd. *m/z*. 281.9572; Calc. *m/z* 281.9578; COSY, H1-H2, H4-H5, H5-H6.

Compound 4.7

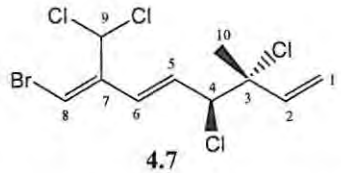

4.7

3,4-erythro-8-bromo-3,4-dichloro-7-(dichloromethyl)-3-methyl-5E,7E-octatriene ***(4.7)****:* colourless oil; $[\alpha]_D$ -10.8; λ_{max} (hexane) 232nm; IR ν_{max} (KBr): 1451, 2849, 2918 cm^{-1}; ^1H and ^{13}C NMR in Table 4.6; EIMS, *m/z* 128/129 (11/20), 165/167 (32/17), 201/203 (45/32), 215/217 (15/16), 277 (basepeak); HRFABMS obsd. *m/z* 349.8795; Calc. *m/z* 349.8798; COSY, H1-H2, H4-H5, H5-H6

4.3.5 Antiplasmodial assay

The assay was carried out at the Division of Pharmacology, University of Cape Town.

Compounds **4.1** – **4.2** and **4.4** – **4.7** were tested in duplicate against CQS *P. falciparum* D10 strain. The continuous *in vitro* culture of the asexual erythrocytic stage used in the experiment was maintained using a modified method of Trager and Jensen (1976). The result was quantitatively assessed to determine the *in vitro* antiplasmodial activity through the lactate dehydrogenase assay according to a modified method of Makler (1993) as discussed in sections 2.3.5. The full dose response experiment of the compounds was started at a concentration of 100 μg/ml and was serially diluted 2-folds to give 10 concentrations with a minimum of 0.195 μg/ml. Chloroquine was tested at a starting concentration of 100 ng/ml. The highest concentration of solvent used did not have any measurable effect on the parasites. The 50% inhibitory concentration (IC_{50}) values were obtained using a non-linear dose-response curve fitting analysis via GraphPad Prism v.4.0 software.

4.3.6 Anti-oesophageal Assay

The Anti-oesophageal assay was conducted by Catherine Whibley of the Department of Medical Biochemistry at the University of Cape Town.

4.3.6.1 Cell culture

The IC_{50} values of compound **4.1** and **4.4** – **4.7** were determined as described by Rajput *et al.* (2004). WHCO1 oesophageal cancer cell were cultured and maintained in DMEM supplemented with 10% fetal calf serum, 100 U/ml penicillin and 100 μg/ml streptomycin in a humidified, 37 °C, CO_2 environment.

4.3.6.2 Crystal violet assay

The cells were plated at 1500 cells/well in 90 μL medium in Cell-Star 96 well plates and incubated for 24 hours at 37 °C. The compounds **4.1** and **4.4** – **4.7** were added to the medium in a 0.2% DMSO solution at varying concentrations and incubated for

another 48 hours. The culture media was drained from each well and 100 μL of absolute methanol was added for 10 minutes. The methanol was drained and replaced with crystal violet solution (1% crystal violet and 50% methanol) for 20 minutes. The plates were rinsed with water and 100 μL of water was added to each well for an hour. The water was discarded and replaced with another 100 μL of water for one hour before reading the plates at 595 nm on Anthos microplate reader 2001.

4.3.6.3 The MTT Assay

The MTT assay was carried out according to the modified method of Mosmann (1983) as described in section 2.3.7. Oesophageal cancer cells (1500) were seeded in cell-star 96 well plates and incubated for 24 hours. Monoterpenes **4.1** and **4.4 – 4.7** were added at varying concentrations in 0.2% final concentration of DMSO and incubated for 48 hours. MTT solution (10 μL) was then added to each well and incubated for another four hours. Solubilization solution (100 μL) was added to each well for further incubation overnight. The plates were read at 595 nm on an Anthos microplate reader 2001.

Supplementary information: NMR, IR and MS supplementary data are available on CD.

References

Abreu, P. M. and Galindro, J. M. Polyhalogenated Monoterpenes from *Plocamium cartilagineum* from the Portuguese Coast. *Journal of Natural Product* **1996**, 59, 1159-1162

Branch, G. M.; Griffiths, C. L.; Branch, M. L. and Beckley, L. E.. *Two Oceans: A Guide to the Marine Life of Southern Africa* **2005**, first edition, David Philips Publishers, South Africa, p. 318.

Crews, P. and Kho, E. Cartilagineal. An Unusual Monoterpene Aldehyde from Marine Alga. *Journal of Organic Chemistry* **1974**, 39, (22), 3303-3304.

Crews, P.; and Kho, E. Plocamene B, a New Cyclic Monoterpene Skeleton from a Red Marine Alga. *Journal of Organic Chemistry* **1975**, 40, (17), 2568 – 2570.

Crews, P.; Meyer, B. L.; Naylor, S.; Clason, E. L.; Jacobs, R. S. and Staal, G. B. Bio-active Monoterpenes from Red Seaweeds. *Phytohemistry* **1984**a, 23, (7), 1449-1451.

Crews, P.; Naylor, S.; Hanke, F. J.; Hogue, E. R.; Kho, E. and Braslau, R. Halogen Regiochemistry and Substituent Stereochemistry Determination in Marine Monoterpenes by ^{13}C NMR. *Journal of Organic Chemistry* **1984**b, 49, 1371 – 1377.

Davies-Coleman, M. T. and Beukes, D. R. Ten Years of Marine Natural Products Research at Rhodes University. *South African Journal of Science* **2004**, 100, 539 – 544.

De Napoli, L.; Fattorusso, E.; Magno, S. and Mayol, L. Acyclic Polyhalogenated Monoterpene from Four Marine Hydroids. *Biochemical Systematics and Ecology* **1984**, 12, (3), 321 – 322.

Faulkner, D. J. and Stallard, M. O. 7-Chloro-3,7-dimethyl-1,4,6-tribromo-1-octen-3-ol, A Novel Monoterpene Alcohol from *Aplysia californica*. *Tetrahedron Letters* **1973**, 14, 1171 – 1174.

Fuller, R. W.; Cardellina II, J. H.; Jurek, J.; Scheuer, P. J.; Alvarado-Lindner, B.; McGuire, M.; Grey, G. N.; Steiner, J. R.; Clardy, J.; Menez, E.; Shoemaker, R. H.; Newman, D. J.; Snader, K. M and Boyd, M. R. Isolation and Structure/Activity Features of Halomon-Related Antitumor Monoterpenes from the Red Alga *Portieria hornemannii*, *Journal of Medicinal Chemistry* **1994**, 37, 4407 – 4411.

Imperato, F.; Minale, L. and Ricco, R., Constituents of the Digestive Gland of Molluscs of the Genus *Aplysia*. II. Halogenated Monoterpenes from *Aplysia limacine*. *Experientia* **1977**, 33, 1273-1274.

Knott, M. G.; Mkwananzi, H.; Arendse, C. E.; Hendricks, D. T.; Bolton, J. J. and Beukes, D. R. Plocoralides A-C: Polyhalogenated Monoterpenes from the Marine Alga *Plocamium corallorhiza*. *Phytochemistry* **2005**, 66, 1108-1112.

Lubke, R. A. and Seagrief, S. C. *In The Field Guide to the Eastern Cape Coast*, **1998**, pp 65, The Grahamstown Centre of the Wildlife Society of South Africa: Port Elizabeth.

Lubke, R. A.; Gess, F. W. and Bruton, M. N. *A Field Guide to the Eastern Cape Coast*, **1988**, pp 56 – 57, The Grahamstown Centre of the Wildlife Society of South Africa.

Mann, M. G. A.; Mkwananzi, H.; Antunes, E. M.; Whibley, C. E.; Hendricks, D. T.; Bolton, J. J. and Beukes, D. R. Halogenated Monoterpene Aldehydes from the South African Marine Alga *Plocamium corallorhiza*. *Journal of Natural Products* **2007**, 70, 596 – 599.

Mynderse, J. S. and Faulkner, D. J. Polyhalogenated Monoterpenes from the Red Alga *Plocamium cartilagineum*. *Tetrahedron* **1975**, 31, 1963 – 1967.

Mynderse, J. S.; Faulkner, D. J.; Finer, J. and Clardy, J. (1R,2S,4S,5R)-1-bromo-trans-2-chlorovinyl-4-5-dichloro-1,5-dimethyl-cyclohexane, a New Monoterpene Skeletal Type from the Red Alga, *Plocamium violaceum*. *Tetrahedron Letters* **1975**, 26, 2175 – 2178.

Rajput, J.; Moss. J. R.; Hutton, A. T.; Hendricks, D. T.; Arendse, C. E. and Imrie, C. Synthesis, Characterization, and Cytotoxicity of some Palladium(II), Platinum(II), Rhodium(I) and Iridium(I) Complexes of Ferrocenylpyridine and Related Ligands. Crystal and Molecular Structure of *Trans*-Dichlorobis(3- ferrocenylpyridine)palladium(II). *Journal of Organometallic chemistry* **2004**, 689, 1553 – 1568.

Stierle, D. B.; Wing, R. M. and Sims, J. J. Marine Natural Products-XVI, Polyhalogenated Monoterpenes from the Red Alga *Plocamium* of Antarctica. *Tetrahedron* **1979**, 35, 2855 – 2859.

Chapter 5

Synthetic modifications of halogenated monoterpenes from *Plocamium cornutum*

5.1 Introduction

With the structures of the antiplasmodial halogenated monoterpenes in hand we were interested in improving on their biological activity. Our first goal was thus to improve on the aqueous solubility of these highly non-polar compounds. We envisaged achieving this by exploring reactions to selectively dihydroxylate the $\Delta^{1,2}$ double bond followed by phosphorylation. A second goal was to develop 1-deoxy-D-xylulose 5-phosphate reductoisomerase (DXR) inhibitors from natural products. DXR is an enzyme present in the non-mevalonate pathway of isoprenoid biosynthesis and is an important new target for the development of antimalarial drugs. This enzyme has become available to us through our collaborators in the Biochemistry, Microbiology and Biotechnology Department at Rhodes University.

5.1.1 The mevalonate non-mevalonate pathway[16] to terpene biosynthesis

For years, the mevalonate pathway was considered the only pathway for the production of isoprene units, IPP (**5.9**) and DMAPP (**5.10**) (Rohdich *et al.*, 2001). The mevalonate pathway starts with the condensation of three molecules of acetyl-coenzyme A (Acetyl-CoA, **5.11**) to form 3-hydroxy-3-methylglutaryl Coenzyme A (HMG CoA, **5.13**). HMG-CoA reductase enzyme reduces HMG-CoA (**5.13**) to mevalonate (**5.14**) which is in turn converted into mevelonate-5-diphosphate (**5.16**) by kinases in two phosphorylation reactions. Decarboxylation of this compound then leads to the formation of IPP (**5.9**) and DMAPP (**5.10**) (Scheme 5.1).

An alternative pathway, the non-mevalonate pathway, was discovered in the early 1990's (Rohmer, *et al.*, 1993). Since its discovery the pathway has been shown to be

[16] The non-mevalonate pathway is also known as mevalonate-independent pathway, DOXP or 2-C-Methyl-D-erythritol 4- phosphate (MEP) pathway.

present in many bacteria, green algae and chloroplast of higher plants (Lichtenthaler, 1999). This pathway has also been found to occur in the apicoplast of the malaria parasite *P. falciparum* (Jomaa *et al.*, 1999).

Rohmer's research group found that the initial stage of the seven step pathway involve the condensation of glyceraldehyde-3-phosphate (**5.2**) and pyruvate (**5.1**) by DOXP synthase (DXS) to form DOXP (**5.3**) (Rohmer, *et al.*, 1993). DOXP (**5.3**) so formed then serve as a substrate for the enzyme DOXP reductoisomerase (DXR or IspC) in the second step. Through intramolecular rearrangement and reduction reaction, DXR converts DOXP (**5.3**) to 2-C-Methyl-D-erythritol 4- phosphate (MEP, **5.4**). For this stage, DXR enzyme has been shown to require NADPH and a divalent cation Mg^{2+}, Co^{2+} or Mn^{2+} for activity (Kuzuyama *et al.*, 1998). In the next step MEP (**5.4**) is cytidilated by 4-diphosphocytidyl-2-C-methyl-D-erythritol (CDP-ME) synthase (or IspD) to produce CDP-ME (**5.5**) with the release of pyrophosphate (Rohdich *et al*, 1999). Subsequent phosphorylation of the 2-hydroxy group on the CDP-ME by CDP-ME kinase (IspE) yields 4-diphosphocytidyl-2-C-methyl-D-erythritol-2-phosphate (CDP-ME-2-phosphate, **5.6**) in an ATP dependent reaction (Luttgen *et al.*, 2000). Cyclization of the intermediate—phosphate by 2-C-methyl-D-erythritol-2,4-cyclodiphosphate (MECDP) synthase (IspF) results in the formation of MECDP (**5.7**) with the release of Cytidine monophosphate (CMP) (Herz *et al.*, 2000). This ring is opened by a reduction reaction to give 1-hydroxy-2-methyl-2-buten-4-yl diphosphate (HMBPP, **5.8**) and the reaction is catalysed by GcpE (or IspG). The overall reaction is a two-electron reduction process that involves the cleavage of two C-O bonds. Two reaction mechanisms involving cysteine residue has been proposed for the conversion (Hecht *et al.*, 2001). The final step of the non-mevalonate pathway is another reduction by the LytB (IspH) enzyme with the removal of a hydroxyl group to give a mixture of IPP (**5.9**) and DMAPP (**5.10**) (Scheme 5.1) (Altincicek *et al.*, 2002).

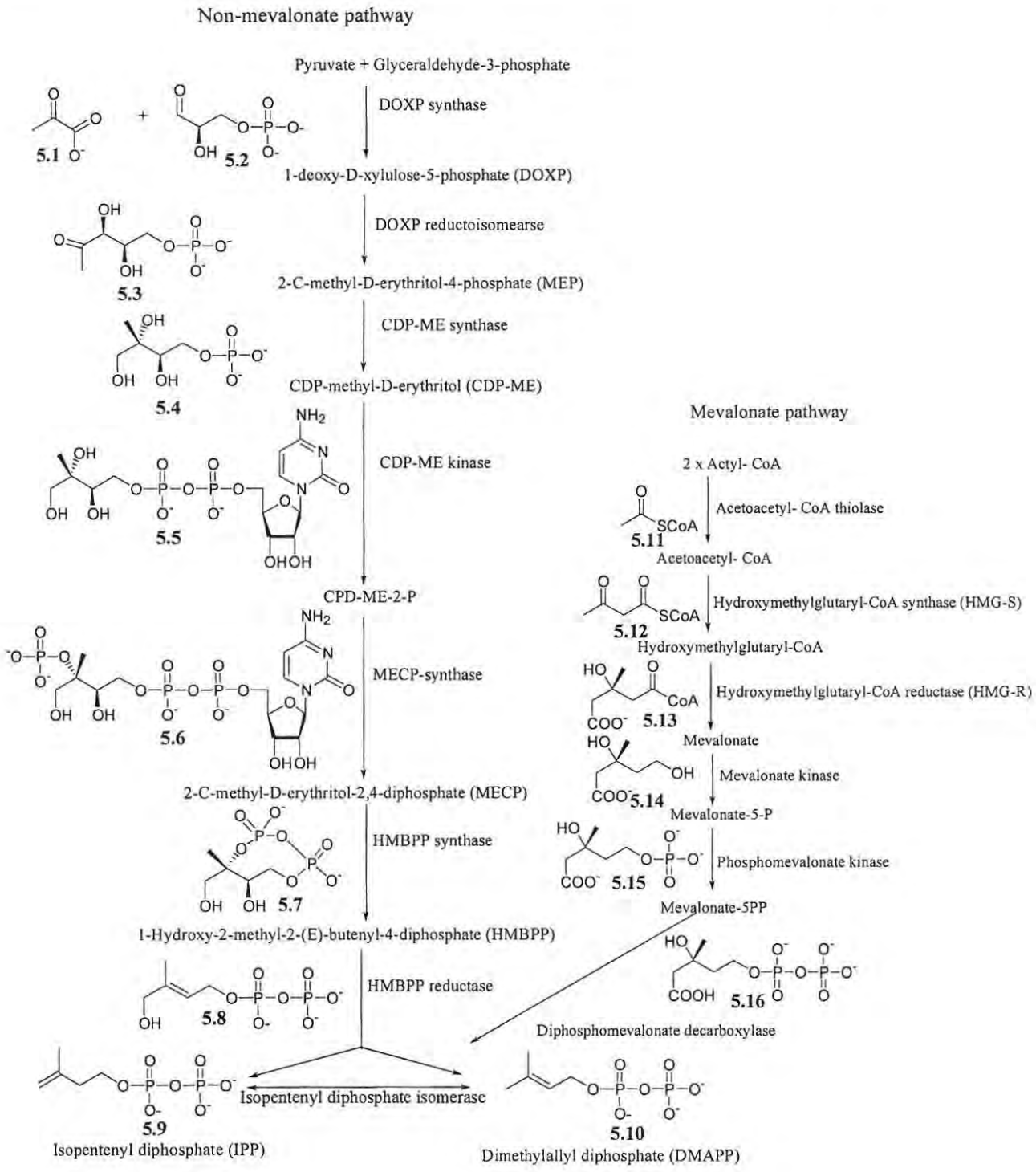

Scheme 5.1 The mevalonate and non-mevalonate pathway (Modified from Testa *et al.*, 2006)

This research project targets the DXR, the second enzyme of the MEP (**5.4**) pathway. DXR has been cloned from different organisms including *Escherichia coli* (Kuzuyama *et al.*, 1998), *P. falciparum* (Jomaa *et al.*, 1999), *Arabidopsis thaliana*

(Schwender *et al.*, 1999) and *Synechocystis* sp. PCC6803 (Yin and Proteau, 2003). DOXP (**5.3**) is not only found in the non-mevalonate pathway but also as a biosynthetic intermediate for thiamine and pyridoxol, therefore the rearrangement and reduction of DOXP (**5.3**) by DXR to MEP (**5.4**) is the first committed step in the production of IPP (**5.9**) and DMAPP (**5.10**) (Kuzuyama *et al.*, 1998).

The enzymes in the pathway have attracted a lot of research attention as they promise to be good targets for antibiotics and antimalarial agents. DXR has been receiving a lot of attention due to the fact that its gene has been cloned and can be easily expressed in *E. coli*. In addition, DXR was available and was thus selected for this project.

5.1.2 1-Deoxy-D-xylulose 5-phosphate reductoisomerase (DXR)

DXR, is a V-shaped homodimer (Figure 5.1). Each monomer has a cleft-like structure that is covered by a flexible loop, and subdivided into three domains:

i. The N-terminal or the amino terminal domain which forms one arm of the V and is responsible for binding NADPH.
ii. A central or catalytic region that contains the binding site for substrate, metal ion and residues required for catalysis. It connects the two arms of the V-shaped monomers.
iii. The carboxyl or C-terminal domain that forms the second arm of the V and appears to play a structural role in supporting the catalytic domain (Fernandes and Proteau, 2006)

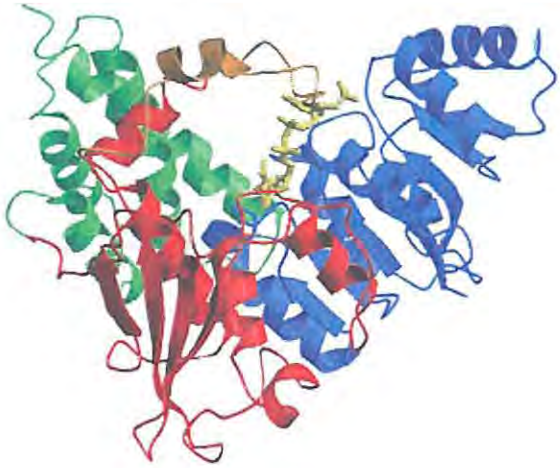

Figure 5.1 A ribbon representation of DXR monomer with NADPH modeled (Reuter *et al.*, 2002)

A cluster of hydrophilic amino acids binds metal ions in the DXR. These acidic residues seemed involved in the complexation of the divalent ion which is known to be Mn^{2+} and necessary for the enzyme activity (Reuter *et al.*, 2002). A flexible loop is suggested to close the active site after the binding of the substrate. The loop appeared to be more ordered when there is a substrate or an inhibitor bound to the enzyme but less defined in the structure of the enzyme alone. The residues making up the loop are thus proposed to promote proper binding of substrate and good orientation (Fernandes and Proteau, 2006). The loop folds over the active site after the binding of the substrate and completely shields the site from solvent. This probably creates a highly specific binding pocket (Reuter *et al.*, 2002). The enzyme has been suggested to work via an ordered sequential mechanism where NADPH binds first followed by the substrate (Proteau, 2004).

5.1.3 DXR catalyzed reaction

The DXR enzyme combines rearrangement and reduction stages so that the formation of MEP (**5.4**) from DOXP (**5.3**) occurs in a single step. The intermediate 2-C-methyl-D-erythrose 4-phosphate (**5.17**) is formed during the conversion of DOXP (**5.3**) to MEP (**5.4**) (Scheme5.2) although it has not been directly detected (Proteau, 2004).

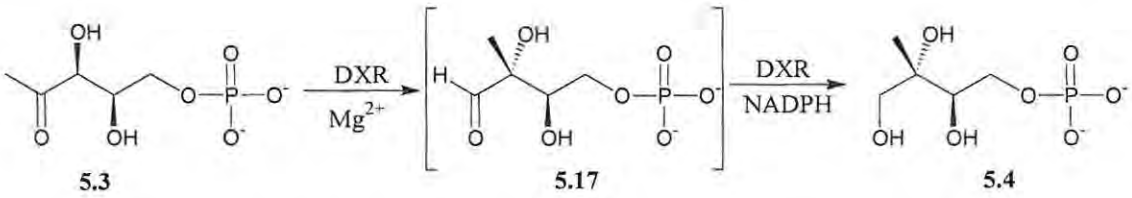

5.3 5.17 5.4

Scheme 5.2 DXR-catalyzed reaction (Modified from Proteau, 2004)

The stereochemistry of the reaction is such that there is delivery of pro*S* hydride from NADPH. This has resulted in the classification of the enzyme as a class B dehydrogenase. The C-3 hydrogen of DOXP (**5.3**) becomes pro*S* hydrogen at C-1 of MEP and the C-1 pro*R* hydrogen is delivered from NADPH (Proteau, 2004).

5.1.4 Mechanism of the rearrangement of DOXP to 2-C-methyl-D-erythrose 4-phosphate

Two mechanisms are currently proposed for the rearrangement of DOXP to the intermediate 2-C-methyl-D-erythrose 4-phosphate (**5.17**) (Scheme 5.3):

i. An α-ketol rearrangement
ii. A retro-aldol/aldol reaction

The α-ketol rearrangement is thought to involve the deprotonation of C-3 hydroxy group of DOXP and subsequent migration of the C-2 unit to form the intermediate 2-C-methyl-D-erythrose 4-phosphate (Hoeffler *et al.*, 2002). A retro-aldol/aldol reaction involves the formation of the enolate of hydroxyacetone and glyceraldehydes phosphate. Attempts to mimic the reaction by incubating DXR with glyceraldehyde and hydroxyacetone have not been successful (Proteau, 2004). To date the two mechanisms have not been ruled out but in both cases the intermediate remain tightly bound to DXR before the NADPH mediated reaction takes place (Singh *et al.*, 2007).

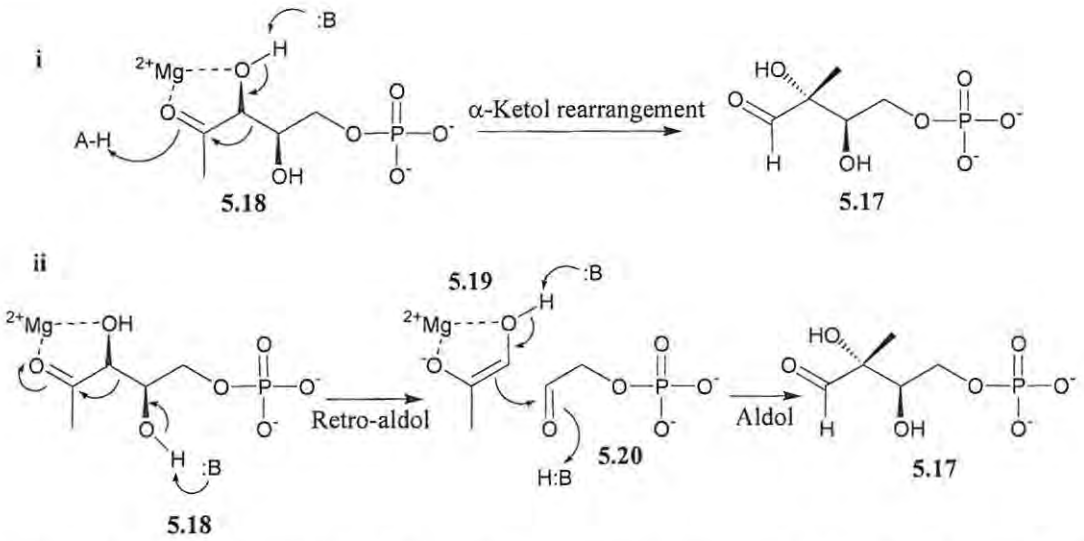

Scheme 5.3 Proposed mechanisms of the rearrangement of DOXP (**5.3**) attached to Mg^{2+} **(5.18)** to the intermediate 2-C-methyl-D-erythrose 4-phosphate (**5.17**) (Proteau, 2004)

5.1.5 Inhibitors of DXR

Various avenues are being exploited for antiplasmodial agents that will be effective and that the *Plasmodium* parasites will have little or no chance of developing resistance to. Also very important is that it should be selective for the *Plasmodium* parasites. DXR catalyses the first committed step of the non-mevalonate pathway which is not found in mammal and thus makes a very good selective target for the *Plasmodium* organisms. Recently inhibition of DXR has been the focus of many antimalarial drug development researches.

Fosmidomycin (**5.21**, Figure 5.2), an antibacterial was reported to be an inhibitor of DXR shortly after the discovery of the enzyme. Studies have shown fosmidomycin as a slow, tight-binding inhibitor that display an initial competitive inhibition of DOXP (**5.3**) and another non-competitive inhibition with DOXP (**5.3**) (Proteau, 2004). FR900098 (**5.22**), natural product derivative of fosmidomycin, has also been shown to inhibit DXR with greater activity than fosmidomycin (**5.21**), both of them with low toxicity in human (Jomaa *et al.*, 1999).

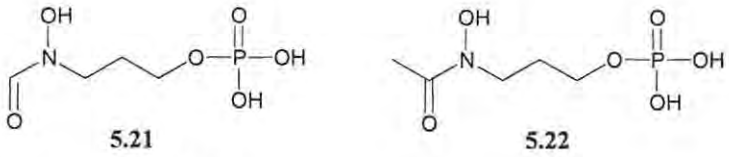

5.21 5.22

Figure 5.2 Inhibitors of DXR

Although active, both fosmidomycin (**5.21**) and FR900098 (**5.22**) have poor oral bioavailability due to their high hydrophilicity as a result of ionization of the phosphonate group at physiological pH (Ortmann *et al.*, 2003). This has led to modification of these compounds to improve on the oral bioavailability. Transformation of the phosphonate moiety on the FR900098 (**5.22**) to a phosphodiaryl ester prodrug (**5.22a**, Figure 5.3) has been shown to improve bioavailability (Reichenberg *et al.*, 2001). These esters however produce phenol, which is toxic, during drug processing. To avoid this complication Ortmann *et al.* (2003) developed acyloxyalkyl esters of the compounds (**5.22b**, Figure 5.3). These have improved oral bioavailability due to the masking of the phosphonate moiety with acyloxyalkyl ester group. The acyloxyalkyl expected to hydrolyze to acetic acid and acetaldehyde (Ortmann *et al.*, 2003).

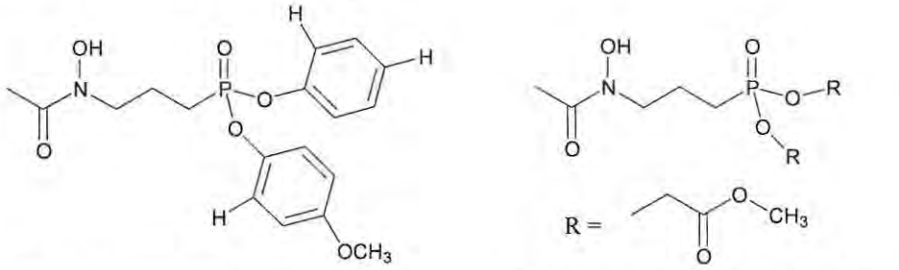

Phosphodiaryl ester derivative (**5.22a**) Acyloxyalkyl ester derivative (**5.22b**)

Figure 5.3 Derivatives of FR900098 (**5.22**)

Fosmidomycin (**5.21**) and FR900098 (**5.22**) α-substituted analogues have also been investigated for better half-life and oral bioavailability. Different analogues of the parent drugs containing phenyl moiety in the α-position have been investigated and have all been shown to surpass fosmidomycin (**5.21**) activity in inhibiting parasite growth. However, all of these compounds are weaker inhibitors of *E. coli* DXR than fosmidomycin (**5.21**) (Haemers *et al.*, 2006). Of particular note is the analogue **5.23** which showed twelve fold more *in vitro* antimalarial activity than fosmidomycin (**5.21**) and also more activity than FR900098 (**5.22**) which is considered the most potent analogue to date. It is suggested that lipophilic and electronegative properties

of the 3,4-dichloro substitution of the α-phenyl group favours the interaction of the compound with *P. falciparum* DXR. It is also suggested that the aromatic ring in the α-position may improve the capacity of the analogues to enter the parasite cells (Haemers *et al.*, 2006).

5.23

Two analogues of DOXP (**5.3**), 3*S*-hydroxypentan-2-one 5-phosphate (**5.24**) and 4*S*-hydroxypentan-2-one 5-phosphate (**5.25**), with only one hydroxyl group have been found to inhibit DXR although at a much higher concentration. These two compounds are not substrate for DXR and therefore they reveal the critical role of both hydroxyl groups in the substrate (Proteau 2004).

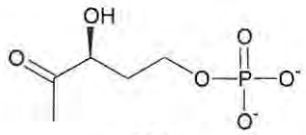

5.24

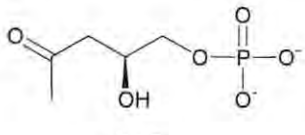

5.25

The substrate and known inhibitor of DXR, DOXP (**5.3**) and fosmidomycin (**5.21**) respectively, have common chemical features. These compounds contain phosphate (compound **5.3**) or phosphonate (compound **5.21**) and carbonyl functionalities which are separated by five bonds (Kuzuyama *et al.*, 1998). The same properties are also found in 2-C-methyl –D-erythrose-4-phosphate, the intermediate product, of the rearrangement and reduction of DOXP to 2-C-Methyl-D-erythritol 4- phosphate (MEP, **5.4**) by DXR (Scheme 5.3). Fosmidomycin (**5.21**) orientate itself within the enzyme active site by the binding of its phosphonate group to the positively charged pocket of the enzyme and the binding of the hydroxamic acid group to the amphipathic region of the enzyme (Sweeney *et al.*, 2005). A phosphate or phosphonate head is thus an important consideration when developing or modifying potential inhibitors for the enzyme.

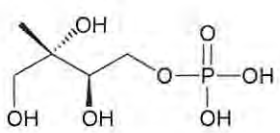

MEP (**5.4**)

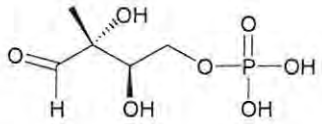

2-C-methyl-$_D$-erythrose-5-phosphate (**5.17**)

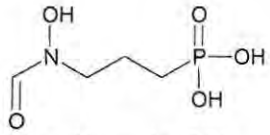

Fosmidomycin (**5.21**)

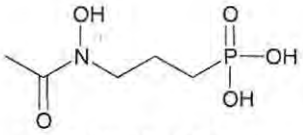

FR900098 (**5.22**)

Starting from monoterpene **4.4** and progressing to modify it by dihydroxylation and phosphorylation our target compound would thus be compound **5.26** (Figure 5.4). This seemed a reasonable proposal since fosmidomycin (**5.21**) analogues with a long acyl chain such as compound **5.27**, still show low micromolar inhibition of DXR (Ortmann *et al.*, 2007).

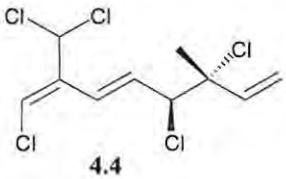

4.4

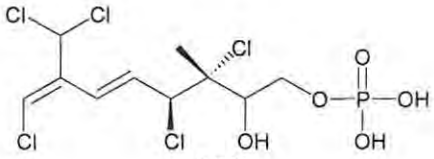

5.26

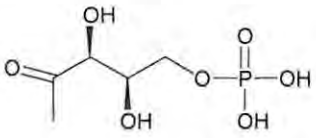

DOXP (**5.3**)

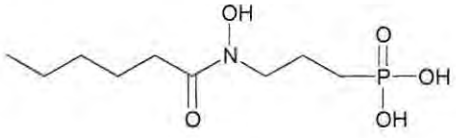

5.27

Figure 5.4 Proposed modifications of halogenated monoterpene **4.4** to phosphate derivative **5.26**

Although there is ample literature precedent for the dihydroxylation of alkenes and phosphorylation of alcohols, performing these modifications on compound **4.4** could still present a significant challenge.

5.1.6 Proposed synthetic modifications of halogenated monoterpene 4.4 (inhibitor design)

The halogenated monoterpenes isolated from the alga *P. cornutum* have already been found to be active against the CQS *P. falciparum* D10 strain. Of the five compounds

isolated, compound **4.4** was selected for synthetic chemical modification to inhibit the DXR as it was the most abundant. The antiplasmodial activity of compound **4.4** as described in the previous chapter was due to the presence of the electronegative gem-dichloride group at position 9 of the compound (Figure 5.5). Although the exact mode of action of the monoterpene is unknown it is unlikely that it disrupts the non-mevelonate pathway as it does not possess the essential phosphate group. Synthetic modifications of the head part of compound **4.4** (the terminal alkene end) is consequently expected to give the compound a more specific activity and in combination with the action of the gemchloride activity establish a dual mode of action on the *Plasmodium* parasite. This dual action approach was expected to improve the chances of discovering a potent antimalarial compound.

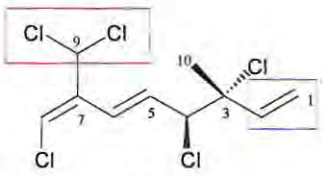

4.4

Figure 5.5 Chemical structure of **4.4** indicating the antiplasmodial active group (red box) and site of modification (blue box) for potential DXR inhibition.

The effect of chlorine atoms at C-3 and C-4 of compound **4.4** was to be investigated. However, these could potentially be sites for covalent bonding to the enzyme. The importance of the two hydroxyl groups in the structure of DOXP (**5.3**) as a substrate is to facilitate the rearrangement of the substrate by the enzyme as these hydroxyl groups serve as the site of chelation for the metal ion (Mg^{2+} or Mn^{2+}) which is essential for the activity of the enzyme (Hoeffler *et al.*, 2002). DOXP analogues, 3*S*-hydroxypentan-2-one 5-phosphate (**5.24**) and 4*S*-hydroxypentan-2-one 5-phosphate (**5.25**), with only one hydroxyl group have been shown to inhibit DXR with the 4-deoxy analogue (i.e. the 2-hydroxy analogue using our monoterpene numbering) 6.7 times more potent than the 3-deoxy analogue (**5.25**). It thus reasons that hydroxylation of compound **4.4** at C-2 and phosphorylation at C-1 to produce a target compound **5.26** (Scheme 5.4) would not only improve the polarity of compound **4.4** but also enhance its binding to DXR.

Critical to the success of this project is the selective dihydroxylation and phosphorylation of compound **4.4** (Scheme 5.4). The presence of three double bonds in halogenated monoterpene **4.4** could present a significant problem. Therefore, the first challenge would be to explore the selective dihydroxylation of the least substituted $\Delta^{1,2}$ double bond in compound **4.4**. In the following section selected dihydroxylation and phosphorylation reactions will be reviewed briefly.

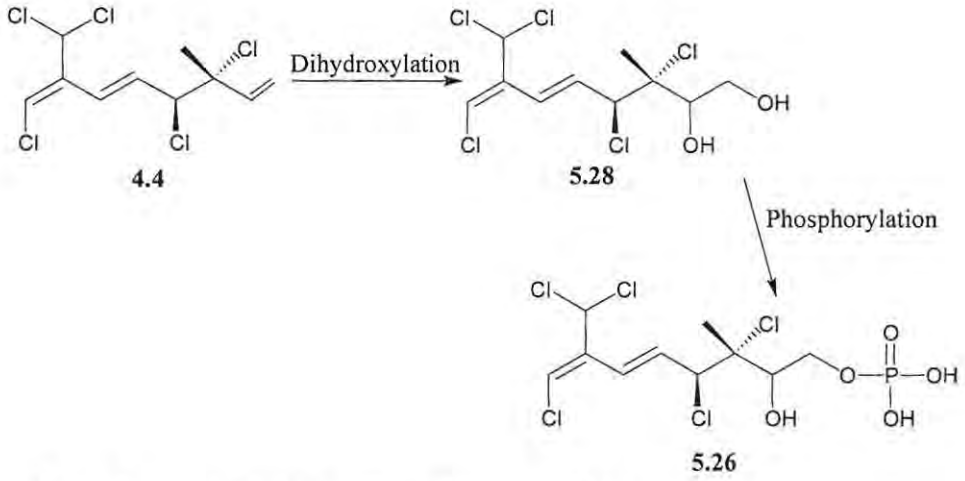

4.4 **5.28** **5.26**

Scheme 5.4 Proposed modification of compound **4.4**

5.1.7 Dihydroxylation reactions of alkenes

The dihydroxylation of alkenes can be achieved by a number of methods. The most common of which often include the use of OsO_4 (VanRheenen *et al.*, 1976), $KMnO_4$ (Weber and Shepherd, 1972) or RuO_4 (Djerassi and Engle, 1953) as catalysts to obtain *syn*-dihydroxylated products. The Woodward reaction (Woodward and Brutcher, 1958) achieves *syn*-dihydroxylation by treating the alkene with I_2-AgOAc in AcOH. The addition of I_2 is followed by the nucleophilic displacement with acetate in the presence of water. The diol is formed by hydrolyzing the ester. Prevost alternatively achieved *anti*-dihydroxylation of alkenes using peroxy acids and I_2-silver benzoate in the absence of water (March, 1977). Each of these methods while affording the diol end product with good yields has its limitations. The OsO_4 catalyzed reaction is very expensive and toxic while overoxidation is a common side reaction in RuO_4-catalyzed reaction. Both the Woodward and Prevost reactions make use of expensive silver salts and stoichiometric amount of molecular halogens and form a large amount of organic and inorganic waste (Emmanuvel *et al.*, 2005). A simple catalytic approach to the

Woodward-Prevost reaction was reported by Emmanuvel *et al.* (2005). This approach utilized $NaIO_4$ as oxidant in a LiBr-catalyzed reaction (Scheme 5.5) and provided a much simpler route to hydroxylation and eliminated the use of expensive silver salts, although high-valent iodine reagents are also relatively expensive. The reaction is proposed to occur *via* the oxidation of the metal halides with $NaIO_4$ to release the electrophilic halogen which reacts with the alkene to form a *trans*-1,2-bromoacetate derivative via a bromonium ion intermediate. The bromoacetate derivative in the presence of $NaIO_4$ and water then gives a *cis*-hydroxy acetate with the release of bromine. A diacetate is formed as a side product.

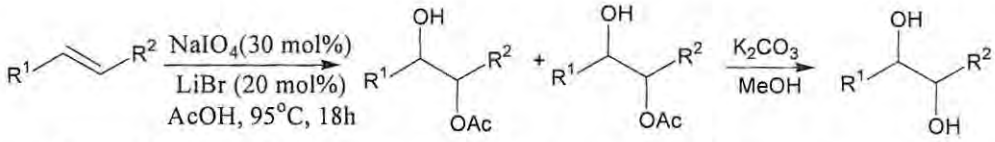

Scheme 5.5 $NaIO_4$/LiBr-mediated dihydroxylation of alkenes (Emmanuvel *et al.*, 2005).

This method has the advantage, particularly for the desired monoterpene modification, of forming a mono-hydroxylated product at the end of the first step. This allows for only one hydroxyl group to be available for the following phosphorylation and thus allow for the formation of a monophosphate product before the basic hydrolysis of the acetate moiety to a hydroxyl group (Scheme 5.5). Although phosphates are known to be unstable under basic conditions, dialkyl phosphates are extremely stable (Brown and Higson, 1957) and thus a dialkyl phosphorylating agent was considered for the proposed reaction.

5.1.8 Phosphorylation of alcohols

Phosphoryl chloride ($POCl_3$) is one of the most commonly used phosphorylating agents for alcohols (Sakakura *et al.*, 2005). It reacts with alcohol in the presence of water and pyridine to form phosphate monoesters with pyridine hydrochloride as byproduct. However, phosphate diesters and triesters are often formed when equimolar amount of alcohol and $POCl_3$ is used because of the high reactivity of $POCl_3$ (Sakakura *et al.*, 2005).

Another interesting method reported by Sakakura *et al.* (2005) involves the direct condensation of the alcohol with H_3PO_4 crystals in equimolar amounts. The reaction is best conducted using aprotic solvents such as DMF, nitroethane or a mixture of aprotic solvents. To aid the dissolution of H_3PO_4 in the solvent, a tertiary amine such as Bu_3N is required. A nucleophilic base such as *N*-methyl imidazole promotes the reaction of H_3PO_4 with alcohol and better catalytic activity is observed when the more lipophilic nucleophiles are used (Sakakura *et al.*, 2005). The reaction has the advantage of producing water as the only byproduct which is easily removed with molecular sieves. This advantage and the fact that only equimolar amount of alcohol and H_3PO_4 is required for the reaction makes this method attractive. The limitation of this method lies in the fact that the reaction is conducted at azeotropic reflux for six hours which when DMF is used as the solvent is 150 °C and may lead to decomposition of the starting material.

Phosphates are often difficult to purify due to their hydrophilic nature. Coupled with the presence of hydroxyl groups, manipulating phosphate compounds is often complicated. Protecting the phosphate group with a less polar moiety such as benzyl or phenyl groups reduces the polarity of the phosphate and improves the solubility of the compound in volatile organic solvents.

A widely used reagent in the synthesis of phosphate esters is dibenzylchlorophosphate ($(BnO)_2P(O)Cl$). It can be synthesized by the chlorination of dibenzyl hydrogen phosphate (Atherton *et al.*, 1945). The advantage of using dibenzylchlorophosphate as a phosphorylating agent is that the benzyl group is easy to remove by simple hydrogenation or catalytic transfer hydrogenolysis (Bajwa, 1992) as opposed to a phenyl group. Dibenzylchlorophosphate is however unstable (Atherton *et al.*, 1945) and the best result is obtained when the reagent is formed *in situ* by reacting carbon tetrachloride (CCl_4) with dibenzyl phosphite in the presence of *N*,*N*-diisopropyl ethylamine with a catalytic amount of *N*,*N*-dimethylaminopyridine (DMAP), and acetonitrile as the solvent (Silverber *et al.*, 1996). Alternatively, diphenylchlorophosphate ($(PhO)_2P(O)Cl$), a more stable phosphorylating agent which is available commercially, can be used in a base-catalyzed phosphorylation reaction to form phosphate esters (Hayakawa *et al.*, 1983). Successful hydrogenolysis of the

phenyl group has been reported with the use of the expensive PtO_2-H_2O as a catalyst (Burgos *et al.*, 2005).

5.2 Results and Discussion

5.2.1 Model studies

5.2.1.1 Attempted phosphorylation and dihydroxylation of geraniol (5.29)

Although compound **4.4** was the most abundant compound isolated form *P. cornutum*, there was not enough available to accommodate for repeated synthetic reactions. A cheap commercially available monoterpene analogue, geraniol (**5.29**), was consequently employed as a model starting material for the proposed phosphorylation and hydroxylation reactions of compound **4.4**.

Since geraniol (**5.29**) already has a hydroxyl group, the first step in its modification was phosphorylation followed by hydroxylation, acetate hydrolysis and hydrogenolysis of the diphenyl ester.

Geraniol (**5.29**) was reacted with sodium hydride at -78 °C followed by treatment of the resulting alkoxide with diphenylchlorophosphate. 1D NMR (^{1}H and ^{13}C) data analysis of the crude product did not show the expected phosphorylated geraniol ester (**5.30**) (Scheme 5.6) nor the starting material. Varying the base used, the reaction temperature, time and molar equivalents of the reagents did not improve the yield. A literature search revealed that a similar reaction of geraniol with diphenylchlorophosphate using $TiCl_4$ as a catalyst and triethylamine as the base resulted in decomposition (Jones and Selitsianos, 2002). However compound **5.30** had previously been synthesized using titanium (IV) tert-butoxide (Ti(*t*-BuO)$_4$) (Jones *et al.*, 2003). At this point it was not clear whether the failure of this reaction was due to the alcohol, reagents or reaction conditions. This reaction was thus repeated using methyl benzyl alcohol (**5.32**) (Section 5.2.1.2)

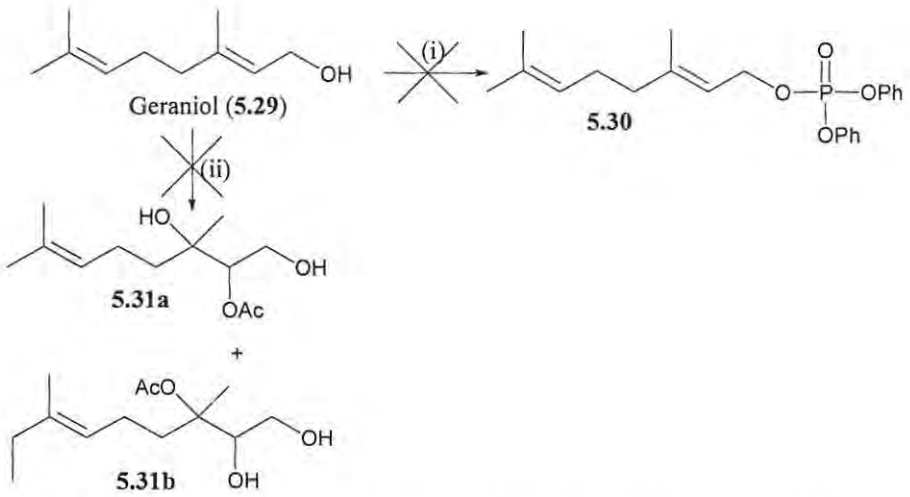

Scheme 5.6 Attempted phosphorylation and dihydroxylation geraniol (**5.29**)
(i) diphenylchlorophosphate, NaH, -78 °C (ii) $NaIO_4$ (30 mol %), NaBr (20 mol %), AcOH, 95 °C, 18h

Selective 2,3-dihydroxylation of geraniol had previously been achieved using triethylethylenediaamine (TMEDA) and osmium tetroxide (Donohoe *et al.*, 1997). However, we were interested in exploring the use of Emmanuvel's. NaBr / NaIO4 / AcOH method (Emmanuvel *et al.* 2005). Unfortunately this reaction also proved to be unsuccessful (Scheme 5.6).

5.2.1.2 Phosphorylation of *p*-methyl benzyl alcohol (5.7) (Hayakawa *et al.* 1983)

Suspecting that geraniol (**5.29**) may be the cause of the failure of the reactions, a new model compound, *p*-methyl benzyl alcohol (**5.32**) was used to further explore reaction conditions. Thus, the alkoxide of benzyl alcohol (**5.33**) was treated with diphenylchlorophosphate to give pure phosphoric acid methylbenzyldiphenyl ester (**5.34**) in 46% yield after chromatography (Scheme 5.7). Some unreacted starting material was also isolated indicating that the reaction could be optimized further.

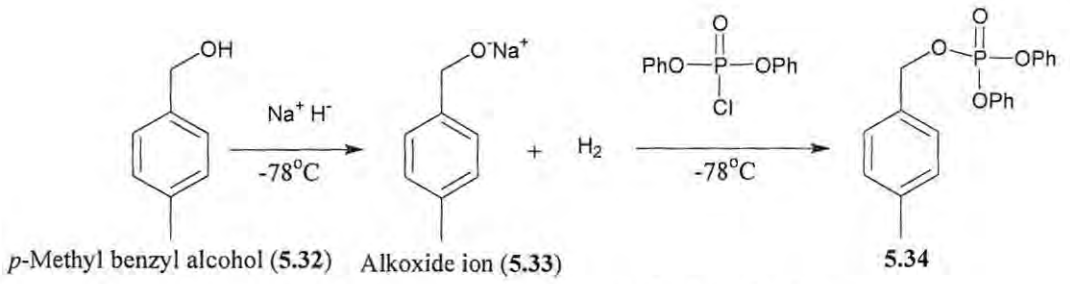

Scheme 5.7 Phosphorylation of *p*-methyl benzyl alcohol (**5.32**)

The ^{1}H NMR spectrum (Figure 5.6) of compound **5.34** showed a methyl signal at δ 2.41 and a characteristic methylene signal at δ 5.27 (J = 8.5 Hz) due to coupling of the phosphorus. The ^{13}C NMR data also showed a splitting of the methylene signal at δ 70.6 (J = 6.1Hz) which is characteristic of phosphate group on neighbouring atoms (Lapper, *et al.*, 1973).

The successful preparation of benzyl phosphate (**5.34**) gave us confidence that this reaction could be suitable to phosphorylate our compounds.

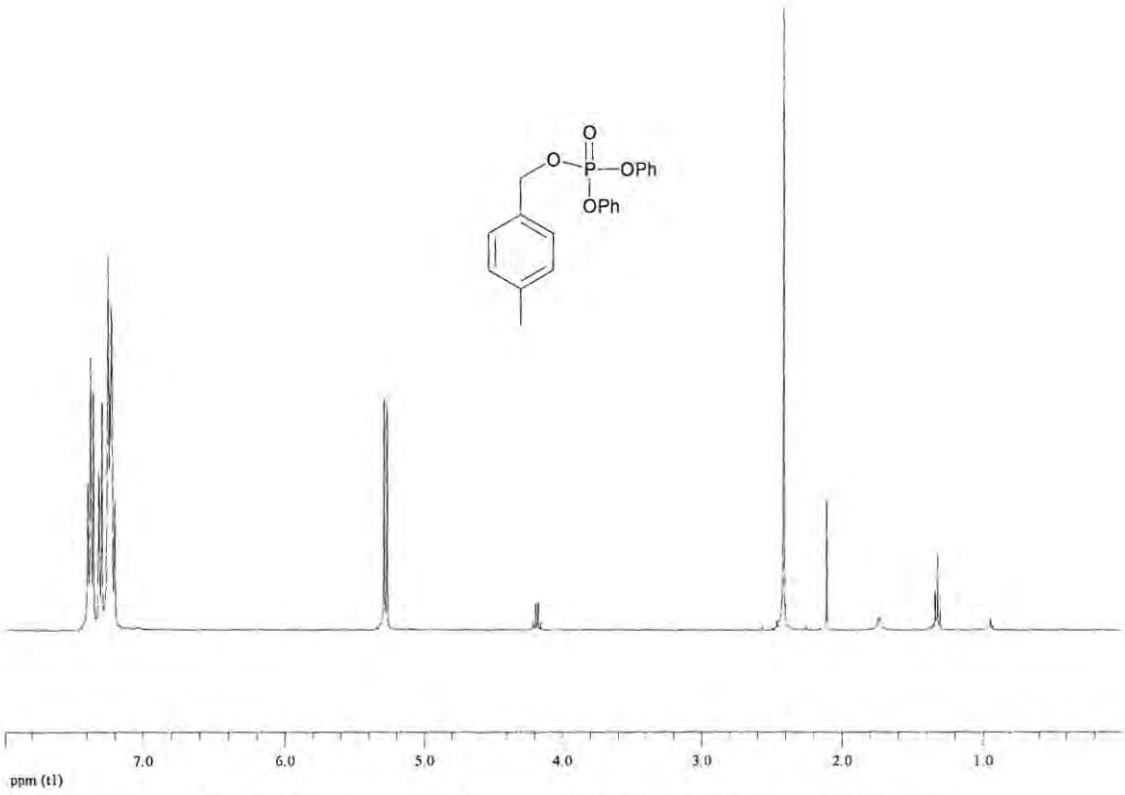

Figure 5.6 ^{1}H NMR spectrum of compound **5.34** ($CDCl_3$, 400MHz)

5.2.1.3 Dihydroxylation of styrene (5.35)

Having failed to successfully hydroxylate geraniol (**5.29**) using the method reported by Emmanuvel *et al* (2005), and once again suspecting the allylic alcohol to be the reason, styrene (**5.35**), another model compound, was employed to further investigate the conditions of the reaction (Scheme 5.8).

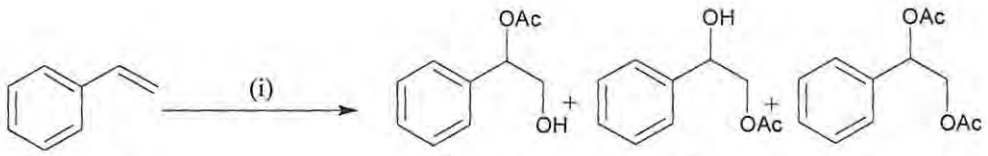

Styrene (**5.35**) **5.36a** **5.36b** **5.37**

Scheme 5.8 Hydroxylation of styrene (**5.35**): (i) 30 mol% $NaIO_4$, 20 mol% NaBr, AcOH, 95 °C, 18h

All three products of the first step of the reaction were obtained albeit at a disappointing yield of 30% combined monoacetate (**5.36a** and **5.36b** at a ratio of 1:3) and 14% diacetate (**5.37**). Compound **5.36b** was purified while **5.36a** was obtained as a mixture with **5.36b**. The isomers were clearly shown in the ^{1}H NMR spectrum (Figure 5.7a) of the mixture. The isomers were differentiated based on the analysis of the spectrum in comparison with the ^{1}H NMR spectrum of pure compound **5.36b** (Figure 5.7b) and literature values (Virsu *et al.*, 2001).

This confirms that the method does result in the formation of dihydroxylated products and could have failed when geraniol (**5.29**) is used as the starting material because of geraniol (**5.29**) itself.

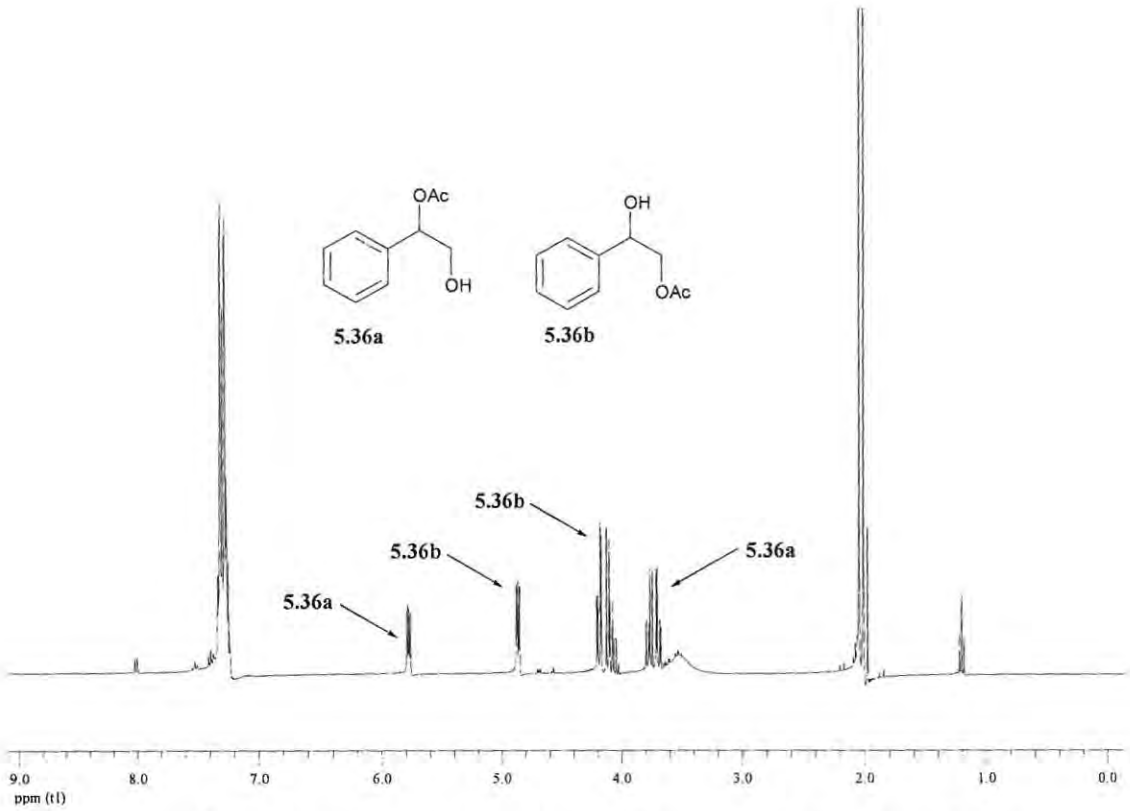

Figure 5.7a ^{1}H NMR spectrum of a mixture of compounds **5.36a** and **5.36b**

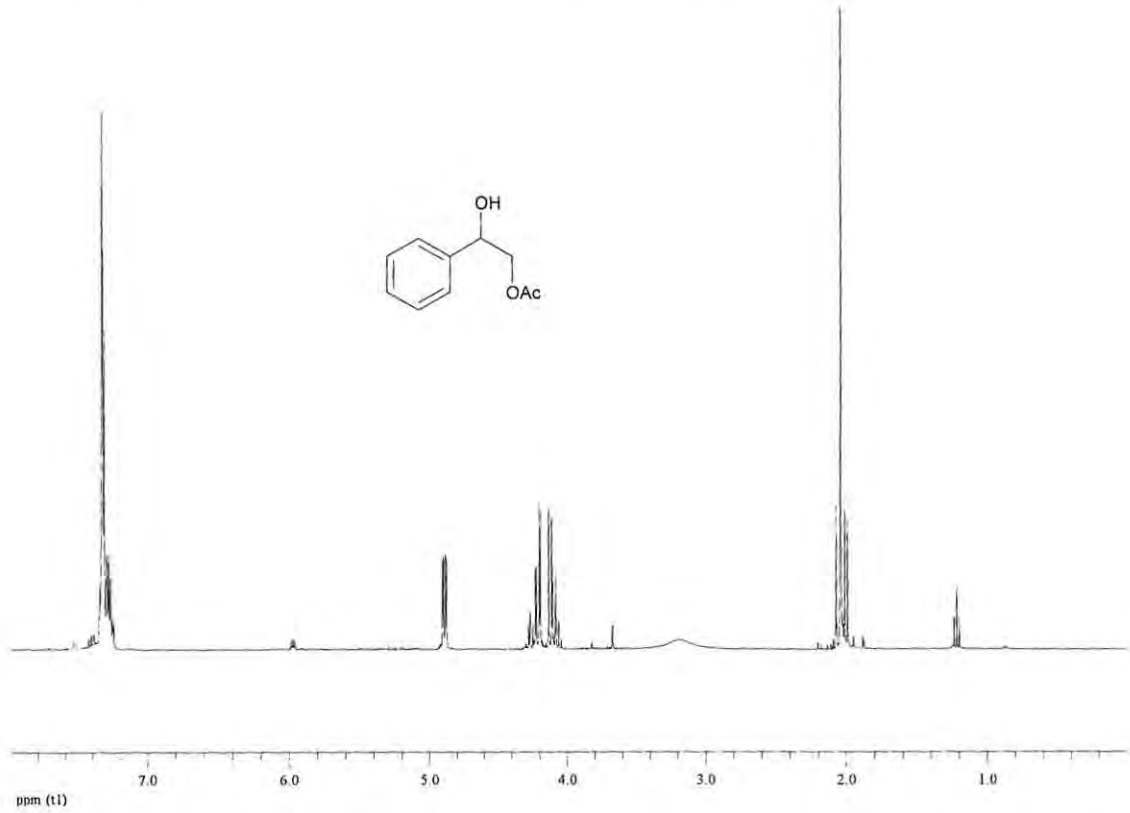

Figure 5.7b ^{1}H NMR spectrum of compound **5.36b** ($CDCl_3$, 400 MHz)

5.2.2 Attempted dihydroxylation of halogenated monoterpene (4.4)

Although attempts to phosphorylate and dihydroxylate geraniol (**5.29**) were not successful due to the allylic alcohol, it was still likely that the isolated double bond in compound **4.4** could be selectively hydroxylated (Andrus *et al.*, 1997). Unfortunately, this reaction also failed to provide the required dihydroxylated product (Scheme 5.9).

These results suggested that the dihydroxylation as described by Emmanuvel *et al.* (2005) is unsuitable for monoterpenes with allylic functional groups.

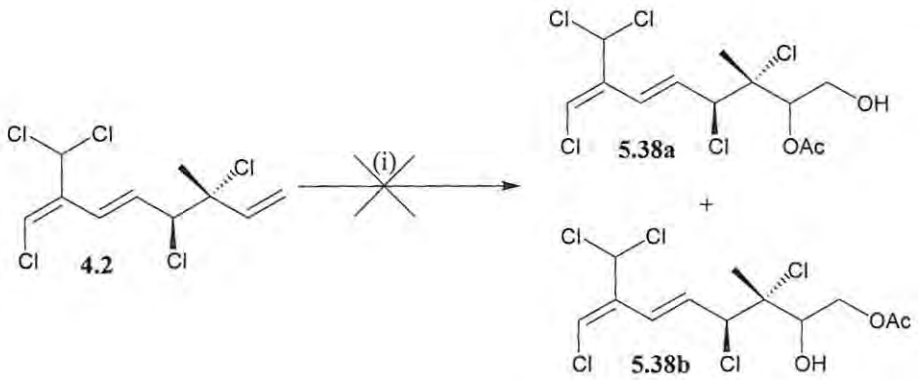

Scheme 5.9 Attempted dihydroxylation of compound **4.4**: (i) Hydroxylation of compound **4.4**: (i) $NaIO_4$ (30 mol %), LiBr (20 mol %), AcOH, 90 °C, 4h followed by room temperature for 16 hours

5.2.3 A simplified approach to the synthesis of potential DXR inhibitors

At this point it was clear that simple dihydroxylation and phosphorylation of halogenated monoterpene **4.4** will not be trivial. Before investing more time in exploring appropriate reactions for the derivatization of compound **4.4** it was more prudent to establish whether these modifications would lead to the production of DXR inhibitors.

We thus turned our attention to simpler analogues of halogenated monoterpene **4.4**. In particular, we wanted analogues of the right-hand hemisphere of compound **4.4**. Scheme 5.10 illustrates some simplified analogues to be synthesized to examine the feasibility of this approach.

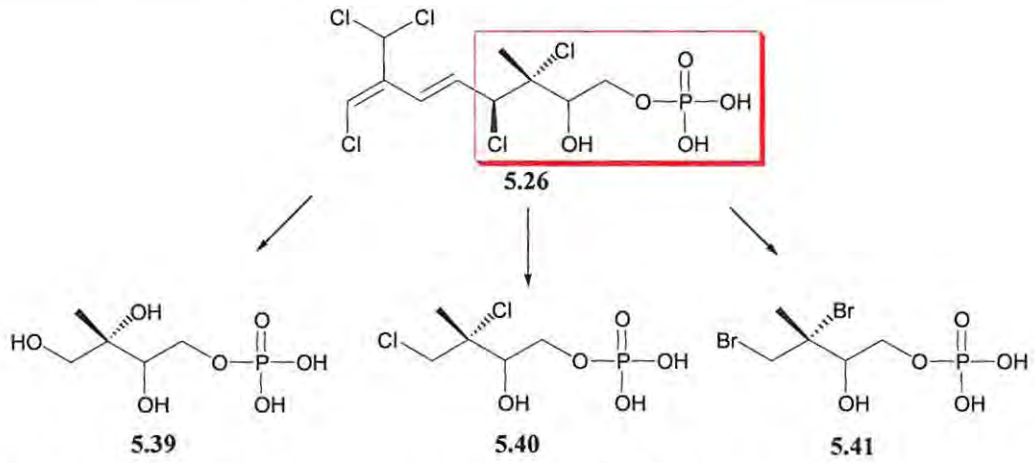

Scheme 5.10 A simplified approach to potential DXR inhibitors

It was proposed that the alcohol group on 3-methyl-3-buten-ol (**5.42**) be phosphorylated followed by dihydroxylation or halogenation of the double bond at the terminal end of the compound to produce structurally similar hemi-terpenes to compound **5.26** (Scheme 5.10).

5.2.3.1 Synthesis of diphenylphosphate esters 5.44a and 5.45

Reaction of compound **5.42** with sodium hydride and the subsequent treatment of the alkoxide formed with diphenylchlorophosphate gave compound **5.43** in 22% yield after column chromatography (Scheme 5.11).

Dihydroxylation of compound **5.43** using $NaIO_4$/NaBr/AcOH afforded compound **5.44a** in a very poor yield of 5% (Scheme 5.11). This, however, yielded sufficient material for characterization and preliminary testing before optimization of reaction conditions.

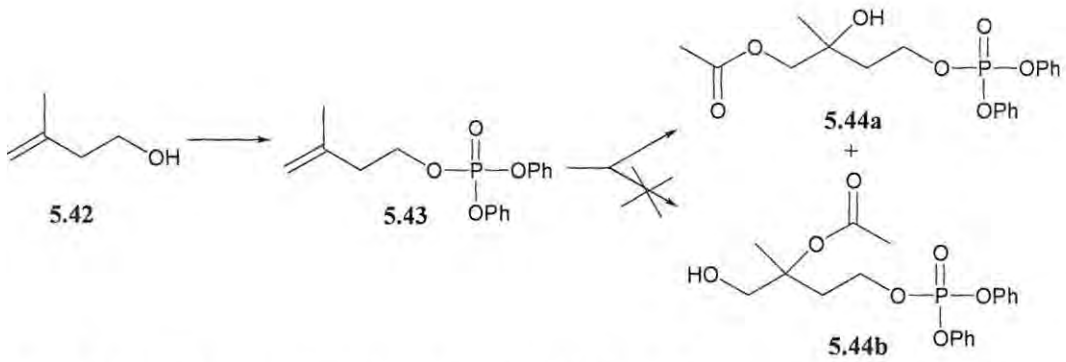

Scheme 5.11 Phosphorylation and dihydroxylation of methyl-3-buten-ol (**5.42**):
(i) Diphenylchlorophosphate, NaH, -78 °C, 24h, (ii) 30 mol% $NaIO_4$, 20 mol% NaBr, AcOH, 95 °C, 20h

The ^{1}H NMR spectrum of compound **5.44a** clearly showed the acetyl group at δ 2.08 and two oxymethylenes at δ 3.95 and 4.45, respectively. The ^{13}C and DEPT-135 NMR spectra supported the pattern observed in the ^{1}H NMR spectrum in that two methyl carbons were observed at δ 20.8 and 24.2 as well as three methylene carbons at δ 38.6, 65.4 and 71.1. A quaternary carbon resonated at δ 70.6 while a carbonyl signal was observed at δ 170.9 (Figure 5.8). The splitting of the methylene carbons at δ 38.6 (J = 6.7 Hz) and 65.4 (J = 6.1 Hz) is indicative of the phosphate component of the compound. The broad IR signal at 3423 cm^{-1} confirmed the presence of hydroxyl group in the structure of compound **5.44a**.

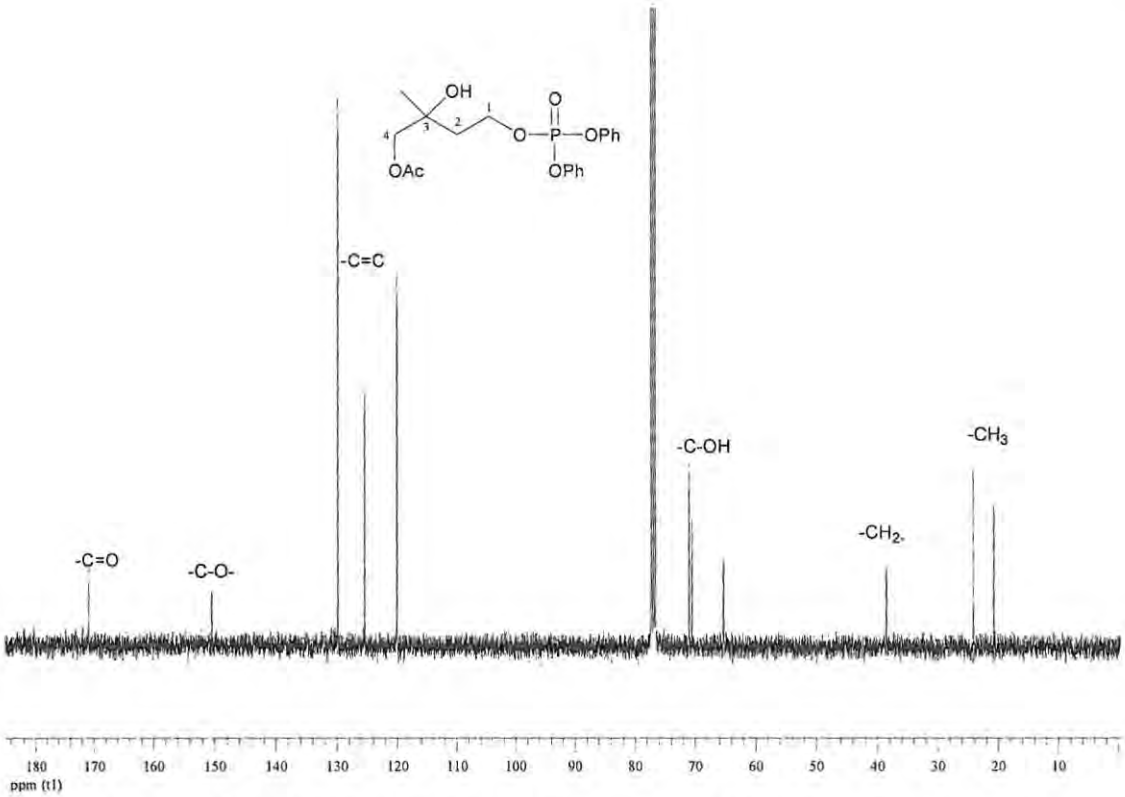

Figure 5.8 ^{13}C ($CDCl_3$, 400 MHz) NMR spectrum of compound **5.44a**

Analysis of the HMBC spectrum confirmed the structure of the compound to be the isomer **5.44a** (Figure 5.9) as opposed to **5.44b** (Scheme 5.8). The EIMS showed a molecular ion at *m/z* 395, a basepeak at *m/z* 377 for $[M^+-OH]$ and fragments *m/z* 335, 251 and 145 corresponding to $[M-OAc]^+$, $[M-C_7H_{12}O_3]$ and $[M-(PhO)_2OP]^+$ respectively.

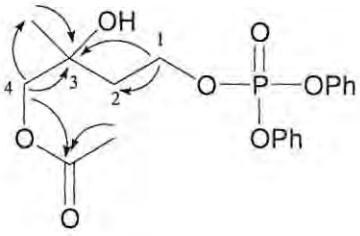

Figure 5.9 Selected HMBC correlations of **5.44a**

Compound **5.45** which was obtained as a side product in the dihydroxylation of compound **5.43** to **5.44a** in 5% yield. The side was product was initially suspected to be compound **5.45** or a diol derivative of compound **5.42** based on the fact that ^1H and ^{13}C (Figure 5.10) NMR spectra of the compound did not show the aromatic protons

observed for the starting material (compound **5.43**) in the region of δ 7.1 – 7.4 or the aromatic carbons in the region of δ120 – 130.

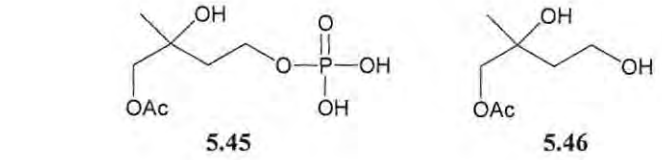

5.45

5.46

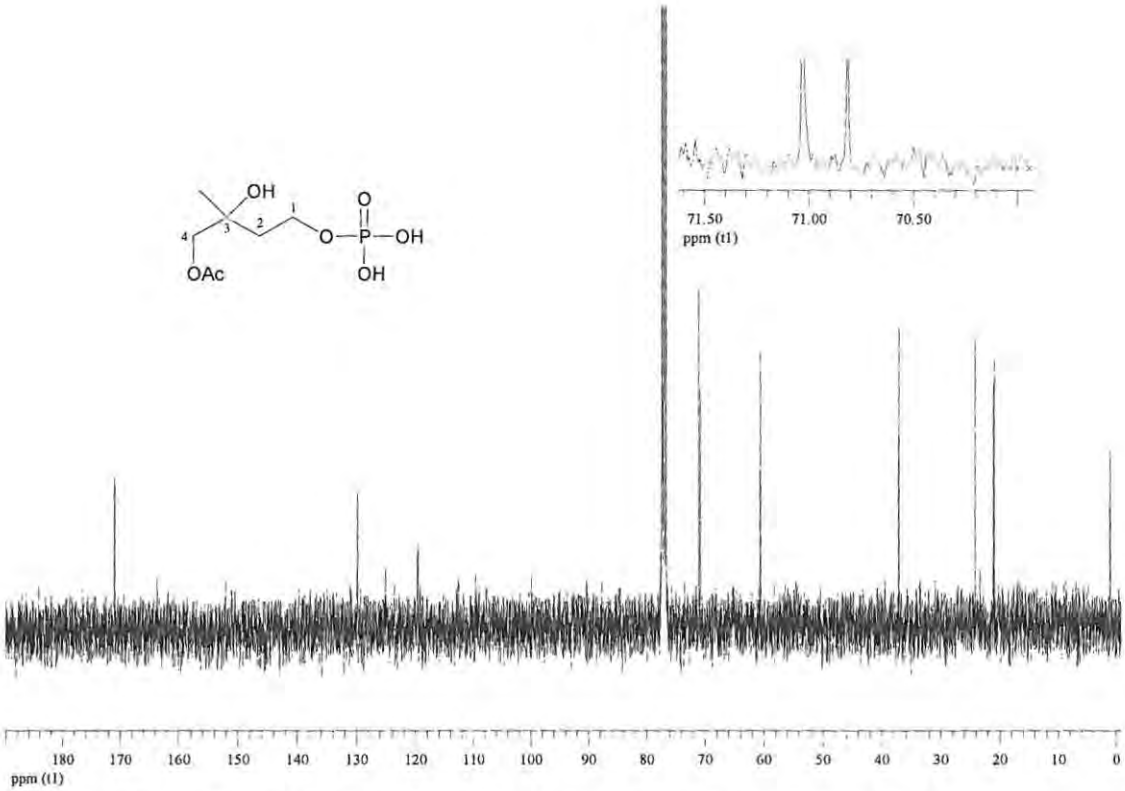

Figure 5.10 ^{13}C ($CDCl_3$, 100 MHz) NMR spectrum of compound **5.45**

Comparison of the 1D NMR spectra of compound **5.45** to those of **5.44a** showed very similar resonances except for the disappearance of the phenyl signals. ^{31}P NMR spectrum of compound **5.45** showed a phosphorus signal at δ -14.39, confirming the presence of the phosphate group. As was observed for compound **5.44a** a broad IR signal indicating the presence of a hydroxyl group was also observed for compound **5.45** at 3443 cm^{-1}. EIMS of compound **5.45** showed a basepeak molecular ion at *m/z* 241.

The fortuitous isolation of phosphate **5.45** essentially bypassed the need to develop reactions for the phosphate ester hydrolysis. In addition, it immediately provided access to another analogue of the target inhibitors (**5.39 – 5.41**).

The formation of compound **5.45** is proposed to be via the hydrolysis of PhO-P bond (Scheme 5.12) to release phenoxide ions that is subsequently protonated to phenols.

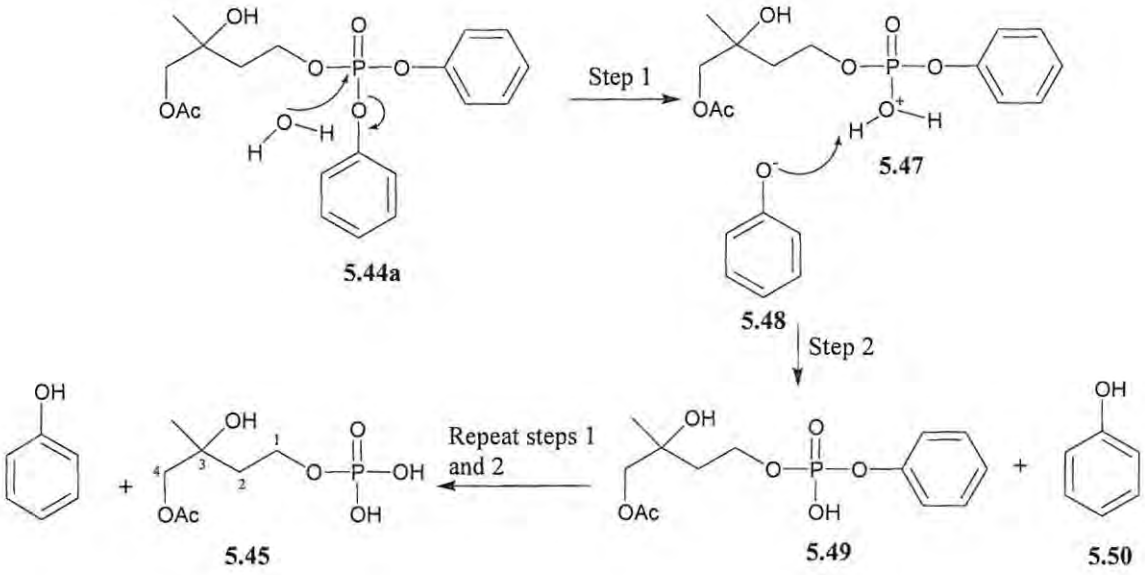

Scheme 5.12 Proposed mechanism for the synthesis of compound **5.45**

5.2.3.2 Synthesis of the dibrominated compound 5.51

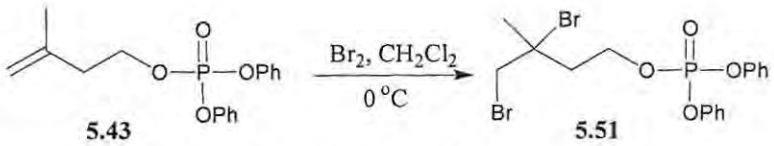

Scheme 5.13 Dibromination of compound **5.43**

The bromination of compound **5.43** was carried out by dropwise addition of a solution of bromine to afford 93% yield of compound **5.51**. The proton ^{1}H NMR data of compound **5.51** showed one methyl resonance at δ1.84, one oxymethylene proton at δ 4.51 and two methylene protons at δ 3.79 and 2.35. The ^{13}C and DEPT-135 NMR (Figure 5.11) spectra were in agreement with the ^{1}H NMR data showing a methyl resonance at δ 30.6, an oxymethylene carbon at δ 66.7, two methylenes at δ 41.6 and

42.6 and a quaternary carbon resonance at δ 63.5. The deshielded ^{1}H NMR resonance at δ 3.79 and ^{13}C NMR resonances at δ 63.5 and 42.6 are indicative of the presence of bromine atoms at C-3 and C-4 respectively.

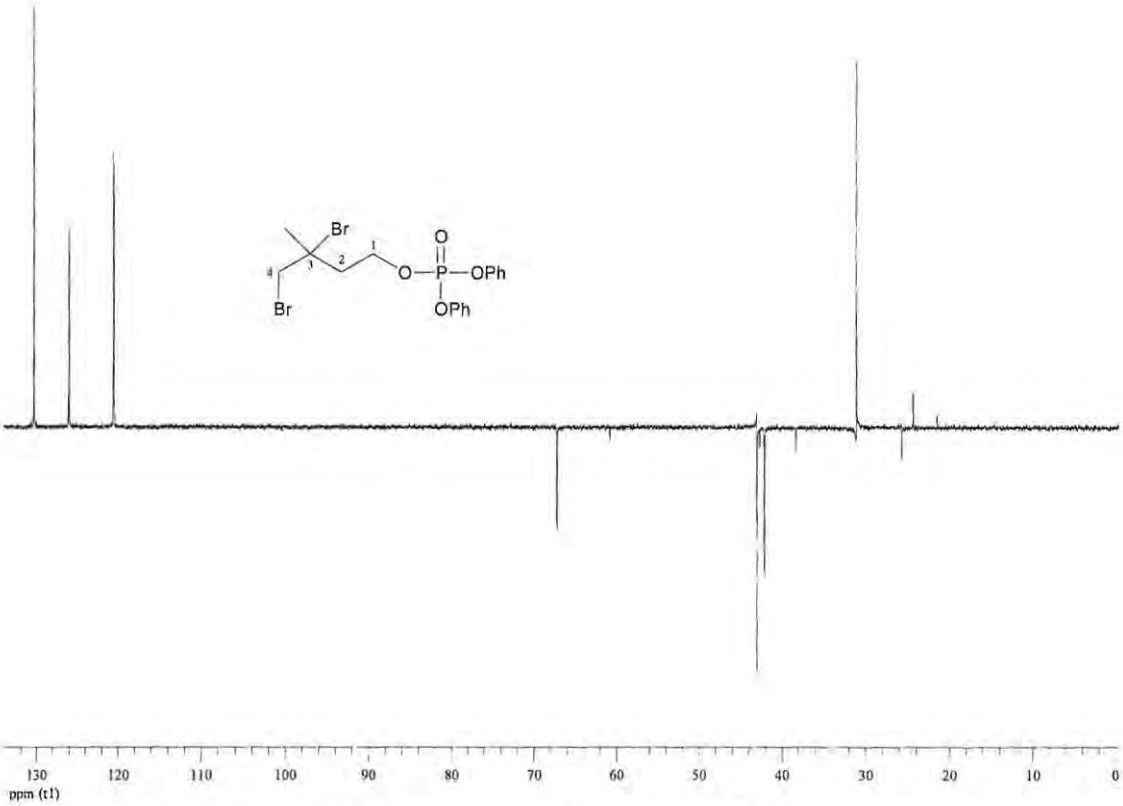

Figure 5.11 DEPT-135 NMR spectrum of compound **5.51**

The structure of compound **5.51** was further confirmed by APCI mass spectrometry which gave a molecular ion peak at *m/z* 476.9486.

5.2.3.3 Attempted synthesis of the dichlorinated compound 5.57

A simple manganese-mediated dichlorination of alkenes using potassium permanganate ($KMnO_4$) and trimethylsilyl chloride (Me_3SiCl) was reported by Markó *et al.* (1997). Although the mechanism of the reaction is unknown, the method involves the generation of a manganese reagent from the treatment of $KMnO_4$ with Me_3SiCl in the presence of a phase transfer reagent (quaternary ammonium salt). Addition of an alkene at room temperature to this mixture gives rise to *trans*-dichlorinated products. Such products include compounds **5.53** and **5.55** which were obtained from compounds **5.52** and **5.54** respectively as shown in Scheme 5.14.

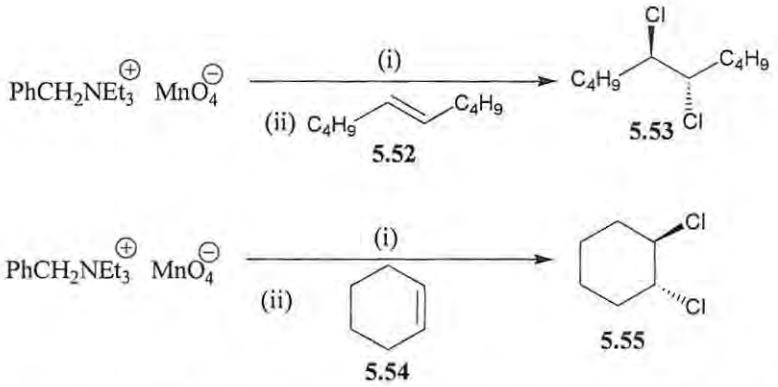

Scheme 5.14 Examples of *trans*-chlorinated alkene reported by Markó *et al.* (1997): (i) Me_3SiCl, CH_2Cl_2, 0 °C (ii) alkene, CH_2Cl_2, 20 °C

The procedure reported by Markó *et al.* (1997) was used in an attempt to synthesize compound **5.56** (Scheme 5.15). ^{1}H NMR data of the crude product however showed the presence of what appeared to be the expected dichlorinated product and was further purified by normal phase HPLC to afford a pure, colourless oil.

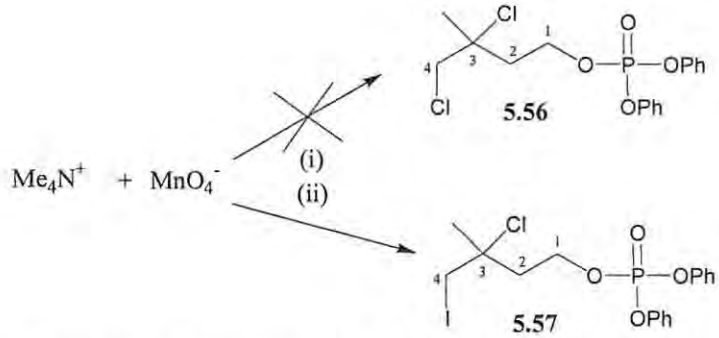

Scheme 5.15 Attempted dichlorination of **5.43** (i) Me_3SiCl, CH_2Cl_2, 0 °C (ii) **5.43**, CH_2Cl_2, 20 °C

The NMR spectra of what was initially thought to be compound **5.56** were very similar to those of compound **5.51**. The ^{1}H NMR spectrum clearly showed the methyl protons resonating at δ 1.71. As was expected, three sets of methylene protons were observed at δ 2.34, 3.36 and 4.48 (J = 6.9, 13.5 Hz). The phenyl protons were observed as multiplets from δ 7.37 – 7.19. The ^{13}C NMR data showed a signal at δ 17.8 which was thought to be a methyl signal but which on analysis of the DEPT-135 spectrum (Figure 5.12) showed to be a methylene carbon. A methyl carbon was observed at δ 30.6, a quaternary carbon at δ 67.8 and sp^2 hybridized carbons at δ 120.0, 125.5 and 129.8.

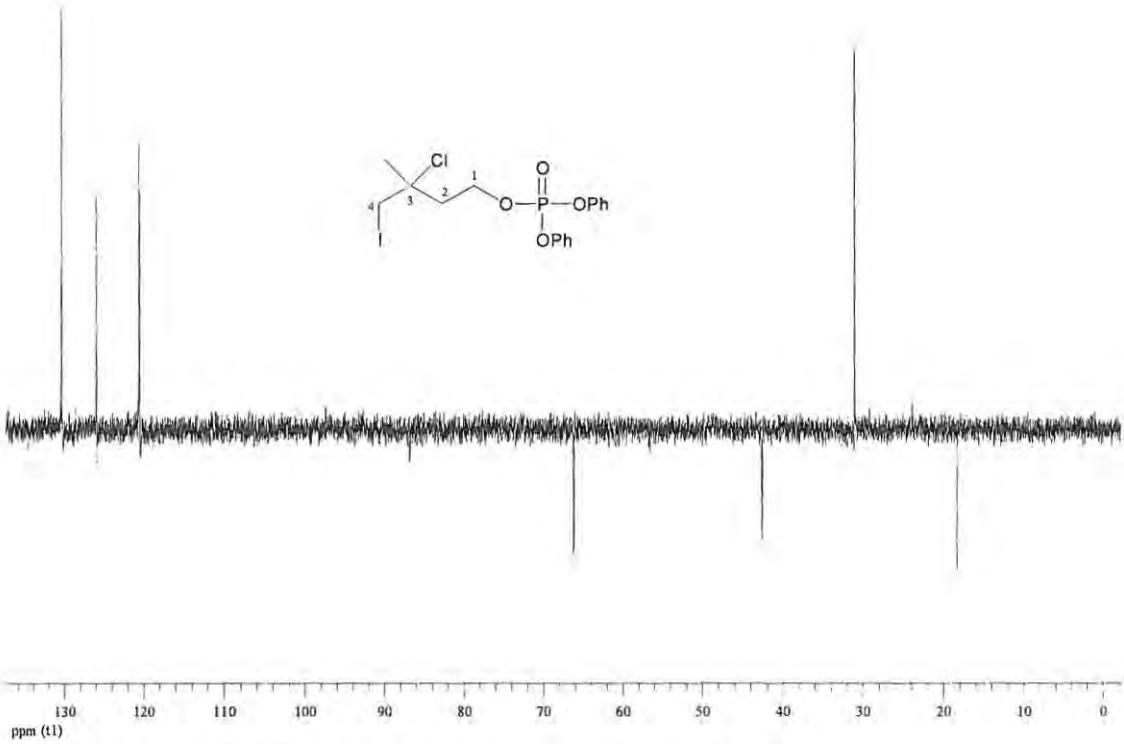

Figure 5.12 DEPT-135 NMR spectrum of compound **5.57**

The major difference observed between the spectra of compound **5.51** and **5.57** was the carbon resonance at C-4 which was observed at δ 17.8 for compound **5.57** and 42.6 for compound **5.51**. However, with an electronegative Cl atom on C-4 a carbon resonance of δ 17.8 was not expected as Cl deshields neighbouring carbons even more than bromine. An evaluation of the reagents and conditions of the chlorination reaction highlighted the use of another halogen in the reaction. Tetramethylammonium iodide was used as phase transfer reagent in the formation of the manganese complex required for the dichlorination of the alkene. The iodine appeared to have reacted with compound **5.43** in place of chlorine at C-4, thus resulting in compound **5.57** (Scheme 5.15). As iodine is considerably less electronegative than chlorine carbon attached to iodine are less deshie1ded than carbons attached to chlorine or bromine atoms which explained the upfield carbon shift observed for compound **5.57** at δ 17.8. The formation of this product could have also been avoided if a chloride as opposed to an iodide salt of the phase transfer reagent had been used.

5.2.3.4 Attempted hydrogenolysis of compounds 5.43 and 5.51

To complete the proposed modifications of the hemi-terpene analogues of compound **4.4**, hydrogenolysis of compound **5.43**, **5.51** and **5.57** to afford free phosphate compounds required. An attempt to hydrogenate compound **5.43** using palladium-on-carbon based on the fact that it works successfully with dibenzylchlorophosphate (Atherton *et al.*, 1948) resulted, not surprisingly, in the reduction of the double bond to give compound **5.58** (Scheme 5.16). Changing the catalyst to the platinum IV oxide dihydrate in an attempted hydrogenolysis of compound **5.51** resulted in dehalogenation of the compound also to give compound **5.58**.

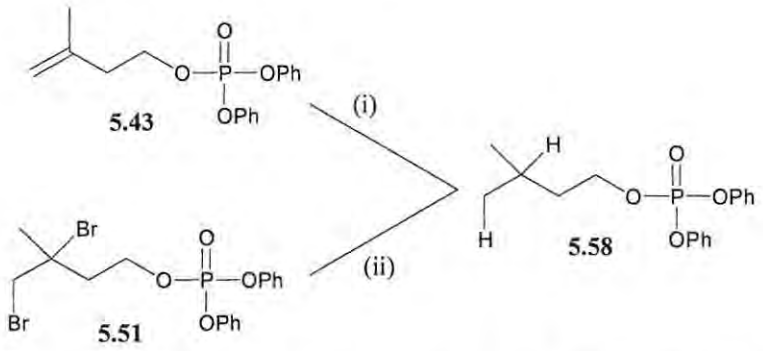

Scheme 5.16 Hydrogenation of compounds **5.43** and **5.51**: (i) H_2, 10% Pd on carbon, EtOH, 2.5 hours (ii) H_2, PtO_2-H_2O, EtOH, overnight

The ^{1}H NMR spectrum of compound **5.58** (Figure 5.13) clearly showed two methyl resonances at δ 0.87 and 0.99 for compound **5.58**. The deshielded oxymethylene protons resonated at δ 4.27. As opposed to compound **5.51** with a quaternary carbon at C-3, the spectrum of compound **5.58** showed the appearance of a proton at δ 1.59 on C-3. The carbon spectrum of Compound **5.58** showed the same pattern observed in the ^{1}H spectrum. As compared to the ^{13}C NMR spectra of compounds **5.43** and **5.51**, there was no double bond signal at δ 140.4 and 112.9 or brominated signals at δ 63.5 and 42.6 at C-3 and C-4, respectively. Instead compound **5.58** had C-3 and C-4 resonances at δ 24.3 and 22.2 respectively, further confirming the formation of the reduced compound and thus the unsuccessful attempt to synthesize the desired phosphate compounds for DXR inhibition. However, the synthesized diphenyl esters as well as compound **5.45** were tested for DXR inhibition as discussed in the next chapter.

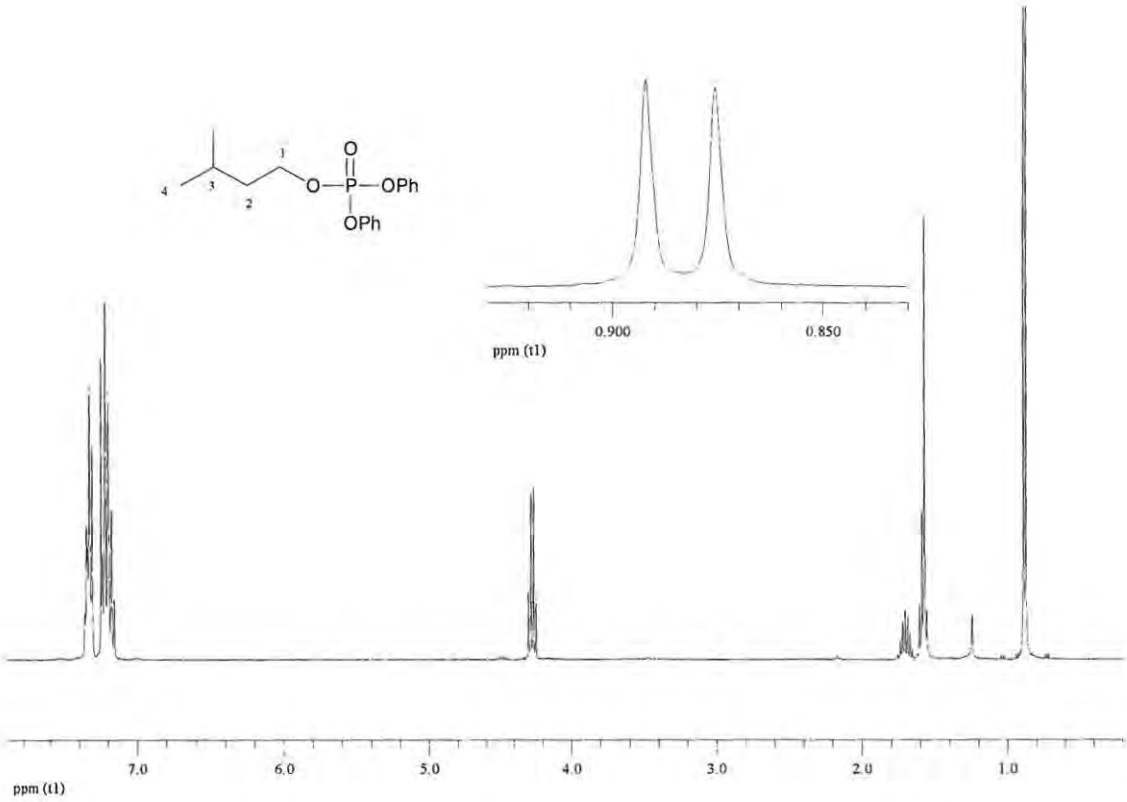

Figure 5.13 ^{1}H NMR ($CDCl_3$, 400 MHz) spectrum of compound **5.58**

Table 5.1 Comparison of the ^{13}C NMR data of the synthesized phosphate esters

δ_C, mult, J_{Hz}						
Carbon no.	**5.18**	**5.19a**	**5.20**	**5.24**	**5.30**	**5.31**
1	67.3, d, 6.4	65.4, d, 6.1	60.6	66.7, d, 6.0	65.7, d, 6.0	68.0, d, 6.6
2	38.0, d, 6.9	38.6, d, 6.7	37.1	41.6, d, 7.5	42.2, d, 7.4	38.7, d, 6.7
3	140.4	70.6	70.8	63.5	67.8	24.3
4	112.9	71.1	71.0	42.6	17.8	22.2
CH_3	22.3	24.2	24.2	30.6	30.6	22.2
Ar-C	129.7– 20.0	129.8–120.0		129.8–120.0	129.8–120.0	129.9–120.1
C-O	150.5, d, 7.2	150.4, d, 7.2		150.7, d, 7.1	150.4, d, 7.0	150.7, d, 7.1
CH_3COO		20.8	20.5			
CH_3COO		170.9	171.0			

5.3 Experimental

5.3.1 General Experimental Procedures

Chemicals and reagents

Compound **4.4** was isolated from *Plocamium cornutum*

The following general procedures were used unless stated otherwise. All solvents used for column chromatography and HPLC were HPLC grade obtained from Sigma-Aldrich (EtOAc) and BDH laboratory supplies. Normal phase TLC was performed on DC-Alufolien Kieselgel $60F_{254}$. The plates were viewed under UV light (254 nm) and developed in iodine tank or by spraying with a solution of 10% H_2SO_4 in MeOH. Column chromatography was performed using Kieselgel 60 (230 – 400 mesh) silica.

Compounds that were purified by HPLC were purified using a Spectra-Physics Isochrom LC HPLC system with a rheodyne injector which was connected to a Spectroseries UV100 UV detector and a Rikadenki cahrt recorder. The UV absorbance was read at a wavelength of 250 nm and a range of 2.0 in AUFs. Normal Phase chromatography was performed using Whatman Partisil 10 column with a 40cm X 10mm i.d.

Low resolution Mass spectroscopy (EIMS) was obtained by Mr. Aubrey Sonemann on a Finnigan MAT GCQ system mass spectrometer at 70 eV. High resolution fast atom bombardment (HRFABMS) were performed at the University of the North West, Potchefstroom by Dr Louis Fourie VG-7070E mass spectrometer and Atmospheric pressure chemical ionization (APCI) by Dr Marietjie Stander of the Mass Spectroscopy unit at Stellenbosch University using Water API Q-TOF Ultima.

Ultraviolet measurements were obtained on the GBC UV/ Vis 916 spectrometer, Infrared spectra were obtained on Perkin-Elmer spectrum 2000 FT-IR spectrometer as films on KBr discs.

The 1D and 2D NMR spectra were recorded on a Bruker Avance 400 NMR spectrometer. Chemical shifts were recorded in ppm and referenced to residual deuterated solvent ($CDCl_3$ δ_H 7.25, δ_C 77.0). All coupling constants are reported in Hz.

All reactions requiring anhydrous conditions were conducted in flame-dried apparatus. THF was dried over sodium wire and benzophenone as described in literature (Casey, 1990). Hexane was dried over calcium hydride.

5.3.2 Synthetic procedures

Phosphoric acid 4-methyl-benzyl ester diphenyl ester (5.34)

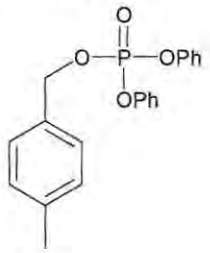

5.34

In a flame dried round bottom flask equipped with a stirring bar and N_2 supply, 60% NaH in mineral oil (0.16 g, 4.09 mmol) was introduced. The base was washed with dry hexane and the hexane was drained off. Dry THF (8 ml) and compound **5.32** (0.50 g, 4.09 mmol) were added to the base at -78 °C. The reaction was followed by TLC and Diphenylchlorophosphate (1.30 g, 4.82 mmol) pre-mixed under N_2 with THF (5 ml) was added after 6 hours. The reaction was stirred for 4 hours at -78 °C and was left for 16 hours during which the temperature rose to -10 °C. The reaction was quenched with brine (10 ml) and extracted with CH_2Cl_2. The organic extract was dried over anhydrous $MgSO_4$ and concentrated under vacuum. Silica gel column chromatography by solvent gradient afforded pure compound **5.34** (0.67 g, 45.6%). Colourless oil; δ_H (400 MHz; $CDCl_3$) 2.41 (3H, s, CH_3), 5.28 (2H, d, J = 8.5 Hz, CH_2), 7.39 – 7.20 (14H, m, Ar-H); δ_C (100 MHz; $CDCl_3$) 21.2 (CH_3), 70.6 (d, J = 6.1 Hz), 120.0 – 138.7 (14C, Ar-C), 150.4 (d, 7.2 Hz).

Acetic acid 2-hydroxy-1-phenyl-ethyl ester (5.36a), acetic acid 2-hydroxy-2-phenyl-ethyl ester (5.36b), acetic acid 2-acetoxy-2-phenyl-ethyl ester (5.37)

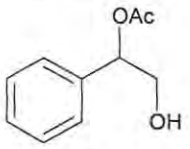

5.36a

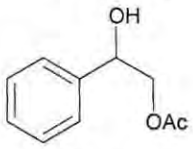

5.36b

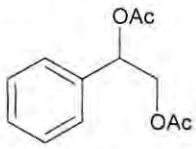

5.37

In a round bottom flask equipped with a stirring bar, styrene (0.9 g, 8.6 mmol), $NaIO_4$ (0.6 g, 2.6 mmol), NaBr (0.12 g, 1.72 mmol) and acetic acid (15 ml) were stirred at 95 ^{o}C for 23 hours. The reaction mixture was cooled and extracted with EtOAc three times. The combined organic phase was washed with saturated solution of sodium thiosulphate, water and aqueous sodium hydrogen carbonate. The crude product was dried over anhydrous Na_2SO_4 and concentrated under reduced pressure. The crude product was then fractionated by silica gel column chromatography using 80:20 hexane-EtOAc as the mobile phase to obtain pure compounds **5.36b**, **5.37** and a mixture of **5.36a** and **5.36b.**

Compound **5.36a** (0.12 g, 8%): Yellow oil; δ_H (400 MHz; $CDCl_3$) 2.01(3H, s, C*H*$_3$COO), 3.73 (2H, , qd, *J* = 4.1, 7.9, 12.1, 28.7 Hz, C*H*$_2$,), 5.78 (1H, dd, *J* = 4.0, 7.8 Hz, C*H*), 7.34 – 7.23 (5H, m, Ar-H); δ_C (100 MHz; $CDCl_3$) 21.6 (*C*H$_3$COO), 66.0 (*C*H$_2$OH), 77.3 (*C*H), 127.1, 128.8, 129.0 and 137.6 (6C, Ar-C), 171.4 (*C*OO).

Compound **5.36b** (0.34 g, 22%): Yellow oil; δ_H (400 MHz; $CDCl_3$); 2.05 (3H, s, C*H*$_3$COO), 4.18 (2H, m, C*H*$_2$), 4.90 (1H, dd, *J* = 3.5, 8.3 Hz, C*H*), 7.36 – 7.26 (5H, m, Ar-H); δ_C (100 MHz; $CDCl_3$), 20.7 (*C*H$_3$COO), 69.0 (*C*H$_2$OH), 72.0 (*C*H), 126.0, 128.0, 128.4 and 139.8 (6C, Ar-C), 171.2 (*C*OO).

Compound **5.37** (0.26 g, 14%): Yellow oil; δ_H (400 MHz; $CDCl_3$) 2.03 (3H, s, C*H*$_3$COOCH$_2$), 2.09 (3H, s, C*H*$_3$COOCH), 4.29 (2H, m, C*H*$_2$), 6.00 (1H, dd, *J* = 4.0, 7.9 Hz, C*H*), 7.35 – 7.30 (5H, m, Ar-H); δ_C (100 MHz; $CDCl_3$) 20.7 (*C*H$_3$COOCH$_2$), 21.0 (*C*H$_3$COOCH), 66.0 (*C*H$_2$), 73.2 (*C*H), 126.6, 128.5, 136.4 (6C, Ar-C), 170.0 (*C*OOCH$_2$), 170.5 (*C*OOCH).

Phosphoric acid 3-methyl-3-but-enyl ester diphenyl ester

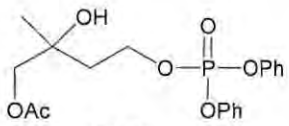

5.44a

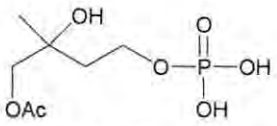

5.45

Into a flame dried two-necked round bottom flask equipped with a stirrer bar and flushed with nitrogen gas 60% NaH in mineral oil (0.40 g equivalent to 0.24g of NaH, 9.9 mmol) was introduced. Dry hexane (2 ml) was added and the mixture was stirred. The hexane was removed from the mixture and dry THF (20 ml) was added. At -78 °C, 3-methyl-3-buten-ol (**5.42**, 0.85 g, 9.9 mmol) was added dropwise. The temperature of the reaction was allowed to rise by 30 °C for 10 minutes to accelerate the formation of alkoxide ion and then cooled to -78 °C for another 4 hours. Diphenyl chlorophosphate (3.19 g, 11.9 mmol), premixed in dry THF (8 ml) was added at once to the alcohol mixture. The reaction was stirred at -78 °C for 4 hours and the reaction was left to stir for 16 hours during which the temperature rose to -10 °C. The reaction was quenched with brine (10 ml), extracted with ethyl acetate, dried over anhydrous Na_2SO_4 and concentrated under reduced pressure. The crude product was purified by column chromatography (hexane-EtOAc, 75:25) to afford pure **5.43** (0.67g, 21.6%). Colourless oil; δ_H (400 MHz; $CDCl_3$) 1.76 (3H, s, CH_3), 2.45 (2H, t, J = 6.7Hz, 2-H), 4.39 (2H, q, J = 7.0, 14.1 Hz, 1-H), 4.82 (2H, br s, 4-4), 7.39-7.19 (10H, m, Ar-H); δ_C (100 MHz; $CDCl_3$) 22.3 (CH_3), 38.03 (d, J = 6.9 Hz, C-2), 67.3 (d, J = 6.4 Hz, C-1), 112.9 (C-4), 120.0, 125.2 and 129.7 (10C, Ar-C), 140.4 (C-3), 150.5 (2C, d, J = 7.2 Hz, C-O); HRFABMS obsd. *m/z* 318.1030 (calcd. for $C_{17}H_{19}O_4P$) [M^+], 318.1020.

Acetic acid 4-(diphenoxy-phosphoryloxy)-2-hydroxy-2-methyl-butyl ester (5.44a) and Acetic acid 2-hydroxy-2-methyl-4-phosphonooxy-butyl ester (5.45)

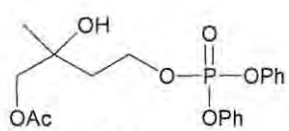

5.44a

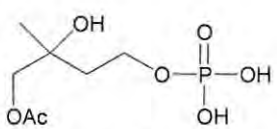

5.45

Compound **5.43** (0.30 g, 0.95 mmol), $NaIO_4$ (0.06g, 0.28 mmol) and NaBr (0.02 g, 0.19 mmol) were mixed and stirred in acetic acid (1.2 ml) at 95 °C for 20 hours. The product was extracted with EtOAc and washed with water, saturated solution of sodium thiosulphate and $NaHCO_3$. The organic fraction was dried over anhydrous Na_2SO_4 and concentrated under reduced pressure. Silica gel column chromatography by solvent gradient gave rise to four fractions. The fraction eluting with 50:50 hexane-EtOAc contained the side product **5.45** (10 mg, 5% yield). HPLC of the 100% EtOAc fraction using 100% EtOAc as the mobile phase yielded compound **5.44a** (20 mg, 5% yield).

Compound **5.44a**: colourless oil which turned pink after an hour; IR ν_{max} (KBr): 3423, 2973, 2355, 1729, 1590, 1483, 1255, 1185, 1020, 948, 769, 689 cm^{-1}; δ_H (400 MHz; $CDCl_3$) 1.21 (3H, s, CH_3), 1.93 (2H, m, 2-H), 2.08 (3H, s, CH_3COO), 3.95 (2H, s, 4-H), 4.45 (2H, q, J = 6.8, 14.4 Hz, 1-H), 7.36 – 7.17 (10H, m, Ar-H); δ_C (100 MHz; $CDCl_3$) 20.8 (CH_3COO), 24.2 (CH_3), 38.6 (d, J = 6.7 Hz, C-2) 65.4 (d, J = 6.1 Hz, C-1), 70.6 (C-3), 71.1 (C-4), 120.0 (d, J = 4.9 Hz), 125.5 and 129.8 (10C, Ar-C), 150.4 (2C, d, J = 7.2 Hz, C-O), 170.9 (CH_3-COO).

Compound **5.45**: colourless oil; IR ν_{max} (KBr): 3443, 2962, 1728, 1489, 1368, 1257, 1032, 943, 798, 690 cm^{-1}; δ_H (400 MHz; $CDCl_3$) 1.24 (3H, s, CH_3), 1.86 (2H, m, 2-H), 2.09 (3H, s, CH_3COO), 3.98 (2H, br s, 4-H), 4.24 (2H, br t, J = 6.7 Hz, 1-H); δ_C (100 MHz; $CDCl_3$) 20.5 (CH_3COO) 24.2 (CH_3), 37.1 (C-2), 60.6 (C-1), 70.8 (C-3), 71.0 (C-4), and 171.0 (CH_3-COO); δ_P (164 MHz; $CDCl_3$) -14.39.

Phosphoric acid 3,4-dibromo-3-methyl-butyl ester diphenyl esters (5.51)

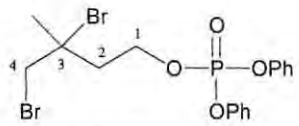

5.51

A solution of Br_2 (0.02 ml, 0.35 mmol) in CH_2Cl_2 (0.1 ml) was added to a CH_2Cl_2 (2 ml) solution of compound **5.43** (0.10 g, 0.31 mmol) at 0 °C. The reaction was

followed by TLC and was completed within 5 minutes. Compound **5.51** was obtained as yellow oil in 93.3% yield; IR ν_{max} (KBr): 3065, 2975, 1589, 1484, 1283, 1194, 1020, 945, 755, 687 cm^{-1}; δ_H (400MHz; $CDCl_3$) 1.84 (3H, CH_3), 2.35 (2H, t, J = 6.8 Hz, 2-H), 3.79 (2H, br s, 4-H), 4.51 (2H, m, 1-H), 7.37 – 7.18 (10H, m, Ar-H); δ_C (100MHz; $CDCl_3$) 30.6 (CH_3), 41.6 (d, J = 7.5 Hz, C-2), 42.6 (C-4), 63.5 (C-3), 66.7 (d, J = 6.0 Hz, C-1), 120.0 (d, J = 4.8 Hz), 125.4 and 129.8 (10C, Ar-C), 150.3 (2C, d, J = 7.3 Hz, C-O); APCI obsd *m/z* 476.9486.

Phosphoric acid 3,4-dichloro-3-methyl-butyl ester diphenyl ester (5.57)

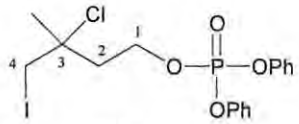

5.57

Potassium permanganate crystals (0.055 g, 0.35 mmol) and tetramethylammonium iodide (0.0695 g, 0.35 mmol) was stirred in $CHCl_2$ until the suspension was purple (45 minutes). Trimethylsilyl chloride (0.18 ml, 1.38 mmol) was added to the mixture. Compound **5.43** (0.11 g, 0.35 mmol) was added when the mixture turned emerald green and stirred at room temperature for 6 days. The crude product was extracted with EtOAc and washed with a saturated solution of sodium thiosulphate. Normal phase HPLC with hexane-EtOAc (70:30) gave pure compound **5.57** (0.085 g, 68.3%). Colourless oil; IR ν_{max} (KBr): 2973, 2355, 1589, 1485, 1283, 1184, 1022, 943, 753, 688 cm^{-1}; δ_H (400 MHz; $CDCl_3$) 1.71 (3H, s, CH_3), 2.34 (2H, t, J = 6.7, 2-H), 3,36 (2H, br s, 4-H), 4.48 (2H, q, J = 6.9, 13.5, 1-H), 7.37-7.19 (10H, m, Ar-H); δ_C (100 MHz; $CDCl_3$) 17.8 (C-4), 30.6 (CH_3), 42.2 (d, J = 7.4, Hz, C-2) 65.7 (d, J = 6.0 Hz, C-1) 67.8 (C-3), 120.0, 125.5 and 129.8 (10C, Ar-C), 150.4 (2C, d, J = 7.0 Hz, C-O).

Phosphoric acid 3-methyl-buttyl ester diphenyl ester (5.58)

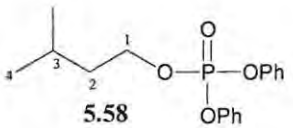

5.58

PtO_2-H_2O (0.006 g) was stirred in EtOH (0.15 ml) under H_2 to activate the catalyst for 1 hour. Compound **5.51** (0.06 g, 0.14 mmol) was added to the activated catalyst and stirred at room temperature for 16 hours. The reaction mixture was filtered and the product was washed with water, saturated solution of sodium thiosulphate and brine. The product was then concentrated under reduced pressure to give compound **5.58** (0.05 g 100%).

In a similar reaction, a round bottom flask equipment with a stirrer bar and fitted with a septum, compound **5.43** (0.05 g) in 2.5 ml EtOH was degassed and flushed with Ar three times. 10% palladium on carbon (0.008 g) was added to the reaction mixture and was again degassed and flushed with argon three times before replacing the argon line with H_2. The reaction was left for 2.5 hours at room temperature and was then filtered. The crude product was passed through a silica gel plug with 70:30 hexane-EtOAC to afford pure compound **5.58** (0.049, 97%). Colourless oil; δ_H (400MHz; $CDCl_3$) 0.88 (3H, CH_3), 0.89 (3H, s, 4-H), 1.57 (2H, s, 2-H), 1.59 (1H, s, 3-H), 4.27 (2H, q, J = 6.8, 7.2 Hz, 1-H), 7.36 – 7.16 (10H, m, Ar-H); δ_C (100MHz; $CDCl_3$), 22.2 (2C, CH_3 and C-4), 24.3 (C-3), 38.7 (d, J = 6.7 Hz, C-2), 68.0 (d, J = 6.6 Hz, C-1), 120.1 (d, J = 4.8 Hz), 125.0 and 129.9 (10C, Ar-C), 150.7 (2C, d, J = 7.1 Hz, C-O).

The molecular ion of compounds **5.44a**, **5.45**, **5.51** and **5.57** were not observed on the HRFABMS or APCI conducted.

Attempted phosphorylation of geraniol

Following the same method as for compound **5.32**, geraniol (**5.29**, 0.45 g, 2.9 mmol) was treated with NaH in mineral oil (0.12 g, 2.9 mmol) and diphenylchlorophosphate (1.3 g, 4.8 mmol) to give a clear yellowish oil. ^1H and ^{13}C NMR of the crude oil did not show the expected phosphorylated geraniol.

Attempted dihydroxylation of geraniol

Using the method as for styrene (**5.35**), Geraniol (**5.29**, 0.45 g, 2.9 mmol) was reacted with $NaIO_4$ (0.184 g, 0.86 mmol) and NaBr (0.06 g, 0.58 mmol) in acetic acid (5 ml). ^1H NMR of the crude yellow oil did not show the expected dihydroxylated products.

Attempted dihydroxylation of compound 4.4

Following the same method described for styrene (**5.35**) with slight modifications, compound **4.4** (0.23 g, 0.76 mmol) was treated with $NaIO_4$ (0.05 g, 0.23 mmol) ans NaBr (0.02 g, 0.15 mmol) in acetic acid (1.25 ml). The mixture was heated at 90 °C for 4 hour and left to stir at room temperature for 16 hours. The mixture was extracted three times with EtOAc and washed with sodium thiosulphate, water and $NaHCO_3$. ^{1}H and ^{13}C NMR of the orangish red crude product did not show the expected dihydroxylated products.

Supplementary information: NMR and MS supplementary data are available on CD.

References

Altincicek, B.; Duin, E. C.; Reichenberg, A.; Hedderich, R.; Kollas, A-K.; Hintz, M.; Wagner, S.; Wiesner, J.; Beck, E.; and Jomaa, H. LytB Protein Catalyzes the Terminal Step of the 2-*C*-Methyl-D-Erythritol-4-Phosphate Pathway of Isoprenoid Biosynthesis. *Federation of European Biochemical Societies* **2002**, 532, 437 – 440.

Andrus, M. B.; Lepore, S. D. and Sclafani, J. A. Selective Dihydroxylation of Non-conjugated Dienes in Favour of the Terminal Olefin. *Tetrahedron Letters* **1997**, 38(23), 4043 – 4046.

Atherton, F. R.; Howard, H. T. and Todd, A. R. Studies on Phosphorylation.Part IV. Further Studies on the Use of Dibenzyl Chlorophosphonate and the Examination of Certain Alternative Phosphorylation Methods. *Journal of Chemical Society* **1948**, 1106 – 1111.

Atherton, F. R.; Openshaw, H. T. and Todd, A. R. Studies on Phosphorylation. Part I. Dibenzyl Chlorophosphonate as a Phosphorylating Agent. *Journal of Chemical Society* **1945**, 382 – 385.

Bajwa, J. S. Chemoselective Deprotection of Benzyl Esters in the presence of Benzyl Ethers, Benzyloxymethyl Ethers and *N*-Benzyl Groups by catalytic Transfer hydrogenation. *Tetrahedron Letters* **1992**, 33 (17), 2299 – 2302.

Brown, D. M. and Higson, H. M. Phospholipids. Part I. The Hydrolysis of Some Esters of Cyclohexanediol Phosphates. *Journal of Chemical Society* **1957**, 2034 – 2041.

Burgos, E.; Roos, A. K.; Mowbray, S. L. and Salmon L. Synthesis of 5-Deoxy-5-phospho-D-ribonohydroxamic Acid: A new Competitive and Selective Inhibitor of Type B Ribose-5-phosphate isomerase from *Mycobacterium tuberculosis*. *Tetrahedron Letters* **2005**, 46, 3691 – 3694.

Casey, M.; Leonard, J.; Lygo, B. and Procter, G. *Advanced Practical Organic Chemistry* **1990**, first edition, Blackie Academic & Professional, Great Britain.

Djerassi, C. and Engle, R. R. Oxidations with Ruthenium Tetroxides. *Journal of American Chemical Society* **1953**, 75, 3838 – 3840.

Donohoe, T. J.; Moore, P. R.; Waring, M. J. and Newcombe, N. J. The Directed Dihydroxylation of Allylic Alcohols. *Tetrahedron Letters* **1997**, 38(28), 5027 – 5030.

Emmanuvel, L.; Shaikh, T. M. and Sudalai, A. $NaIO_4$/LiBr-Mediated Diastereoselective Dihydroxylation of Olefins: A catalytic Approach to the Prevost-Woodward Reaction. *Organic Letters* **2005**, 7 (22), 5071 – 5074.

Fernandes, R. P. M. and Proteau, P. J. Kinetic Characterization of *Synechocystis* sp. PCC6803 1-Deoxy-D-xylulose -5-Phosphate Reductoisomearse Mutants. *Biochimica et Biophysica Acta* **2006**, 1764, 223 – 229.

Haemers, T.; Wiesner, J.; Van Poecke, S.; Goeman, J.; Henschker, D.; Beck, E.; Jomaa, H. And Van Calenbergh, S. Synthesis of α-substituted Fosmidomycin analogues as Highly Potent *Plasmodium falciparum* Growth Inhibitors. *Bioorganic & Medicinal Chemistry Letters* **2006**, 16, 1888 – 1891.

Hayakawa, Y.; Aso, Y.; Uchiyama, M. and Noyori, R. Facile Nucleoside Phosphorylation via Hydroxyl Activation. *Tetrahedron Letters* **1983**, 24 (11), 1165 – 1168.

Hecht, S.; Eisenreich, W.; Adam, P.; Amslinger, S.; Kis, K.; Bacher, A.; Arigoni, D. And Rohdich, F. Studies on the Nonmevalonate Pathway to Terpenes: The Role of the GcpE (IspG) Protein. *Proceedings of National Academy of Sciences* **2001**, 98 (26), 14837 – 14842.

Herz, S.; Wungsintaweekul, J.; Schuhr, C. A.; Hecht, S.; Luttgen, H.; Sagner, S.; Fellermeier, M.; Eisenreich, W.; Zenk, M. H.; Bacher, A. and Rohdich, F. Biosyntheis of Terpenoids: YgbB Protein Converts 4-Diphosphocytidyl-2C-Methyl-D-Erythritol 2-Phosphate to 2C-Methyl-D-Erythritol 2,4-Cyclodiphosphate. *Proceedings of National Academy of Sciences*, **2000**, 97 (6), 2486 – 2490.

Hoeffler, J-F.; Tritsch, D.; Grosdemange-Billiard, C. and Rohmer, M. Isoprenoid biosynthesis via the methylerythritol phosphate pathway: Mechanistic investigations of the 1-deoxy-D-xylulose 5-phosphate reductoisomerase. *European Journal of Biochemistry* **2002**, 269, 4446 – 4457.

Jomaa, H.; Wiesner, J.; Sanderbrand, S.; Altincicek, B.; Weidemeyer, C.; Hintz, M.; Türbachova, I.; Eberl, M.; Zeidler, J.; Lichtenthaler, H. K.; Soldati, D. and Beck, E. Inhibitors of the Nonmevalonate Pathway of Isoprenoid Biosynthesis as Antimalarial Drugs. *Science* **1999**, 285, 1573 – 1576.

Jones, S. and Selitsianos, D. A Simple and Effective Method for Phosphoryl Transfer Using $TiCl_4$ Catalysis. *Organic Letters* **2002**, 4 (21), 3671 – 3673.

Jones, S.; Selitsianos, D.; Thompson, K, J. and Toms, S. M. An Improved Method for Lewis Acid Catalyzed Phosphoryl Transfer with Ti(*t*-BuO)$_4$. *Journal of Organic Chemistry* **2003**, 68(13), 5211 – 5216.

Kuzuyama, T.; Takahashi, S.; Watanabe, H. and Seto, H. Direct Formation of 2-C-Methyl-D-Erythritol 4-Phosphate from 1-Deoxy-D-xylulose -5-Phosphate by 1-Deoxy-D-xylulose -5-Phosphate Reductoisomerase, a New Enzyme in the Non-Mevalonate Pathway to Isopentenyl Diphosphate. *Tetrahedron Letters* **1998**, 39, 4509 – 4512.

Lapper, R. D.; Mantsch, H. H. and Smith I. C. P. A Carbon-13 Nuclear Magnetic Resonance Study of the Conformations 3',5'-Cyclic Nucleotides. *Journal of American Chemical Society* **1973**, 95(9), 2878 – 2880.

Lichtenthaler, H. K. The 1-Deoxy-D-xylulose -5-Phosphate Pathway of Isoprenoid Biosynthesis in Plants. *Annual Review of Plant Physiology and Plant Molecular Biology* **1999**, 50, 47 – 65.

Lüttgen, H.; Rohdich, F.; Herz, S.; Wungsintaweekul, J.; Hecht, S.; Schuhr, C. A.; Fellermeier, M.; Sagner, S.; Zenk, M. H.; Bacher, A. and Eisenreich, W. Biosyntheis of Terpenoids: YchB Protein of *Escherichia coli* Phosphorylates the 2-Hydroxy Group of 4-Diphosphocytidyl-2C-Methyl-D-Erythritol. *Proceedings of National Academy of Sciences* **2000**, 97 (3), 1062 – 1067.

March, J. Advanced Organic Chemistry Reactions, Mechanisms and Structure **1977**, second edition, pp 749 – 750, McGraw-Hill Book Company, U.S.A.

Markó, I. E.; Richardson, P. R.; Bailey, M.; Maguire, A. R. and Coughlan, N. Selective Manganese-Mediated Transformations Using the Combination: $KMnO_4/Me_3SiCl$. *Tetrahedron Letters* **1997**, 38 (13), 2339 – 2342.

Ortmann, R.; Wiesner, J.; Reichenberg, A.; Henschker, D.; Beck, E.; Jomaa, H. and Schlitzer, M. Acyloxyalkyl Ester Prodrugs of FR900098 with Improved *In Vivo* Anti-malarial Activity. *Bioorganic & Medicinal Chemistry Letters* **2003**, 13, 2163 – 2166.

Ortmann, R.; Wiesner, J.; Silber, K. Klebe, G.; Jomaa, H. and Schlitzer, M. Novel Deoxyxylulosephosphate-Reductoisomerase Inhibitors: Fosmidomycin Derivatives with Spacious Acyl Residues. *Archiv der Pharmazie-Chemistry in Life Sciences* **2007**, 340(9), 483 – 490.

Proteau, P. J. 1-Deoxy-D-xylulose -5-Phosphate reductoisomerase: An Overview. *Bioorganic Chemistry* **2004**, 32, 483 – 493.

Reichenberg, A.; Wiesner, J.; Weidemeyer, C.; Dreiseidler, E.; Sanderbrand, S.; Altincicek, B.; Beck, E.; Schlitzer, M. and Jomaa, H. Diaryl Ester Prodrug of FR900098 with Improved *In Vivo* Antimalarial Activity. *Bioorganic & Medicinal Chemistry Letters* **2001**, 11, 833 – 835.

Reuter, K.; Sanderbrand, S.; Jomaa, H.; Wiesner, J.; Steinbrechers, I.; Beck, E.; Hintz, M.; Klebe, G. and Stubbs, M. T. Crystal Structure of 1-Deoxy-D-xylulose -5-Phosphate Reductoisomerase, a crucial Enzyme in the Non-Mevalonate Pathway of Isoprenoid Biosynthesis. *The Journal of Biological Chemistry* **2002**, 277 (7), 5378 – 5384.

Rohdich, F.; Kis, K.; Bacher, A and Eisenreich, W. The Non-Mevalonate Pathway of Isoprenoids: Genes, Enzymes and Intermediates. *Current Opinion in Chemical Biology* **2001**, 5, 535 – 540.

Rohdich, F.; Wungsintaweekul, J.; Fellermeier, M.; Sagner, S.; Herz, S.; Kis, K.; Eisenreich, W.; Bacher, A. and Zenk, M. H. Cytidine 5'-Triphosphate-dependent Biosynthesis of Isoprenoids: YgbB Protein of *Escherichia coli*, Catalyzes the Formation of 4-Diphosphocytidyl -2-*C*-Methylerythritol. *Proceedings of National Academy of Sciences* **1999**, 96 (21), 11758 – 11763.

Rohdich, F.; Zepeck, F.; Adam, P.; Hecht, S.; Kaiser, J.; Laupitz, R.; Grawert, T.; Amslinger, S.; Eisenreich, W.; Bacher, A. and Arigoni, D. The Deoxyxylulose Phosphate Pathway of Isoprenoid Biosynthesis: Studies on the Mechanisms of the Reactions Catalyzed by IspG and IspH Protein. *Proceedings of National Academy of Sciences* **2003**, 100 (4), 1586 – 1591.

Rohmer, M.; Kani, M.; Simonin, P.; Sutter, B. and Sahm, H. Isoprenoid Biosynthesis in Bacteria. *Biochemistry Journal* **1993**, 295, 517 – 524.

Sakakura, A.; Katsukawa, M. and Ishihara, K. Selective Synthesis of Phosphate Monoesters by Dehydrative Condensation of Phosphoric Acid and Alcohols Promoted by Nucleophilic Bases. *Organic Letters* **2005**, 7 (10), 1999 – 2002.

Schwender , J.; Muller, C.; Zeidler, J. and Lichtenthaler H. K. Cloning and Heterogenous Expression of a cDNA Encoding 1-Deoxy-D-xylulose -5-Phosphate reductoisomerase of *Arabidopsis thaliana. Federation of European Biochemical Societies* **1999**, 455, 140 – 144.

Silverber, L. J.; Dillion, J. L. and Vemishetti, P. A Simple, Rapid and efficient Protocol for the Selective Phosphorylation of Phenols with Dibenzyl Phosphite. *Tetrahedron Letters* **1996**, 37 (6) 771 – 774.

Singh, N.; Cheve, G.; Avery, M. A. and McCurdy, C. R. Targeting the Methyl Erythritol Phosphate (MEP) Pathway for Novel Antimalarial, Antibacterial and Herbicidal Drug Discovery: Inhibition of 1-Deoxy-D-xylulose -5-Phosphate Reductoisomerase (DXR) Enzyme. *Current Pharmaceutical Design* **2007**, 13, 1161 – 1177.

Sweeney, A. M.; Lange, R.; Fernandes, R. P. M.; Schulz, H.; Dale, G. E.; Douangamath, A.; Proteau, P. J. and Oefner, G. The Crystal Structure of E. coli 1-Deoxy-D-xylulose-5-phosphate Reductoisomerase in a Ternary Complex with the Antimalarial Compound Fosmidomycin and NADPH Reveals a Tight-binding Closed Enzyme Conformation. *Journal of Molecular Biology*, **2005**, 345, 115 – 127.

Testa, C. A.; Lherbet, C.; Pojer, F.; Noel, J. P. and Poulter, C. D. Cloning and Expression of *IspDF* from *Mesorhizobium loti*. Characterization of Bifunctional Protein that Catalyzes Non-consecutive Steps in the Methylerythritol Phosphate Pathway. *Biochimica et Biophysica Acta* **2006**, 1764, 85 – 96.

VanRheenen, V.; Kelly, R. C. and Cha, D. Y. An Improved Catalytic OsO_4 Oxidation of Olefins to *cis*-1,2,-Glycols Using Tertiary Amine Oxides as the Oxidant. *Tetrahedron Letters* **1976**, 23, 1973 – 1976.

Virsu, P.; Liljeblad, A.; Kanerva, A. and Kanerva, L. Preparation of the Enantiomers of 1-Phenylethan-1,2-diol. Regio- and Enantioselectivity of Acylase I and *Candida Antarctica* Lipases A and B. *Tetrahedron Asymmetry* **2001**, 12, 2447 – 2455.

Weber,W. P. and Shepherd, J. P. An Improved Procedure for the $KMnO_4$ Oxidation of Olefins to *cis*-1,2,-Glycols by Use of Phase Transfer Catalysis. *Tetrahedron Letters* **1972**, 48, 4907 – 4908.

Woodward, R. B. and Brutcher, F. V. *cis*-Hydroxylation of a Synthetic Steroid Intermediate with Iodine, Silver Acetate and Wet Acetic acid. *Journal of American Chemical Society* **1958**, 80, 209 – 211.

Yin, X. and Proteau, P. J. Characterization of Native and Histidine-tagged Deoxyxylulose 5-Phosphate Reductoisomerase from the Cyanobacterium *Synechocystis* sp. PCC6803. *Biochimica et Biophysica Acta* **2003**, 1652, 75 – 81.

Chapter 6

Over-expression, purification and preliminary assessment of inhibitors of DOXP reductoisomerase

6.1 Introduction

One of the great developments in Biochemistry and Biotechnology is the ability to produce recombinant DNA. This has several applications in molecular biology and genetic engineering. Virtually any DNA segment can now be cloned or expressed in bacterial host cells. One of the objectives of this research project was to test for inhibition of 1-deoxy-$_D$-xylulose 5-phosphate reductoisomerase (DXR) by natural products and their analogues, therefore it was necessary to produce and purify a relatively large quantity of this enzyme for the inhibition assay. In this chapter the expression and purification of DXR will be discussed followed by use of the recombinant enzyme to test the inhibition potential of selected natural products and their analogues.

6.1.1 Plasmid as a cloning Vector

Bacteria carry plasmids, which are self-replicating, extrachromosomal, circular pieces of double stranded DNA that contains genetic information for their growth (Madigan and Martinko, 2006). Plasmids seemed to have evolved in nature to carry genetic information such as antibiotic resistance and impart this characteristic to any bacteria that takes up such a plasmid. Scientists have exploited this natural mechanism by using it to transfer and amplify a gene of interest. Requirements for a plasmid vector include (i) an origin of replication, (ii) a selectable marker such as antibiotic resistance and (iii) a cloning site where restriction endonuclease can cleave the plasmid and allow for insertion of a foreign DNA fragment (Garret and Grisham, 1999). Recombinant plasmid or chimeric constructs are plasmids which have been artificially modified to carry a gene of interest. This

chimeric plasmid can then be inserted into a competent bacterial cell for amplification of the gene.

6.1.2 Production and purification of recombinant protein in *E. coli*

Escherichia coli (*E. coli*) is one of the bacteria favoured by molecular biologists to effect expression of DNA. This bacterium has been well characterized and its simple genetics and rapid growth rates are of advantage to researchers. One of the techniques that have been developed for production, isolation and purification of proteins in *E. coli* is fusion protein expression. This involves a carrier protein and a fusion partner. The carrier protein, which is a sequence encoding for the amino terminus or the whole length of the highly expressed proteins, facilitates solubility and high-level expression of the protein while the fusion partner encodes an affinity tag to facilitate purification of the expressed protein (Studier *et al.*, 1990).

Purification of proteins in this new age is mostly achieved by affinity-based techniques which allows for the purification of proteins either by their biological function or by chemical structure. Metal chelate affinity chromatography is a technique that involves binding of metal ion to solid chromatographic matrices which in turn interact and bind to the imidazole and thiol groups of the protein (Chaga, 2001). In order to improve on the system, researchers have tagged proteins e.g. with poly histidine tag to allow for purification of the protein on a nickel charged column without interfering with the expression of the protein.

6.1.3 Over-expression of *Plasmodium falciparum* recombinant proteins

DXR (discussed in Section 5.1.2) is an enzyme found in the non-mevalonate isoprenoid biosynthetic pathway of some bacteria, green algae, higher plants and *Plasmodium falciparum* (Lichtenthaler, 1999). The DXR gene of several organisms including *P. falciparum* and *E. coli* has been cloned and *P. falciparum* DXR (*Pf*DXR) has been successfully expressed in *E. coli* (Jomaa *et al.*, 1999).

However, difficulties have also been encountered with the expression of *P. falciparum* proteins, including DXR, in *E. coli* due to various reasons. One of the reasons include the codon bias with *P. falciparum* which exhibits an AT genome composition of approximately 80% (Ahuja *et al.*, 2006). The codons that are often used in the parasite are rarely used in *E. coli* (Baca and Hol, 2000), and thus protein synthesis in the bacteria is hindered by translational problems such as premature termination of translation and mistranslational amino acid substitutions (Ahuja *et al.*, 2006). This problem was eliminated by designing a plasmid which encodes for the genes of tRNAs which are not well expressed in *E coli* (Baca and Hol, 2000). Another problem encountered in the expression of *Pf*DXR in *E. coli* is protein toxicity which has been countered by the co-expression with pMICO[17] plasmid. This allows for the expression of toxic proteins in *E. coli* host system (Cinquin, *et al.*, 2001). Alternatively as opposed to using *E. coli* a different host system such a yeast cell can be used to express the *P. falciparum* proteins to avoid the problems that are often experienced with the expression.

For the purpose of this project the expression of *Ec*DXR in *E. coli* was conducted. *Pf*DXR and *Ec*DXR have been reported to be 36% identical with 54% similar amino acid residues at the catalytic centre. Most of these residues are involved in the binding of DOXP (**5.3**) and NADPH and are involved in coordination of the divalent metal ion (Kaiser *et al.*, 2007). An inhibitor of *Ec*DXR is therefore expected to inhibit *Pf*DXR. Thus *E. coli* DXR can be used as a model for the inhibition assay.

6.1.4 Enzyme Kinetics

The rearrangement and reduction of DOXP (**5.3**) to MEP (**5.4**) by DXR is dependent on the availability of NADPH. As such determination of the rate of activity of *Ec*DXR can be carried out in an NADPH-dependent DOXP assay. The activity of the enzyme is then measured by the rate at which NADPH is depleted (Takahashi *et al.*, 1998).

[17] pMICO is a hybrid pLysS plasmid with a tRNA gene insert. The pLysS plasmid contains genes that produce low levels of T7 lysozyme which allows for the expression of toxic proteins in *E. coli*. Within the pLysS plasmid a gene insert that encode for tRNA that are rarely used in *E.coli* is included giving rise to the hybrid pMICO plasmid.

The study of enzyme kinetics involves the study of chemical reactions that are catalyzed by the enzyme and reveals the catalytic mechanism of the enzyme (Garret and Grisham, 1999). Enzymes catalyze single-substrate and multi-substrate reactions. DXR has a single substrate, DOXP (**5.3**), and can therefore be quantified by Michaelis-Menten Kinetics used for single-substrate reactions. The Michaelis-Menten kinetics applies to situations where there are fewer enzymes than substrate. In this type of reaction the rate of reaction increases with increasing substrate concentration up to a point where the enzyme is saturated with the substrate and the enzyme reaches its maximum rate of activity, V_{max}. The equation:

$$V = \frac{V_{max}[S]}{[S] + K_m}$$

Known as the Michaelis-Menten equation can then be used to calculate the rate of reaction of the enzyme where V_{max} is the maximum rate of activity of the enzyme, [S] is the substrate concentration and K_m, the Michealis constant, is the substrate concentration at which the enzyme reaction rate is half V_{max} ($V_{max}/2$) (Garret and Grisham, 1999).

The actual kinetic parameters V_{max} and K_m are determined from the Michaelis-Menten plot which is a plot of the reaction rate (v) as a function of substrate concentration [S]. This plot is non-linear although it starts off linear at low substrate concentration but bends and become constant as the enzyme is saturated (Figure 6.1A).

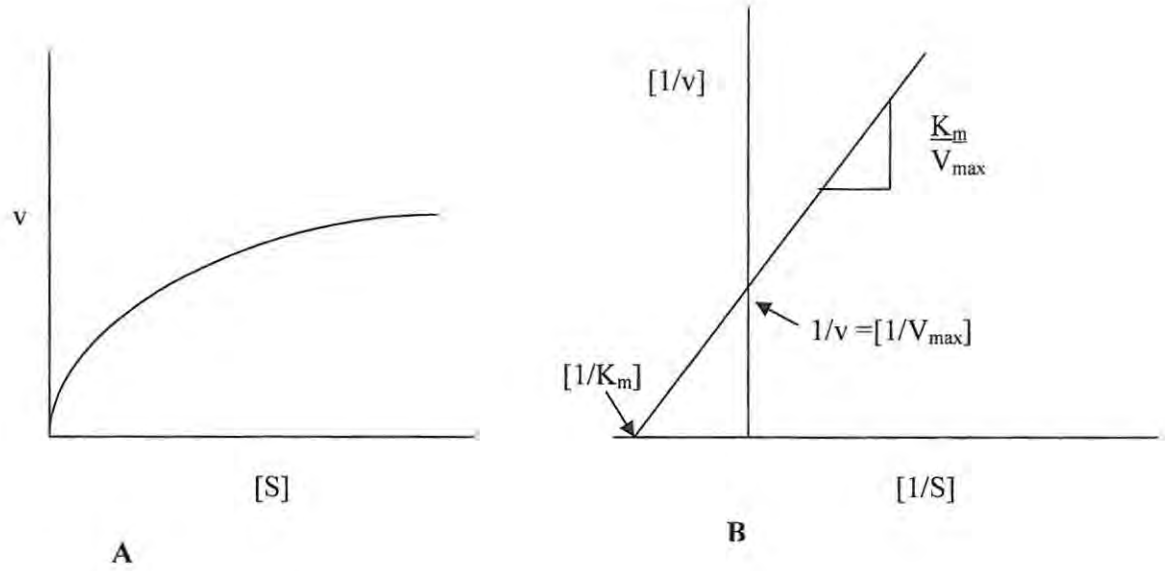

Figure 6.1 A schematic representation of Michaelis-Menten plot (A) and Lineweaver-Burke plot (B) (Garret and Grisham, 1999)

In the absence of computer programs that can accurately measure the V_{max} and K_m, a linear plot of Michaelis-Menten plot, known as Lineweaver-Burke plot (Fugure 6.1B) or double reciprocal plot can be used for easier determination of these parameters. This is a plot of the reciprocal values of the reaction rate (1/v) and substrate concentration (1/[S]) with a linear equation of:

$$\frac{1}{V} = \frac{K_m}{V_{max}[S]} + \frac{1}{V_{max}}$$

The y-intercept of the plot is thus $1/V_{max}$ and the x-intercept is $-1/K_m$. The x-intercept is however an extrapolation of experimental data at positive concentration since no experimental value can be taken as negative 1/[S] and 1/[S] = 0 (y-intercept) represent an infinite concentration of substrate in order that $1/v = 1/V_{max}$.

To determine the V_{max} and K_m of overproduced enzyme a series of experiment with increasing concentration of substrate is therefore required.

As this was a project designed for inhibition study the K_i which is the concentration of inhibitor which produces half the maximum inhibition is required. An inhibitor is a compound that binds to an enzyme to reduce the activity of such an enzyme. The type of kinetics displayed by the enzyme gives an indication of the type of inhibition exhibited by the inhibitor. There are reversible and irreversible inhibitions. In the case of an irreversible inhibition the enzyme is covalently modified that the activity is permanently reduced. Different types of reversible inhibition exist and include:

i. Competitive inhibition – In this type of inhibition the inhibitor competes with the substrate to bind to the enzyme and an enzyme-substrate (ES) or enzyme-inhibitor (EI) complex is formed. With increasing concentration of the substrate the inhibitor can be displaced and the enzyme can eventually reach its V_{max} (i.e. the V_{max} is unchanged) but the K_m will change as more of the substrate is required to reach the V_{max} (Garret and Grisham, 1999).

ii. Non-competitive inhibition – this type of inhibition involves the inhibitor binding to the ES complex and slows down the rate at which the product is formed. Increases in the concentration of the substrate thus have no effect on the inhibition of the enzyme. Here the V_{max} is changed but the K_m remains unchanged.

iii. Uncompetitive inhibition – The inhibitor in this case binds to the enzyme and enhances the binding of the substrate, thus reducing K_m. However, the enzyme-inhibitor-substrate complex forms product slowly thereby reducing the V_{max} as well. This type of inhibition is uncommon.

To determine the type of inhibition exhibited by an inhibitor a series of experiments with increasing substrate concentration for a set of increasing inhibitor concentration is thus necessary. The inhibition constant K_i gives an indication of how potent an inhibitor is. Determining K_i involves setting up a series of experiment with increasing inhibitor concentration and repeating this experiment for different concentrations of the substrate.

Plotting a curve of 1/v against inhibitor concentration, [I], at different concentrations of the substrate gives a group of intersecting lines. Where the lines intersect above the x-axis, the inhibitor is competitive and the value of [I] where the lines intersect is the K_i. For a non-competitive inhibitor the lines converge on the x-axis and the [I] at this point is the K_i (Garret and Grisham, 1999).

The aim of this part of the project was thus to express and purify *E. coli* DXR and conduct an enzyme inhibition assay of the expressed protein using the isolated compounds from *P. cornutum* and the synthesized derivatives of 3-methyl-3-butenol (**5.42**).

6.2 Results and Discussion

The plasmid construct pQE9EcDXR was kindly provided by Jomaa Pharmaka GmbH (Germany). The plasmid incorporated an *N*-terminal $(His)_6$ fusion tag to facilitate nickel affinity purification. The plasmid also included an ampicillin cassette as a selectable marker and different diagnostic restriction enzyme sites (Figure 6.1).

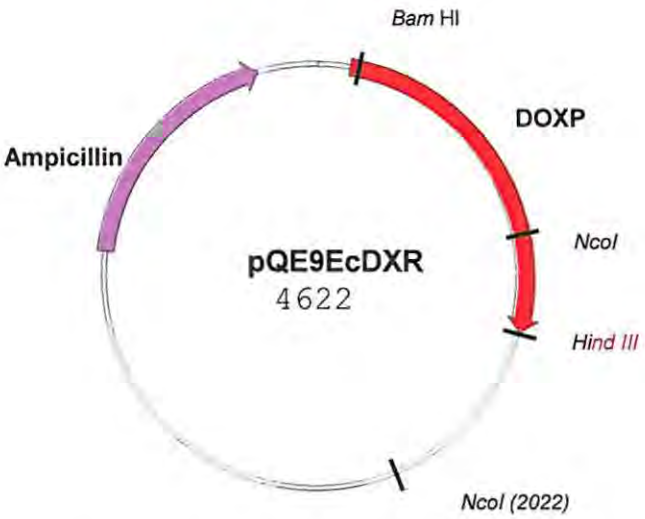

Figure 6.2 Plasmid map of pQE9EcDXR (Tanner, 2004)

6.2.1 Confirmation of pQE9EcDXR plasmid construct (restriction analysis)

In order to confirm that the construct provided contains the *E. coli* DXR gene, a series of small scale enzymes digests were done on the construct. This involved the incubation of the pQE9EcDXR plasmid with different restriction enzymes that "cut" the circular plasmid into linear fragments. The fragments have different weights depending on the number of base pairs (bp) and when run on agarose gel moved different distances. Restriction enzymes are mostly isolated from bacteria. For the confirmation of the pQE9EcDXR plasmid the restriction enzymes used included *NcoI* obtained originally from *Nocardia corallina, HindIII* originally from *Haemophilus influenzae* and *BamHI* from the bacterium *Bacillus amyloliquefaciens* which recognize and "cuts" specific DNA sequences on the plasmid (Figure 6.2). Samples of the different digests were run on the agarose gel and the result as shown in Figure 6.2 confirmed the presence of the *Ec*DXR.

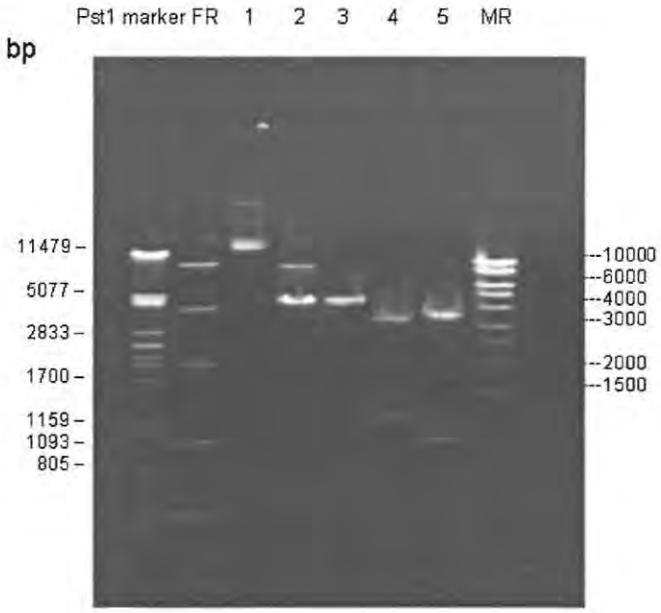

Figure 6.3 Confirmation of the pQE9EcDXR plasmid construct: Pst1 marker – molecular marker, lamda DNA restricted with pstI and expressed in base pairs; Fr- fast ruler™ DNA ladder as a molecular marker; lane 1 – uncut pQE9EcDXR; lane 2 – plasmid linearized with *BamHI*; Lane 3 – Linearized plasmid with *HindIII*; Lane 4 – double digest with *BamI* and *HindIII*; Lane 5 – Restriction with *NCoI*; MR – Mass ruler™ DNA ladder as a molecular marker in base pair.

The linearized pQE9EcDXR plasmid has 4622 bp which was observed in lanes 2 and 3 which were linearized by *BamHI* and *HindIII*, respectively. These enzymes cut the plasmid once giving the 4622 bp. The release of the DXR gene occurred as a result of a double digest with *BamHI* and *HindIII* which were incubated with the plasmid to give two linear fragments (Figure 6.3, lane 4) of 1203 and 3419. The last digest to confirm the correct coding sequence of both the vector and the DXR recombinant protein in the construct plasmid, involved digestion with *NcoI*. This also digests the plasmid at two points and results in two fragments with 1023 and 3599 bp (Figure 6.3, lane 5). This result confirms the presence of the correct pQE9EcDXR plasmid construct.

6.2.2 Transformation of competent *E. coli* XL1 Blue cells with pQE9EcDXR construct

Having confirmed the identity of the pQE9EcDXR plasmid construct, they were incorporated into XL1 Blue[18] *E. coli* competent cells in a process of transformation. Transformation is the process by which foreign plasmids are introduced into a bacterial cell in order to use the bacteria as hosts to amplify the plasmid (Madigan and Martinko, 2006). The cell membrane of bacteria is hydrophobic and DNA is very hydrophilic, making these two components incompatible. Therefore, in order for transformation to take place the bacterial cells need to be made "competent" to take up the hydrophilic plasmid. This is done by suspending the cells in a high concentration of calcium and as a result create small holes in the bacterial cell membrane through which the plasmid can be taken up. The DNA is then forced into the cell by incubating the DNA with the bacterial cells on ice, heat-shocking the cells at 42 °C and putting the cells back on ice (Dagert and Ehrlich, 1979).

E. coli XL1 Blue cells were transformed with the pQE9EcDXR plasmid. The success of the transformation process was confirmed by plating the cells on agar plates containing ampicillin. The plates were incubated overnight at 37 °C. The growth of ampicillin resistant (plasmid marker) bacteria on the agar plate confirmed that the *E. coli* DXR plasmid and therefore the DXR gene has been transferred to the cells.

6.2.3 Induction studies

An initial induction study of the over-production of the *Ec*DXR enzyme was conducted to determine the optimum time of harvest after inducing the bacterial cells to over-produce the enzyme. This was done by inoculating autoclaved broth agar containing 0.15 mg/ml ampicillin with transformed *E. coli* cells. The cells were induced after one hour with isopropyl-β-D-galactopyranoside (IPTG). The IPTG acts on the *lac* operon of the

[18] XL1 Blue is a strain of *E. coli* which has a T5 promoter that is compatible with the IPTG induction Maguire *et al.*, 2001)

vector system to promote transcription of the DXR encoding region of the construct (Yadava and Ockenhouse, 2003). A 1 ml aliquot of the cells was taken before induction and every hour after induction for 6 hours. The last aliquot was taken after the cells had been incubated overnight.

The induction profile of the protein was analyzed by discontinuous SDS-PAGE and Coomassie Blue staining (Figure 6.4).

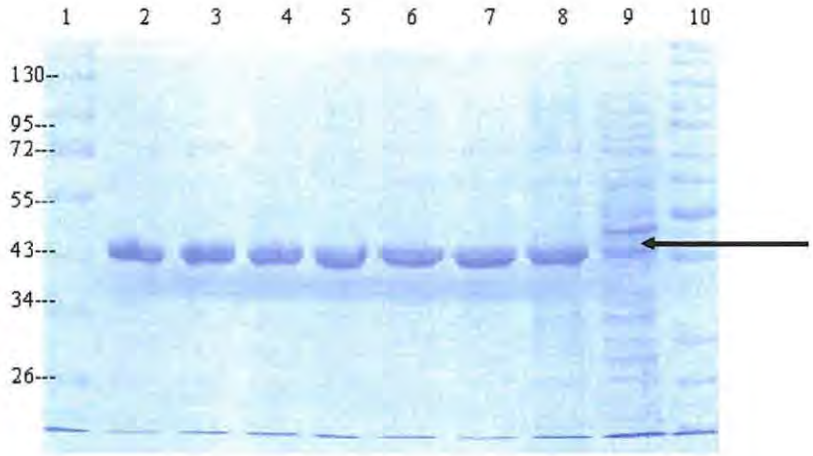

Figure 6.4 Over-production of recombinant *E. coli* DXR in XL1 Blue cells induced by IPTG: Lane 1 – peqGOLD Protein marker IV (kDa); Lane 2 – pre-induction sample removed after 1 hour of incubation in 250 ml 2xYT broth; Lanes 3-8 – Samples removed hourly after induction with IPTG; Lane 9 – Overnight sample with IPTG; Lane 10 – peqGOLD Protein Marker II (kDa).

The $(His)_6$-DXR subunit has a molecular mass of 43.5 kDa which is clearly seen (Figure 6.4) on the SDS-PAGE as the area with the highest intensity. This represents the over-expression of the DXR enzyme with optimal production between 4 – 6 hours (lanes 6-8). The protein degraded overnight probably due to depletion of nutrients required to continue the overproduction of the enzyme as well as the need for the cell to manufacture other proteins for survival. A low level of the protein was expected in the pre-induced sample (lane 2) but it appeared that the protein was already being over-produced before the addition of IPTG to the cultured cells. This could have happened due to a natural

trigger of the bacterial cells to produce more of the enzyme or from a stimulus from the environment.

6.2.4 Purification of recombinant *E. coli* DXR

Since the protein had degraded overnight from the induction study, a fresh overproduction was made to harvest the protein after induction for four hours. The cells were lysed with lysozyme and sonication. The supernatant obtained after centrifuging the lysed cells contained the expressed DXR and was purified by nickel chelate affinity chromatography.

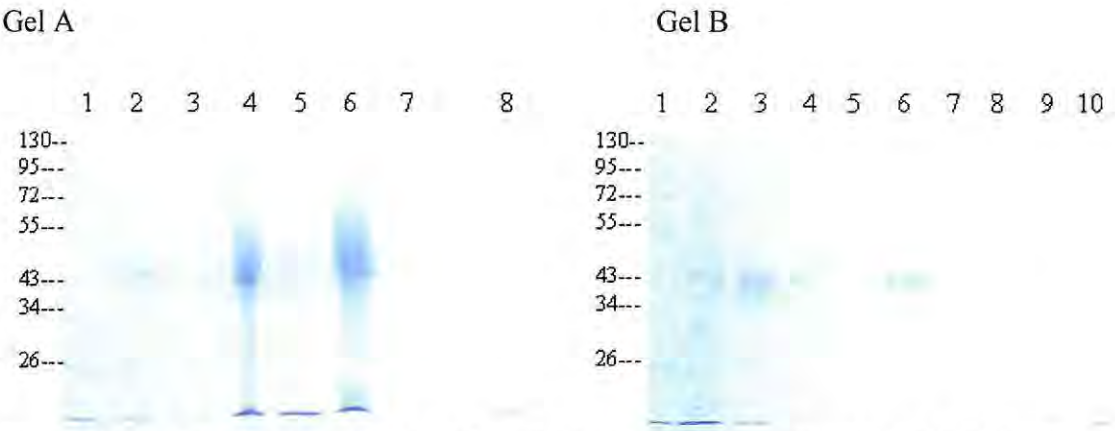

Figure 6.5 Purification Profile of $(His)_6$ *E. coli* DXR monitored by SDS-PAGE; Gel A: Lane 1 – peqGOLD protein marker IV (kDa), Lane 2 – sample 1 after 4 hours of induction, Lane 3 – sample 2 after 4 hours of induction, Lane 4 – sonicated fraction, Lane 5 – soluble fraction, Lane 6 – insoluble fraction, Lane 7 – Beads, Lane 8 – peqGOLD protein marker II (kDa); Gel B: Lane 1 – peqGOLD protein marker IV (kDa), Lane 2 – Flow-through, Lane 3-5 – native wash 1, 2 and 3 respectively, Lane 6-8 – native elutions 1, 2 and 3 respectively, Lane 9 – elution 1 dialysate, Lane 10 – peqGold protein marker II (kDa)

The over production of DXR was done in 4x 250 ml 2xYT[19] broth with ampicillin and were combined into two fractions. Lanes 2 and 3 of gel A (Figure 6.5) contained whole

[19] 2xYT broth is a bacterial growth nutrient medium containing 16 g tryptone, 10 g yeast extract and 5 g NaCl dissolved in 1 L of deionized water.

cells from each of the two samples after 4 hours of induction. Both samples showed that *Ec*DXR had been over-expressed as the intensity of the stain at 43.6 kDa is higher than for other proteins. Lanes 4 and 6 contained the sonicated fraction and insoluble fraction respectively, which also showed the presence of the DXR protein. The sonicated fraction was yet to be cleared while although the insoluble fraction had been cleared of the protein showed that some protein was still present. The smudged appearance of these fractions could be due to cell debris. Lane 5 of gel A contained the soluble fraction i.e. the cleared lysate with the DXR enzyme. The intensity of the stain was not as high as expected probably due to high dilution of the lysate.

As compared to gel A, gel B shows a progressive clearing of other proteins until only *Ec*DXR is observed (lanes 4 – 9), highlighting the efficiency of the protein purification process. The flow-through (lane 2) which was the supernatant obtained after agitating the cleared lysate on nickel charged resin contained some $(His)_6$ tag *Ec*DXR which could have been due to saturation of the beads. Washing the beads removes other unwanted impurities from the resin and wash 1 (lane 3) removed more impurity proteins including a considerable amount of *Ec*DXR. Less *Ec*DXR was removed from washes 2 and 3 (lane 4 and 5) and no other protein appeared in the washes indicating that the beads are cleared of impurities. The *Ec*DXR was removed and collected by gentle agitation of the beads with elution buffer three times. The first elution or elution 1 (Figure 6.5, gel B, lane 6) showed a clean fraction with high intensity at 43.5 kDa indicating a large amount of the expressed protein is being removed. By the third elution (lane 8) most of the protein had been displaced from the beads and is cleared of impurities. Elution 1 was dialyzed in PEG 20 000 to concentrate and remove imidazole from the protein. However from the gel (Figure 6.5, gel B), the dialysate (lane 9) did not appear as concentrated as elution 1.

6.2.5 *In vitro* activity of over-expressed *Ec*DXR

The *in vitro* DXR assay was conducted using a modified method described by Takahashi *et al.* (1998). The assay was carried out in a flat-bottom 96-well microtitre plate in a total volume of 200 µL. A satisfactory result had been obtained for the enzyme assay when 20 µL of 8.73 µM concentration of the enzyme was used (Tanner, 2004). A concentration of 6.87 µM was obtained for the over-produced *Ec*DXR from the Bradford Assay. A 25 µL volume of the produced enzyme was then calculated and observed (data not shown) to be the optimal volume for the assay. The enzyme catalyzed reaction i.e. the conversion of DOXP (**5.3**) to MEP (**5.4**) was initiated by the addition of the enzyme. The activity of the enzyme was observed by measuring the depletion of NADPH, which is an important cofactor in the conversion of DOXP (**5.3**) to MEP (**5.4**). The depletion of NADPH was monitored spectrophotometrically at 340 nm over 10 minutes. The reaction was essentially complete after 5 minutes and the slope of the curve over 5 minutes was -54.61 mOD/min[20] (Figure 6.6). The slope of the curve represents the rate at which NADPH is consumed by the enzyme in the catalytic process. The activity of the enzyme was also tested in the absence of the substrate (Appendix 2, Figure 6A2) and the presence of the inhibitor fosmidomycin (**5.21**) (Figure 6.7). The slope of the curve over 5 minutes when no substrate was added to the assay was 5.04 mOD/min while it was -3.93 mOD/min when fosmidomycin (**5.21**) was incorporated into the assay. No depletion of NADPH was observed when the substrate was not included indicating that no reaction involving the consumption of NADPH took place. In the presence of the inhibitor minimum activity of the enzyme was observed. This result showed the successful expression of an active *Ec*DXR.

[20] mOD/min = milli optical density

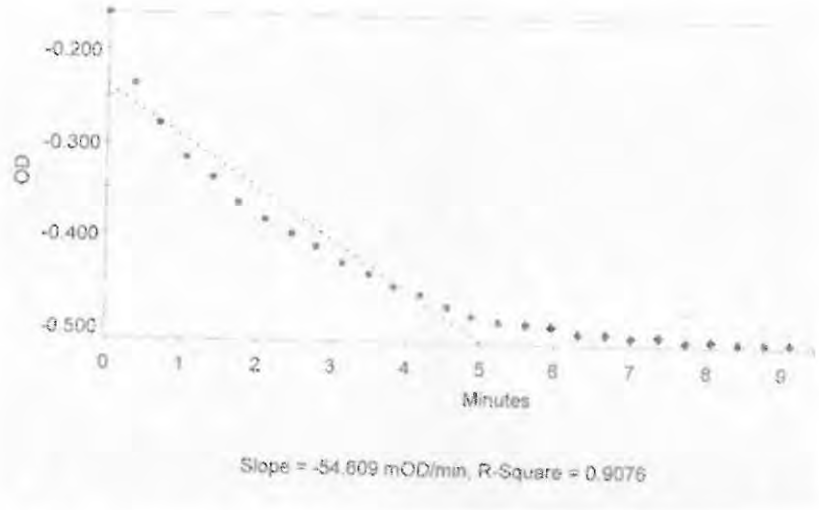

Figure 6.6 *In vitro* activity of the purified recombinant *Ec*DXR

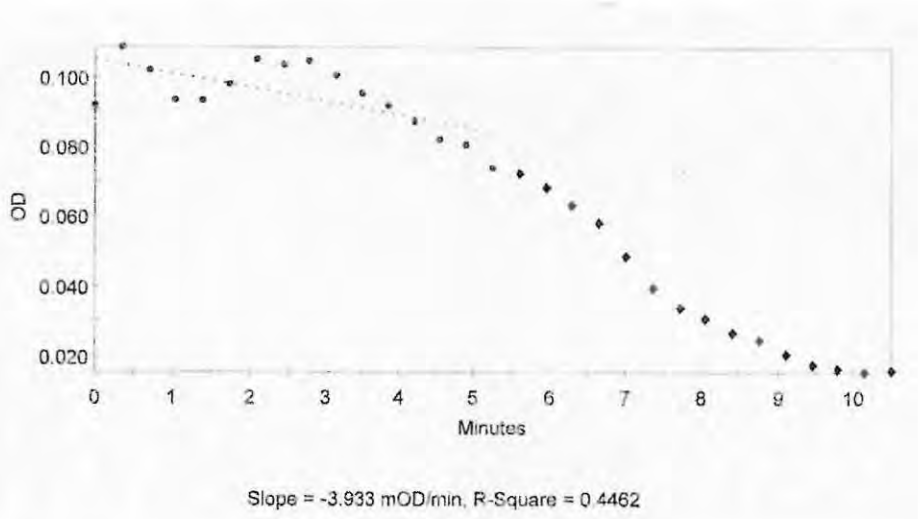

Figure 6.7 Activity of purified recombinant *Ec*DXR in the presence of the inhibitor Fosmidomycin **(5.21)**

The kinetics of the expressed *Ec*DXR was not determined as the potential inhibitors to be tested were yet to be modified. A fresh overproduction of the enzyme for the inhibition assay was envisaged once the potential inhibitors had been prepared. Unfortunately, the expressed *Ec*DXR was no longer active after seven months even though the enzyme had been stored at -80 °C. A fresh batch of *Ec*DXR was produced and purified for the inhibition assay with an added purification step which included a buffer exchange of the

eluted protein into 0.1M Tris –HCl (pH 7.5) by size exclusion column chromatography to remove imidazole from the protein fraction. However the newly purified enzyme did not show any significant activity (Appendix 2, Figure 6A2). A repeat of the over-production without the buffer exchange step also did not produce active enzyme. Due to time constraints the reasons for failed experiment could not be investigated.

6.2.6 Preliminary assessment of over-expressed *Pf*DXR

Fortunately, a small volume of over-produced *Pf*DXR was available[21]. The concentration of the enzyme was determined to be 20.5μM with the optimum final concentration of 1.03 μM in the assay at a final volume of 200 μL. Due to the small amount of enzyme available, kinetics study of the enzyme was not determined. Goble (2007) however determined the K_m and V_{max} of the *Pf*DXR to be 417 μM and 0.076μmol/min/mg respectively although investigation is still in ongoing on the enzyme kinetics.

A number of preliminary tests were conducted to verify the activity of the enzyme. This included conducting the assay in the absence of the DOXP (**5.3**) substrate, NADPH, in the presence of fosmidomycin (**5.21**), and with heat denatured enzyme. The standard assay was made up of Tris-HCl, $MnCl_2$, NADPH, DOXP substrate, *Pf*DXR and water to make up the volume to 200 μL (Assay A). Assay A showed progressive depletion of the NADPH (Figure 6.8) and the reaction appeared to be complete after 6 minutes.

[21] *Pf*DXR was kindly donated by Jessica Goble, Department of Biochemistry, Microbiology and Biotechnology, Rhodes University.

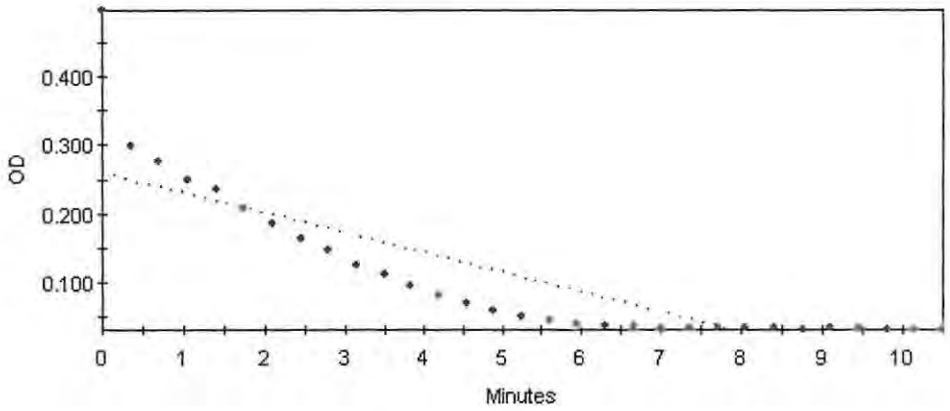

Figure 6.8 A plot of the consumption of NADPH in Assay A[22]

Since the V_{max} and the K_m of the enzyme was unknown this particular assay, the activity of each assay conducted was based on comparison of the slopes with the slope of assay A (-28.84 mOD/min) which was set to be 10 minutes.[23] The assay when conducted without NADPH (Figure 6.9), without substrate (Figure 6.10), with heat denatured enzyme (Figure 6.11) and with concentration of fosmidomycin (**5.21**) (Figure 6.12) showed no activity. Results obtained from these preliminary tests show that the enzyme is active.

[22] In figures 6.5 to 6.10 the red line shows the activity of DXR. The blue line represent the rate of consumption of NADPH i.e. the slope of the curve.

[23] The slope of the curves of all *Pf*DXR was determined over 10 minutes even though on some of the curves it appeared otherwise.

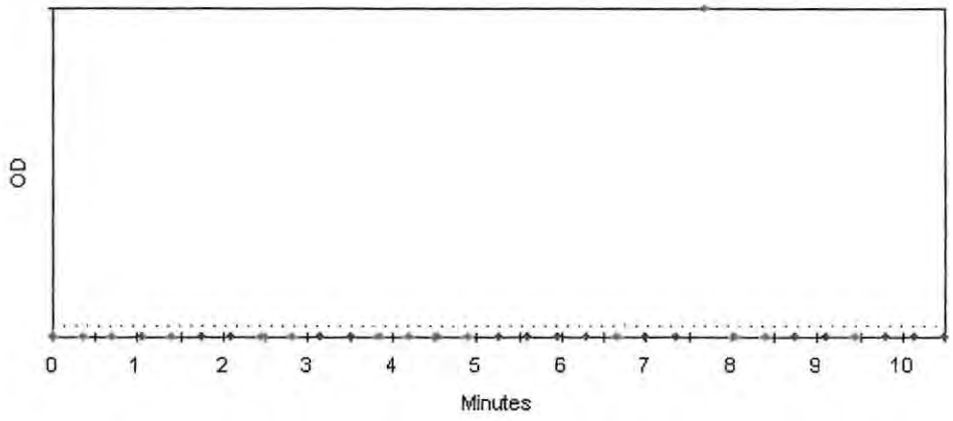

Slope = 0.000 mOD/min, R-Square = 0.0204

Figure 6.9 A plot of *Pf*DXR assay in the absence of NADPH

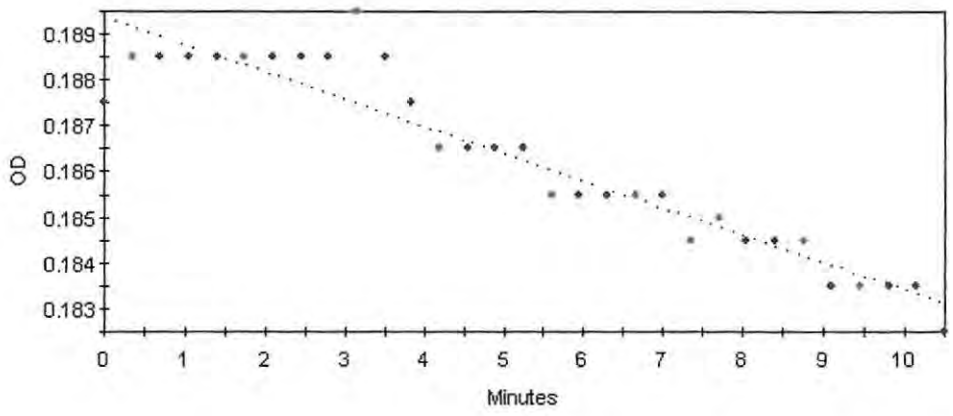

Slope = -0.595 mOD/min, R-Square = 0.8932

Figure 6.10 A plot of *Pf*DXR assay in the absence of DOXP (**5.3**) substrate

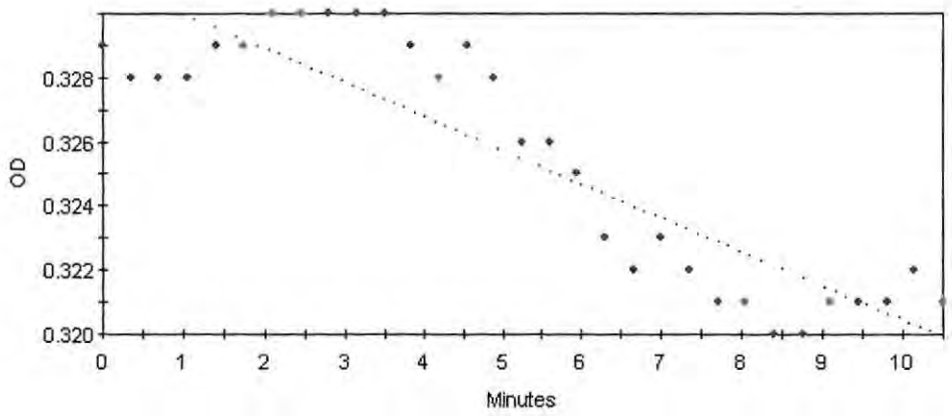

Slope = -1.058 mOD/min, R-Square = 0.7982

Figure 6.11 A plot of *Pf*DXR assay in the presence of boiled enzyme

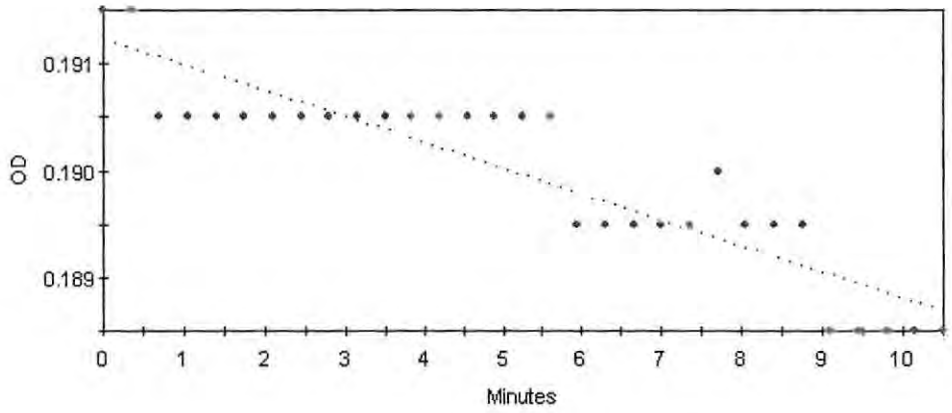

Slope = -0.241 mOD/min, R-Square = 0.8244

Figure 6.12 A plot of *Pf*DXR assay in the presence of fosmidomycin (**5.21**)

6.2.7 Inhibition studies of selected compounds on *Pf*DXR

After confirming the activity of the enzyme, selected compounds obtained from *P. cornutum* and the synthetic derivatives of **5.42** (Figure 6.13) were tested as potential inhibitors of *Pf*DXR. Although compounds **4.4**, **4.5 and 4.7** were included in this assay it is unlikely that they would act as inhibitors of DXR due to their very non-polar nature and lack of the phosphate group. The inhibitors were dissolved in a 50:50 EtOH-H_2O but

only compounds **5.43**, **5.44a** and **5.45** dissolved in the solution. The remaining compounds were tested as suspensions. Each sample was prepared to a concentration of 50 μM and from this solution 10 μL was added to the assay of each inhibitor was included in the assay. The highest concentration of EtOH used did not affect the activity of the enzyme.

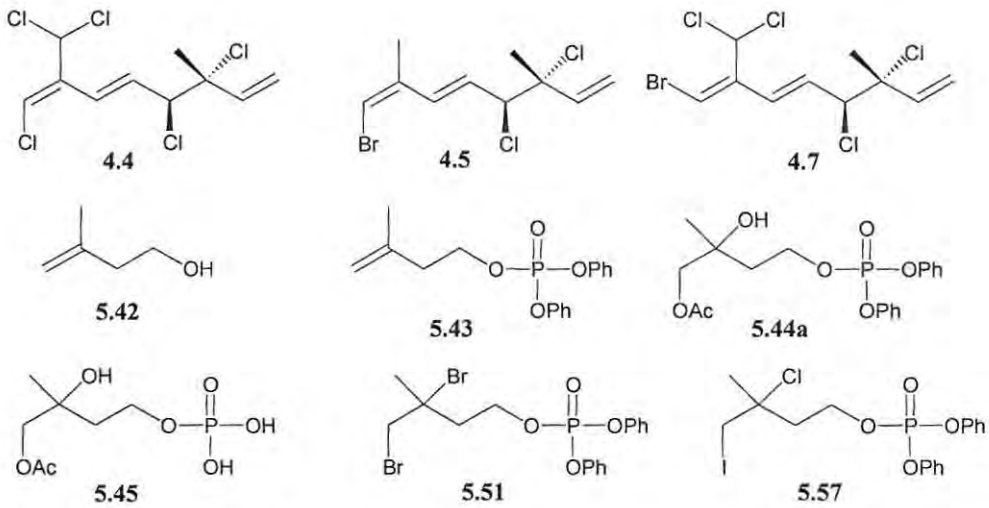

Figure 6.13 Potential DXR inhibitors tested

Table 6.1 Results of *Pf*DXR inhibition assay

Compound	**Slope (OD/min)**
Assay A (no inhibitor)	-28.84
Fosmidomycin (**1.35**)	-0.24
4.4	-21.49
4.5	-25.26
4.7	-23.31
5.42	-29.79
5.43	-15.58
5.44a	-30.65
5.45	-1.27
5.51	-14.34
5.57	-13.95

The assay containing fosmidomycin (**5.21**) as the inhibitor was used as a positive control for the inhibition assay while Assay A served as a negative control with no inhibitor. The K_i of the enzyme could not be determined due to limited enzyme therefore a comparison of the inhibitory activity of compounds against fosmidomycin (**5.21**) was done. The result (Table 6.1) showed that none of the compounds tested was as potent as fosmidmycin (**1.35**) (final concentration of 0.05 μM) even at the final concentration of 2.5 μM.

Not surprisingly, compound **5.45** showed a promising inhibitory activity with a slope of -1.27 at a final concentration of 2.5 μM in the assay. For a better comparison of the activity with fosmidomycin (**5.21**) a 1 μM solution of compound **5.45** was prepared and added to a fresh assay at a final concentration of 0.05 μM. The result shows that compound **5.45** was active against the enzyme at this concentration (Figure 6.14) although it is 27.5 times less potent than fosmidomycin (**5.21**).

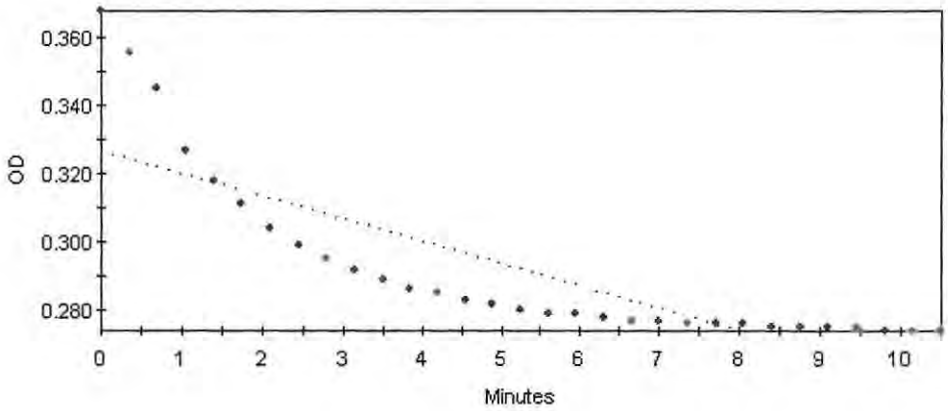

Figure 6.14 A plot of *Pf*DXR with the addition of 10 μM of compound **5.45**

The chemical structure of compound **5.45**, with its free phosphate group was analogous to the substrate and inhibitors (fosmidomycin (**5.21**), FR900098 (**5.22**)) of DXR. The phosphate moiety could have aided the binding of the enzyme to the active site. The tail end of the molecule with the C-hydroxyl C-acetyl group is suspected to be the inhibiting

part in a similar manner to the N-formyl-N-hydroxy group of fosmidomycin (**5.21**) and FR900098 (**5.22**) which inhibit the enzyme. Compound **5.45** was not as active as fosmidomycin (**5.21**) probably because it contains C-hydroxyl C-acetyl as opposed to a N-formyl-N-hydroxy moiety at the tail end. The presence of a N atom at the tail end of fosmidomycin (**5.21**) and FR900098 (**5.22**) has been suggested to be one of the main reasons for their inhibitory properties and an introduction of a N atom on compound **5.45** might be able to improve the potency of this compound against *Pf*DXR. Compound **5.45** could thus serve as a lead compound for anti-malarial drug development. The derivative of this compound (**5.44a**) showed no activity which can be attributed to the fact that compound **5.44a** carries the diphenyl group and was unable to orientate itself to bind to the enzyme.

Compounds **5.43, 5.51** and **5.57** showed some inhibitory activity (Table 6.1) relative to assay A towards the *Pf*DXR. The hydrolysis of the diphenyl moiety might result in compounds with very potent activity against the *Pf*DXR and thus may be used as lead compounds for the development of antimalarial agents. The activity of these compounds might also improve with the replacement of C-3 with a N atom, giving an N-X functionality. *In vivo* testing of the compounds might also show significant DXR inhibition as esterase enzymes within the host or the parasite should be able to hydrolyse the diphenyl component of the compounds and release the free phosphate to bind t the DXR enzyme.

The preliminary results obtained in this work showed that a free phosphate head and electronegative groups at positions 3 and 4 of a hemiterpene could give rise to a potential antimalarial compound and in essence provide initial evidence that dihydroxylation and phosphorylation of halogenated monoterpenes from *Plocamium cornutum* might produce inhibitors of DXR

6.3 Experimental

6.3.1 General experimental

The centrifuges used included Eppendorf centrifuge 5810 R, Eppendorf benchtop centrifuge 5495 and Avanti® JE centrifuge. SDS-PAGE was carried out on BioRad MinigGel Electrophoresis Set. Ultraviolet visualisation of the result of Agarose Gel Electrophoresis (AGE) was performed with the BioRad Universal Hood II chemi/Gel Doc system.enzyme assay was performed in flat bottom 96 well microtitre plates. Assays were read on the PowerWave X plate reader from Bio-Tek instruments at a wavelength of 340 nm. A table of materials and reagents used is attached as appendix (Table 6A1).

6.3.2 Confirmation of the pQE9EcDXR construct

A small scale restriction digest was conducted to confirm the identity of the pQE9EcDXR construct. A series of reaction mixture of a total volume of 20 µL containing ~ 200 ng of plasmid construct, 10 units of restriction enzyme with 20 units of the appropriate buffer was made up in eppendorf tubes. The appropriate volume of water was added to each mixture and was incubated at 37 °C for 2 hours after which 4 µL of 6x loading buffer (30% glycerol, 0.25% bromophenol blue) was added and loaded into the agarose gel. The agarose gel had been made up of 0.4g agarose in 0.5x TBE buffer (45mM Tris, 45mM borate, 1mM EDTA, pH 8.3) and 0.1 µg/ml ethidium bromide. The gel was run at 100V for 1 hour before visualizing the gel under UV.

6.3.3 Competent cells

E. coli XL1 Blue cells was inoculated into 5 ml 2xYT broth and incubated at 37 °C overnight with shaking. 500 µL of the overnight culture was added to a fresh 25 ml 2xYT broth and allowed to incubate at 37 °C for 4 hours. The cells were collected via centrifugation (5000 rpm for 5 minutes at 4 °C). The cell pellets was resuspended in 15

ml cold 0.1 $MnCl_2$ and left on ice for 1 minute then centrifuged as before. The cells were resuspended in 20 ml ice-cold 0.1M $CaCl_2$ and left on ice for 2 hours after which they were harvested again by centrifugation. 5 ml of 0.1 M $CaCl_2$ and 5 ml 30% glycerol was added and aliquots of 200 µL were stored at -80 °C.

6.3.4 Transformation of XL1 Blue with *E. coli*

DXR plasmid construct (~ 200 ng) was incubated with 100 µL competent *Ec* XL1 Blue cell for 20 minutes on ice. The reaction mixture was heat-shocked for 2 minutes at 42 °C then returned to ice for 2 minutes. Pre-incubated 2xYT broth (900 µL, 37 °C) was added to the reaction mixture and incubated with shaking at 37 °C for 1 hour. The reaction culture was microcentrifuged (12 000x g) for 1 minute and 800 µL of the supernatant was removed. The cells were resuspended in the remaining supernatant. The transformed cells were then spread onto 2xYT broth agar plate containing 0.15mg/ml ampicillin. The plates were inverted and incubated for 16 hours at 37 °C. Confirmation of a successful transformation was observed when colonies were seen on the agar plates.

6.3.5 Over-production of *Ec*DXR (Induction studies)

Cultures of transformed *E. coli* cells were incubated in 25 ml 2xYT broth containing ampicillin (0.15 mg/ ml) overnight with shaking at 37 °C. The culture was then diluted 1:10 by inoculating the 25 ml into fresh 225 ml 2xYT broth with 0.15 mg/mL ampicillin and incubated at 37 °C for 1 hour until the mid-logarithmic growth phase was reached (A_{600} = 0.6 – 1). A sample (1 ml) was removed and the culture was then induced with IPTG (final concentration of 1mM). Samples were taken out every hour after induction for 6 hours then overnight and the A_{600} of each sample was determined. Each sample was centrifuged (13 000x g, 1 minute) and the cell pellet was resuspended in 150 µL PBS buffer for every 0.5 OD. To 20 µL of each sample, 4 µL SDS loading buffer (62.5 mM Tris-HCl, pH6.8; 10% (vlv) glycerol; 2% (w/v) SDS, 5% (v/v) β-mercaptoethanol; 0.05% (w/v) bromophenol blue) was added and the samples were boiled at 95 °C for 5 minutes.

The samples were loaded onto 0.1% SDS 12% PAGE (10% acrylamide resolving gel, 4% stacking gel)and run at 150 V for 1 hour in SDS running buffer (25mM Tris-HCl, 250mM glycine, 0.1% SDS, pH 8.0). The protein was visualized with coomassie blue stain (0.1% (w/v) commassie brilliant R-250, 40% (v/v) methanol, 10% glacial acetic acid) and destained in destain (40% (v/v) methanol, 10% glacial acetic acid.

6.3.6 Heterologous production and nickel affinity purification of *Ec*DXR.

Cultures of transformed XL1 Blue cells were inoculated into sterile 2xYT broth (4 x 25ml) containing 0.15mg/ml ampicillin at 37 °C with shaking overnight. The overnight cultures were inoculated into 225ml fresh 2xYT broth and incubated for 37 °C with shaking for 1 hour after which it was induced with 250 µL of 1M IPTG (final concentration 1mM). The cultures were further incubated for 4 hours at 37 °C. The cells were harvested by centrifugation (5 000x g, 20 minutes, 4 °C) and the cell pellets were resusupended in 2.5 ml native lysis buffer (20mM Tris-HCl, 300mM NaCl, 10mM imidazole, pH 8.0). The four cultures were combined to make two cultures and 65 µL of 1 mM phenylmethylsulfonyl (PMSF) and 650 µL of 100 µg/ml lysozyme were added to each fraction and stored at -80 °C overnight. The cells were sonicated with three times 30 second pulse at 4 °C and the debris were removed via centrifugation (13 000x g; 4 °C; 25 minutes). Samples (80 µL) of the soluble (supernatant) and insoluble (cell debris) fractions were visualized on SDS-PAGE as described in section 6.3.4.

Nickel charged sepharose resins (1 ml) was added to the cleared lysate and agitated on ice for 4 hours. The resins were collected by centrifugation (4 000x g; 5 minutes; 4 °C) and a sample of the flow-through (supernatant) was visualized by SDS-PAGE. The resins was washed with 5 ml Native wash Buffer (20mM Tris-HCl, 300mM NaCl, 100mM imidazole; pH 8.0) three times (washes 1 – 3). The protein was displaced from the resins by gentle agitation three times (elutions 1 – 3) with 5 ml Native elution Buffer (20mM Tris-HCl, 300mM NaCl, 1M imidazole; pH 8.0). In between each wash and elution, the resin was collected by centrifugation (4 000x g; 5 minutes; 4 °C). Samples from each wash and elution was visualized by SDS-PAGE to monitor the purification profile of the

protein. Elution 1 was dialyzed in PEG 20 000 in a dialysis tubing at 4 °C overnight. The protein concentration was then determined by Bradford's Assay. A series of concentrations of the (0 – 300 μg/ml) standard protein (Bovine Serum Albumin) were prepared for the determination of the standard curve. 10 μL of each standard and 10 μL of the dialyzed *Ec*DXR was incubated with 200 μL of Bradford's Reagent at room temperature for 5 minutes. The absorbance of the standards and the sample (DXR) was measured at 595 nm using a PowerWave Microtitre Plate Reader.

6.3.7 *In vitro* assay of *Ec*DXR activity

The assay mixture was prepared in a flat bottom 96-well microtitre plate to a final volume of 200 μL. The assay mixture consisted of 100 mM Tris-HCl, (pH 7.5, final concentration 10 mM), 1 mM $MnCl_2$ (final concentration 0.1 mM), 0.3 mM NADPH (final concentration 0.009 mM), 0.3 mM of DOXP (**5.3**) substrate (final concentration 0.009 mM), 6.87 μM *Ec*DXR (final concentration 0.857 μM) and water to makeup to 200 μL. The assays were blanked against the reaction mixture with no enzyme present. The assay was initiated by the addition of enzyme and the oxidation of NADPH was monitored at 340 nm over a period of 10 minutes although the slope was calculated over 5 minutes. The reaction was conducted at 37 °C on a powerwave microtitre plate reader. Negative controls which included (1) no substrate and (2) no NADPH were used to determine the activity of the *Ec*DXR enzyme.

6.3.8 Sample preparation

Each tested potential inhibitor was dissolved or suspended in 50:50 solution of EtOH:water to a concentration of 50μM. Sample of compound **5.45** solution was further diluted to a 1 μM solution. The maximum concentration of EtOH used did not have a any noticeable effect on the enzyme assay.

6.3.9 *In vitro* assay of *Pf*DXR activity

The purified *Pf*DXR was donated by Jessica Goble, (department of Biochemistry, Microbiology, and Biotechnology, Rhodes University, Grahamstown) The DOXP substrate was kindly provided by Professor Philip Proteau, Department of Pharmaceutical Sciences, College of Pharmacy, Oregon State University, Corvallis) on a 96-well microtitre plate. The assay mixture consisted of 100 mM Tris-HCl, (pH 7.5, final concentration 10 mM), 1 mM $MnCl_2$ (final concentration 0.1 mM), 0.3 mM NADPH (final concentration 0.12 mM), 0.3 mM of DOXP (**5.3**) substrate (final concentration 0.015 mM), 20.5μM *Pf*DXR (final concentration 1.03 μM) and water to make a final volume of 200 μL. Each assay was blanked against water. The assay had been initially blanked against the reaction mixture without the enzyme. However, this resulted in a curve which appeared to be fluctuating, although the slope was close to zero (-0.374 mOD/min) with a difference of 0.003 OD between the highest and the lowest readings (appendix 6.5). Water blank was thus used to obtain a constant base line absorbance with a slope of zero over 10 minutes. The assay, which measured the depletion or oxidation of NADPH to NADP at 340nm, was initiated by the addition of the purified DXR at 37 °C over 10 minutes. The negative controls used included (1) heat denatured enzyme, (2) no NADPH and (3) no substrate. The inhibition assays included the compounds tested at a final concentration of 2.5 μM. A second assay of compound **5.45** as the test inhibitor included 0.05 μM of the compound. Fosmidomycin (**5.21**) (1mM) was used as the positive control for the inhibition assays also at a final concentration of 0.05 μM.

References

Ahuja, S.; Ahuja, S.; Chen, Q. And Wahlgren, M. Prediction of Solubility on Recombinant Expression of *Plasmodium falciparum*, Erythrocyte Membrane Protein I in *Escherichia coli*. *Malarial Journal* **2006**, 5, 52 – 60.

Baca, A. M. and Hol, G. J. Overcoming Codon Bias: A Method for High-Level Overexpression of *Plasmodium* and Other AT-Rich Parasite Genes in *E. coli*. *International Journal of Parasitology* **2000**, 30, 113 – 118.

Chaga, G. S. Twenty-five Years of Immobilized Metal Ion Affinity Chromatography: Past, present and Future. *Journal of Biochemical and Biophysical Methods* **2001**, 49, 313 – 334.

Cinquin, O.; Christopherson, R. I. and Menz, R. I. A Hybrid Plasmid for Expression of Toxic malarial Proteins in *E. coli*. *Molecular and Biochemical Parasitology* **2001**, 117, 245 – 247.

Dagert, M. and Ehrlich, S. D. Prolonged Incubation in Calcium Chloride Improves the Competence of *Escherichia coli*. *Gene* **1979**, 6, 23 – 28.

Garret, R.H. and Grisham, C. M. **1999**. *Biochemistry*, Second edition, pp 395 – 399 and 426 – 459, Saunders College Publishing, Harcourt Brace Colledge Publishers, New York.

Goble, J. Honours Thesis, **2007**, The purification and Kinetic Chracterization of the Malaria Protein 1-Deoxy-$_D$-xylulose-5-phosphate Reductoisomerase (*Pf*DXR).

Jomaa, H., Wiesner, J., Sanderbrand, S., Altincicek, B., Weidemeyer, C., Hintz, M., Türbachova, I., Eberl, M., Zeidler, J., Lichtenthaler, H. K., Soldati, D. and Beck, E. Inhibitors of the Nonmevalonate Pathway of Isoprenoid Biosynthesis as Antimalarial Drugs. *Science* **1999**, 285, 1573 – 1576.

Kaiser, J.; Yassin, M.; Prakash, S.; Safi, N.; Agami, M; Lauw, S.; Ostrozhenkova, E.; Bacher, A.; Rohdich, F.; Eisenreich, W; Safi, J. and Golan-Goldhirsh, A. Anti-malarial Drug Targets: Screening for Inhibitors of 2C-Methyl-$_D$-erythritol 4-phosphate Synthase (IspC Protein) in Mediterranean Plants. *Phytomedicine* **2007**, 14, 242 – 249.

Lichtenthaler, H. K. The 1-Deoxy-D-xylulose -5-Phosphate Pathway of Isoprenoid Biosynthesis in Plants. *Annual Review of Plant Physiology and Plant Molecular Biology* **1999**, 50, 47 – 65.

Madigan, M. T. and Martinko, J. M. **2006**. *Brock Biology of Microorganisms*, Eleventh edition, 268 – 269, 288, Pearson Prentice Hall, USA.

Maguire, B. A.; Manuilov, A. V. and Zimmermann, R. A. Differential Effects of Replacing *Escherichia coli* Ribosomal Protein L27 with Its Homologue from *Aquifex aeolicus*. *Journal of Bacteriology* **2001**, 183 (22), 6565 – 6572.

Studier, F. W.; Rosenberg, A. H.; Dunn, J. J. and Dubendorff, J. W. Use of T7 RNA Polymerase to Direct Expression of Cloned Genes. *Methods in Enzymology* **1990**, 185, 61 – 89.

Takahashi, S.; Kuzuyama, T.; Watanabi H. and Seto, H. A. 1-Deoxy-D-Xylulose 5 Phosphate Reductoisomerase Catalizing the Fformation of 2-C-Methyl-D-Erythritol 4-Phosphate in an Alternative Non-mevalonate Pathway for Terpenoid Biosynthesis. *Proceedings of National Academy of Sciences* **1998**, 95, 9879 - 9884.

Tanner, D. Msc Thesis, **2004**, Over-Expression, Purification and Biochemical Characterization of DOXP Reductoisomerase and the Rational Design of Novel anti-malarial Drugs.

Yadava, A. and Ockenhouse, C. F. Effect of Codon Optimization on Expression Levels of Functionally Folded Malaria Vaccine Candidate in Prokaryotic and Eukaryotic Systems. *Infection and Immunity* **2003**, 71 (9), 4961 – 4969.

Chapter 7

Summary and Conclusions

Not many antiplasmodial compounds have been reported in the literature from the marine environment. This study revealed that a large number of marine algae in the South African coast could be a potential source of antiplasmodial compounds in that 50% of the 22 marine algae extracted gave extracts with antiplasmodial activity. *S. heterophyllum*, *P. cornutum*, *A. ephedrea* and *P. cloiophylla* gave the extracts with the most promising antiplasmodial results. Three tetraprenyl toluquinols (**3.1**, **3.2** and **3.5**) and *all-tans*-fucoxanthin (**3.6**) showed good antiplasmodial activity towards CQS *P. falciparum* D10 strain.

Five halogenated monoterpenes comprising of three new (**4.5**, **4.6** and **4.7**) and two known compounds (**4.1** and **4.2**) were isolated from *P. cornutum* and tested against CQS *P. falciparum* D10 strain. The most potent antiplasmodial activity was exhibited by compounds **4.4** and **4.7** indicating that a gem-dichloride moiety at position 9 of these halogenated monoterpenes is important for antiplasmodial activity.

In order to impart a dual mode of action on the halogenated monoterpenes and make them more selective antiplasmodial agents attempts were made to synthetically modify halogenated compound **4.4** into an analogue of the DXR substrate and inhibitor, DOXP and fosmidomycin respectively. A $NaIO_4$/NaBr-catalyzed dihydroxylation reaction of compound **4.4** was unsuccessful. However hemiterpene analogue **5.42** was successfully phosphorylated to compound **5.43** that was in turn successfully dihydroxylated and halogenated to compounds **5.44a**, **5.45**, **5.51**, and **5.57**. An unexpected de-phenylated analogue of compound **5.44a**, compound **5.45**, was isolated as a side product from the dihydroxylation reaction of compound **5.18**. Attempts to hydrolyze the phenyl group from the phosphate moiety of the synthesized analogues were unsuccessful and instead yielded a saturated analogue (**5.58**) of compound **5.43**.

An *in vitro* inhibition assay of the halogenated monoterpenes **4.4**, **4.6** and **4.7** and the synthesized hemiterpene analogues **5.42** – **5.45**, **5.51** and **5.57** with *Pf*DXR showed only compound **5.45** with a free phosphate moiety to be the inhibitor of the enzymes. This result indicated the important role of a free phosphate in the inhibition of the DXR enzyme.

Future work and recommendations

Now that the antiplasmodial property of the halogen at position 9 of the halogenated monoterpenes and the importance of a free phosphate head group has been determined, an effective alternative method of phosphorylation and hydroxylation of the compounds is recommended. Perhaps a change of phosphorylating agent to dibenzylchlorophosphate would give products that can easily be hydrolyzed to free phosphates.

Compound **5.45** was found to be 27.5 times less potent than fosmidomycin at inhibiting the *Pf*DXR enzyme. The inhibitory property of this compound may be improved by the substitution of the C-3 carbon with N to produce a closer analogue to fosmidomycin and FR90098 whose activity have been reported to be due to the N-hydroxyl-N-formyl group.

Finally more isolation and screening of compounds from marine algae against the plasmodium parasite is recommended as more interesting compounds are envisage to be in store for discovery against the deadly parasite.

Appendix 1

Table 2A1 Antiplasmodial and cytotoxicity data of marine algal extracts

Algae, dry weight after extraction	Algae code	Mass of crude extract (mg)	% Parasite survival			D10 IC_{50} (µg/ml)	CHO IC_{50} (µg/ml)	SI
			50 µg/ml	25 µg/ml	12.5 µg/ml			
Caulacanthus ustulatus 26.5.g	KB 06-8-A	96	34.7	85.9	101.7	nd	nd	nd
	KB 06-8-B	190.5	19.8	57.1	77.6	nd	nd	nd
Pterosiphonia cloiophylla 8.8 g	KB 06-9-A	95.4	10.8	41.3	42.6	nd	nd	nd
	KB 06-9-B	324	3.6	14.3	47.0	nd	nd	nd
	KB 06-9-C	36.4	2.5	14.7	67.8	nd	nd	nd
	KB 06-9-D	237.8	4.1	2.5	5.7	4.7	75.0	16
	KB 06-9-E	33.9	3.6	8.8	19.3	11.4	nd	nd
Bifurcaria brassicaeformis 14.3 g	KB 06-5-A	331.2	48.9	80.3	83.6	nd	nd	nd
	KB 06-5-B	654.7	12.7	49.6	67.9	nd	nd	nd
	KB 06-5-D	65.4	35.6	69.6	80.0	nd	nd	nd
Grateloupia filicina 16.9 g	KB 06-4-A	244.4	84.8	96.6	91.9	nd	nd	nd
	KB 06-4-B	169.5	13.4	49.5	74.1	nd	nd	nd
	KB 06-4-D	312.1	107.9	107.4	98.7	nd	nd	nd
Laurencia flexuosa 33.3 g	NDK 06-6-A	306.5	9.7	24.6	64.5	nd	nd	nd
	NDK 06-6-B	554.4	5.5	14.9	37.8	nd	nd	nd
	NDK 06-6-D	38.5	30.2	59.6	75.1	nd	nd	nd
Trematocarpus flabellatus 73.2 g	NDK 06-9b-A	212.4	33.0	27.9	54.1	nd	nd	nd
	NDK 06-9b-B	302.3	4.2	17.6	30.0	7.8	45.9	5.9
	NDK 06-9b-D	33.9	50.1	74.4	86.0	nd	nd	nd
	NDK 06-9b-E	46.7	8.7	25.5	42.3	nd	nd	nd
Sargassum heterophyllum 52.6 g	NDK 06-5-A	2012.9	3.5	19.5	40.0	nd	nd	nd
	NDK 06-5-B	2031.9	3.9	2.7	5.6	2.8	3.7	1.3
	NDK 06-5-C	108.2	5.2	8.9	22.8	5.9	12.3	2.1
	NDK 06-5-D	891.5	5.4	33.6	54.8	nd	nd	nd
	NDK 06-5-E	87.4	6.1	7.3	10.2	4.1	9.8	2.4
Gelidium capense 55.3 g	NDK 06-10-A	320.5	30.0	63.5	86.5	nd	nd	nd
	NDK 06-10-B	530.0	13.4	28.3	54.4	nd	nd	nd
	NDK 06-10-C	34.6	22.4	55.9	62.3	nd	nd	nd
	NDK 06-10-D	110.5	39.1	71.9	90.7	nd	nd	nd
Plocamium corallorhiza 33.8 g	NDK 06-1b-A	800.4	2.2	2.5	15.2	3.5	35.1	10
	NDK 06-1b-B	749.3	8.2	7.8	21.0	6.6	14.0	2.1
	NDK 06-1b-C	39.2	44.9	57.1	61.5	nd	nd	nd
	NDK 06-1b-D	55.7	3.0	17.5	38.1	nd	nd	nd

n = average number of data set, KB = Kalk Bay, NDK = Noordhoek and KOS = Kenton on Sea, nd = not determined.

Table 2A1 continue

Algae, dry weight after extraction (g)	Algae code	Mass of crude extract (mg)	% Parasite survival			D10 IC_{50} (µg/ml)	CHO IC_{50} (µg/ml)	SI
			50 µg/ml	25 µg/ml	12.5 µg/ml			
Polysiphonia incompta 28.9 g	NDK 06-19-A	128.6	48.0	90.2	103.4	nd	nd	nd
	NDK 06-19-B	345.1	25.6	67.9	80.5	nd	nd	nd
	NDK 06-19-C	41.5	5.8	12.7	8.7	6.1	19.2	3.1
	NDK 06-19-D	371.8	21.2	26.9	58.5	nd	nd	nd
Plocamium cornutum 26.0 g	KB 06-3-A	784.0	0.0	7.3	12.3	6.2	7.9	1.3
	KB 06-3-B	706.0	0.0	2.0	18.5	4.6	57.8	12.6
	KB 06-3-C	135.0	26.6	49.4	59.6	nd	nd	nd
Gracilaria aculeate 21.6 g	KOS 06-1-A	356.4	29.4	67.5	66.2	nd	nd	nd
	KOS 06-1-B	346.8	62.4	73.3	72.1	nd	nd	nd
	KOS 06-1-C	64.8	35.3	45.8	67.9	nd	nd	nd
	KOS 06-1-D	1400	75.4	86.0	94.8	nd	nd	nd
Gelidium abbottiorum 106.5 g	KOS 06-2-A	1000.0	67.3	91.5	90.6	nd	nd	nd
	KOS 06-2-B	250.0	10.2	38.6	68.2	nd	nd	nd
	KOS 06-2-D	300.0	36.3	64.0	83.6	nd	nd	nd
Gelidium pteridifolium 26.0 g	KOS 06-3A	394.6	84.1	89.0	98.3	nd	nd	nd
	KOS 06-3-B	147.6	25.8	37.7	61.6	nd	nd	nd
	KOS 06-3-C	73.0	56.6	78.0	82.9	nd	nd	nd
	KOS 06-3-D	385.0	46.0	64.2	83.3	nd	nd	nd
Amphiroa ephedraea 101.3 g	KOS 06-23-A	301.7	23.0	67.3	77.1	nd	nd	nd
	KOS 06-23-B	223.7	0.0	3.7	23.9	8.3	>100	>12.1
	KOS 06-23-C	55.4	15.0	55.9	63.5	nd	nd	nd
	KOS 06-23-D	169.1	6.1	47.3	71.7	nd	nd	nd
Codium extricatum 57.1 g	KOS 06-13B-A	207.1	17.7	57.6	85.6	nd	nd	nd
	KOS 06-13B-B	270.9	0.0	0.0	0.8	5.9	32.1	5.4
	KOS 06-13B-C	250.9	3.5	7.5	22.0	8.2	59.3	7.2
	KOS 06-13B-D	182.2	54.6	76.7	87.4	nd	nd	nd
Cladophora rugulosa 21.0 g	KOS 06-11-A	197.9	0.0	0.8	7.0	11.4	nd	nd
	KOS 06-11-B	236.6	1.9	5.5	48.4	nd	nd	nd
	KOS 06-11-C	54.1	28.4	66.7	88.0	nd	nd	nd
	KOS 06-11-D	76.5	36.1	77.7	86.0	nd	nd	nd
Spyridia cupressina 9.0 g	KOS 06-20-A	50.3	19.3	48.2	75.6	nd	nd	nd
	KOS 06-20-B	28.8	28.7	36.7	67.2	nd	nd	nd
	KOS 06-20-C	15.5	3.7	6.2	16.8	17.8	nd	nd
	KOS 06-20-D	ND	39.6	79.8	86.7	nd	nd	nd
Polysiphonia incompta 35.1 g	KOS 06-15A	151.3	84.9	99.7	97.5	nd	nd	nd
	KOS 06-15B	407.5	24.1	64.6	90.5	nd	nd	nd
	KOS 06-15C	144.9	29.7	46.8	88.2	nd	nd	nd
	KOS 06-15D	61.1	10.3	25.5	54.9	nd	nd	nd

n = average number of data set, KB = Kalk Bay, NDK = Noordhoek and KOS = Kenton on Sea, nd = not determined.

Table 2A1 continued

Algae, dry weight after extraction (g)	Algae code	Mass of crude extract (mg)	% Parasite survival			D10 IC_{50} (µg/ml)	CHO IC_{50} (µg/ml)	SI
			50 µg/ml	25 µg/ml	12.5 µg/ml			
Laurencia flexuosa 15.0 g	KOS 06-6A	241.7	0.0	6.7	37.2	nd	nd	nd
	KOS 06-6B	228.8	8.7	38.6	62.4	nd	nd	nd
	KOS 06-6C	30.0	61.2	76.8	83.3	nd	nd	nd
	KOS 06-6D	123.0	11.2	23.7	49.6	nd	nd	nd
Sargassum elegans 15.1 g	KOS 06-17A	405.4	30.4	38.2	64.0	nd	nd	nd
	KOS 06-17B	234. 0	22.7	27.3	42.5	nd	nd	nd
	KOS 06-17C	717.8	9.2	17.6	46.4	nd	nd	nd
	KOS 06-17D	35.9	31.5	33.1	44.6	nd	nd	nd
Plocamium corallorhiza 33.6 g	KOS 06-14b-A	1440	20.4	24.5	28.2	9.6	41.8	4.4
	KOS 06-14b-B	378	11.1	14.9	32.8	7.6	50.7	6.7
	CQ (n=7)					9.3ng/ml		
	Emetine (n=5)						0.07	

n = average number of data set, KB = Kalk Bay, NDK = Noordhoek and KOS = Kenton on Sea, nd = not determined.

Appendix 2

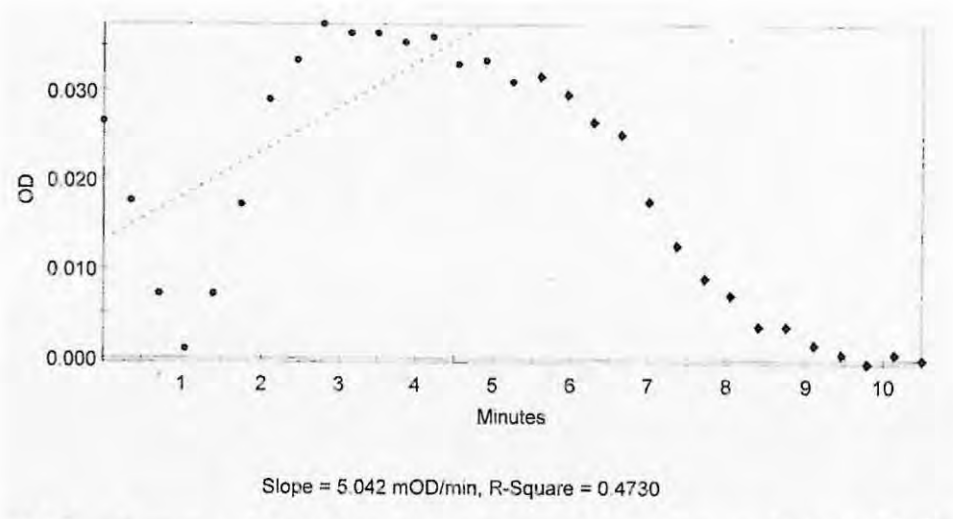

Figure 6A1 Activity of *Ec*DXR in the absence of the substrate DOXP (**1.20**)

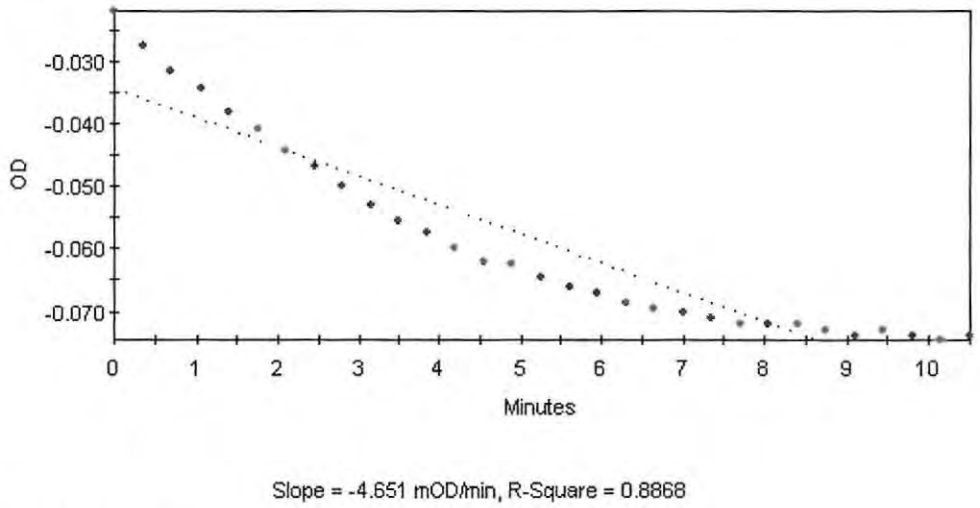

Figure 6A2 Activity of a second over-produced *Ec*DXR

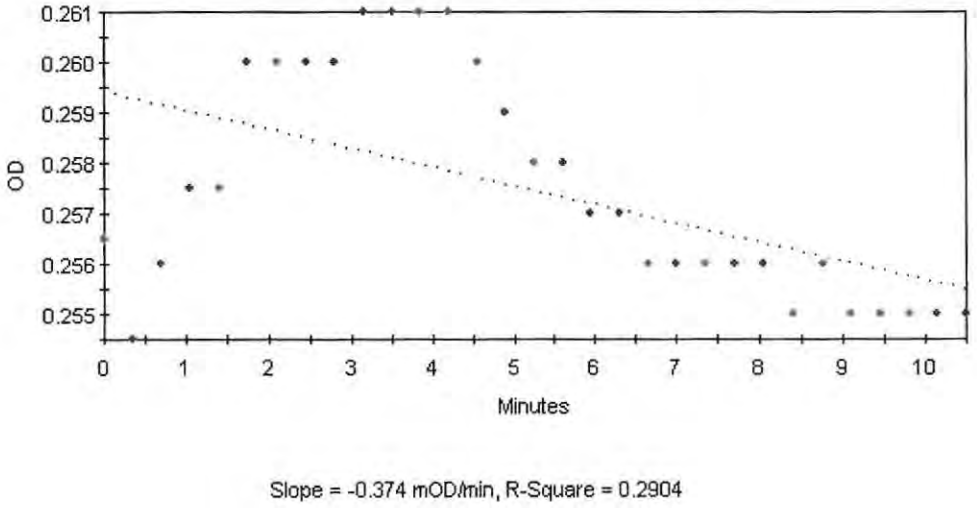

Figure 6A3 Water blanked assay mixture without *Pf*DXR

Table 6A1 Materials and reagents used

Reagents	**Suppliers**
Agar	Oxoid, UK
Agarose	Whitehead Scientific, South Africa
Ampicillin	Sigma-Aldrich, USA.
Bradford's Reagent	Sigma-Aldrich, USA.
Bromophenol blue	Sigma-Aldrich, USA.
Coomassie brilliant blue R250	Saarchem, South Africa
Ethanol	BDH laboratory supplies
Ethidium bromide	Sigma-Aldrich, USA.
Imidazole	Sigma-Aldrich, USA.
IPTG	Peqlab, Germany
Magnesium Chloride	Saarchem, South Africa
Nickel sulphate	Sigma-Aldrich, USA.
PMSF	Sigma-Aldrich, USA.
Polyethylene glycol 20000	Saarchem, South Africa
SDS-PAGE and Agarose gel markers	Peqlab, Germany
SDS	Saarchem, South Africa
Calcium chloride	Merk laboratory supplies, South Africa
E. coli XL1 Blue	Stratagene, USA
Glycerol	BDH laboratory supplies
B-mercaptoethanol	Merck laboratory supplies
Coomassie blue stain	Sigma-Aldrich, South Africa
Methanol	BDH laboratory supplies
Glacial acetic acid	BDH laboratory supplies
Sodium Chloride	Saarchem, South Africa
Bovine serum albumin	Roche, South Africa
Fosmidomycin	Jomaa, Germany
DOXP	Echelon Biosciences Inc.
NADPH	Roche, Japan
Restriction endonucleases	New England Biolabs